UNIVERSIDAD DE CONCEPCIÓN

FACULTAD DE CIENCIAS NATURALES Y OCEANOGRÁFICAS

Programa de Doctorado en Ciencias con mención en Manejo de Recursos Acuáticos Renovables

EFECTO DE LA HIPOXIA SOBRE LA RESPUESTA MOLECULAR, MICROBIANA Y EPITRANSCRIPTÓMICA DE *Mytilus chilensis*

POR: MILTON GABRIEL MONTÚFAR ROMERO

Tesis presentada a la Facultad de Ciencias Naturales y Oceanográficas de la Universidad de Concepción para optar al grado académico de

Doctor en Ciencias con mención en Manejo de Recursos Acuáticos Renovables

Profesor Guía: Cristian Jorge Gallardo Escárate

Septiembre de 2025
Concepción, Chile

TABLA DE CONTENIDO

ÍNDICE DE TABLAS

ÍNDICE DE ILUSTRACIONES

RESUMEN

La expansión de zonas hipóxicas en ambientes marinos costeros representa una de las consecuencias más críticas del cambio climático y del aumento de las actividades humanas. Este fenómeno se ha intensificado en áreas de alta productividad, como la Región de Los Lagos en el sur de Chile. En esta zona, factores como la limitada renovación de aguas, el aumento de la temperatura, la acumulación de materia orgánica y los residuos generados por actividades acuícolas han favorecido procesos de eutrofización, disminuyendo progresivamente los niveles de oxígeno disuelto. Estas condiciones amenazan directamente la supervivencia y el desempeño fisiológico de especies marinas de interés económico, entre ellas *Mytilus chilensis* (chorito), un bivalvo ampliamente cultivado en la región. En los moluscos bivalvos, la exposición prolongada a hipoxia altera el equilibrio homeostático, forzando la redistribución del gasto energético hacia mecanismos de compensación. Esto ocurre a expensas de funciones biológicas esenciales como el crecimiento, la reproducción y la inmunidad. Aunque existen mecanismos adaptativos frente a la hipoxia, la magnitud y el tipo de respuesta pueden variar entre especies, tejidos y escalas temporales. En el caso específico de *M. chilensis*, aún se desconocen con precisión las

respuestas moleculares, microbianas y epitranscriptómicas que se activan frente a condiciones hipóxicas sostenidas y su posterior reoxigenación. Esta tesis tuvo como objetivo general caracterizar de manera integrada las respuestas transcriptómicas, epitranscriptómicas y microbianas de *M. chilensis* expuesto experimentalmente a condiciones de hipoxia (2,0 mg de oxígeno por litro) y reoxigenación (7,2 mg de oxígeno por litro). Para ello, se aplicó una estrategia metodológica de múltiples niveles, que incluyó análisis transcriptómicos mediante RNA-seq, caracterización del microbioma a través de la secuenciación del gen 16S rRNA, y secuenciación directa de ARN de molécula única utilizando la plataforma Oxford Nanopore Technologies. Los análisis se realizaron en tres tejidos fisiológicamente relevantes: branquias, glándula digestiva y músculo aductor. Los resultados transcriptómicos revelaron la expresión diferencial de 15.056 genes en branquias, 11.864 en glándula digestiva y 9.862 en músculo aductor. Se observaron cambios relevantes en vías como la señalización Toll-like, mTOR, metabolismo del ciclo del ácido cítrico y apoptosis. Estos hallazgos sugieren una transición hacia el metabolismo anaeróbico y una supresión de la respuesta inmunitaria. También se identificó una regulación génica específica en los cromosomas 1, 9 y 10, vinculada al estrés del retículo endoplásmico, la generación de especies

reactivas de oxígeno, la autofagia y el metabolismo energético. En paralelo, el análisis del microbioma evidenció un desequilibrio significativo inducido por la hipoxia. Se registró una disminución en la abundancia de bacterias comensales, como las pertenecientes al orden *Rhodobacterales*, y un aumento de patógenos oportunistas como *Vibrio* y *Aeromonas*. Estas alteraciones microbianas estuvieron asociadas a la pérdida de funciones metabólicas e inmunológicas esenciales, lo que podría afectar la estabilidad fisiológica del organismo hospedador. A nivel epitranscriptómico, se obtuvieron 476.915 y 587.120 lecturas limpias en condiciones de normoxia e hipoxia, respectivamente, con tasas de mapeo superiores al 50 %. Se construyeron 3.260 transcritos consenso en normoxia y 4.437 en hipoxia. Además, se identificaron 5.237 transcritos nuevos, de los cuales 4.796 no presentaron similitud con anotaciones genómicas previas. El análisis de expresión diferencial detectó 289 transcritos significativamente regulados, con 90 sobreexpresados y 199 subexpresados en hipoxia. Se identificaron múltiples sitios de metilación m^6A y m^5C, y se observaron 48 transcritos con metilación m^6A diferencial. Asimismo, se detectaron diferencias en la metilación m^5C entre condiciones y se reconocieron sitios de pseudouridina (Ψ), modificando potencialmente la funcionalidad de los transcritos involucrados. En

conjunto, los hallazgos de esta investigación proporcionan una visión completa y detallada de los mecanismos de adaptación de *M. chilensis* frente a la hipoxia. La interacción entre el transcriptoma, la microbiota y las modificaciones epitranscriptómicas constituye un eje central en la respuesta del organismo al estrés ambiental. Esta información es clave para desarrollar estrategias de manejo acuícola más sostenibles y resilientes, considerando el impacto creciente del cambio climático sobre los ecosistemas marinos.

INTRODUCCIÓN

1. Cambio climático e hipoxia

El oxígeno es un factor ecológico dominante sobre la biomasa y la composición de especies bentónicas (Levin, 2003). La hipoxia es el déficit de oxígeno disuelto disponible en la columna de agua, siendo un importante factor de estrés para la mayoría de los animales marinos que requieren oxígeno para sobrevivir y completar sus ciclos (Calle et al., 2019; García et al., 2008; Haider et al., 2020). El incremento de las áreas hipóxicas en los sistemas costeros se produce principalmente por acción combinada de la eutrofización y el calentamiento global (Breitburg et al., 2018; Capet et al., 2013; Conley et al., 2009; Haider et al., 2020). La eutrofización es un proceso inducido por la acumulación excesiva de nutrientes inorgánicos, principalmente nitrógeno y fósforo. Aunque estos compuestos no constituyen materia orgánica por sí mismos, estimulan una elevada productividad primaria, lo que conduce a la generación y acumulación de materia orgánica autóctona. La posterior degradación microbiana de esta materia incrementa la respiración heterótrofa, provocando una disminución significativa en las concentraciones de oxígeno disuelto en el ecosistema acuático. (Ledesma et al., 2013; Silva &

Vargas, 2014). En las aguas superficiales, las concentraciones de oxígeno disuelto son el resultado de un equilibrio entre la producción de oxígeno a través de la fotosíntesis, el consumo provocado por la respiración y el intercambio con la atmósfera, donde el último tiende a mantener el oxígeno disuelto cerca de la saturación, según la temperatura y la salinidad (Silva & Vargas, 2014). El aumento de temperatura provoca una disminución de la solubilidad de oxígeno en el agua y un incremento de la estratificación (Melzner et al., 2013; Scanes et al., 2021; Scanes et al., 2020). En los ecosistemas marinos costeros se han utilizado umbrales de referencia considerando los efectos biológicos y ecológicos en los que interviene la cantidad de oxígeno disuelto (OD) en el océano (Choumiline et al., 2019; Conley et al., 2009; Diaz & Rosenberg, 2008; Hofmann et al., 2011; McArley et al., 2018; Moffitt et al., 2015; Sattari et al., 2013). Por ejemplo, hiperoxia (10,0 mg $L^{-1} \leq$ OD < 6,0 mg L^{-1}), normoxia (6,0 mg $L^{-1} \leq$ OD < 3,0 mg L^{-1}), baja concentración de oxígeno (3,0 mg $L^{-1} \leq$ OD < 2,0 mg L^{-1}), hipoxia moderada (2 mg $L^{-1} \leq$ OD < 0,7 mg L^{-1}), hipoxia severa (0,7 mg $L^{-1} \leq$ OD < 0,1 mg L^{-1}), y anoxia (OD $\leq$ 0,1 mg L^{-1}) (Choumiline et al., 2019; Conley et al., 2009; Diaz & Rosenberg, 2008; Hofmann et al., 2011; McArley et al., 2018; Moffitt et al., 2015; Sattari et al., 2013). Estos umbrales de hipoxia han sido ampliamente utilizados en

los organismos marinos, sin embargo, algunos pueden variar de acuerdo a la región y a la especie (Choumiline et al., 2019; Conley et al., 2009; Diaz & Rosenberg, 2008; Hofmann et al., 2011; McArley et al., 2018; Moffitt et al., 2015; Sattari et al., 2013). Por ejemplo, en Chile el umbral de hipoxia de 2 mL L^{-1} (2,9 mg L^{-1} mediante el factor de conversión 1 mL L^{-1}= 1,43 mg L^{-1}), se ha utilizado para distinguir condiciones hipóxicas en el mar interior de la Patagonia (Diaz, 2001; Diaz & Rosenberg, 1995; Silva & Vargas, 2014). Los eventos de surgencia, que se caracterizan por el ascenso de masas de agua bajas en oxígeno disuelto producido por el viento (transporte de Ekman), aumentarán debido al calentamiento global, favoreciendo así la intensidad y magnitud de las hipoxias naturales (sin intervención antropogénica) entre 1 y 7% durante el próximo siglo (Bakun et al., 2015; Cerda et al., 2010; Gattuso et al., 2015; Hernández-Miranda et al., 2017; Schmidtko et al., 2017). El cambio climático afecta a las precipitaciones y a la descarga de los ríos en los fiordos (Bianchi et al., 2020; Iriarte et al., 2014). Esto repercutirá en el grosor y la extensión de la capa de baja salinidad en la parte superior de los fiordos, lo que ralentizará el ritmo de la circulación y la renovación de las aguas profundas, afectando así a las concentraciones de oxígeno del fondo (Bianchi et al., 2020; Iriarte et al., 2014), dando como resultado

consecuencias perjudiciales para la pesca y las economías costeras (Schmidtko et al., 2017).

2. Efecto de la hipoxia en organismos marinos bentónicos

Durante los eventos de hipoxia, los moluscos bivalvos sésiles cierran sus valvas para mantener concentración óptima de oxígeno disuelto en su interior (Kim et al., 2021; Levin et al., 2009), a diferencia de los organismos acuáticos móviles que pueden migrar lejos de las áreas con poco oxígeno. Cuando la duración o exposición severa a eventos de hipoxia superan la tolerancia de los organismos marinos, esto conduce a múltiples efectos negativos, que pueden ser letales y subletales con consecuencias a largo plazo (Breitburg et al., 2018; Hernández-Miranda et al., 2017).

La exposición a hipoxia puede ser de corta duración (horas a días), estacional (semanas a meses), y permanente (Breitburg et al., 2018; Haider et al., 2020; Hernández-Miranda et al., 2017). Los eventos a corto plazo pueden originarse por el ascenso de aguas hipóxicas asociado a procesos de surgencia, o por los ciclos diurnos de fotosíntesis y respiración (Breitburg et al., 2018; Haider et al., 2020). Por ejemplo, en la bahía de

Coliumo, frente a la costa centro-sur de Chile, se ha reportado un evento hipóxico con una duración de 5 días que provocó una mortalidad masiva y varamiento de moluscos bivalvos (Hernández-Miranda et al., 2010; Hernández-Miranda et al., 2017; Hernández-Miranda et al., 2012; Labra et al., 2015). Estacionalmente, por ejemplo, en la bahía de Tongoy se han registrado eventos hipóxicos en noviembre y diciembre, con un importante aumento de la mortalidad de adultos de *Argopecten purpuratus* (>45 mm) (Lagos et al., 2015). La hipoxia permanente ocurre naturalmente en algunos mares y zonas de mínimo oxígeno como cuencas marinas aisladas y fiordos (Breitburg et al., 2018; Greenwood et al., 2010; Haider et al., 2020; Levin et al., 2009). Por ejemplo, en la bahía de Mejillones, ubicada en el norte de Chile, se han registrado valores de oxígeno disuelto inferiores a 0,7 mg L^{-1} a menos de 50 m de profundidad, lo que constituye una barrera química para la distribución y migración vertical de varias especies (Escribano et al., 2000; Valdés & Ortlieb, 2001).

Se ha informado con frecuencia que el estrés por hipoxia y reoxigenación tiene efectos negativos en la fisiología de organismos bentónicos (Follo et al., 2019; Haider et al., 2020; Kim et al., 2021;

Rabalais et al., 2014; Shen et al., 2019; Steckbauer et al., 2015; Tripp-Valdez et al., 2019). Por ejemplo, algunos eventos naturales de hipoxia, como los provocados por la surgencia costera, pueden disminuir la supervivencia, causar mortalidad masiva y provocar varamientos a gran escala. (Breitburg et al., 2018; Chu et al., 2018; Conley et al., 2009; Grantham et al., 2004; Haider et al., 2020; Hernández-Miranda et al., 2010; Hernández-Miranda et al., 2017; Levin et al., 2009; Rabalais et al., 2014; Reed & Harrison, 2016; Yu & Wu, 2006). La hipoxia provocada por alta demanda respiratoria provoca una disminución de las tasas de alimentación y muerte en invertebrados marinos bentónicos (Bell & Eggleston, 2005; Goodman & Campbell, 2007; Roberts et al., 2011). El nivel exacto de oxígeno disuelto que produce efectos negativos sobre la fisiología depende de la especie (Essington & Paulsen, 2010). En consecuencia, debido a las condiciones cambiantes y la no linealidad de los procesos ecológicos, los ecosistemas no vuelven a su estado de perturbación previa de oxígeno disuelto en el agua, incluso si se alivian las condiciones que causaron la desoxigenación inicial (Duarte et al., 2009).

El efecto de la hipoxia puede ser dramático y tener importantes consecuencias para las especies bentónicas que no están adaptadas a superar entornos con baja concentración de oxígeno disuelto durante largos períodos de tiempo (Hernández-Miranda et al., 2017; Rabalais et al., 2014). Por lo tanto, la creciente aparición de hipoxia en aguas costeras se considera un problema medioambiental global y un importante factor de estrés para los organismos acuáticos, afectando a miles de kilómetros cuadrados (Breitburg et al., 2018; Conley et al., 2009; Diaz & Rosenberg, 2008; Gutiérrez et al., 2009; Haider et al., 2020; Rabalais et al., 2014; Yu & Wu, 2006). Además, a finales de este siglo se proyecta una reducción del índice metabólico de la capa superior del océano en un 20% a nivel mundial. Este índice representa la relación entre el oxígeno disponible en el ambiente y la cantidad mínima que un organismo necesita en reposo. Cuando este valor disminuye, se reduce el margen fisiológico necesario para funciones vitales como el movimiento, la alimentación y la reproducción, limitando así la habitabilidad del medio marino (Deutsch et al., 2015).

3. Efecto de la hipoxia en la fisiología de moluscos bivalvos

Los moluscos bivalvos están expuestos con frecuencia a niveles fluctuantes de oxígeno, provocando estrés por hipoxia y reoxigenación en las zonas costeras (Babarro & De Zwaan, 2008; Breitburg et al., 2018; Chu et al., 2018; Diaz & Rosenberg, 2008; Haider et al., 2020; Hill et al., 2012; Kim et al., 2021). Estudios experimentales reportan para *Mytilus edulis* un aumento en la tasa de aclaramiento y de respiración (Gu et al., 2019). La tasa de aclaramiento se define como el volumen de agua filtrada por unidad de tiempo y se calcula mediante la diferencia de concentraciones de microalgas al principio y al final de un período de tiempo en un volumen determinado de agua de mar (Munari et al., 2020). La tasa de respiración se define como la cantidad de oxígeno disuelto consumido en un período de tiempo y se calcula en un respirómetro mediante la diferencia de concentraciones de oxígeno disuelto al principio y al final del período de una hora en un volumen de agua determinado (Wang et al., 2015)

4. Efecto de la hipoxia en las células de moluscos bivalvos

A nivel celular, el efecto por hipoxia-reoxigenación puede producir aumento de la autofagia, el estrés oxidativo y la disminución de la viabilidad celular (Falfushynska et al., 2020; Follo et al., 2019; Haider et al., 2020; Kim et al., 2021; Rabalais et al., 2014; Shen et al., 2019; Steckbauer et al., 2015; Tripp-Valdez et al., 2019). La autofagia es un proceso homeostático mediante el cual la célula degrada su propio contenido (proteínas mutantes y orgánulos defectuosos) mediante enzimas lisosomales como la catepsina D para utilizarlo como fuente de energía (Antunes et al., 2018; Falfushynska et al., 2020; Kroemer et al., 2009; White, 2012). La hipoxia provoca el cierre de las valvas y el cese de la alimentación en los moluscos bivalvos, por lo tanto, la autofagia se utiliza como un mecanismo de tolerancia a la hipoxia en el corto plazo. Sin embargo, cuando la hipoxia es prolongada, se genera una activación de autofagia excesiva y descontrolada provocando la pérdida de moléculas y organelos esenciales y, por consiguiente, una muerte celular autofágica (Peña-Sanoja & De Sanctis, 2013; Ramírez-Sagredo et al., 2016). El estrés oxidativo es el aumento significativo de las moléculas oxidantes sobre las moléculas antioxidantes y para su identificación se utiliza como biomarcador las variantes del grado de peroxidación lipídica, evidenciado

por el aumento en los niveles de malondialdehído (MDA) a nivel de la membrana lipídica en la célula (Moret et al., 2014). La viabilidad celular es el número de células vivas en la hemolinfa que sobreviven a períodos de hipoxia y se puede determinar mediante la adición del colorante Rojo Neutro a los hemocitos, en donde las células vivas tienen la capacidad de retener el colorante y ser teñidas (Borenfreund & Puerner, 1985; Falfushynska et al., 2020; Fang & Trewyn, 2012; King, 2000; Kroemer et al., 2009).

5. Efecto de la hipoxia a nivel molecular en moluscos bivalvos

Estudios a nivel molecular reportan el estrés por hipoxia prolongado produce la detención de la síntesis y el aumento del catabolismo de las proteínas, así también, cambios en el ciclo de la urea y cambios en la expresión de genes asociados a apoptosis, mecanismos de respuesta inflamatoria y neoplasia (Falfushynska et al., 2020; Haider et al., 2020; Kim et al., 2021; Sokolova, 2018; Storey & Storey, 2004). En condiciones de normoxia el gen HIF -1α (factor inducible por hipoxia) funciona como regulador de la homeostasis del oxígeno en los moluscos bivalvos (Huang & Zhou, 2020; Jung-whan et al., 2006). La homeostasis es el conjunto de reacciones coordinadas y automáticas que mantienen la constancia en la

composición y propiedades del medio interno de un organismo (Grijalba-Uche & Echarte, 2015). En condiciones de hipoxia, la transcripción del gen HIF genera cambios en el metabolismo celular como el incremento del catabolismo que consiste en la degradación de proteínas en aminoácidos (Huang & Zhou, 2020; Jung-whan et al., 2006). El metabolismo se define como las reacciones químicas en el interior de la célula para procesar y aprovechar los nutrientes (moléculas orgánicas ingeridas en los alimentos) como fuente de energía (Alonso et al., 2016). Los aminoácidos están compuestos por un grupo amino y un ácido (Haider et al., 2020; Sokolov & Sokolova, 2019). Cuando se agrega una molécula de hidrógeno al grupo amino se forma el amonio, el cual es tóxico (Haider et al., 2020). Este amonio debe ser transformado en urea a través del ciclo de la urea para que pueda ser acumulado en los músculos, siendo un mecanismo de tolerancia a la hipoxia por su menor toxicidad (Haider et al., 2020; Soldatov et al., 2010; Soldatov et al., 2009; Velasco-Martínez et al., 2016). Durante la hipoxia, el aspartato es un aminoácido que sirve como sustrato anaeróbico para la producción de alanina en el citosol y la generación mitocondrial de succinato, importante para la generación de energía a través de ATP (Grieshaber et al., 1994; Haider et al., 2020). En el ciclo de la urea se convierten los iones amonio en urea mediante los

intermediarios ornitina, citrulina, argininosuccinato y arginina (Haider et al., 2020). El exceso de moléculas oxidantes (ROS) producidas durante el metabolismo anaeróbico activa la apoptosis o muerte celular programada, a través de la vía intrínseca regulada por los genes p53 (gen supresor de tumores) y BAX (proteína X asociada a bcl-2) (Falfushynska et al., 2020; Sokolova et al., 2019). El desequilibrio metabólico provoca la activación de la vía extrínseca de apoptosis mediante la caspasa 2 (enzima iniciadora) y la caspasa ejecutora 3 (enzima ejecutora) (Fava et al., 2012; Movassagh & Foo, 2008). El incremento de las moléculas oxidantes (ERO) promueven la activación de la vía inflamatoria a través de la activación del gen TBK1 (proteína Quinasa Serina/treonina) y del factor de transcripción NF-kB (factor nuclear potenciador de las cadenas ligeras kappa de las células B activadas) (Adli et al., 2010; Angelo et al., 2008; Falfushynska et al., 2020; Kaltschmidt et al., 2000; Moret et al., 2014; Thornton et al., 2017). La estimulación de la vía NF-kB promueve la apoptosis (Carella et al., 2015).

Estudios realizados evidencian que la hipoxia tiene poco impacto en la expresión de las proteínas mitocondriales en las células, sin embargo, eleva el contenido de ADNmt (ADN mitocondrial) (Pastukh et al., 2016).

Algunos tipos de células responden a la hipoxia incrementando el número de copias de ADNmt en algunos tejidos, como el cerebro, el hígado, el corazón, la placenta, el esperma y las células sanguíneas, seguido por modificaciones oxidativas en el genoma mitocondrial (en la región del bucle D) (Lacedonia et al., 2015; Luo et al., 2013; Pastukh et al., 2016). Las ROS generadas durante la hipoxia conducen a un daño oxidativo del ADN y a la activación de la reparación por escisión de bases en secuencias promotoras clave (Pastukh et al., 2016). Las lesiones oxidativas del bucle D bajo exposición hipóxica son de carácter transitorio y finalmente son reparadas mediante enzimas de reparación del ADN (Pastukh et al., 2016; Perillo et al., 2008; Pohjoismäki et al., 2012).

6. Respuesta inmune en moluscos bivalvos expuestos a hipoxia y *Vibrio anguillarum*.

El sistema inmune innato de los moluscos bivalvos es el encargado de la defensa del huésped, posee una especificidad limitada, y responde a patógenos y estresores ambientales como la hipoxia (Bouallegui, 2019; Toche, 2012). Se ha determinado que la hipoxia tiene un mayor efecto en la respuesta inmune de los moluscos bivalvos adultos debido a su mayor

capacidad de acumular productos derivados del estrés oxidativo en los hemocitos (Clark et al., 2013). Esta acumulación puede ser tóxica para las células; por lo tanto, la respuesta inmune es generar la producción de moléculas antioxidantes reguladas por los genes catalasa y superóxido dismutasa (Carvajal, 2019; Clark et al., 2013; Echeverri & Mockus, 2008). El *Vibrio anguillarum* es una de las especies de *Vibrio* más peligrosas y es el agente causante de la vibriosis, la cual es devastadora para las empresas mitícolas (Hickey & Lee, 2018). Los esfuerzos para comprender y controlar la virulencia de *V. anguillarum* han sido de alta prioridad entre los estudios internacionales de investigación acuática debido a lo costoso de sus medidas de prevención o tratamiento (Hickey & Lee, 2018). Estos vibrios suelen entrar en la hemolinfa de los moluscos bivalvos cuando las valvas de la concha están abiertas para alimentarse, respirar y excretar residuos (Todgham & Stillman, 2013). El aumento de la temperatura de la superficie del mar y los eventos climáticos que causan una gran escorrentía terrestre provocados por el cambio climático promoverán la abundancia de *V. anguillarum* en las zonas costeras (Hernroth & Baden, 2018). El efecto a través del patógeno bacteriano *Vibrio anguillarum* comienza con la activación del gen LITAF (factor alfa de necrosis tumoral inducido por lipopolisacáridos) en el citoplasma para que se transcriba en

el núcleo y promueva la expresión de citoquinas como TNF-α (factor de necrosis tumoral alfa) (Hickey & Lee, 2018; Li et al., 2012; Zou et al., 2015). Las citoquinas son proteínas cuya función es coordinar la respuesta del sistema inmunológico a través de los hemocitos entre sí para eliminar a los vibrios (Bouallegui, 2019; Hopkins, 2003). La Mitilina b es un péptido antimicrobiano (antibiótico natural con efecto microbicida) que se almacena en los gránulos y se libera hacia la hemolinfa con el objetivo de neutralizar y eliminar el *Vibrio* (Bouallegui, 2019). Cuando existe más de un factor estresante, los organismos responden al tipo y magnitud de sus efectos sincronizados (Todgham & Stillman, 2013). En este caso los organismos utilizan los mismos mecanismos de protección, elevando la tolerancia a un segundo factor o haciéndolo más susceptible (Todgham & Stillman, 2013). Debido a que la hipoxia altera el desarrollo de hemocitos, es posible inferir que en bivalvos expuestos a hipoxia habrá un efecto negativo en la respuesta inmune haciéndolos susceptibles a patógenos. Por ejemplo, algunas especies de *Vibrio* no patógenas que son importantes para la digestión de las algas en bivalvos pueden provocar mortalidad al combinarse con factores de estrés adicionales (Green et al., 2019; Li et al., 2019; Lokmer & Mathias, 2015; Tanaka et al., 2016).

7. Efecto de la hipoxia en el transcriptoma de moluscos bivalvos

En la última década, el desarrollo y aplicación de herramientas transcriptómicas ha revolucionado la comprensión de las respuestas moleculares frente a la hipoxia en organismos no modelo, incluyendo bivalvos (Amorim et al., 2021; Cheng et al., 2024). La transcriptómica permite analizar simultáneamente la expresión de miles de genes, lo que proporciona una visión global de las rutas metabólicas y mecanismos celulares activados o reprimidos en condiciones hipóxicas. Las técnicas de RNA-seq, microarrays y qRT-PCR han sido aplicadas para caracterizar los perfiles transcriptómicos de múltiples especies de bivalvos bajo diferentes regímenes de exposición a hipoxia (Giannetto et al., 2015; Hall et al., 2023). Los resultados revelan una reprogramación génica compleja, especie-específica y dependiente del tejido, tiempo de exposición, intensidad del estrés y condiciones ambientales concomitantes, como la temperatura o la salinidad (Martínez et al., 2023).

La expresión de HIF-1 alfa, un regulador clave de las respuestas a la hipoxia, y de genes asociados con el metabolismo anaeróbico se incrementa en condiciones de hipoxia, mientras que los genes

relacionados con el metabolismo aeróbico y la expresión de hemoglobina disminuyen notablemente (Hatano et al., 2025). A pesar del creciente número de estudios transcriptómicos sobre hipoxia en bivalvos, persisten vacíos importantes en el conocimiento. Muchos trabajos se han enfocado en un número limitado de especies, frecuentemente de interés comercial, lo que limita la extrapolación de resultados a un contexto ecológico más amplio (Wang et al., 2022). Asimismo, existe una heterogeneidad metodológica significativa en términos de diseño experimental, parámetros fisiológicos medidos, tiempos de muestreo y análisis bioinformáticos empleados (Falfushynska et al., 2020). Estas diferencias dificultan la comparación inter-específica y la identificación de patrones transcriptómicos conservados o adaptativos (Steffen et al., 2020). La mayoría de los trabajos se han enfocado en tejidos específicos, como las branquias o el hepatopáncreas, dejando de lado una visión sistémica que integre múltiples órganos o niveles de organización biológica (Wang et al., 2019).

Otro aspecto crítico es la limitada integración de la transcriptómica con otras capas de análisis ómico, como la epigenómica, proteómica y metabolómica, lo que impide una comprensión holística de las respuestas

biológicas frente a la hipoxia (Falfushynska et al., 2020). Asimismo, aún se requiere avanzar en la validación funcional de genes candidatos identificados mediante estudios transcriptómicos, así como en la elucidación de sus interacciones reguladoras y su papel en la fisiología adaptativa (Giannetto et al., 2015). También es escasa la información sobre la heredabilidad y estabilidad transgeneracional de los cambios transcriptómicos inducidos por hipoxia, aspectos clave en un contexto de cambio climático global (Martínez et al., 2023).

En este contexto, el objetivo específico uno de la presente tesis se orienta a caracterizar los mecanismos moleculares implicados en la tolerancia de *M. chilensis* expuestos a condiciones experimentales de hipoxia y etapas de reoxigenación, mediante el análisis comparativo del transcriptoma en branquias, glándula digestiva y músculo aductor, con énfasis en las rutas de señalización asociadas al metabolismo, la respuesta inmune y el estrés del retículo endoplasmático.

8. Efecto de la hipoxia en la microbiota de moluscos bivalvos

Los moluscos bivalvos constituyen un grupo filogenéticamente diverso de invertebrados acuáticos que cumplen funciones ecológicas y

productivas clave en ecosistemas costeros y sistemas de acuicultura. Una de sus características fisiológicas más distintivas es su estrategia trófica por filtración, la cual no solo facilita la captura eficiente de partículas en suspensión, sino que también los expone de manera constante a los cambios fisicoquímicos del ambiente circundante (Kueh & Chan, 1985). Este modo de alimentación promueve el establecimiento de comunidades microbianas complejas en sus tejidos, particularmente en las branquias y el aparato digestivo, configurando un microbioma específico que comprende géneros como *Vibrio*, *Pseudomonas*, *Acinetobacter*, *Photobacterium*, *Moraxella*, *Aeromonas*, *Bacillus*, *Alcaligenes*, *Flavobacterium*, *Cytophaga*, *Spongiobacter*, *Shewanella*, *Escherichia*, *Chromobacterium*, *Desulfovibrio*, *Rhodococcus*, *Microbacterium* y *Micrococcus* (Beleneva et al., 2003; Cavallo et al., 2009; Dunkai et al., 2023; Kueh & Chan, 1985; Li et al., 2018). Esta relación simbiótica es altamente dinámica y está modulada por variables fisiológicas, ontogénicas y ambientales (Beleneva et al., 2003; Cavallo et al., 2009; Dunkai et al., 2023; Li et al., 2018; Paillard et al., 2022; Zannella et al., 2017).

El microbioma cumple funciones esenciales para el hospedador, tales como la digestión de macromoléculas, la biosíntesis de compuestos bioactivos, la inmunomodulación y la defensa frente a agentes patógenos (Hashem, 2025; Kim, 2018; Kogut et al., 2020). En *Crassostrea gigas*, por ejemplo, se ha demostrado que la exposición temprana a ambientes microbianos complejos durante el desarrollo larval contribuye a la maduración del sistema inmunológico mediante mecanismos epigenéticos, fortaleciendo la inmunocompetencia en fases posteriores del ciclo vital (Destoumieux-Garzón et al., 2024). Sin embargo, esta asociación mutualista es especialmente vulnerable a factores ambientales estresantes, siendo la hipoxia uno de los principales disruptores de dicha homeostasis (Pollock et al., 2007).

Aunque los bivalvos presentan una tolerancia fisiológica moderada a condiciones hipóxicas en comparación con otros organismos bentónicos, esta situación puede desencadenar una serie de efectos deletéreos sobre el metabolismo del hospedador (Song et al., 2024; Vaquer-Sunyer & Duarte, 2008). Entre ellos se encuentran la disminución de la tasa de filtración, la reprogramación del metabolismo energético hacia rutas anaeróbicas, la inmunosupresión y, en casos severos, la mortalidad (Song et al., 2024;

Vaquer-Sunyer & Duarte, 2008). La susceptibilidad a la hipoxia varía significativamente entre especies, y está influenciada por el tamaño corporal, la fisiología interna y el estadio de desarrollo del organismo. En este contexto, estudios realizados en *Argopecten irradians*, *Crassostrea virginica*, *Mytilus edulis* y *Mercenaria mercenaria* han evidenciado patrones divergentes de tolerancia a la hipoxia, destacando la necesidad de abordajes específicos por especie (Mizutani et al., 2025; Stevens & Gobler, 2018).

Además del impacto sobre el hospedador, la hipoxia impone una presión selectiva directa sobre las comunidades microbianas del agua, sedimentos y tejidos de los moluscos (Mizutani et al., 2025). Investigaciones recientes en *Anadara kagoshimensis* han demostrado que esta condición ambiental altera de forma significativa la composición bacteriana, con un aumento en la abundancia de familias como Arcobacteraceae y Alkalispirochaetaceae en branquias, y Metamycoplasmataceae en el hepatopáncreas (Mizutani et al., 2025). Este último órgano, clave en el metabolismo y la inmunidad, mostró una marcada sensibilidad a la hipoxia, presentando rutas metabólicas asociadas a la reducción de sulfato y respiración del hierro, lo que sugiere

una reconfiguración funcional adaptativa (Mizutani et al., 2025). En *C. virginica*, se ha documentado un incremento en la diversidad y carga bacteriana en condiciones hipóxicas, incluyendo especies potencialmente patógenas como *Vibrio vulnificus*, lo cual apunta a un estado de disbiosis con implicancias clínicas relevantes (Khan et al., 2018). Asimismo, se ha vinculado la exposición prolongada a hipoxia con una mayor susceptibilidad a infecciones por *Perkinsus marinus*, como resultado de una respuesta inmunológica comprometida (Breitburg et al., 2015; Keppel et al., 2015).

Desde un enfoque holístico, el concepto de holobionte —entendido como la unidad funcional integrada por el hospedador y su microbiota asociada— ofrece un marco teórico robusto para interpretar la complejidad de estas interacciones (Lasa & Romalde, 2021). La estabilidad funcional del holobionte en bivalvos depende de la resiliencia de su microbiota frente a perturbaciones ambientales (Dittami et al., 2021). La hipoxia, al inducir el desplazamiento de taxa aerobios por anaerobios facultativos, puede alterar profundamente funciones simbióticas clave, tales como la digestión, la síntesis de metabolitos inmunomoduladores y la inhibición competitiva de patógenos.

A pesar de los avances recientes en la caracterización del microbioma de moluscos bivalvos, persiste una importante brecha de conocimiento respecto a los efectos específicos de la hipoxia sobre la composición, funcionalidad y estabilidad de estas comunidades microbianas. Esta limitación obstaculiza el desarrollo de modelos predictivos precisos para evaluar la respuesta del holobionte frente a escenarios de cambio ambiental, así como la implementación de estrategias acuícolas basadas en la manipulación dirigida del microbioma. En este contexto, el objetivo específico dos de la presente tesis se orienta a evaluar el impacto del estrés hipóxico en la composición, estructura y potencial funcional de las comunidades microbianas asociadas a las branquias y la glándula digestiva de *M. chilensis*, mediante secuenciación directa del ADN mediante tecnología Oxford Nanopore y análisis funcional, para identificar cambios microbianos relevantes para la homeostasis del hospedador bajo condiciones de oxigenación fluctuante.

9. Efecto de la hipoxia en el epitranscriptoma de moluscos bivalvos

La regulación de la expresión génica en eucariotas es un proceso complejo que no se limita exclusivamente al control transcripcional, sino que incluye una amplia gama de mecanismos postranscripcionales capaces de modular la estabilidad, localización, procesamiento y traducción de los transcritos (Chokkalla et al., 2020). En este contexto, la epitranscriptómica ha emergido como un campo de estudio innovador que examina las modificaciones químicas reversibles que ocurren en los ácidos ribonucleicos (ARN), sin alterar la secuencia nucleotídica subyacente (Boo & Kim, 2020; Chokkalla et al., 2020; Gatsiou & Stellos, 2018; Radbakhsh et al., 2025). Estas modificaciones, conocidas colectivamente como marcas epitranscriptómicas, constituyen una capa adicional de regulación génica de gran dinamismo y especificidad, permitiendo una respuesta celular rápida frente a señales ambientales y endógenas sin necesidad de transcripción génica de novo.

Actualmente, se han identificado más de 170 modificaciones postranscripcionales distribuidas entre diversas clases de ARN, entre las que destacan la N6-metiladenosina (m^6A), 5-metilcitosina (m^5C), 7-

metilguanosina (m^7G), 1-metiladenosina (m^1A), pseudouridina (Ψ), acetilación en C4 de citidina (ac4C) y 2′-O-metilación de ribosa (2′-O-Me) (Boccaletto et al., 2018; Jung & Goldman, 2018; Radbakhsh et al., 2025). Estas modificaciones están reguladas por un sistema enzimático dinámico compuesto por "escritores", que catalizan la adición de marcas químicas; "lectores", que reconocen e interpretan estas modificaciones modulando procesos como splicing, traducción y degradación del ARN; y "borradores", encargados de remover dichas marcas, permitiendo una regulación reversible y específica en tiempo y espacio (Radbakhsh et al., 2025; Yang et al., 2018). Esta compleja maquinaria de regulación ha sido asociada con múltiples procesos fisiológicos, incluyendo diferenciación celular, desarrollo embrionario, plasticidad neuronal, respuestas inmunológicas, y adaptación al estrés (Alkhammash, 2025; Chokkalla et al., 2020; Gatsiou & Stellos, 2018; Kumar & Mohapatra, 2021; Radbakhsh et al., 2025).

En organismos modelo como mamíferos, peces y plantas, la epitranscriptómica ha demostrado ser sensible a condiciones de estrés ambiental tales como temperatura extrema, radiación UV, estrés oxidativo y, particularmente, hipoxia (Hu et al., 2022; Yang & Chen, 2021). La

exposición a ambientes con bajo oxígeno desencadena reprogramaciones rápidas en los patrones de modificación del ARN, posibilitando una adaptación celular eficiente sin requerir nuevos eventos transcripcionales. Esta plasticidad regulatoria representa una ventaja adaptativa sustancial frente a fluctuaciones ambientales agudas o crónicas, facilitando la homeostasis celular en condiciones adversas (Park et al., 2020).

Sin embargo, a pesar del creciente cuerpo de conocimiento en modelos experimentales clásicos, el estudio de la epitranscriptómica en invertebrados marinos continúa siendo incipiente (Du et al., 2025; Frye et al., 2016; Gilbert et al., 2016; Nishikura, 2016; Patil et al., 2018; Roundtree et al., 2017). Dentro de este grupo, los moluscos bivalvos representan un modelo de estudio particularmente relevante debido a su estilo de vida bentónico y su exposición constante a condiciones ambientales variables, tales como cambios en temperatura, salinidad, pH y niveles de oxígeno disuelto (Liao et al., 2025; Sleight et al., 2025). Específicamente, *M. chilensis*, una especie clave para la acuicultura en el cono sur, se ve frecuentemente sometida a episodios de hipoxia en zonas costeras y estuarinas con alta carga orgánica o influencias antropogénicas (León-Muñoz et al., 2021). A pesar de la importancia ecológica y

económica de esta especie, los mecanismos moleculares que subyacen a su tolerancia hipóxica, y en particular el papel de la epitranscriptómica en este proceso, permanecen sin caracterizar.

Uno de los principales obstáculos históricos en la investigación epitranscriptómica ha sido la falta de metodologías capaces de detectar de manera precisa y sensible estas modificaciones a escala de nucleótido (Cerneckis et al., 2024). No obstante, avances recientes en tecnologías de secuenciación directa de ARN, particularmente mediante plataformas como Oxford Nanopore Technologies, junto con algoritmos bioinformáticos especializados, han permitido el mapeo sistemático de modificaciones epitranscriptómicas en organismos no modelo (Cerneckis et al., 2024; Gatsiou & Stellos, 2018; Gilbert et al., 2016; Roundtree et al., 2017; Zhang et al., 2018). Estos avances han impulsado el reconocimiento del campo, culminando con la concesión del Premio Nobel de Fisiología o Medicina 2023 a Katalin Karikó y Drew Weissman por sus descubrimientos sobre las modificaciones del ARNm y su impacto en la inmunogenicidad y traducción (Karikó et al., 2005; Karikó et al., 2008; Kumar & Mohapatra, 2021; Liu et al., 2025; Nance & Meier, 2021). Estas herramientas posibilitan una caracterización integral del epitranscriptoma

bajo diferentes condiciones fisiológicas y ambientales, incluyendo estrés hipóxico.

En este contexto, el objetivo específico tres de la presente tesis se orienta a Caracterizar el epitranscriptoma de *M. chilensis* mediante secuenciación directa de ARN utilizando tecnología Oxford Nanopore, con el fin de obtener una visión integral de las modificaciones post-transcripcionales, incluyendo tanto modificaciones químicas de nucleótidos como m^6A y m^5C, como la caracterización estructural del ARN a través del análisis de la longitud de las colas poliadeniladas y la identificación de transcritos de longitud completa.

10. *M. chilensis* como modelo de estudio

Mytilus chilensis, comúnmente llamado chorito, es un molusco bivalvo filtrador, con una talla mínima de extracción de 5 cm y tamaños máximos de 8 cm (Subpesca, 2021). Sexualmente son gonocóricos (con sexos separados) con fecundación externa y dimorfismo sexual interno (Oyarzún et al., 2011). El macho presenta la gónada color amarillo

cremoso, y la hembra un tono anaranjado (Oyarzún et al., 2011). Mediante sus palpos bucales es capaz de separar los alimentos que no va a ingerir, y al generar pseudofecas puede eliminar el material capturado sin ingerir (Salas-Yanquin et al., 2018). Posee branquias desarrolladas que intervienen en la alimentación y la respiración (Puerta, 1995). En condiciones normales, un mejillón adulto filtra de 4 a 5 litros de agua por hora (Puerta, 1995). Se distribuye desde la costa del Océano Pacífico en Chile central hasta la costa de la Patagonia Argentina en el Atlántico (Navarro et al., 2016; Ríos et al., 2018). Es capaz de vivir en un amplio rango de salinidad, destacándose una alta abundancia en fiordos (Osores et al., 2017; Taraska & Anne, 2013). Se considera un recurso marino importante para el ecosistema en virtud de ser fuente vital de alimento, y proporcionar servicios ecológicos (Osores et al., 2017; Scanes et al., 2021). La sobreexplotación de este recurso trajo consigo un aumento en su valor comercial. Esto significó un estímulo para aumentar la producción de choritos a través del cultivo, debido al menor tiempo de crecimiento en sistemas suspendidos (IFOP, 2000). Comenzando con la captación de semilla en su medio natural, luego son transportadas hasta las concesiones de acuicultura para el proceso de engorde hasta alcanzar la talla comercial, donde son procesados para su comercialización (IFOP,

2000). En Chile la actividad miticultora genera 17.000 empleos y representa el 25% del total de las cosechas acuícolas, convirtiéndola en el tercer productor de moluscos a nivel mundial por debajo de China y Corea del Sur (Blanc et al., 2018; Lohrmann et al., 2019; Subpesca, 2019; Yevenes et al., 2019). En los últimos años la producción de choritos se ha incrementado alcanzando la producción de 399 millones de toneladas, equivalente a más de 200 millones de dólares en exportaciones dirigidas en su mayor parte a Europa (Blanc et al., 2018; FAO, 2018; IFOP, 2000; Lohrmann et al., 2019; Subpesca, 2019). La captación de semilla de chorito se concentra en el fiordo de Reloncaví y la engorda se realiza en sistemas de cultivos ubicados en la Isla de Chiloé, Región de Los Lagos (Yevenes et al., 2019). En ambas zonas se producen eventos de hipoxia que son provocados principalmente por la surgencia y la eutrofización (Silva & Vargas, 2014). La eutrofización es provocada principalmente por efecto de la actividad acuícola y por la baja tasa de recambio de agua en la zona (Daneri et al., 2012; Mardones et al., 2021; Montero et al., 2011; Silva & Vargas, 2014).

El mar interior de Chiloé alberga la totalidad de la industria de chorito, sin embargo, esta región se ve cada vez más afectada por eventos

ambientales relacionados tanto con la variabilidad climática como con la influencia humana (Narváez et al., 2019). La elevada variabilidad del oxígeno disuelto puede tener importantes implicaciones para la adaptación local de las poblaciones marinas ante los cambios en las condiciones oceánicas (Vargas et al., 2017), y justifica una investigación a nivel experimental de los choritos, para evaluar la capacidad de adaptación ante la variabilidad de las condiciones ambientales a diferentes escalas espaciales y temporales (Narváez et al., 2019). Por lo tanto, una mejor comprensión de la respuesta del chorito a condiciones experimentales de hipoxia es relevante para tenerse en cuenta en la gestión y planificación de la industria acuícola en el contexto de los futuros escenarios climáticos en esta región altamente productiva y socioeconómicamente importante (Narváez et al., 2019).

Debido a las alteraciones en condiciones ambientales derivadas del cambio climático y a la importancia de *M. chilensis* en la producción acuícola de Chile y en el ecosistema, este estudio busca determinar la medida en que la hipoxia costera influye en la alteración del transcriptoma, el microbioma y el epitranscriptoma del chorito.

HIPÓTESIS

H1: El estrés ambiental en *M. chilensis* producido por la hipoxia genera una modulación a nivel transcriptómico asociada con cambios epitranscriptómicos y en la comunidad microbiológica de los organismos expuestos a bajos niveles de oxígeno disuelto.

OBJETIVOS

Objetivo general

Analizar las respuestas a nivel de transcriptoma, microbiota y epitranscriptoma de *Mytilus chilensis* expuesto a condiciones de hipoxia.

Objetivos específicos

1. Caracterizar los mecanismos moleculares implicados en la tolerancia de *M. chilensis* expuestos a condiciones experimentales de hipoxia y etapas de reoxigenación, mediante el análisis comparativo del transcriptoma en branquias, glándula digestiva y

músculo aductor, con énfasis en las rutas de señalización asociadas al metabolismo, la respuesta inmune y el estrés del retículo endoplasmático.

2. Evaluar el impacto del estrés hipóxico en la composición, estructura y potencial funcional de las comunidades microbianas asociadas a las branquias y la glándula digestiva de *M. chilensis*, utilizando secuenciación directa del ADN con tecnología Oxford Nanopore y análisis funcional, para identificar cambios microbianos relevantes para la homeostasis del hospedador bajo condiciones de oxigenación fluctuante.
3. Caracterizar el epitranscriptoma de *M. chilensis* mediante secuenciación directa de ARN utilizando tecnología Oxford Nanopore, con el fin de obtener una visión integral de las modificaciones post-transcripcionales, incluyendo tanto modificaciones químicas de nucleótidos como m^6A y m^5C, como la caracterización estructural del ARN a través del análisis de la longitud de las colas poliadeniladas y la identificación de transcritos de longitud completa

METODOLOGÍA

La comprensión de las respuestas fisiológicas y microbiológicas de los bivalvos marinos frente al estrés hipóxico constituye un eje central en la evaluación de los impactos derivados del cambio climático y la eutrofización en ecosistemas costeros, especialmente en aquellas especies con relevancia para la acuicultura. A pesar de que múltiples estudios han documentado los efectos de la hipoxia aguda, con exposiciones que varían entre 15 minutos y 36 horas, así como los procesos subsecuentes de reoxigenación de entre 10 minutos y 24 horas, persiste una importante brecha de conocimiento en torno a las consecuencias fisiológicas y ecológicas de exposiciones crónicas a concentraciones persistentemente bajas de oxígeno disuelto (Adzigbli et al., 2024; Adzigbli et al., 2022; Amorim et al., 2021; Falfushynska et al., 2020; Haider et al., 2020; Ivanina & Sokolova, 2016; Liu et al., 2024; Sokolov et al., 2019; Steffen et al., 2020). Esta laguna reviste especial gravedad considerando que en ambientes litorales se han registrado eventos hipóxicos prolongados, con duraciones de hasta seis días e incluso 25 días en condiciones extremas, lo que pone de relieve la urgencia de incorporar estos escenarios prolongados en los esquemas experimentales destinados a comprender las estrategias adaptativas y de tolerancia desarrolladas por los bivalvos frente

a dichos desafíos ambientales (Haider et al., 2020; Li et al., 2014; Linford et al., 2024; Yang et al., 2023; Yang et al., 2020).

Bajo este marco, el presente estudio fue concebido para evaluar los efectos de la hipoxia progresiva de largo plazo, superando las limitaciones metodológicas de los enfoques convencionales centrados en eventos hipóxicos agudos (Yang et al., 2023). El diseño experimental se basó en condiciones ambientales reales observadas en los fiordos del sur de Chile, caracterizados por su morfología compleja, e intercambio hidrodinámico limitado como lo indica un tiempo de residencia del agua cercano a los 98 días en el fiordo de Reloncaví (Calvete & Sobarzo, 2011; Cáceres et al., 2002; Silva & Vargas, 2014). Con el propósito de reproducir estas condiciones de manera realista, se emplearon coeficientes de marea obtenidos de fuentes públicas (https://tablademareas.com, consultado el 7 de marzo de 2022), que reflejan las fluctuaciones en la amplitud de las mareas dentro del área de estudio durante aproximadamente 10 días. Esta aproximación metodológica ofrece una plataforma sólida para la investigación de los mecanismos de resiliencia fisiológica y de reconfiguración microbiana que emergen en bivalvos sometidos a

condiciones hipóxicas prolongadas, proporcionando así una visión más integral de su capacidad adaptativa en entornos costeros vulnerables.

Objetivo 1. Caracterizar los mecanismos moleculares implicados en la tolerancia de *M. chilensis* expuestos a condiciones experimentales de hipoxia y etapas de reoxigenación, mediante el análisis comparativo del transcriptoma en branquias, glándula digestiva y músculo aductor, con énfasis en las rutas de señalización asociadas al metabolismo, la respuesta inmune y el estrés del retículo endoplasmático.

Aclimatación de los ejemplares de *M. chilensis*

Durante el mes de abril de 2022, se recolectaron especímenes adultos de chorito en bancos naturales de Puerto Montt, Chile, registrando una longitud valvar promedio de 6,26 ± 0,50 cm y un peso fresco medio de 18,57 ± 3,85 g. Los individuos fueron trasladados en condiciones controladas a la Estación de Biología Marina de Dichato, dependiente de la Universidad de Concepción. Antes del inicio de los ensayos experimentales, se realizó una rigurosa selección morfológica,

excluyéndose aquellos individuos que presentaban fracturas en las valvas o evidencia de epibiosis. Posteriormente, se efectuó una limpieza mecánica para eliminar organismos incrustantes y otras formas de biofouling adheridas a las conchas.

Los ejemplares fueron sometidos a un periodo de aclimatación de 38 días en un sistema de recirculación cerrado, empleando un tanque de fibra de vidrio con capacidad de 7 m^3, bajo condiciones fisicoquímicas estándar: temperatura de 12,5 ± 0,94 °C, salinidad de 34,5 ± 0,32 unidades prácticas de salinidad (UPS), pH de 7,2 ± 0,12 y concentración de oxígeno disuelto de 7,5 ± 1,11 mg/L. Estos parámetros fueron monitorizados diariamente mediante una sonda multiparamétrica HI9829 (Hanna Instruments®). La alimentación se llevó a cabo mediante suministro pasivo diario de una mezcla de microalgas (*Isochrysis sp.* y *Pavlova sp.*), complementada con una renovación del 80 % del volumen total de agua cada 24 horas, a fin de mantener condiciones óptimas de calidad ambiental. Conforme a la normativa nacional vigente, *M. chilensis* no se encuentra categorizada bajo ninguna condición de conservación por la UICN, por lo cual no fue necesario gestionar permisos específicos para su recolección y manipulación.

Diseño experimental

El diseño experimental se basó en un modelo de series temporales de oxígeno disuelto, con el objetivo de simular las fluctuaciones naturales de OD observadas en bancos de cultivo del sur de Chile (Narváez et al., 2019). Finalizado el periodo de aclimatación, un total de 480 individuos fueron asignados aleatoriamente a dos condiciones experimentales con tres réplicas por tratamiento (n = 80 individuos/réplica):

1. Grupo Control (Normoxia): Tres réplicas (N1, N2 y N3) mantenidas bajo niveles normales de OD (7,2 ± 0,2 mg/L).

2. Grupo Experimental (Hipoxia): Tres réplicas (H1, H2 y H3) expuestas a condiciones de hipoxia controlada (2,0 mg/L de OD).

Las condiciones experimentales de temperatura (12,5 ± 1 °C) y salinidad (34,5 ± 0,5 UPS) se mantuvieron constantes durante toda la fase de exposición. En el tratamiento hipóxico, se aplicó diariamente una inyección controlada de burbujas de nitrógeno para alcanzar y mantener la concentración deseada de OD (2,0 mg/L) en el sistema de recirculación.

Preparación de muestras para secuenciación del transcriptoma

Se recolectaron muestras de ARN total a partir de tres tipos de tejido: branquias, glándula digestiva y músculo aductor, obtenidas en distintos intervalos temporales tanto del grupo control como del grupo expuesto a hipoxia. Se extrajeron tres muestras biológicas independientes por tipo de tejido, condición experimental y punto temporal. Todos los tejidos, incluyendo el líquido extrapalial, fueron congelados inmediatamente a −80 °C para su posterior procesamiento.

Extracción de ARN y Preparación de la Biblioteca

Para la secuenciación del transcriptoma, se tomaron muestras de tejidos de las branquias, la glándula digestiva y el músculo aductor de los grupos de control y expuestos a hipoxia a los 10, 20, 40, 50 y 60 días. Los tejidos se almacenaron en RNA Later (Ambion, Austin, TX, EE. UU.) a −80 °C hasta la extracción del ARN. Las extracciones de ARN se realizaron por triplicado para cada grupo experimental utilizando el reactivo Trizol (Invitrogen, Carlsbad, CA, EE. UU.) de acuerdo con las instrucciones del fabricante. Se crearon grupos de 9 individuos para cada réplica. La concentración de ARN extraído se midió utilizando el

instrumento QUBIT 4 (Thermo Fisher Scientific, Pittsburgh, Pensilvania, EE. UU.), y la calidad se determinó utilizando el instrumento TapeStation 2200 (Agilent Technologies Inc., Santa Clara, California, EE. UU.). Las bibliotecas de ADNc de doble cadena se prepararon utilizando el kit TruSeq RNA Sample Preparation Kit v2 (Illumina®, San Diego, CA, EE. UU.), siguiendo las instrucciones del fabricante, utilizando 1 μg de ARN tisular por grupo. Cada una de las tres réplicas biológicas por grupo experimental se envió a la República de Corea, donde Macrogen, Inc. realizó la secuenciación del transcriptoma de novo utilizando la plataforma Illumina. El tipo de lectura fue paired-end, con una longitud de lectura de 101.

Análisis transcriptómico y anotación funcional

Las lecturas obtenidas fueron sometidas a un proceso de control de calidad y eliminación de adaptadores mediante el software CLC GenomicWorkbench v23 (Qiagen Bioinformatics, Redwood City, CA, EE. UU.), utilizando un umbral de calidad de 20, longitud mínima de lectura de 50 pb y ventana deslizante de 4 pb, con recorte en ambos extremos. La cuantificación de la expresión génica se basó en valores normalizados de TPM. La asignación se realizó sobre el genoma V1 de *M.*

chilensis. Se utilizó distancia Euclidiana para la construcción de la matriz de expresión y agrupamiento k-means con 5-6 iteraciones.

Las transcripciones con un cambio relativo >|2| y un valor $p < 0.05$ se consideraron diferencialmente expresadas. Los valores p fueron corregidos para múltiples comparaciones mediante la tasa de descubrimientos falsos (False Discovery Rate, FDR), de modo que se controla la proporción esperada de falsos positivos entre los hallazgos declarados significativos (Korthauer et al., 2019; Pawitan et al., 2005; Storey & Tibshirani, 2003). Las anotaciones funcionales se realizaron utilizando BLAST contra bases de datos Nr, Nt, eggNOG, Pfam, Swiss-Prot, GO, KO y KEGG, con un valor de corte de 1×10^{-5} (Aleksander et al., 2023; Altschul et al., 1998; Bateman et al., 2022; Kanehisa et al., 2022; Tatusov et al., 2001). Posteriormente, los transcritos fueron organizados en matrices de Excel, filtrados y clasificados para generar mapas de calor con TBtools v2.007. Se construyeron diagramas de Venn con la herramienta en línea Venny.

El análisis de enriquecimiento de términos GO se efectuó mediante ShinyGO, empleando listas de genes y anotaciones GO obtenidas desde TBtools. Se utilizó un umbral FDR de 0,05, y se aplicaron funciones para

reducir redundancia y abreviar vías funcionales. La representación gráfica se realizó con ggplot2 (R). Para los mapas de calor, se utilizó agrupamiento jerárquico y medidas de distancia Euclidiana. La selección de genes se basó en criterios de expresión diferencial, relevancia fisiológica y asociación con rutas biológicas clave.

Análisis de la Expresión Génica Cromosómica (CGE)

Los datos sin procesar fueron alineados al genoma V1 de *M. chilensis* para estimar el índice de expresión génica cromosómica (CGE), siguiendo la metodología descrita en investigaciones previas (Gallardo-Escarate et al., 2023; Valenzuela-Muñoz et al., 2022). El CGE evalúa la variabilidad transcripcional entre condiciones normóxicas e hipóxicas, estimando la cobertura media de transcripción en regiones cromosómicas específicas. Se emplearon ventanas móviles de cinco posiciones con un rango de umbral de 2.000 a 100.000 lecturas. Los cálculos se realizaron con la herramienta Graph Threshold Areas del software CLC GenomicsWorkbench v23. Aquellos cromosomas con valores de CGE superiores al 60 % fueron visualizados con Circo (versión 0.69-9), incorporando mapas de cobertura de transcripción para cada condición experimental (Cui et al., 2021).

Disponibilidad de los Datos

Los datos del transcriptoma para el análisis del ARNm se depositaron en la base de datos NCBI-SRA (Sequence Read Archive) con el número de acceso PRJNA1099139.

Objetivo 2. Evaluar el impacto del estrés hipóxico en la composición, estructura y potencial funcional de las comunidades microbianas asociadas a las branquias y la glándula digestiva de *M. chilensis*, utilizando secuenciación directa del ADN con tecnología Oxford Nanopore y análisis funcional, con el fin de identificar cambios microbianos relevantes para la homeostasis del hospedador bajo condiciones de oxigenación fluctuante.

Diseño Experimental (Aclimatación de *M. chilensis*, Exposición a Hipoxia y Muestreo para Análisis Microbiológico)

Este estudio se estructuró bajo un enfoque experimental controlado, orientado a evaluar los efectos sistémicos de la hipoxia y la reoxigenación prolongada en *M. chilensis*, con especial énfasis en las alteraciones microbiológicas de los tejidos branquiales y de la glándula digestiva. El

experimento, de 50 días de duración, consistió en fases alternas de hipoxia (2,0 mg/L de oxígeno disuelto) y normoxia (7,2 ± 0,2 mg/L). A partir de una población inicial de 480 individuos, se seleccionaron 36 ejemplares que fueron distribuidos aleatoriamente en tres réplicas experimentales (n = 12 individuos por réplica). La duración de cada fase hipóxica se definió con base en protocolos metodológicos previamente establecidos.

El régimen de muestreo fue estructurado para captar la dinámica temporal de la microbiota. Se recolectaron muestras de branquias y glándulas digestivas de tres mejillones por réplica en condiciones hipóxicas en el día 10 (n = 9), en normoxia tras reoxigenación en los días 20 (n = 9) y 40 (n = 9), y nuevamente bajo hipoxia el día 50 (n = 9). En total, se analizaron 18 muestras provenientes de condiciones hipóxicas y 18 correspondientes a condiciones de reoxigenación. No se incluyó un grupo control adicional, dado que el diseño comparativo entre fases hipóxicas y normóxicas respondió al objetivo de evaluar directamente los efectos de la fluctuación de oxígeno sobre la microbiota. La inclusión de múltiples puntos temporales permitió detectar alteraciones progresivas y acumulativas, fundamentales en escenarios de cambio climático y eutrofización.

El oxígeno disuelto fue monitoreado y ajustado diariamente mediante inyección de nitrógeno en el sistema de recirculación para mantener los niveles deseados. Se priorizó el análisis de tejidos branquiales por su rol en la respiración, alimentación por filtración y su alta exposición a factores ambientales (Mardones et al., 2024; Sun et al., 2024). La glándula digestiva se seleccionó por su relevancia en la digestión, metabolismo e inmunorrespuesta (Borkovic-Mitic et al., 2013; Sforzini et al., 2018). Bajo hipoxia, el cierre valvar reduce la filtración y respiración, lo que puede inducir disbiosis (Porter & Porter, 2018; Tang & Riisgård, 2018). El objetivo buscó identificar patrones microbianos perturbados como posibles biomarcadores del estrés hipóxico.

Para minimizar la variabilidad interindividual, se agruparon tejidos de tres individuos por réplica, lo que generó muestras representativas de nueve mejillones por condición experimental (Sun et al., 2020). Las muestras se conservaron en etanol grado molecular, transportadas a 4 °C y almacenadas a −80 °C hasta su procesamiento.

Aislamiento de ADN y Amplificación del gen 16S rRNA

El ADN bacteriano total se extrajo de tejidos homogeneizados de branquias y glándulas digestivas mediante el protocolo fenol-cloroformo. Se utilizaron entre 20 y 30 mg de tejido por muestra (n = 9 por tratamiento), que fueron descongelados, lavados, picados y homogeneizados con perlas cerámicas en vórtex. Se adicionó 1 mL de tampón de lisis (10 mM Tris-HCl, 400 mM NaCl, 100 mM EDTA, 0.4 % SDS y 100 µg/mL proteinasa K, pH 8.0) e incubado a 37 °C durante 2 h (Valenzuela-Miranda et al., 2024). Posteriormente, se realizaron extracciones sucesivas con fenol-cloroformo y cloroformo puro, seguidas de una precipitación con etanol absoluto. La fase acuosa purificada fue transferida a columnas DNeasy Blood and Tissue (Qiagen®) para completar la extracción.

La calidad y pureza del ADN se evaluaron con espectrofotometría (Nanodrop One), su integridad mediante electroforesis en gel de agarosa al 1 % (tampón TAE) y la concentración por fluorometría (Qubit 4) utilizando el kit dsDNA BR. Para la amplificación del gen 16S rRNA se emplearon 50 ng/µL de ADN como molde en reacciones de 25 µL con

LongAmp Taq DNA Polimerasa (New England Biolabs®) y cebadores universales 27F y 1492R (Valenzuela-Miranda et al., 2024). Las condiciones térmicas incluyeron desnaturalización inicial a 95 °C (1 min), 25 ciclos de 95 °C (20 s), 56 °C (30 s), 65 °C (2 min), y extensión final a 65 °C (5 min). La amplificación se confirmó por electroforesis en gel de agarosa al 1.2 %.

Preparación de la Biblioteca y Secuenciación Nanopore

Los amplicones generados se purificaron con perlas Agencourt AMPure XP para eliminar productos no específicos y cuantificados mediante Qubit 4. Las bibliotecas fueron construidas con el kit 16S Barcoding Kit (SQK-16S024, Oxford Nanopore Technologies®) conforme a las instrucciones del fabricante. Los amplicones fueron codificados por PCR adicional y purificados. La calidad y distribución de tamaño fueron verificadas en TapeStation 2200 (Agilent®) con DNA ScreenTape. La concentración final fue validada con D5000 ScreenTape.

Se incluyó un control estándar (ZymoBiomics® Microbial Community Standard) para asegurar calidad y reproducibilidad. Las bibliotecas se normalizaron equimolarmente, agrupadas para multiplexación y cargadas en una celda de flujo Spot-ON para

secuenciación en la plataforma MinION (Oxford Nanopore Technologies®). La ejecución y rendimiento fueron monitoreados en tiempo real mediante MinKNOW (versión 5.8.12).

Procesamiento de Datos y Asignación Taxonómica

Las lecturas se sometieron a basecalling con Guppy (v6.3.2) y filtrado por calidad ($Q \geq 7$). Se empleó Porechop para eliminación de adaptadores y demultiplexación (Bonenfant et al., 2023). Las lecturas clasificadas se analizaron con el algoritmo Emu, optimizado para secuencias completas de 16S rRNA generadas por secuenciación Nanopore (Curry et al., 2022). Se utilizó una base de datos personalizada y se estableció un umbral mínimo de abundancia de 0.01. Las lecturas fueron agrupadas en unidades taxonómicas operativas (OTU) con un umbral de similitud del 97 %.

Perfilado de la Comunidad y Análisis Estadístico

Las tablas OTU se analizaron en MicrobiomeAnalyst v2.0. Se eliminaron OTU únicas, se aplicó transformación logarítmica y se generaron análisis de coordenadas principales (PCoA) utilizando la distancia Bray-Curtis. Se

realizaron pruebas ANOSIM para evaluar diferencias entre grupos y curvas de rarefacción con el paquete Vegan de R (Dixon, 2003).

Visualización del Árbol de Calor

Los datos se analizaron en R (v4.3.3) mediante los paquetes Metacoder, Dplyr y Vegan (Beckerman et al., 2017; Dixon, 2003). Se eliminaron taxa con <5 lecturas y aquellos sin presencia en al menos el 20 % de las muestras. Se generaron árboles de calor jerárquicos, estructurando la jerarquía taxonómica con taxmap. Los nodos fueron dimensionados por abundancia y coloreados según diferencias estadísticas entre condiciones.

Análisis Discriminante Lineal (LEfSe) y Redes de Correlación

Se aplicó LEfSe para identificar taxa diferenciales (FDR <0.05; LDA ≥4.0). Las 15 características discriminativas principales se visualizaron mediante gráficos de puntos. Las redes de coocurrencia se construyeron con SparCC (100 permutaciones, $p < 0.05$, $r \geq 0.3$).

Predicción del Potencial Funcional Metagenómico

Se utilizó PICRUSt2 y el paquete ggpicrust2 para inferencias funcionales a partir de regiones V3-V4 extraídas con HyperEx (Douglas et al., 2020). Se empleó la base MetaCyc para construcción de vías y el uso del software R v4.3.3 para visualización (Caspi et al., 2016). Se aplicó STAMP con corrección FDR de Benjamini-Hochberg (FDR <0,05), seleccionando vías con ≥0,5 % de abundancia relativa (Parks et al., 2014).

Disponibilidad de los Datos

Los datos de secuenciación Nanopore se encuentran disponibles en la base NCBI-SRA bajo el número de acceso BioProject RJNA1240298.

Objetivo 3. Caracterizar el epitranscriptoma de *M. chilensis* mediante secuenciación directa de ARN utilizando tecnología Oxford Nanopore, con el fin de obtener una visión integral de las modificaciones post-transcripcionales, incluyendo tanto modificaciones químicas de nucleótidos como m^6A y m^5C, como la caracterización estructural del ARN a través del análisis de la longitud de las colas poliadeniladas y la identificación de transcritos de longitud completa.

Preparación de Bibliotecas de ARN Directo

Este estudio empleó una aproximación metodológica avanzada basada en la secuenciación directa de ARN de molécula única, utilizando la plataforma Nanopore (Oxford Nanopore Technologies®) (Reddy et al., 2020). Esta tecnología de tercera generación permitió superar las limitaciones inherentes a la secuenciación de ARN complementario (cADN), como los sesgos de amplificación, la ambigüedad en la identificación de isoformas y las restricciones en la longitud de lectura, ofreciendo una resolución integral del transcriptoma a nivel de molécula completa y específica de cadena.

La preparación de las bibliotecas comenzó con la extracción selectiva de ARN mensajero poliadenilado [ARN poli(A)]. Posteriormente, se realizó la ligación de adaptadores dT y adaptadores motores conforme al protocolo del fabricante, lo que permitió la secuenciación directa sin necesidad de retrotranscripción ni síntesis enzimática. Este método conservó la orientación nativa del ARN y permitió preservar modificaciones epitranscriptómicas.

Secuenciación y Control de Calidad de los Datos

Las bibliotecas generadas fueron cargadas en un flowcell de secuenciación Nanopore. Durante la lectura, las moléculas individuales de ARN generaron perturbaciones características en la corriente iónica al atravesar los nanoporos. Estas señales eléctricas fueron decodificadas en secuencias de bases mediante una red neuronal recurrente (RNN) implementada en el software GUPPY.

Los archivos obtenidos en formato fast5 fueron convertidos a formato fastq y sometidos a control de calidad. Se aplicaron filtros estrictos que excluyeron lecturas con puntuaciones de calidad inferiores

a Q7 y longitudes inferiores a 50 pb, asegurando así la integridad y confiabilidad de los datos empleados en los análisis posteriores.

Mapeo al Genoma de Referencia y Análisis de Transcritos

Las lecturas depuradas fueron alineadas contra un genoma de referencia. Se conservaron únicamente aquellas con alineamiento único. Para la construcción de transcritos consenso y su cuantificación, se utilizó el software FLAIR (v1.5.0) (Tang et al., 2020). Posteriormente, la estructura de los transcritos fue refinada con el software StringTie (v2.1.4), mapeando las secuencias consenso al genoma de referencia de forma conservadora (Pertea et al., 2015).

Para identificar genes y transcritos previamente no anotados, se implementó el software gffcompare (v0.12.1), el cual permitió comparar las nuevas secuencias con las anotaciones genómicas existentes, revelando un total de 5.237 transcritos nuevos, de los cuales 4.796 no presentaron homología con regiones previamente conocidas (Pertea & Pertea, 2020).

Predicción de Secuencias Codificantes (CDS)

Se utilizó TransDecoder (v5.5.0) para predecir las regiones codificantes (CDS) en los transcritos no anotados (Cossío-Bayúgar et al., 2024). Este paso permitió distinguir entre transcritos codificantes y no codificantes, y facilitó el análisis funcional y estructural de nuevas regiones génicas.

Optimización de la Estructura de los Transcritos

La estructura de los transcritos consenso fue comparada con las anotaciones conocidas del genoma mediante gffcompare (v0.12.1). Las regiones 5’ y 3’ de los transcritos fueron extendidas cuando se detectaron límites no coincidentes, lo cual permitió una corrección y optimización de las regiones no traducidas (UTRs) y una mejor definición de los límites génicos (Pertea & Pertea, 2020).

Análisis de Expresión Diferencial

El análisis de expresión diferencial se realizó con el software edgeR (v3.32.1), a partir de los conteos de lecturas por transcripto. Se consideraron como diferencialmente expresados aquellos transcritos con

FDR < 0,05 y |logFC| > 1, permitiendo identificar los genes con expresión significativamente alterada entre condiciones experimentales (Robinson et al., 2010).

Identificación de Metilaciones en ARN (m^6A y m^5C)

La identificación de sitios metilados se realizó para las modificaciones epitranscriptómicas m^5C y m^6A. Para m^5C, se empleó el modelo alternativo de Tombo (Zhang et al., 2020), mientras que para m^6A se utilizó el modelo de novo del mismo software, complementado con el pipeline MINES (Lorenz et al., 2020). Este enfoque permitió detectar con alta precisión sitios metilados a nivel de base.

Análisis de Motivos de Metilación

Se analizaron los motivos nucleotídicos asociados a los sitios de metilación, dado que las enzimas responsables del establecimiento o eliminación de estas modificaciones reconocen secuencias específicas. Estos motivos se analizaron para comprender la relación entre la metilación y la regulación de la expresión génica.

Análisis Diferencial de Sitios m^5C

Para detectar diferencias significativas en los patrones de metilación m^5C entre grupos experimentales, se utilizó el software methylKit (Akalin et al., 2012). En presencia de múltiples réplicas, se aplicó regresión logística; en caso contrario, se empleó la prueba exacta de Fisher. Esta estrategia permitió identificar sitios diferencialmente metilados con alta sensibilidad.

Análisis de Pseudouridina (Ψ)

La modificación de pseudouridina (Ψ), reconocida como la más abundante en ARN, fue evaluada mediante el software Nanopsu, utilizando un umbral de probabilidad posterior $P > 0,9$ (Jain et al., 2022). Esta modificación estructural fue incluida en el análisis epitranscriptómico como marcador potencial de estabilidad y funcionalidad de las moléculas de ARN.

RESULTADOS

Capítulo 1: La hipoxia en el mejillón azul *Mytilus chilensis* induce un cambio en el transcriptoma asociado con el estrés del retículo endoplásmico, el metabolismo y la respuesta inmunitaria.

Cita entera del artículo publicado: Montúfar-Romero, M.; Valenzuela-Muñoz, V.; Valenzuela-Miranda, D.; Gallardo-Escárate, C. Hypoxia in the Blue Mussel *Mytilus chilensis* Induces a Transcriptome Shift Associated with Endoplasmic Reticulum Stress, Metabolism, and Immune Response. *Genes* 2024, 15, 658. https://doi.org/10.3390/genes15060658

Resumen

El aumento de los episodios de hipoxia, como consecuencia del cambio climático en los ecosistemas costeros y fiordos, afecta a la salud y la supervivencia de los mejillones. Estos organismos despliegan respuestas fisiológicas y moleculares como mecanismo de adaptación para mantener la homeostasis celular bajo estrés ambiental. Sin embargo, se desconocen los efectos específicos de la hipoxia en mejillones de interés socioeconómico, como *Mytilus chilensis*. Mediante secuenciación de ARN, investigamos los perfiles transcriptómicos de las branquias, la glándula digestiva y el músculo aductor de *M. chilensis* en condiciones de hipoxia (10 días a 2 mg L−1) y reoxigenación (10 días a 6 mg L−1). Se identificaron 15.056 transcritos expresados de forma diferencial en

las branquias, 11,864 en la glándula digestiva y 9,862 en el músculo aductor. La respuesta varió entre los tejidos, mostrando cambios cromosómicos en Chr1, Chr9 y Chr10 durante la hipoxia. La hipoxia reguló los genes de señalización en las vías Toll-like, mTOR, ciclo del citrato y apoptosis en las branquias, lo que indica alteraciones metabólicas e inmunológicas. Estos cambios sugieren que la hipoxia indujo un cambio metabólico en los mejillones, reduciendo la dependencia de la respiración aeróbica y aumentando la dependencia del metabolismo anaeróbico. Además, la hipoxia pareció suprimir la respuesta inmunitaria, lo que podría aumentar la susceptibilidad a las enfermedades, con implicaciones negativas para la industria del cultivo de mejillones y las poblaciones de lechos naturales. Este estudio proporciona información fundamental sobre las adaptaciones metabólicas e inmunológicas a la hipoxia en *M. chilensis*, y ofrece genes candidatos para rasgos adaptativos.

genes

MDPI

Article

Hypoxia in the Blue Mussel *Mytilus chilensis* Induces a Transcriptome Shift Associated with Endoplasmic Reticulum Stress, Metabolism, and Immune Response

Milton Montúfar-Romero [1,2,3], Valentina Valenzuela-Muñoz [1,4], Diego Valenzuela-Miranda [1,2] and Cristian Gallardo-Escárate [1,2,*]

[1] Interdisciplinary Center for Aquaculture Research (INCAR), Universidad de Concepción, P.O. Box 160-C, Concepción 4030000, Chile; mmontufar@institutopesca.gob.ec (M.M.-R.); valentina.valenzuela@uss.cl (V.V.-M.); divalenzuela@udec.cl (D.V.-M.)
[2] Biotecnology Center, Universidad de Concepción, Concepción 4030000, Chile
[3] Instituto Público de Investigación de Acuicultura y Pesca (IPIAP), Guayaquil 090314, Ecuador
[4] Escuela de Medicina Veterinaria, Facultad de Ciencias de la Naturaleza, Universidad San Sebastián, Concepción 4030000, Chile
* Correspondence: crisgallardo@udec.cl; Tel.: +56-412204402

Abstract: The increase in hypoxia events, a result of climate change in coastal and fjord ecosystems, impacts the health and survival of mussels. These organisms deploy physiological and molecular responses as an adaptive mechanism to maintain cellular homeostasis under environmental stress. However, the specific effects of hypoxia on mussels of socioeconomic interest, such as *Mytilus chilensis*, are unknown. Using RNA-seq, we investigated the transcriptomic profiles of the gills, digestive gland, and adductor muscle of *M. chilensis* under hypoxia (10 days at 2 mg L^{-1}) and reoxygenation (10 days at 6 mg L^{-1}). There were 15,056 differentially expressed transcripts identified in gills, 11,864 in the digestive gland, and 9862 in the adductor muscle. The response varied among tissues, showing chromosomal changes in Chr1, Chr9, and Chr10 during hypoxia. Hypoxia regulated signaling genes in the Toll-like, mTOR, citrate cycle, and apoptosis pathways in gills, indicating metabolic and immunological alterations. These changes suggest that hypoxia induced a metabolic shift in mussels, reducing reliance on aerobic respiration and increasing reliance on anaerobic metabolism. Furthermore, hypoxia appeared to suppress the immune response, potentially increasing disease susceptibility, with negative implications for the mussel culture industry and natural bed populations. This study provides pivotal insights into metabolic and immunological adaptations to hypoxia in *M. chilensis*, offering candidate genes for adaptive traits.

Keywords: bivalve mollusks; hypoxia; oxidative stress; reoxygenation; gills; transcriptome; metabolism; immunity

Citation: Montúfar-Romero, M.; Valenzuela-Muñoz, V.; Valenzuela-Miranda, D.; Gallardo-Escárate, C. Hypoxia in the Blue Mussel *Mytilus chilensis* Induces a Transcriptome Shift Associated with Endoplasmic Reticulum Stress, Metabolism, and Immune Response. *Genes* **2024**, *15*, 658. https://doi.org/10.3390/genes15060658

Academic Editor: Chunjin Li

Received: 28 March 2024
Revised: 1 May 2024
Accepted: 15 May 2024
Published: 22 May 2024

1. Introduction

Hypoxia is the dissolved oxygen deficiency in the water column and is a significant stress factor for most marine animals that require oxygen to survive [1–3]. It can disrupt biodiversity and productivity in aquatic ecosystems [1–4]. Recently, the increase in hypoxic areas in coastal systems, primarily caused by the combined action of eutrophication and global warming, has attracted significant attention from the scientific community due to its potential ecological repercussions worldwide [3,5–8]. In surface waters, dissolved oxygen concentrations result from a balance between oxygen production through photosynthesis, consumption caused by respiration, and exchange with the atmosphere, where the latter tends to maintain dissolved oxygen close to saturation, depending on temperature and salinity [9]. According to projections of increased sea surface temperatures in southern Chile caused by climate change, there would be a decrease in the solubility of oxygen in

the water and an intensification of the stratification [10–13]. Furthermore, climate change affects precipitation and river discharge into fjords [14,15]. This could disturb the thickness and extent of the low-salinity layer at the top of the fjords, slowing down the rate of circulation and renewal of deep waters, thereby affecting bottom oxygen concentrations and resulting in detrimental consequences for fisheries and coastal economies [14–16].

Under hypoxia conditions, bivalve mollusks display several physiological and molecular responses as an adaptive coping mechanism for environmental stress [17]. Sessile bivalve mollusks can close their valves or reduce water flow during hypoxic events, decreasing oxygen consumption, energy expenditure, and ATP production [18–20]. In contrast, mobile aquatic organisms can migrate away from areas with low oxygen [19,21]. When the duration or severe exposure to hypoxic events exceeds the tolerance of marine organisms, it leads to various detrimental effects, which can be lethal or sublethal, with long-term consequences [5,22]. Hypoxia is involved in molecular mechanisms that trigger mass mortality during the summer, explaining the negative impacts on benthic organisms during these events [23,24]. Adaptation in response to hypoxia is critical for maintaining cellular and organismal homeostasis [25]. Gills play an essential role in gas exchange, where the increase in reactive oxygen species (ROS) caused by hypoxia decreases antioxidant agents, causing cellular damage [26–28]. Molecular studies report that the duration of hypoxia stress leads to the cessation of protein synthesis and increased protein catabolism, as well as changes in the urea cycle and the expression of genes associated with apoptosis, inflammatory response mechanisms, and neoplasia [3,18,25,29–31]. Hypoxia is a common feature of numerous diseases and a frequent player in several cell malignancies and neoplasia [32]. Under normoxia conditions, the HIF-1α gene is the primary regulator of oxygen homeostasis in bivalve mollusks [33,34], promoting the ability of cells to adapt to hypoxia and playing an essential role in immune system cells [35,36]. Excessive production of reactive oxygen species (ROS) during anaerobic metabolism activates apoptosis or programmed cell death through the intrinsic pathway regulated by the *p53* and *BAX* genes [29,37]. Additionally, metabolic imbalance activates the extrinsic apoptosis pathway through caspases 2 and 3 [38,39]. Increased ROS stimulates the inflammatory pathway by activating the TBK1 gene and the NF-kB transcription factor, which promotes apoptosis [29,40–45].

Sequencing technology development based on short and long reads provides an indispensable tool for a better understanding of RNA biology, giving pivotal insights about when and where transcription occurs in response to a set of ecological processes [46–48]. Notably, the recently published chromosome-level genome assembly for *M. chilensis* (Hupe, 1854) represents a valuable resource for exploring the molecular responses of mussel's genomes facing the marine environment [49]. For instance, transcriptome studies conducted in *M. chilensis* generated molecular markers related to environmental and biological stressors [50–52]. Furthermore, the exploration of molecular markers linked to immune response resulted in the identification of saxitoxin immunoreceptors present in harmful algal blooms, the use of mitochondrial genes as biomarkers for environmental fluctuations such as temperature and salinity, and the exploration of genes related to shell biomineralization, which functions as protection against predators and anatomical support [50–53]. These analyses help determine the adaptation of populations when transferred from natural seed banks to aquaculture farms [50–52]. These genes could be affected by variations in pH caused by ocean acidification [53].

The Chilean mussel, *M. chilensis* (commonly known as "chorito" in Chile), is Chile's most commercially crucial filter-feeding bivalve mollusk and holds socio-ecological relevance. Its distribution ranges from the Pacific Ocean coast in central Chile to Patagonia in southern Argentina [54–58] The minimum size for extraction is 5 cm, and individuals can reach up to 8 cm [58]. They are gonochoric, with external fertilization and internal sexual dimorphism [59]. Males have a creamy yellow gonad, while females have an orangish tone [59]. Through their buccal palp, they can sort out food particles, eliminating captured material without ingestion through pseudofeces [60]. They can tolerate a wide range of salinity and are particularly abundant in fjords [55].

M. chilensis is an essential marine resource because it provides ecosystem services [55,61]. The cultivation of mussels begins with collecting seedlings from their natural environment, which are then transported to farms for growing until they reach commercial size [62]. They are then processed for marketing purposes [62]. The species accounts for 98.4% of the shellfish cultivation in Chile and ranks first in worldwide exports [63,64]. In 2021, 424.3 thousand tons were produced, equivalent to over USD 271 million in exports, with the majority directed to Europe [54,62,63,65]. However, in recent years, the mussel farming industry has faced an increased risk of exposure to hypoxia events mainly caused by upwelling and eutrophication in the Los Lagos Region, where 100% of the seed collection and mussel harvesting occurs [9,63,66].

Sessile bivalve mollusks have traditionally been used as indicators of water quality. In this context, the feasibility of using *Mytilus* sp. as an environmental biosensor model organism through the characterization of its transcriptome has been proposed, as it can adapt its metabolism to ecological changes [67–69]. In recent decades, hypoxia has caused massive mortality and bivalve mollusks' stranding along Chile's central southern coast [22,70–72]. Therefore, understanding the tolerance mechanisms of bivalve mollusks to hypoxia is currently of utmost importance in contributing to the sustainability of this industry [3,73–85]. Thus, the effects of hypoxia on the physiological energetics, intermediary metabolites, cell survival, and inflammatory responses of the genus *Mytilus* suggest that hypoxia significantly affects the adaptation mechanisms of *M. chilensis* [3,29,74]. Despite the number of studies conducted on the subject and the available technology for carrying them out, the molecular mechanisms generated in response to the stress adaptation of mussels caused by hypoxia still need to be discovered.

This study adopted the RNA-seq approach to investigate the transcriptomic profiles of the gills, digestive gland, and adductor muscle of *M. chilensis* under hypoxia and reoxygenation conditions. This work aimed to identify differentially expressed genes and their expression patterns under low oxygen levels to gain a better understanding of transcriptomic regulation in response to hypoxia–reoxygenation stress and to investigate the hypoxia-induced changes in the expression of gene pathways involved in hypoxia regulation in *M. chilensis*. Meanwhile, the differentiated response in each analyzed tissue in *M. chilensis* under experimental hypoxia conditions was investigated. These results provide a deep understanding of the molecular regulatory mechanism in different tissues that adapt to hypoxia–reoxygenation in *M. chilensis*. Additionally, the findings of this study can help develop strategies to mitigate the adverse effects of hypoxia in the mussel farming industry. Therefore, studying the transcriptomic response of the native Chilean blue mussel, *M. chilensis*, to hypoxia is crucial for better understanding marine organism biology and addressing current environmental issues.

2. Materials and Methods

2.1. Mussel Acclimation, Hypoxia Challenge, and Sample Preparation

In April 2022, adult mussels measuring 6.26 ± 0.50 cm in length and weighing 18.57 ± 3.85 g were collected from Puerto Montt, Chile. They were transported from the cultivation area to the laboratory, where mussels with shell defects were discarded, and the rest were cleaned to remove shell fouling. The mussels were acclimated for 38 days in a 7-ton fiberglass tank containing water at 12.5 ± 0.94 °C and a 34.5 ± 0.32 ppt salinity. Other water quality parameters were measured during the experiment (pH: 7.2 ± 0.12, dissolved oxygen: 7.5 ± 1.11 mg/L). All mussels were fed a mixture of *Isochrysis* sp. and *Pavlova* sp. once a day before and after the hypoxia challenge. The water was changed daily to remove waste products from the mussels. *M. chilensis* is a native species without risk of extinction or protection status, so no special permits were required for this research.

The exposure time for the hypoxia assays was based on the average values of the tidal coefficient progression in the area where this organism is cultured. This information is available at the following link: https://tablademareas.com/ (accessed on 7 March 2022). The experimental design for this study is visually outlined in Figure 1A. After acclimation,

a total of 480 mussels were randomly divided into two groups and three replicates for the following treatments: (1) control group in normoxia (N1, N2, and N3) maintained at normal oxygen levels (7.2 ± 0.2 mg/L); (2) experimental group subjected to hypoxia (H1, H2, and H3) maintained at a low oxygen concentration (2.0 mg/L). The dissolved oxygen concentration in the recirculation system was controlled daily by injecting nitrogen bubbles until reaching a dissolved oxygen value of 2.0 mg/L. The oxygen content and salinity of the seawater were measured using a multiparameter device (HI9829) (Hanna Instruments Inc., Woonsocket, RI, USA). The water temperature and salinity were 12.5 ± 1 °C and 34.5 ± 0.5 ppt, respectively. For transcriptome sequencing, samples of total RNA were extracted from the gill, digestive gland, and adductor muscle from the control and hypoxia-exposed groups at different time intervals. Each sample was obtained in triplicate. The extracted tissues and extrapallial fluid were frozen at −80 °C for further processing.

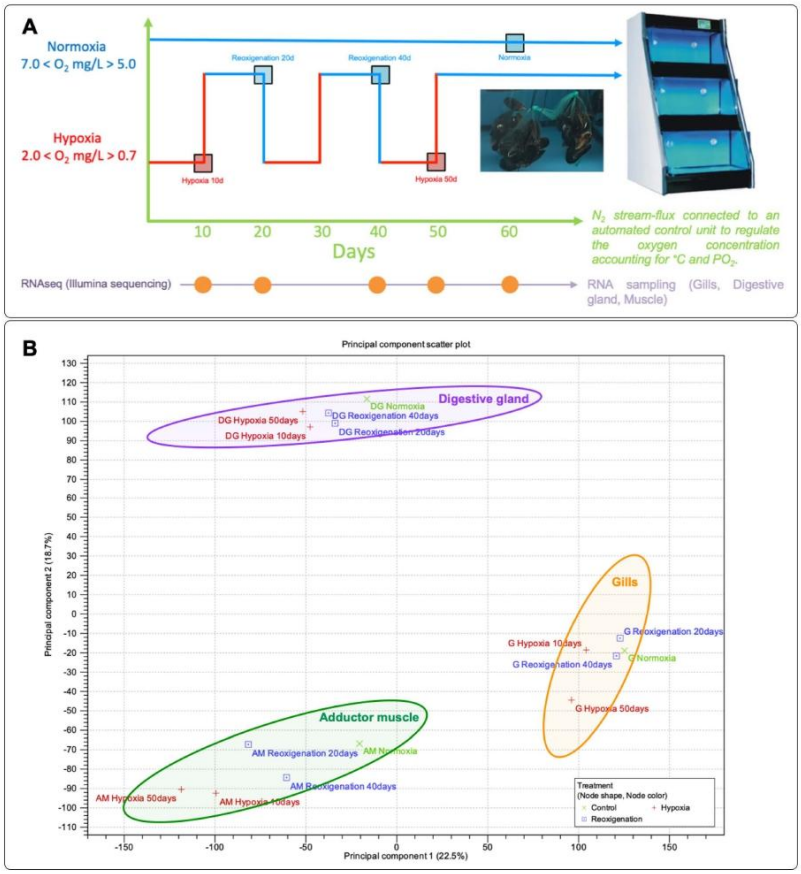

Figure 1. Experimental design and principal component analysis (PCA). (**A**) Experimental design of *M. chilensis* under hypoxia and reoxygenation conditions for 60 days. (**B**) PCA of genes expressed in gills (G), digestive gland (DG), and adductor muscle (AM) under hypoxia and reoxygenation conditions. Circles indicate a differential response by tissue.

2.2. RNA Extraction and Library Preparation

Tissues from the gills, digestive gland, and adductor muscle of the control and hypoxia-exposed groups were sampled at 10, 20, 40, 50, and 60 days. The tissues were stored in RNA Later (Ambion, Austin, TX, USA) at −80 °C until RNA extraction for transcriptome sequencing. RNA extractions were performed in triplicate for each experimental group using the Trizol reagent (Invitrogen, Carlsbad, CA, USA) according to the manufacturer's instructions. Pools made each replicate of 9 individuals. The extracted RNA concentration was measured using the QUBIT 4 instrument (Thermo Fisher Scientific, Pittsburgh, PA, USA), and the quality was determined using the TapeStation 2200 instrument (Agilent Technologies Inc., Santa Clara, CA, USA). Double-stranded cDNA libraries were prepared using the TruSeq RNA Sample Preparation Kit v2 (Illumina®, San Diego, CA, USA), following the manufacturer's instructions, using 1 µg of tissue RNA per group. Each of the three biological replicates per experimental group was sent to the Republic of Korea, where de novo transcriptome sequencing was performed by Macrogen, 180 Inc., using the Illumina platform. The type of read was paired-end, with a read length of 101.

2.3. Transcriptome Analysis and Gene Ontology Annotation

The reads obtained from sequencing were trimmed by quality, and the adapters were removed using the CLC Genomic Workbench software v23 (Qiagen Bioinformatics, Redwood City, CA USA). The trimming parameters included a quality score threshold of 20, a minimum read length of 50 nucleotides, and a sliding window size of 4 nucleotides, and trimming was performed at both ends. Transcriptomic analysis was performed using the *M. chilensis* genome V1 as a reference [49]. RNA-seq analyses were based on all contigs' normalized TPM (transcripts per million mapped reads) values per sample. The Euclidean distance method was employed to compute the distance metric, and it involved subtracting the mean expression level from 5–6 iterations of k-means clustering. All expression analyses and statistical comparisons included the three biological replicates for each experimental group. The group conducted statistical assessments on TPM values, achieving this by calculating the fold change concerning the control group (normoxia) and then applying Kal's test for filtering. Transcripts displaying a fold change exceeding |2| and a p-value below 0.05 were identified as differentially expressed and subsequently extracted for gene annotation. The p-values reported in the analysis were adjusted using the FDR correction to ensure the robustness and reliability of the results. Differentially expressed transcripts were annotated using the BLAST algorithm against the Nr, Nt, egg NOG, Pfam, Swiss-Prot, GO, Ko, KO, and KEGG databases [86–90]. The BLAST E-value cut-off used for annotating the differentially expressed transcripts was set at 1×10^{-5}. To conduct the analysis of differential gene expression, these transcripts were translated into an Excel matrix. Subsequently, using filters, the transcripts were sorted in descending order, and those showing the highest level of differentiation were selected for generating heatmaps in TBtools Version No.2.007. For the construction of Venn diagrams, online software available at https://www.biotools.fr/misc/venny (accessed on 6 March 2023) was utilized.

Functional enrichment analysis of Gene Ontology (GO) terms was conducted to identify key pathways regulated during the experiment. TBtools, available for free download from https://github.com/CJ-Chen/TBtools-II (accessed on 10 April 2023), was utilized to prepare the gene list for analysis with ShinyGO (http://bioinformatics.sdstate.edu/go/ (accessed on 15 May 2023)), an online gene enrichment tool [91,92].

For the TBtools analysis, gene IDs and a corresponding GO annotation file are necessary. The software conveniently provides a downloadable "go-basis.obo" file accessible within its "GO & KEGG" and "GO Enrichment" options.

The analysis focused on the blue mussel, employing a significance threshold (FDR) of 0.05 in ShinyGO. To ensure the clarity of the results, options to remove redundant terms and abbreviate pathways were employed. Visualization plots were generated using the ggplot2 tool implemented in R.

Hierarchical clustering methods were used in the analysis of the heatmaps to classify the data, and Euclidean distance measures were employed to assess the similarity between genes. Not all differentially expressed genes (DEGs) were necessarily included, but rather those considered most relevant for the condition under study. The selection of genes was based on criteria such as their level of differential expression, their association with known biological pathways, and their involvement in physiological functions relevant to the study.

2.4. Chromosome Gene Expression (CGE) Analysis

The unprocessed data from each sequencing process were aligned to the *M. chilensis* genome V1 [49] to evaluate the CGE index, according to Valenzuela-Muñoz et al., 2022 [93]. The CGE index measures the transcriptional variation across the two experimental groups (hypoxia and normoxia). To do this, we determined the average transcript coverage in normoxia within a specific chromosomal region and compared it under different experimental conditions. We applied a threshold range of 2000 to 100,000 reads within a 5-position window to calculate transcript coverage values. The Graph Threshold Areas tool within CLC Genomics Workbench v23 software computed these threshold values for each chromosomal region. Chromosomes exhibiting CGE index values exceeding 60% were visualized alongside the transcript coverage in each dataset using Circo's software version 0.69-9 [94].

2.5. Data Availability

The transcriptome data for mRNA analysis were deposited in the NCBI-SRA (Sequence Read Archive) database under the accession number PRJNA1099139.

3. Results

3.1. Principal Component Analysis (PCA) of Gene Expression Profiles in M. chilensis Tissues under Hypoxia and Reoxygenation

In this study, principal component analysis (PCA) was carried out to identify and compare the gene expression patterns in the gills, digestive gland, and muscle, which contributed to 40.5% of the total variability present in the dataset (Figure 1B). The PCA results indicated that PC1 was mainly related to the separation in gene expression observed in the digestive gland tissue. On the other hand, PC2 allowed a clear distinction in gene expression patterns between gill and adductor muscle tissues (Figure 1B). Likewise, along the PC2 axis, a relationship in the expression of transcripts between the gill tissues and the adductor muscle was identified. Generally, it was possible to observe a lower dispersion of the expression data in the digestive gland, gill, and abductor muscle. However, both reoxygenation and hypoxia conditions were observed grouped for all tissues evaluated.

3.2. Differential Regulation of Transcripts under Normoxia and Hypoxia Conditions in Multiple Tissues of M. chilensis

To determine gene expression patterns for normoxia, reoxygenation, and hypoxia conditions simultaneously, this study identified two data clusters with marked differences in transcript regulation under normoxia and hypoxia conditions (Figure 2A). Performing RNA-seq analyses revealed distinctive patterns between the experimental groups. For example, cluster 1 showed upregulation of genes in response to hypoxia. In contrast, cluster 2 stood out for the downregulation of genes in all tissues analyzed, including gills, digestive gland, and adductor muscle (Figure 2B). When the UpSet plot was examined to compare the transcriptional regulation of tissues under hypoxic conditions, it was observed that a more significant number of genes were upregulated in cluster 1 in all tissues analyzed. In particular, the gills presented the highest number of upregulated transcripts, followed in order by the adductor muscle and the digestive gland (Figure 2C). In cluster 1, 137 transcripts were identified that were differentially expressed in the tissues evaluated. In cluster 2, 34 transcripts were shared among tissues (Figure 2C).

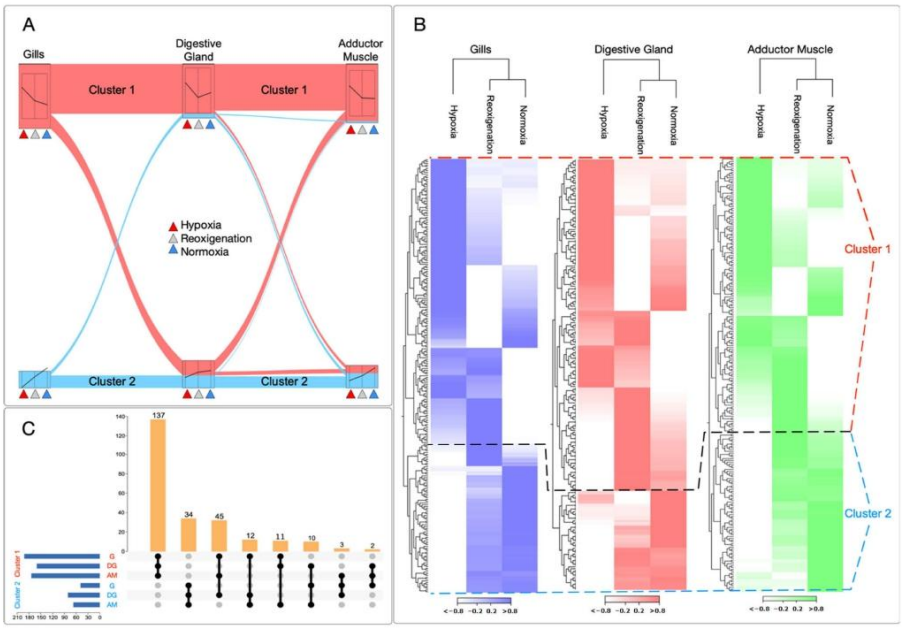

Figure 2. Transcript cluster analysis. (**A**) K-medoids analysis of relevant transcripts for each tissue under normoxia, hypoxia, and reoxygenation conditions. (**B**) Heatmap representation of transcripts for each tissue under normoxia, hypoxia, and reoxygenation conditions. Main clusters 1 and 2 are identified in red and blue, respectively. (**C**) The UpSet plots of transcripts differentially expressed in cluster 1 and cluster 2. Each horizontal bar represents the size of the set of differentially expressed transcripts at a particular time point and treatment. The vertical bars indicate the number of transcripts present in the clusters for each tissue.

For cluster 1, 20 significantly enriched Gene Ontology (GO) terms were identified (Figure 3A), and for cluster 2, 23 terms significantly enriched GO terms were identified (Figure 3C). These terms formed a network connecting the differentially expressed genes (Figure 3B,D). In total, 43 GO terms were identified in both categories. GO category mapping for both clusters ultimately revealed a wide variety of biological processes, including terms such as "Negative regulation of endoplasmic reticulum unfolded protein response", "TORC1 signaling", and "Regulation of nucleotide-binding oligomerization domain containing signaling pathway" for cluster 1 and "Host cellular component", "Symbiont-containing vacuole membrane", and "Thiopurine S-methyltransferase activity" for cluster 2.

Gene expression cluster analysis was used to identify differentially expressed genes (DEGs) associated with hypoxia in the gill, digestive gland, and adductor muscle tissues (see genes marked in red in Figure 4). Evaluation of the DEGs was performed by analyzing the transcriptome in clusters, visualized using a Circos plot to identify specific loci where the DEGs were highly transcribed. The calculated fold-change values revealed elevated levels of transcription on chromosomes Chr1, Chr9, and Chr10, which exhibit more excellent modulation in response to the hypoxia event (Figure 4A). On the other hand, genes present on chromosomes 5, 7, and 12 showed expression during normoxia events.

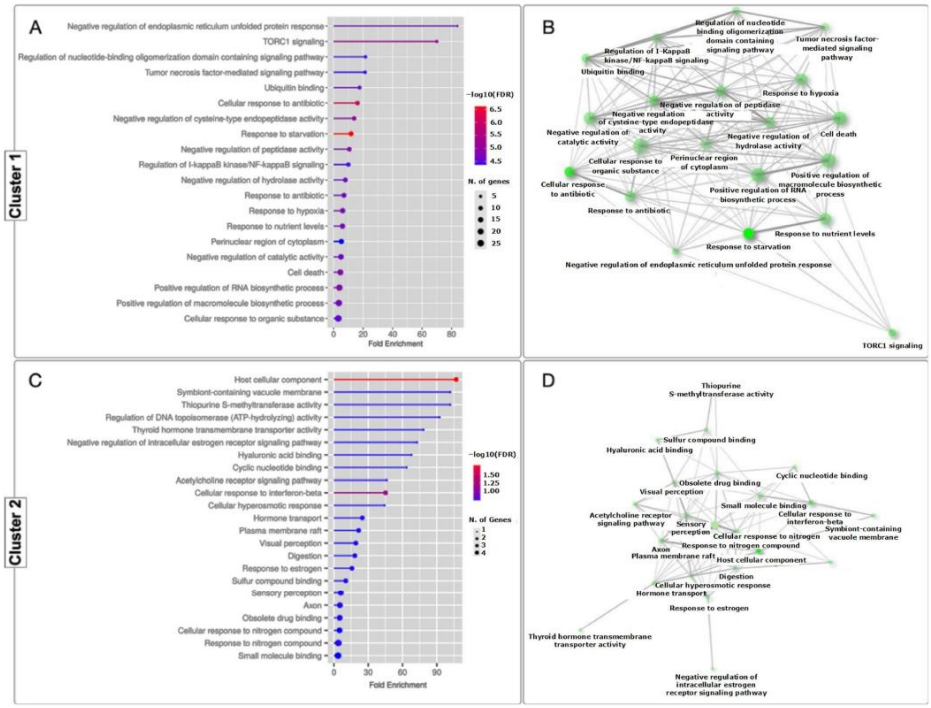

Figure 3. Gene Ontology (GO) enrichment analysis of differentially expressed genes (DEGs). (**A**) GO enrichment analysis of DEGs found in Cluster 1. (**B**) Network analysis of relevant GO terms identified in cluster 1. (**C**) GO enrichment analysis of DEGs found in cluster 2. (**D**) Network analysis of relevant GO terms identifies in cluster 2.

The analysis of the *M. chilensis* genome allowed the identification of 25 genes with a high identity index with hypoxia. Among them, the MCH002084.1 gene (haloacid dehalogenase-like hydrolase) located on chromosome 1 stands out, and its association with hypoxia in bivalve mollusks is reported for the first time. The HAD (haloacid dehalogenase-like hydrolase) gene superfamily was activated in response to phosphate deprivation induced by environmental stressors [95,96]. This superfamily comprises a diversity of proteins involved in the hydrolysis of specific substrates, including phosphatases and ATPases [97]. This finding suggests a possible explanation for how oxygen availability may influence the ability of cells to synthesize ATP through aerobic respiration, which could eventually result in metabolic changes and energy production.

When analyzing the genes that were directly involved in the hypoxia events, their relationship with key biological processes such as "Regulation of miRNA transcription", "nuclear ubiquitin ligase complex", and "negative regulation of RNA biosynthetic process" was observed (Figure 4B).

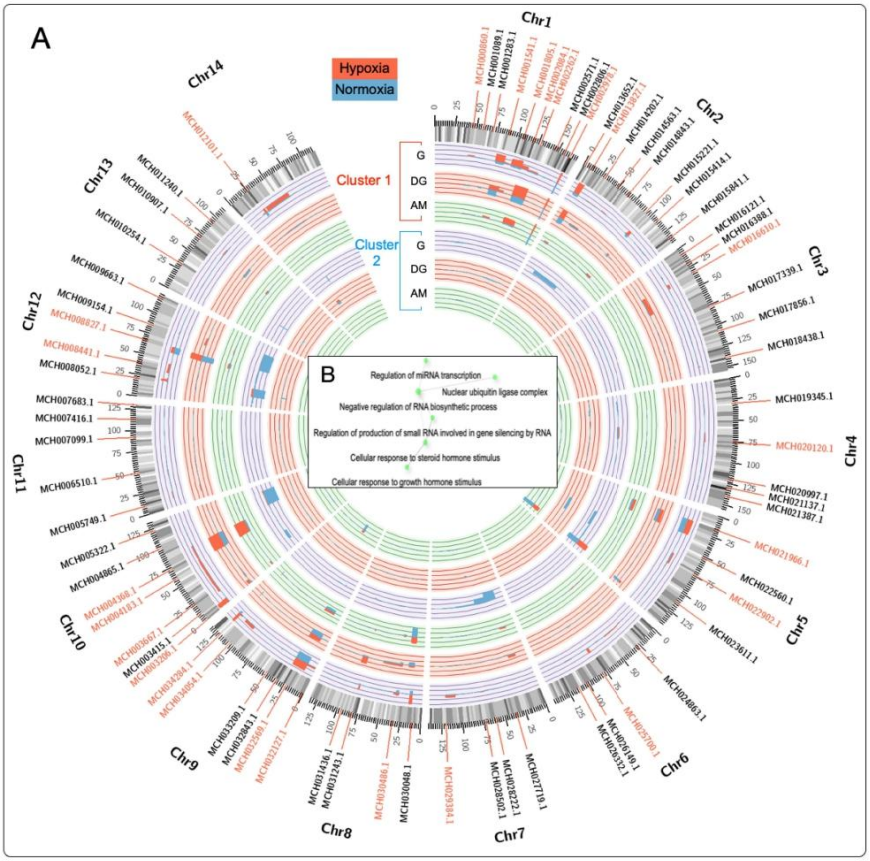

Figure 4. Differentially expressed genes (DEGs) analyzed in *M. chilensis* under hypoxia and normoxia conditions and evaluated through transcriptome analysis in clusters. (**A**) The Circos plot depicts the genomic features of the 14 chromosomes. The DEGs identified in the two analyzed clusters are shown in the Circos plot. From outer to inner circle: gene density, DEG cluster 1, and DEG cluster 2. Red genes represent DEGs associated with hypoxia. Histograms display transcriptional expression levels of G (gill), DG (digestive gland), and AM (adductor muscle). Cluster 1 corresponds to hypoxia (red), and cluster 2 to normoxia (blue). (**B**) Gene Ontology (GO) enrichment network of highly regulated transcripts.

3.3. Differential Expression Analysis of Transcripts Expressed in M. chilensis Gills under Hypoxic and Reoxygenation Conditions

The gills subjected to 10 and 50 days of hypoxia experienced significant modifications in their transcriptome, as evidenced in the heatmap (Figure 5A). However, at 20 and 40 days of reoxygenation, the modification in the transcriptome was less pronounced compared to hypoxia (Figure 5A). However, during reoxygenation, recovery and adaptation processes were observed in the gills. Six transcript clusters with different expression patterns were identified (Figure 5A). In particular, clusters 5 and 6 showed upregulation in the control

group, whereas clusters 1 to 4 displayed downregulation (Figure 5A). A total of 15,056 transcripts were identified, showing regulation during the 10- and 50-day hypoxia periods, as well as during the 20- and 40-day reoxygenation periods, and a core set of 1221 transcripts were found to be commonly present in all periods of hypoxia and reoxygenation (Figure 5B). The highest amount of differentially expressed transcripts was observed after 10 days of hypoxia, followed by hypoxia at 50 days, reoxygenation at 20 days, and finally reoxygenation at 40 days (Figure 5B). This suggests a more pronounced transcriptome response to hypoxia compared to reoxygenation (Figure 5B). Furthermore, an apparent adaptation of the transcriptome over time in response to hypoxia and reoxygenation exposures was evident (Figure 5B). In the Venn diagram analysis (Figure 5C) it was interesting to observe that the number of differentially expressed transcripts was higher under hypoxic conditions compared to reoxygenation. In particular, the gill presented more transcripts that were only expressed in hypoxia than those that were only expressed in reoxygenation. Transcripts regulated in both hypoxia and reoxygenation were found to be less numerous compared to those expressed exclusively in one or the other state (Figure 5C).

A GO enrichment analysis was performed to examine the response at the metabolic level and in the immune system under hypoxic and reoxygenating conditions in the gills of *M. chilensis* (Figure 5D). Compared to reoxygenation, hypoxia showed an association with a series of significant biological processes and molecular functions (Figure 5D). In hypoxia, GO terms related to stress response, response to external stimuli, regulation of response to stimuli, cellular response to stimuli, and response to oxygen-containing compounds were observed (Figure 5D). In addition, terms related to biosynthetic processes, defensive response, immunological response, and regulation of metabolic processes were highlighted. These results indicate a metabolic and immune system response under hypoxic conditions in the gills of *M. chilensis* (Figure 5D). In the case of reoxygenation, a lower abundance of annotated terms was recorded compared to hypoxia (Figure 5D). However, important terms were still identified, such as small-molecule metabolic processes, stress response, response to external stimuli, lipid metabolic processes, immune response, defensive response, carbohydrate metabolic processes, and biological processes related to interaction with the host (Figure 5D). In summary, the results suggest a marked response at the metabolic level and in the immune system under conditions of hypoxia and reoxygenation in *M. chilensis*, being more pronounced in hypoxia (Figure 5D).

3.4. Differential Expression Analysis of Transcripts Observed in the Digestive Gland of M. chilensis under Hypoxic and Reoxygenation Conditions

The digestive gland subjected to 10 and 50 days of hypoxia experienced significant modifications in its transcriptome, as reflected in the heatmap (Figure 6A). However, at 20 and 40 days of reoxygenation, the modification in the transcriptome was less marked compared to hypoxia (Figure 6A). During reoxygenation, a recovery and adaptation process was evident in the digestive gland. Three transcript clusters with different expression patterns were identified in this organ (Figure 6A). Specifically, clusters 2 and 3 showed upregulation. In contrast, cluster 1 showed downregulation (Figure 6A). A total of 11,864 transcripts were identified that underwent regulation during both the 10- and 50-day hypoxia periods and the 20- and 40-day reoxygenation periods, and a core group of 1064 transcripts was found to be consistently present in all the periods of hypoxia and reoxygenation (Figure 6B). The highest number of differentially expressed transcripts was observed at 50 days of hypoxia, followed by hypoxia at 10 days, reoxygenation at 20 days, and finally reoxygenation at 40 days (Figure 6B). These findings suggest a more pronounced response of the transcriptome to hypoxia compared to reoxygenation (Figure 6B). Venn diagram analysis (Figure 6C) revealed that more transcripts were exclusively expressed in response to hypoxia compared to those that underwent regulation during reoxygenation. On the other hand, the transcripts that showed regulation in both the hypoxia and reoxygenation periods turned out to be significantly less numerous compared to those that expressed exclusively in one or the other state (Figure 6C).

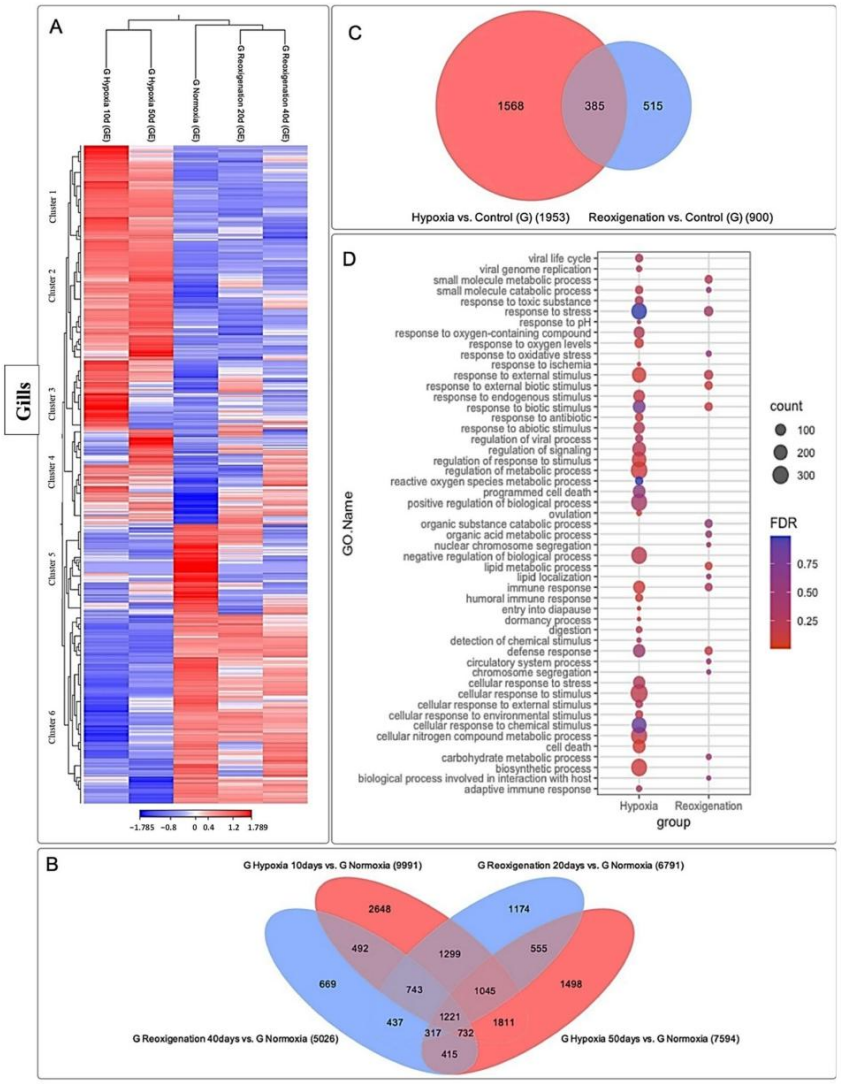

Figure 5. RNA-seq transcriptome analysis in gills illustrating differential RNA-seq expression data. (**A**) The heatmap shows comparisons for each group (normoxia, hypoxia 10 days, reoxygenation 20 days, hypoxia 50 days, and reoxygenation 40 days). Red, positive log fold-change (log FC) indicates higher expression in each treatment; blue, negative log FC. Log FC was calculated using the base 2 logarithm. Grouping was applied by columns (groups compared) and rows (transcripts analyzed), divided into clusters. (**B**) Venn diagram shows the number of unique and overlapping transcripts differentially expressed after exposure to hypoxia–reoxygenation. Sampling was performed at 10 and 50 days of hypoxia and 20 days and 40 days of reoxygenation. A total of 2648 transcripts were differentially expressed

in the gill only at 10 days subjected to hypoxia and were not differentially expressed in any other sampling. The most common overlapping transcripts were 1299 differentially expressed at 10 days subjected to hypoxia and 20 days subjected to reoxygenation. Genes regulated in hypoxia are highlighted in red, while those regulated in reoxygenation are highlighted in blue. (**C**) Venn diagram shows overlapping genes differentially expressed compared with aerated controls in hypoxia and reoxygenation in gills. Genes regulated in hypoxia are highlighted in red, while those regulated in reoxygenation are highlighted in blue. (**D**) Function annotation and Gene Ontology (GO) term enrichment analysis of DEGs in upregulated and downregulated genes in response to hypoxia in gills. FDR: false discovery rate. The most representative and significant molecular functions, biological processes, and cellular components are shown. The circumference size indicates the number of DEGs associated with the process, and the dot color indicates the significance of the enrichment (FDR-corrected *p*-values).

3.5. GO Enrichment Analysis in the Digestive Gland of M. chilensis under Hypoxia and Reoxygenation Conditions

Hypoxia showed a significant association with a variety of biological processes (Figure 6D). Among the GO terms identified were stress response, response to external stimuli, response to endogenous stimuli, response to abiotic stimuli, regulation of molecular function, regulation of biological processes, immune response, immunological effector process, cellular response to stimuli, cell development, cell population proliferation, cell motility, cell growth, cell death, cell communication, cell adhesion, catabolic processes, biosynthetic processes, and development of anatomical structures (Figure 6D). These results indicate a metabolic and cellular response in growth and the immune system in the digestive gland of *M. chilensis* under hypoxic conditions. In comparison, reoxygenation showed fewer annotated GO terms relative to hypoxia. However, transcript counts per term were similar (Figure 6D). Terms identified include response to external stimuli, protein folding, molting cycle, immune response, and cell adhesion. In addition, terms that were not found in hypoxia were recorded in reoxygenation, such as glycosylation, embryonic implantation, digestion, demethylation, and coagulation. These findings revealed a marked difference in the metabolic and immune system response of the digestive gland of *M. chilensis* under hypoxic conditions compared to reoxygenation.

3.6. Differential Expression ANALYSIS of transcripts Observed in the Adductor Muscle of M. chilensis under Hypoxic and Reoxygenation Conditions

The adductor muscle exhibited significant changes in its gene expression profile after 10 and 50 days of hypoxia, which was reflected in the heatmap (Figure 7A). However, during days 20 and 40 of reoxygenation, modifications in the transcriptome were less marked compared to what was observed during hypoxia (Figure 7A). During the reoxygenation phase, a recovery and adaptation process was recorded. Four groups of transcripts with different expression patterns could be identified in the adductor muscle (Figure 7A). Specifically, clusters 3 and 4 consisted of upregulated transcripts, while clusters 1 and 2 included downregulated transcripts (Figure 7A). A total of 9862 transcripts were identified that underwent regulation during both the 10- and 50-day hypoxia periods and the 20- and 40-day reoxygenation periods, and a core group of 1129 transcripts was found that remained consistent across all periods of hypoxia and reoxygenation (Figure 7B). The highest number of differentially expressed transcripts was observed at 50 days of hypoxia, followed by hypoxia at 10 days, reoxygenation at 40 days, and finally reoxygenation at 20 days (Figure 7B). These results suggested a more pronounced response of the transcriptome to hypoxia compared to reoxygenation and also indicated a greater sensitivity of this tissue to hypoxic and reoxygenating conditions over time (Figure 7B). Venn diagram analysis (Figure 7C) highlighted that there was a more significant number of differentially expressed transcripts in the hypoxic conditions compared to the reoxygenation conditions. In the adductor muscle, a more substantial number of transcripts were observed that were

only expressed during hypoxia, in contrast to those that showed exclusive regulation in reoxygenation (Figure 7C). Interestingly, transcripts that experienced upregulation in both the hypoxia and reoxygenation periods were found to be more numerous compared to those that were exclusively manifested during reoxygenation.

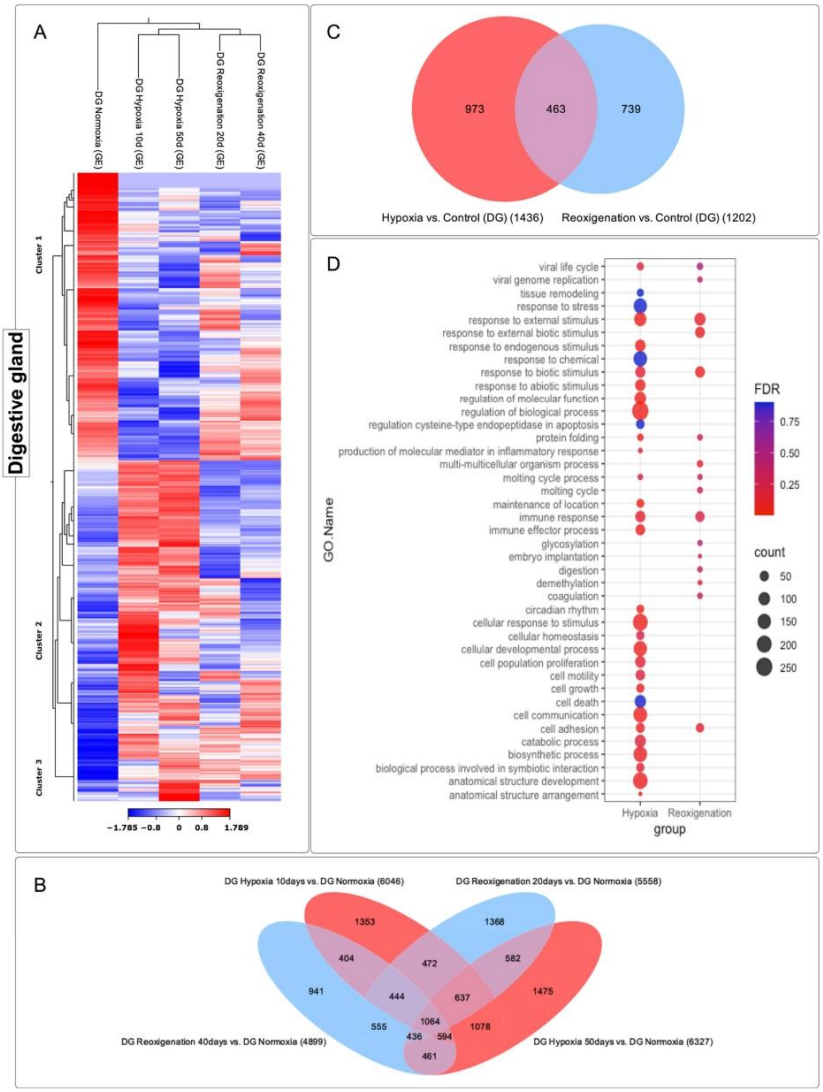

Figure 6. Comparative analysis of the transcriptome in the digestive gland of *M. chilensis*. (**A**) The heatmap shows comparisons for each group (normoxia, hypoxia 10 days, reoxygenation 20 days,

hypoxia 50 days, and reoxygenation 40 days). Red, positive log fold-change (log FC) indicates higher expression in each treatment; blue, negative log FC. Grouping was applied by columns (groups compared) and rows (transcripts analyzed), divided into clusters. (**B**) Venn diagram shows the number of unique and overlapping transcripts differentially expressed after exposure to hypoxia–reoxygenation. Sampling was performed at 10 and 50 days of hypoxia and 20 days and 40 days of reoxygenation. A total of 1475 transcripts were differentially expressed in the digestive gland at 50 days subjected to hypoxia and were not differentially expressed in any other sampling. There were 1078 most common overlapping transcripts, which were differentially expressed both at 10 days and 50 days under hypoxia conditions. Genes regulated in hypoxia are highlighted in red, while those regulated in reoxygenation are highlighted in blue. (**C**) Venn diagram shows overlaps of genes differentially expressed compared with aerated controls in hypoxia and reoxygenation in the digestive gland. Genes regulated in hypoxia are highlighted in red, while those regulated in reoxygenation are highlighted in blue. (**D**) Function annotation and Gene Ontology (GO) term enrichment analysis of DEGs in upregulated and downregulated genes in response to hypoxia in the digestive gland. FDR: false discovery rate. The most representative and significant molecular functions, biological processes, and cellular components are represented. The circumference size indicates the number of DEGs associated with the process, and the dot color indicates the significance of the enrichment (FDR-corrected *p*-values).

3.7. GO Enrichment Analysis in the Adductor Muscle of M. chilensis under Hypoxic and Reoxygenation Conditions

To identify the altered biological processes in the adductor muscle of *M. chilensis* under hypoxic and reoxygenating conditions, GO enrichment analysis was performed (Figure 7D). This analysis revealed that hypoxia is significantly associated with a variety of biological processes, including response to oxygen, response to extracellular stimuli, response to external stimuli, response to abiotic stimuli, regulation of membrane potential, regulation of localization, recognition of phagocytosis, immune response, effector process of the immune response, humoral immune response, defense response, cellular response to external stimuli, cellular response to environmental stimuli, cellular recognition, cellular mobilization, cell death in response to oxidative stress, bone remodeling, and movement based on actin filaments (Figure 7D). In comparison, reoxygenation showed a lower number of annotated GO terms relative to hypoxia (Figure 7D). Furthermore, the transcript count at the terms was lower (Figure 7D). Common terms identified in reoxygenation and hypoxia included response to extracellular stimuli, response to external stimuli, response to abiotic stimuli, and hormone level regulation (Figure 7D). In addition, terms that were not found in hypoxia were recorded in reoxygenation, such as vitamin metabolism, transport, regulation of hormone levels, keratinocyte differentiation, localization establishment, and digestion. These results suggest that hypoxia induced a series of biological changes in the adductor muscle of *M. chilensis*. These changes included activating the immune response, the cellular response to external stimuli, and regulating energy metabolism. Reoxygenation, however, was associated with less activation of these processes.

3.8. Identification and Expression of the mTOR Signaling Pathway in M. chilensis under Hypoxia

In this study, gene expression analysis was carried out in the gills, digestive gland, and adductor muscle of *M. chilensis* under hypoxic conditions. Through the transcripts generated from sequencing, 38 key genes involved in different stages of the mTOR signaling pathway were identified in *M chilensis* under hypoxia. These findings allowed the construction of a putative model of the mTOR signaling pathway under hypoxic conditions (Figure 8A). Some key genes stood out in these clusters. Different regulatory patterns were recorded in several tissues in response to hypoxia and reoxygenation (Figure 8B). For example, TELO2 showed similar behavior in the digestive gland and gills, being downregulated in hypoxia and upregulated in reoxygenation. In contrast, in the adductor muscle, it was upregulated

in both conditions. The MTOR gene showed differential regulation in the three tissues, with both downward and upward responses depending on hypoxia and reoxygenation.

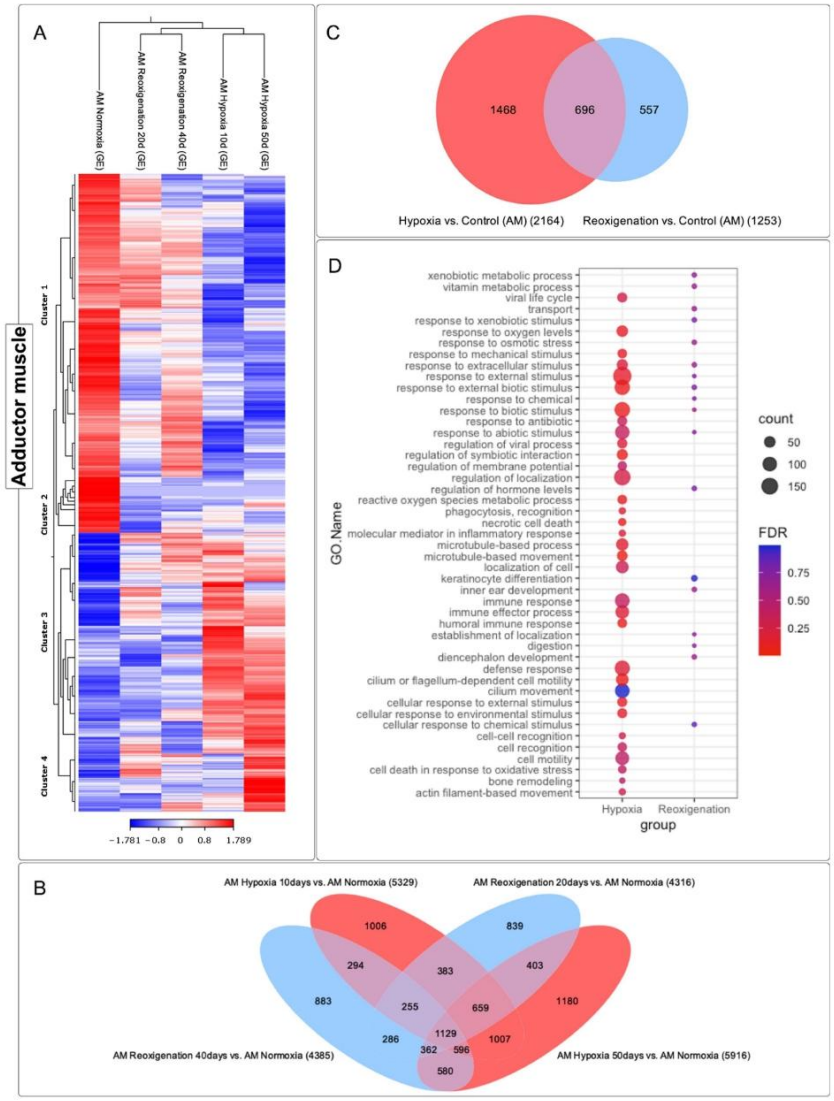

Figure 7. Gene expression analysis of the differentially expressed genes during hypoxia in the adductor muscle of *M. chilensis*. (**A**) Heatmap and hierarchical clustering show the most robust upregulated genes

in red and downregulated genes in blue. The dendrogram clusters genes with similar expression change patterns. (**B**) Venn diagram shows the number of unique and overlapping transcripts differentially expressed after exposure to hypoxia–reoxygenation. Sampling was performed at 10 and 50 days of hypoxia and 20 days and 40 days of reoxygenation. A total of 1180 transcripts were differentially expressed in the adductor muscle at 50 days subjected to hypoxia and were not differentially expressed in any other sampling. There were 1129 most common overlapping transcripts, which were differentially expressed at both 10 and 50 days under hypoxia conditions, as well as at 20 and 40 days under reoxygenation conditions. Genes regulated in hypoxia are highlighted in red, while those regulated in reoxygenation are highlighted in blue. (**C**) Venn diagram shows overlapping genes differentially expressed compared with aerated controls in hypoxia and reoxygenation in adductor muscle. Genes regulated in hypoxia are highlighted in red, while those regulated in reoxygenation are highlighted in blue. (**D**) Function annotation and Gene Ontology (GO) term enrichment analysis of DEGs in upregulated and downregulated genes in response to hypoxia. FDR: false discovery rate. The most representative and significant molecular functions, biological processes, and cellular components are represented. The circumference size indicates the number of DEGs associated with the process, and the dot color indicates the significance of the enrichment (FDR-corrected *p*-values).

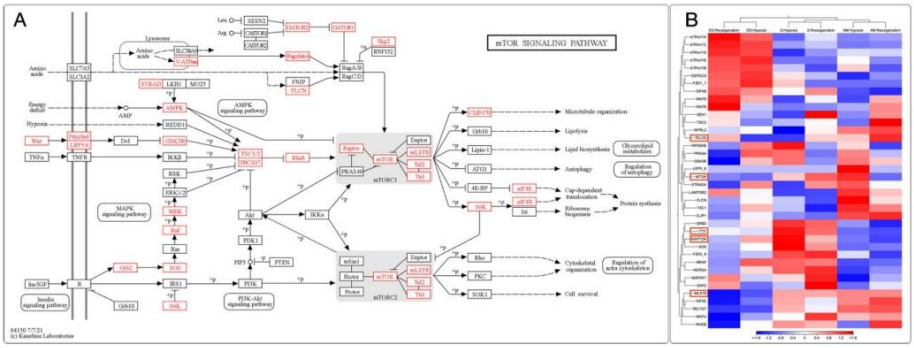

Figure 8. Illustration of the mTOR signaling pathway in *M. chilensis* under hypoxia conditions. (**A**) Interaction between hypoxia and the mTOR signaling pathway in gills. (**B**) Heatmap and hierarchical clustering to show MTOR under hypoxic conditions and reoxygenation in the digestive gland (DG), gill (G), and adductor muscle (AM).

3.9. Transcriptional Response of HIF and PHD in Different Tissues of M. chilensis during Hypoxia and Reoxygenation Phases

The HIF gene is located on chromosome 9, while PHD resides on chromosome 4 (Figure 9A). The relative expression levels of HIF and PHD mRNA in each tissue revealed heterogeneous regulation patterns (Figure 9B). In the gill, HIF experienced upregulation in all treatments including the control group, while PHD showed downregulation in all treatments including the control group (Figure 9B). An increase in the expression of transcripts for HIF and a decrease in transcripts for PHD was observed in the gill after the first 10 days of exposure to hypoxia, followed by a stabilization of the levels of both transcripts from day 20 to day 50 (Figure 9C). Similarly, upregulation of HIF and PHD was detected in this tissue during hypoxia compared to reoxygenation (Figure 9C). Subsequently, after reoxygenation on day 40, the upregulation of HIF and PHD was higher compared to reoxygenation on day 20 (Figure 9C). In the adductor muscle, an upregulation of HIF and PHD was observed in the control group and in reoxygenation at 40 days, while in the rest of the treatments, HIF was downregulated and PHD was upregulated (Figure 8B). HIF and PHD exhibited upregulation in the digestive gland in all cases (Figure 9B).

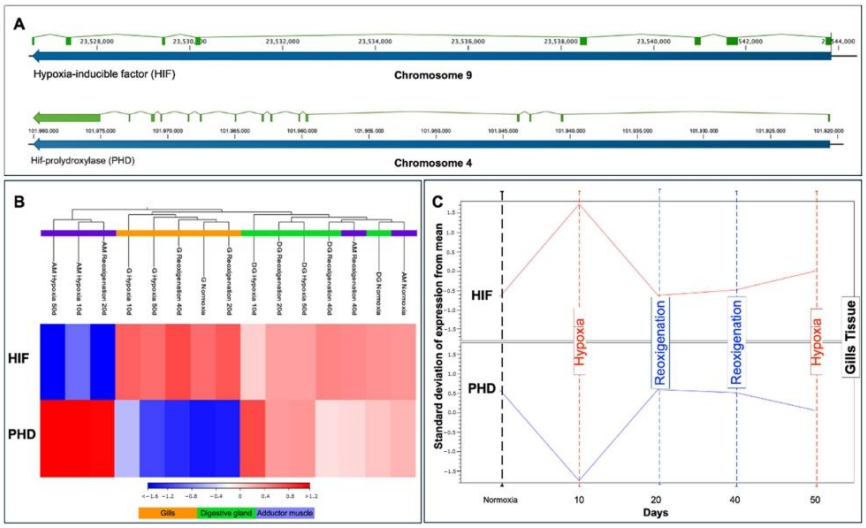

Figure 9. Comparative analysis of HIF and PHD genes in *M. chilensis* under hypoxia conditions. (**A**) Localization of Hif-α and Phd on chromosomes. HIF is located in chromosome 9, and PHD in chromosome 4. (**B**) Heatmap and hierarchical clustering to show HIF and PHD mRNA regulation patterns in gills, digestive gland, and adductor muscle under hypoxia and reoxygenation conditions. (**C**) Standard deviation of HIF and PHD expression in gills versus mean expression in reoxygenation and hypoxia. At 10 days in hypoxia, HIF is upregulated, and PHD is downregulated. The red line represents HIF, while the blue line represents PHD.

3.10. Identifying and Expressing Transcripts in the Toll-like Receptor, Citrate Cycle (TCA), and Apoptosis Signaling Pathways in the Gills of M. chilensis under Hypoxia

Through the de novo assembly of the transcripts obtained by sequencing, key genes involved in various stages of the Toll-like receptor signaling pathway, the citrate cycle (TCA), and apoptosis in the context of hypoxia were identified, which allowed the construction of putative models for each of these pathways (Figures 10A,C and 11A). The results revealed significant changes in the expression of genes related to Toll-like receptor signaling pathways, citrate cycle (TCA), and apoptosis in the gills of *M. chilensis* under hypoxia. In the case of the Toll-like receptor signaling pathway, three hierarchical clusters of RPKM values were generated, allowing a detailed view of its regulation to be obtained (Figure 10B). This analysis highlighted significant changes in gene expression of genes related to this pathway. Cluster 1, which includes genes such as TLR2, NF-κB, and RAC1 related to immune response, showed downregulation during the reoxygenation process at 20 days (Figure 10B). Regarding the apoptosis signaling pathway, six clusters were generated to identify differentially expressed transcripts (Figure 10D). Cluster 2 of this pathway was composed of the genes ENDOG, ITPR 1, CASP 9, CTSF, and CTSL, which play a critical role in cell death (Figure 10C). These genes exhibited upregulation under normoxia conditions and downregulation under hypoxia and during reoxygenation (Figure 10D). Finally, regarding the citrate cycle (TCA), eight hierarchical clusters were generated to identify differentially expressed transcripts (Figure 11B). This also revealed significant changes in the gene expression of genes related to this pathway. Cluster 1 of this pathway was composed of the MDH1 and FH genes, and cluster 2, formed by the DLD and ACO genes, plays a fundamental role in the enzymatic reactions that convert carbohydrates, fats,

and proteins into energy. These genes showed upregulation under hypoxic conditions and downregulation during normoxia and reoxygenation (Figure 11B).

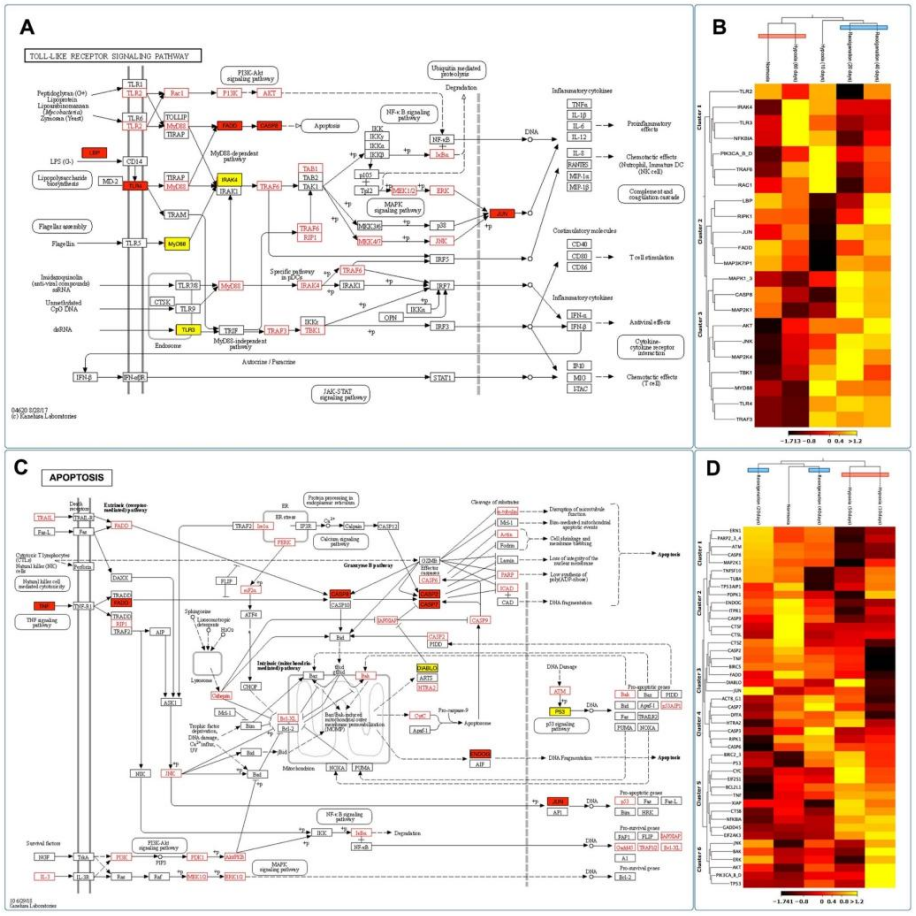

Figure 10. Illustration of the Toll-like receptor signaling and apoptosis pathways in *M. chilensis* gills under hypoxia conditions. (**A**) Toll-like receptor is an inducible transcription factor that inactivates JUN, thereby regulating the hypoxia process. (**B**) Heatmap and hierarchical clustering show JUN downregulated under hypoxic conditions and upregulated under reoxygenation. (**C**) In the intrinsic apoptotic pathway, cellular stress leads to Bak oligomerization, which permeates the mitochondrial outer membrane, releasing apoptogenic factors, including cytochrome c. In the cytosol, cytochrome c activates caspase 9, which cleaves and activates executioner caspases, such as caspase 6 and 7. In the extrinsic apoptotic pathway, ligating death receptors lead to the recruitment of adaptor proteins and subsequent activation of caspase 8, which activates executioner caspases. In addition, activation of apoptosis by the extrinsic pathway was mediated by TNF-α. (**D**) Heatmap and hierarchical clustering show genes regulated under hypoxia conditions and reoxygenation in the apoptosis pathway.

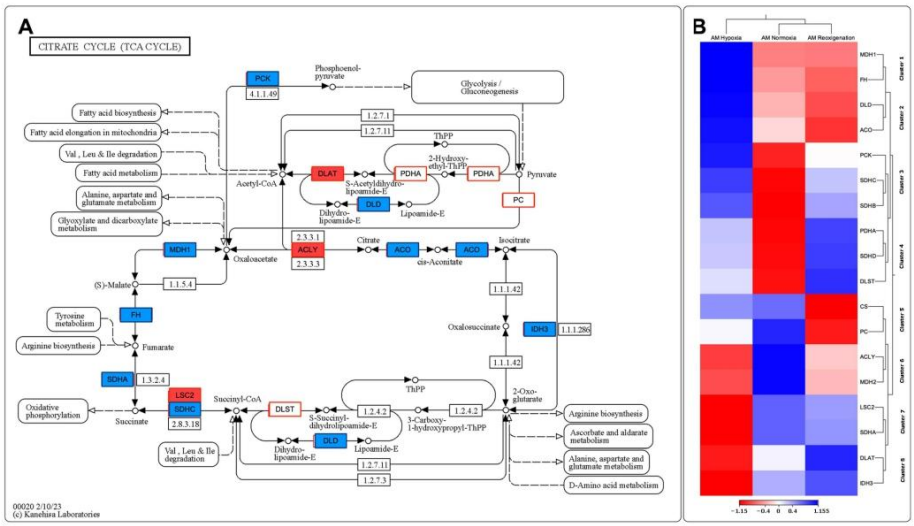

Figure 11. Illustration of the citrate cycle (TCA cycle) in *M. chilensis* gills under hypoxia conditions (**A**). Under hypoxic conditions, the metabolic activity shifted from oxidative to glycolytic metabolism. This metabolic switch was primarily regulated by increased hypoxia-inducible factor (HIF) activity and enhanced glycolysis. Genes upregulated of the cycle are highlighted in blue. Genes downregulated of the cycle are highlighted in red. (**B**) Heatmap and hierarchical clustering show genes related to the citrate cycle under hypoxic and reoxygenation conditions. Genes with similar expression patterns are grouped through hierarchical clustering, providing insights into the coordinated regulation of genes involved in the citrate cycle under hypoxia and reoxygenation conditions.

4. Discussion

Oxygen is a dominant ecological factor affecting benthic organisms' biomass and species composition [98]. Therefore, the effect of hypoxia can be dramatic and have essential consequences on benthic species that are not adapted to low dissolved oxygen environments for extended periods [22,99]. The Chilean mussel's capacity for adaptation to hypoxia has yet to be well known. Thus, this study aimed to analyze the transcriptome of *M. chilensis* and elucidate the specific gene expression in three tissues (gills, digestive gland, and adductor muscle) subjected to hypoxia. Most Chilean aquaculture farms are in Chiloé Island in the Los Lagos Region. Therefore, the mussels were collected from a farm in Puerto Montt, where there was a risk of hypoxic events caused by upwelling and eutrophication. This study is the first conducted on the effect of hypoxia in *M. chilensis*.

Hypoxia activates various molecular pathways in bivalve mollusks as an adaptive mechanism to restore oxygen homeostasis [100]. In recent decades, transcriptomic responses to hypoxia have been studied in several marine bivalve species [82,101–103]. In this study, a transcriptomic reaction was observed in the gills, adductor muscle, and digestive gland in response to hypoxic stress, indicating the importance of these tissues in regulating hypoxia in the Chilean mussel. Different tissue-specific changes in gene expression were observed in the three analyzed tissues, suggesting a tissue-specific response in the mussel. The insulin-like growth factor binding protein complex acid labile subunit gene was expected to be expressed in all tissues. This is a growth factor known to activate signal transduction pathways that lead to the expression of HIF-1α, thereby stabilizing HIF-1α under normoxic conditions [104].

According to the PCA of differential expression, PC1 and PC2 play a significant role in explaining the global variation in gene expression. The findings also reveal noticeable disparities in expression patterns across different tissue types, providing valuable insights into the underlying gene expression patterns in the studied tissues. These results help identify crucial components responsible for gene expression variation and highlight tissue-specific differences in the transcriptome, consistent with previous studies [3,29].

For aerobic organisms, post-hypoxic reoxygenation is associated with additional challenges due to the energy needed to restore cellular homeostasis and replenish energy stores [29]. The re-establishment of oxygen and nutrient supply, along with the restart of mitochondrial energy production, leads to oxidative damage through an increase in reactive oxygen species (ROS) from the mitochondrial electron transport system (ETS) [29,105]. However, a partial recovery of the gene transcription profiling after hypoxia was observed during reoxygenation, consistent with prior research [29,106]. This is the first time it has been reported that hypoxia generates a more significant response to regulatory patterns than reoxygenation.

In contrast to other studies where changes are more pronounced during reoxygenation, such as in the profile of apoptotic, inflammatory, and autophagic biomarkers [29], the current findings indicate that physiological and cellular stress associated with reoxygenation typically occurs within minutes to hours after the return of oxygen [3]. These findings highlight the importance of regulating cell survival pathways in tolerating intermittent hypoxia in marine bivalves and demonstrate the effectiveness of molecular markers in sentinel marine bivalves for monitoring hypoxia-induced stress in estuarine and coastal habitats.

This section addresses the increasing contribution of the unfolded protein response (UPR) in the endoplasmic reticulum (ER) under hypoxic conditions for the first time in bivalve mollusks. The ER is a dynamic intracellular organelle with multiple critical functions in a wide range of processes, including cellular homeostasis; development; the stress response; protein synthesis, folding, modification, and transport; lipid transport; storage of calcium ions within its lumen and their regulated release to the cytoplasm; metabolic regulation; reactive oxygen species (ROS) signaling; autophagy; and signaling and adaptation to constantly changing environments [107]. High protein synthesis, folding, modification, and transport levels are required to initiate and maintain effective immune responses, all coordinated by the endoplasmic reticulum [108]. It is important to note that various conditions inside and outside the cell can affect the ability of this organelle to process proteins, resulting in a state known as "endoplasmic reticulum stress", which activates the unfolded protein response (UPR) [108]. The UPR is a cellular signaling system that readjusts the folding capacity of the ER to restore protein homeostasis in response to endoplasmic reticulum stress [109]. Unfolded or misfolded proteins activate the UPR pathway to cope with ER stress, activating a series of cell death pathways [110]. Apoptotic proteins such as caspase 3, calpains, and cytochrome c interact with and regulate IP3Rs, playing a crucial role in apoptotic cell death [111]. On the other hand, increased ROS levels result in misfolded/unfolded proteins accumulating, activating the unfolded protein response (UPR) [112]. Furthermore, abnormal activation of the UPR may contribute to the development of various diseases, such as neoplasia and metabolic disorders [108].

Endoplasmic reticulum (ER) stress and the activation of the unfolded protein response (UPR) have been associated with intracellular lipid accumulation [113]. The ER, as a site of synthesis of a variety of essential lipids, including cholesterol, triacylglycerols, and phospholipids, plays a critical role in the lipid homeostasis of organisms, including bivalve mollusks [114,115].

Furthermore, the fact that the proteins and lipids that make up the Golgi apparatus originate in the endoplasmic reticulum (ER) underlies this organelle's importance in synthesizing and processing molecules destined for cellular secretion [116]. The close association between the UPR and lipid homeostasis in the context of metabolic diseases

suggests the possible involvement of these processes in the pathogenesis of various diseases [105,117]. Despite significant advances in treating some pathologies, there is still a gap in our complete understanding of the role of the UPR. Therefore, additional research is required to explore the broad therapeutic opportunities that UPR could offer to treat several diseases [118].

In the GO enrichment analysis, differentially expressed transcripts assigned to KEGG pathways related to metabolism, cellular processes, and environmental sensing were observed, in addition to ubiquitin binding as shown in Figure 3C, consistent with what was found in other studies [119].

A differential expression of transcripts associated with enzymes involved in the metabolism of amino acids, such as V-ATPase as shown in Figure 8A and in the amino acids alanine, aspartate, glutamate, tyrosine, and arginine as shown in Figure 11A, was also observed. Amino acids are essential in the anaerobic metabolism of bivalves [119]. Protein catabolism has also been demonstrated in bivalves during hypoxia as a potential mechanism for maintaining amino acid stores, as amino acids are essential in the osmotic balance [3,119,120]. In the present study, differential expression of transcripts associated with amino acid metabolism was observed; for example, MDH1 was upregulated in hypoxia and downregulated in normoxia and reoxygenation, PCK was upregulated in hypoxia and downregulated in reoxygenation, ACLY was downregulated in hypoxia and reoxygenation and upregulated in normoxia, and IDH3 was downregulated in hypoxia and upregulated in reoxygenation and normoxia. This mechanism may be associated with maintaining free amino acids as an essential strategy for survival under hypoxic conditions [119]. Aspartate is usually depleted during anaerobic transamination reactions [121].

Figure 11 records an underexpression of transcripts associated with critical enzymes related to aerobic respiration and the progression of the citric acid cycle, which is consistent with what was found in other studies [119].

The increased upregulation of ACO during hypoxia, concomitant with a decrease in normoxia and reoxygenation, points to a critical role of this enzyme in isocitrate production under conditions of low oxygen availability. Similarly, the upregulation of PCK during hypoxia and a decrease in normoxia and reoxygenation indicate its involvement in pyruvate production under hypoxic conditions. These changes in transcript expression are significant findings, given that these genes are associated with aerobic respiration, and their modification in expression could indicate an alteration in aerobic metabolic pathways [119].

Furthermore, it is essential to highlight that the UPR, an adaptive response to hypoxia, nutrient deprivation, and stress, plays a crucial role in several types of neoplasia, acting as a dynamic promoter in developing these diseases. This finding suggests that regulation of the UPR could be a promising strategy for cancer treatment [118].

A fundamental characteristic of neoplastic cells is their ability to metabolize glucose rapidly and their high proliferation rate [122]. This phenomenon may result in poor vascularization of the tumor mass, leading to insufficient oxygen supply [122]. Furthermore, neoplastic cells require high levels of protein synthesis to maintain their uncontrolled growth and proliferation [123]. The endoplasmic reticulum (ER) stress and activation of the UPR typically trigger these oncogenic conditions [124].

Several oncogenic, transcriptional, and metabolic abnormalities in various malignancies collaborate to create hostile microenvironments that perturb ER homeostasis in malignant cells [124]. These changes induce a persistent stress state in the ER, which has been shown to regulate multiple tumor-promoting characteristics in neoplastic cells [124]. Therefore, ER stress sensors' abnormal activation and subsequent signaling pathways have emerged as critical tumor growth and metastasis regulators [124]. Physiological or pathological activation of the UPR can affect the survival, metabolism, function, and fate of immune cells [108].

Efficient cellular function depends on oxygen availability to maintain normal cell function. However, using oxygen at this level generates free radicals, which can lead to oxidative stress. An intricate network of surveillance mechanisms is required to regulate

this system effectively to maintain adequate oxygen homeostasis [125]. Maintaining the organism's homeostasis depends on integrating external and systemic signals and the ability to perceive cellular perturbations to trigger adaptive responses [117].

Furthermore, enriched with a high concentration of mitochondria, cells exhibit a demanding requirement for glucose as an energy substrate. This heightened energy demand generates intense mitochondrial activity, inevitably producing free radicals as a byproduct. Cells resort to adaptive stress response pathways, which allow them to survive oxidative stress and minimize cellular damage to preserve this balance. These stress response pathways depend on optimal endoplasmic reticulum (ER) function and activation. The UPR is a critical cellular pathway that maintains normal ER function and cell survival [125]. The UPR transmits information about the folding state of proteins to the nucleus and cytosol to adjust the protein folding capacity of the cell [117].

Interestingly, the UPR consists of two opposing signaling pathways: one that promotes cell survival by reducing ER damage during stressful situations and another that induces apoptosis if the stress is prolonged or not adequately mitigated [125]. As described in Figure 3A, the homeostasis of the endoplasmic reticulum (ER) is achieved thanks to the presence of the response to misfolded proteins (UPR), which is essential for the maintenance of the integrity and function of the ER in the context of hypoxic situations. Figure 8A describes, for the first time in bivalve mollusks, the effect of the UPR on cellular metabolism by attenuating general protein translation through the phosphorylation of eIF4B activated by S6K. This downregulation reduces protein loading in the ER and increases ATP availability for processes such as protein folding and degradation, consistent with other studies [105].

Apoptosis, autophagy, translation, energy metabolism, and inflammation are fundamental cellular processes coordinated by intracellular signaling pathways, particularly the regulatory complex known as mTOR and the endoplasmic reticulum stress response (UPR) [126]. mTOR, a protein kinase, is crucial in regulating cell proliferation, survival, metabolism, and immune response. On the other hand, adenosine monophosphate-activated protein kinase (AMPK) acts as a critical sensor of cellular energy, influencing lipid homeostasis and glucose metabolism. These pathways converge in autophagy [127]. The induction of the UPR arises in response to the decrease in cellular ATP resulting from glucose deprivation, which affects the function of the endoplasmic reticulum calcium pump and intracellular calcium levels. Under prolonged endoplasmic reticulum stress, mTORC1 participates in apoptotic signaling by inhibiting the survival kinase Akt and selectively activating the JNK protein kinase pathway [126].

When the ability of the UPR to maintain proteostasis is overwhelmed due to ER stress, it triggers activation of the canonical apoptosis pathway, which involves conformational activation of proapoptotic members of the BCL-2 family in the mitochondria, BAX, and BAK, with simultaneous assembly of the apoptosome and activation of executioner caspase 3. The BCL-2 family proteins, including PUMA and NOXA, are essential factors mediating ER-stress-induced apoptosis in various cellular systems, where activation mechanisms involve only transcriptional regulation and post-translational modifications of proapoptotic BCL-2 proteins. The UPR is widely involved in the signal transduction of inflammatory responses. PERK-mediated phosphorylation of eIF2α attenuates global protein synthesis and promotes the activation of nuclear factor-κB to induce pro-inflammatory genes [117]. PERK-mediated phosphorylation of eIF2α is observed in Figure 10C, in addition to the activation of the nuclear factor-κB signaling pathway.

In genomics and molecular biology, regulating gene expression in response to oxygen availability is vital for cellular adaptation to changing conditions caused by climate change. In this context, hypoxia-inducible factor-1 (HIF-1) emerges as a central figure in orchestrating cellular responses to hypoxia as an adaptive response. Under normoxia conditions, HIF-1α, one of the subunits of HIF-1, is constantly synthesized but undergoes rapid degradation mediated by the HIF–prolyl hydroxylase (PHD) complex. This pro-

cess depends on intracellular oxygen since PHD requires molecular oxygen as a cofactor. Hydroxylation of specific residues on HIF-1α by PHD marks the protein for proteasomal degradation. Therefore, HIF-1α is maintained at low levels under normoxia conditions due to its continuous degradation, which prevents the activation of target genes associated with the hypoxia response [128].

However, in a hypoxic environment, oxygen availability decreases, inhibiting PHD activity. Lack of oxygen prevents the hydroxylation of HIF-1α, stabilizing this subunit. Stabilized HIF-1α undergoes translocation to the cell nucleus, where it forms an active complex with HIF-1β, and together, they act as a transcription factor that binds to hypoxia response regulatory elements (HREs) in target gene promoters. The activation of HIF-1 triggers a cascade of molecular events that impact cellular physiology in multiple ways. HIF-1-regulated target genes are involved in anaerobic glycolysis, cell signaling, and oxidative phosphorylation. This allows the cell to adapt to hypoxia by increasing glucose uptake and utilization, improving cell survival, and modulating the immune response. These results, in addition to suggesting post-translational regulation of HIF-α through PHD, strongly indicate that an oxygen-dependent mechanism plays a fundamental role in the stability and activity of HIF-α. Although HIF-α is regulated through PHD, the latter is controlled by HIF-α, forming a negative feedback loop. The results of the present study, as described in Figure 6B, show a differential transcriptional response of Hif-α and PHD in the tissues analyzed. Gills showed a prominent expression that was less marked in the digestive gland, which is consistent with other studies. The high sensitivity of the oxygen-sensing pathway in the gills to hypoxia can be attributed to their direct exposure to seawater, thus making them the first tissue to feel the detrimental effects of hypoxia [82].

Furthermore, these structures play a fundamental role in regulating essential biological processes, such as gas transfer and osmotic balance, and activating adaptive responses to hypoxia [128]. The upregulation of Hif-α in the gills indicates an adaptation to hypoxic conditions. At the same time, the decrease in PHD in this tissue could be involved in stabilizing Hif-α.

In the adductor muscle, after 40 days of reoxygenation, transcript expression resembles the control group, suggesting long-term adaptation. In the subsequent reoxygenation phase at 20 days (Figure 6C), the expression of hif-α mRNA was not affected by normoxia, while the reduction observed in the amount of HIF-α protein at 40 days of reoxygenation could be attributable to degradation by PHD activity, being consistent with other studies [128]. Furthermore, the significant role played by HIF-α may be restricted to initiating the sequence of events that occur a few hours after oxygen deprivation [128]. There were no significant differences in the digestive gland regulation of Hif-α and PHD in the different treatments.

In summary, this study's findings revealed that the gills and adductor muscles were more sensitive to the effects of hypoxia than the digestive gland. These results provided a better understanding of the regulation of Hif-α and PHD in various tissues. They established a basis for future investigations into the function of these genes in adaptive and pathological responses.

Marine organisms subjected to hypoxia face the critical challenge of reduced energy supply due to oxygen deficiency, as energy is essential for the normal functioning of all biological systems [129]. To cope with energy shortages under hypoxic conditions, these organisms rely heavily on hypoxia-inducible factor-1 (HIF-1), which plays a crucial role in regulating oxygen transport genes and energy production through processes such as glycolysis [130]. Various investigations in mussels have reported findings on the impact of hypoxia on gene expression related to oxidative stress and the activity of antioxidant enzymes [17,131]. This is directly related to increased production of reactive oxygen species (ROS) in cells, posing a potential risk of oxidative damage. Exposure to hypoxia may also have repercussions beyond cellular biochemistry [84]. In bivalve mollusks, hypoxia can inhibit gonadal development [132]. These effects can be attributed to changes in energy balance due to hypoxia, which, in turn, negatively affects reproduction and population

dynamics [133]. HIF-1 activation and accumulation depend on the presence of reactive oxygen species (ROS), posing an exciting paradox [78]. Although these species are necessary for HIF-1 signaling, they can also induce oxidative stress in the organism [79]. It is in this context that superoxide dismutase (SOD) emerges as an irreplaceable enzyme. SOD specifically catalyzes the decomposition of excess superoxide, playing an essential role in protecting the organism against oxidative stress [78]. Previous research in marine animals has confirmed the importance of SOD by significantly increasing its activity under hypoxic conditions [83].

Blue mussels lack adaptive immunity, relying instead on innate immunity for survival and defense against biological and environmental threats [78]. Hypoxia negatively impacts the immunity of blue mussels by suppressing their immunocompetence [78,134]. Therefore, it is crucial to understand the ability of mussels to maintain their innate immunity under hypoxic conditions, which determines their adaptation and survival in changing and challenging environments [78]. This study is the first to record hypoxia's effect on the mussel immune system in multiple tissues, including the gill, adductor muscle, and digestive gland. The results indicate that this effect was maintained mainly in the gill and digestive gland during reoxygenation. Interestingly, in all tissues analyzed, the impact on the immune system was more pronounced during hypoxia than reoxygenation. This finding raises important questions about adapting the mussels' immune system to fluctuations in oxygen levels. The specificity of the immune response in the gill and digestive gland suggests the existence of unique regulatory mechanisms in these tissues, which could be related to their direct exposure to variations in oxygen concentration. It is crucial to highlight that, uniformly in all tissues analyzed, hypoxia caused a more pronounced impact on the immune system than reoxygenation. This fact highlights the importance of thoroughly understanding the effects of hypoxia on mussel immunity and its potential implications for the health of marine populations in the context of environmental change. This study lays the foundation for future research to unravel the molecular mechanisms underlying these specific immune responses in mussels, which could have significant implications for the conservation and management of marine ecosystems.

The blue mussel is known for its outstanding tolerance to hypoxia [78]. It is considered a conformist organism in terms of its response to dissolved oxygen in the environment [78]. This behavior means it adapts to the amount of oxygen available in its environment without adequate regulation, and its respiration rate varies directly with the external oxygen level [78]. When the dissolved oxygen concentration drops below 5–6 mg L-1, the blue mussel decreases its respiration rate and reduces its total energy requirement [78]. This ability to adjust their metabolism in the face of hypoxic conditions is an impressive example of an adaptation of marine organisms to changing and challenging environments [78]. In previous research on the gills of *Mytilus galloprovincialis*, it has been suggested that these mollusks have an adaptive response to hypoxic conditions [79]. In the present study, a notable decrease in gene expression in the gills was observed when comparing the first and third exposures of mussels to hypoxia, as evidenced in Figure 2. This finding reinforces the growing body of evidence showing that mytilids can adapt to environments with reduced oxygen levels, hinting at a genomic response to these challenging conditions. It is essential to highlight that the adaptation mechanism differs between different tissues since the digestive gland and the adductor muscle do not follow this same trend observed in the gills. This suggests that the gill, being the tissue most exposed to hypoxia due to its function in gas exchange, is the one that adapts most quickly to these adverse conditions. These findings provide valuable insight into the molecular mechanisms underlying mussel adaptation to hypoxia and highlight the importance of understanding how different tissues can respond differently to the same environmental challenges.

5. Conclusions

For the first time, this study investigated the transcriptomic response of three tissues in *M. chilensis* under hypoxic stress using the Illumina platform technology. It provides new insights and a comprehensive understanding of the molecular mechanisms underlying tolerance and resistance to hypoxia in the Chilean mussel. The differential expression of transcripts detected in the gills, digestive gland, and adductor muscle offers a list of candidate adaptive genes that control multiple fitness-related traits in populations subjected to hypoxia. It highlights the adaptation mechanisms of the Chilean mussel to hypoxia induced by climate change. These candidate adaptive genes could be used to select future breeding lines of *M. chilensis* broodstock for laboratory production of seedlings intended for cultivation or restocking.

Moreover, the identified Gene Ontology terms, such as negative regulation of endoplasmic reticulum unfolded protein response and TORC1 signaling, offer valuable insights into the molecular mechanisms underlying the adaptation of *M. chilensis* to hypoxic conditions. The negative regulation of endoplasmic reticulum unfolded protein response suggests potential mechanisms for downregulating cellular stress and maintaining protein homeostasis under oxygen-deficient conditions. The involvement of TORC1 signaling indicates a potential role in coordinating cellular responses to hypoxia, providing insights into metabolic pathway regulation and environmental adaptation. The GO enrichment analysis revealed that Wnt and β-catenin are key signaling pathways involved in the adaptation mechanism of the Chilean mussel to hypoxia, offering valuable information for further investigation of critical molecules regulating hypoxia tolerance and gaining new insights into mechanisms of resistance to stress caused by hypoxia in marine bivalves.

Furthermore, these findings serve as biomarkers for detecting natural seed beds and farms that have experienced hypoxic events. These new genomic resources provide tools for designing a genetic selection plan for this commercially important species in aquaculture and contribute to the sustainable expansion management of an industry threatened by climate change. Additionally, they lay the groundwork for future research using RNA-seq and gene expression patterns on proteins involved in hypoxia, which can help explain the amount of genetic information inherited through epigenetic changes and the response of mussels to other environmental stressors or pathogenic agents.

Author Contributions: Conceptualization, M.M.-R., V.V.-M. and C.G.-E.; methodology, M.M.-R., V.V.-M. and C.G.-E.; software, V.V.-M. and C.G.-E.; validation, M.M.-R., V.V.-M., D.V.-M. and C.G.-E.; formal analysis, M.M.-R., V.V.-M., D.V.-M. and C.G.-E.; investigation, M.M.-R., V.V.-M. and C.G.-E.; resources, M.M.-R., V.V.-M. and C.G.-E.; data curation, M.M.-R., V.V.-M. and C.G.-E.; writing—original draft preparation, M.M.-R., V.V.-M. and C.G.-E.; writing—review and editing, M.M.-R., V.V.-M., D.V.-M. and C.G.-E.; visualization, M.M.-R., V.V.-M., D.V.-M. and C.G.-E.; supervision, M.M.-R., V.V.-M., D.V.-M. and C.G.-E.; project administration, M.M.-R., V.V.-M. and C.G.-E.; funding acquisition, M.M.-R., V.V.-M. and C.G.-E. All authors have read and agreed to the published version of the manuscript.

Funding: This research was funded by ANID-Chile, FONDAP #1523A0007, and FONDECYT #1210852. Secretaría de Educación Superior, Ciencia, Tecnología e Innovación (SENESCYT)—Ecuador/Contrato Nro. CZ05-000735-2018, Agencia Nacional de Investigación y Desarrollo (ANID)—Chile/Subdirección de Capital Humano/Beca de Doctorado Nacional 2019—Folio 21190791.

Institutional Review Board Statement: The animal study protocol was approved by the Ethics Committee of CONCEPCION UNIVERSITY (protocol code CEBB 1356-2023 approved in March 2023).

Informed Consent Statement: Not applicable.

Data Availability Statement: The original contributions presented in the study are included in the article, further inquiries can be directed to the corresponding author.

Conflicts of Interest: The authors declare no conflicts of interest.

References

1. Calle, X.; Jiménez-Gallegos, D.; Muñoz-Córdova, F.; Sánchez, P.; Lavandero, S. Mecanismo sensor y de adaptación a los niveles de oxígeno y su implicancia en las enfermedades cardiovasculares: A propósito del Premio Nobel de Fisiología-Medicina 2019. *Rev. Chil. Cardiol.* **2019**, *38*, 225–235. [CrossRef]
2. García, N.; Puentes, O.; Montalvo, J. Contaminación orgánica en el sector de la Bahía de Buena Vista cercano a la desembocadura de Río Guanó, Villa Clara, Cuba. *Rev. Cuba. Química* **2008**, *20*, 39–46.
3. Haider, F.; Falfushynska, H.; Timm, S.; Sokolova, I. Effects of hypoxia and reoxygenation on intermediary metabolite homeostasis of marine bivalves *Mytilus edulis* and *Crassostrea gigas*. *Comp. Biochem. Physiol. Part A Mol. Integr. Physiol.* **2020**, *242*, 110657. [CrossRef]
4. Ali, J.; Yang, Y.; Pan, G. Oxygen micro-nanobubbles for mitigating eutrophication induced sediment pollution in freshwater bodies. *J. Environ. Manag.* **2023**, *331*, 117281. [CrossRef]
5. Breitburg, D.; Levin, L.; Oschlies, A.; Grégoire, M.; Chavez, F.; Conley, D.; Garçon, V.; Gilbert, D.; Gutiérrez, D.; Isensee, K.; et al. Declining oxygen in the global ocean and coastal waters. *Science* **2018**, *359*, eaam7240. [CrossRef]
6. Capet, A.; Beckers, J.; Grégoire, M. Drivers, mechanisms and long-term variability of seasonal hypoxia on the Black Sea northwestern shelf—Is there any recovery after eutrophication? *Biogeosciences* **2013**, *10*, 3943–3962. [CrossRef]
7. Conley, D.; Carstensen, J.; Vaquer-Sunyer, R.; Duarte, C. Ecosystem thresholds with hypoxia. *Hydrobiologia* **2009**, *629*, 21–29. [CrossRef]
8. Sagasti, A.; Schaffner, L.; Duffy, J. Effects of periodic hypoxia on mortality, feeding and predation in an estuarine epifaunal community. *J. Exp. Mar. Biol. Ecol.* **2001**, *258*, 257–283. [CrossRef]
9. Silva, N.; Vargas, C. Hypoxia in Chilean Patagonian Fjords. *Prog. Oceanogr.* **2014**, *129*, 62–74. [CrossRef]
10. Melzner, F.; Thomsen, J.; Koeve, W.; Oschlies, A.; Gutowska, M.; Bange, H.; Hansen, H.; Körtzinger, A. Future ocean acidification will be amplified by hypoxia in coastal habitats. *Mar. Biol.* **2013**, *160*, 1875–1888. [CrossRef]
11. Scanes, E.; Scanes, P.; Ross, P. Climate change rapidly warms and acidifies Australian estuaries. *Nat. Commun.* **2020**, *11*, 1803. [CrossRef]
12. Scanes, E.; Parker, L.; Seymour, J.; Siboni, N.; King, W.; Danckert, N.; Wegner, K.; Dove, C.; O'Connor, A.; Ross, P. Climate change alters the haemolymph microbiome of oysters. *Mar. Pollut. Bull.* **2021**, *164*, 111991. [CrossRef]
13. Yáñez, E.; Lagos, N.; Norambuena, R.; Silva, C.; Letelier, J.; Muck, K.; Martin, G.; Benítez, S.; Broitman, B.; Contreras, H.; et al. Impacts of Climate Change on Marine Fisheries and Aquaculture in Chile. In *Climate Change Impacts on Fisheries and Aquaculture: A Global Analysis*; Phillips, B., Pérez-Ramírez, M., Eds.; John Wiley & Sons Ltd.: Hoboken, NJ, USA, 2017; Volume I, pp. 239–332.
14. Bianchi, T.; Arndt, S.; Austin, W.; Benn, D.; Bertrand, S.; Cui, X.; Faust, J.; Koziorowska-Makuch, K.; Moy, C.; Savage, C.; et al. Fjords as Aquatic Critical Zones (ACZs). *Earth-Sci. Rev.* **2020**, *203*, 103145. [CrossRef]
15. Iriarte, J.; Pantoja, S.; Daneri, G. Oceanographic Processes in Chilean Fjords of Patagonia: From small to large-scale studies. *Prog. Oceanogr.* **2014**, *129*, 1–7. [CrossRef]
16. Schmidtko, S.; Stramma, L.; Visbeck, M. Decline in global oceanic oxygen content during the past five decades. *Nature* **2017**, *542*, 335–339. [CrossRef]
17. Nogueira, L.; Ferraz, D.; Trevisan, R.; Garcia, D.; Da Silva, D.; Luiz, A.; Alves, E. Hypoxia effects on oxidative stress and immunocompetence biomarkers in the mussel *Perna perna* (Mytilidae, Bivalvia). *Mar. Environ. Res.* **2017**, *126*, 109–115. [CrossRef]
18. Kim, C.; Park, C.; Kim, E.; Nam, Y. Transcriptional modulation patterns of abalone *Haliotis discus hannai* hypoxia inducible factor-1α (HIF-1α) in interdependent crosstalk between hypoxia, infection, and environmental stresses. *Aquac. Rep.* **2021**, *19*, 100566. [CrossRef]
19. Levin, L.; Ekau, W.; Gooday, A.; Jorissen, F.; Middelburg, J.; Naqvi, S.; Neira, C.; Rabalais, N.; Zhang, J. Effects of natural and human-induced hypoxia on coastal benthos. *Biogeosciences* **2009**, *6*, 2063–2098. [CrossRef]
20. Grieshaber, M.; Hardewig, I.; Kreutzer, U.; Pörtner, H. Physiological and metabolic responses to hypoxia in invertebrates. *Rev. Physiol. Biochem. Pharmacol.* **1994**, *125*, 43–147. [CrossRef]
21. Chu, J.; Curkan, C.; Tunnicliffe, V. Drivers of temporal beta diversity of a benthic community in a seasonally hypoxic fjord. *R. Soc. Open Sci.* **2018**, *5*, 172284. [CrossRef]
22. Hernández-Miranda, E.; Veas, R.; Anabalón, V.; Quiñones, R. Short-term alteration of biotic and abiotic components of the pelagic system in a shallow bay produced by a strong natural hypoxia event. *PLoS ONE* **2017**, *12*, e0179023. [CrossRef]
23. Tirpe, A.; Gulei, D.; Ciortea, S.; Crivii, C.; Berindan-Neagoe, I. Hypoxia: Overview on Hypoxia-Mediated Mechanisms with a Focus on the Role of HIF Genes. *Int. J. Mol. Sci.* **2019**, *20*, 6140. [CrossRef]
24. Kodama, K.; Horiguchi, T. Effects of hypoxia on benthic organisms in Tokyo Bay, Japan: A review. *Mar. Pollut. Bull.* **2011**, *63*, 215–220. [CrossRef]
25. Batie, M.; Del Peso, L.; Rocha, S. Hypoxia and Chromatin: A Focus on Transcriptional Repression Mechanisms. *Biomedicines* **2018**, *6*, 47. [CrossRef]
26. Soldatov, A.; Gostyukhina, O.; Golovina, I. Antioxidant enzyme complex of tissues of the bivalve *Mytilus galloprovincialis* Lam. under normal and oxidative-stress conditions: A review. *Appl. Biochem. Microbiol.* **2007**, *43*, 556–562. [CrossRef]
27. Vale, G.; Mehennaoui, K.; Cambier, S.; Libralato, G.; Jomini, S.; Domingos, R. Manufactured nanoparticles in the aquatic environment-biochemical responses on freshwater organisms: A critical overview. *Aquat. Toxicol.* **2016**, *170*, 162–174. [CrossRef]

28. Pytharopoulou, S.; Sazakli, E.; Grintzalis, K.; Georgiou, C.; Leotsinidis, M.; Kalpaxis, D. Translational responses of *Mytilus galloprovincialis* to environmental pollution: Integrating the responses to oxidative stress and other biomarker responses into a general stress index. *Aquat. Toxicol.* **2008**, *89*, 18–27. [CrossRef]
29. Falfushynska, H.; Piontkivska, H.; Sokolova, I. Effects of intermittent hypoxia on cell survival and inflammatory responses in the intertidal marine bivalves *Mytilus edulis* and *Crassostrea gigas*. *J. Exp. Biol.* **2020**, *223*, jeb217026. [CrossRef]
30. Sokolova, I. Mitochondrial Adaptations to Variable Environments and Their Role in Animals' Stress Tolerance. *Integr. Comp. Biol.* **2018**, *58*, 519–531. [CrossRef]
31. Storey, K.; Storey, J. Metabolic rate depression in animals: Transcriptional and translational controls. *Biol. Rev. Camb. Philos. Soc.* **2004**, *79*, 207–233. [CrossRef]
32. Liao, C.; Liu, X.; Zhang, C.; Zhang, Q. Tumor hypoxia: From basic knowledge to therapeutic implications. *Semin Cancer Biol* **2023**, *88*, 172–186. [CrossRef]
33. Huang, R.; Zhou, P. HIF-1 signaling: A key orchestrator of cancer radioresistance. *Radiat. Med. Prot.* **2020**, *1*, 7–14. [CrossRef]
34. Jung-whan, K.; Tchernyshyov, I.; Semenza, L.; Dang, V. HIF-1-mediated expression of pyruvate dehydrogenase kinase: A metabolic switch required for cellular adaptation to hypoxia. *Cell Metab.* **2006**, *3*, 177–185. [CrossRef]
35. Bailey, P.; Nathan, J. Metabolic Regulation of Hypoxia-Inducible Transcription Factors: The Role of Small Molecule Metabolites and Iron. *Biomedicines* **2018**, *6*, 60. [CrossRef]
36. Krzywinska, E.; Stockmann, C. Hypoxia, Metabolism and Immune Cell Function. *Biomedicines* **2018**, *6*, 56. [CrossRef]
37. Sokolova, I.; Sokolov, E.; Haider, F. Mitochondrial Mechanisms Underlying Tolerance to Fluctuating Oxygen Conditions: Lessons from Hypoxia-Tolerant Organisms. *Integr. Comp. Biol.* **2019**, *59*, 938–952. [CrossRef]
38. Fava, L.; Bock, F.; Geley, S.; Villunger, A. Caspase-2 at a glance. *J. Cell Sci.* **2012**, *125*, 5911–5915. [CrossRef]
39. Movassagh, M.; Foo, R. Simplified apoptotic cascades. *Heart Fail. Rev.* **2008**, *13*, 111–119. [CrossRef]
40. Adli, M.; Merkhofer, E.; Cogswell, P.; Baldwin, A. IKKalpha and IKKbeta each function to regulate NF-kappaB activation in the TNF-induced/canonical pathway. *PLoS ONE* **2010**, *5*, e9428. [CrossRef]
41. Angelo, A.; Rovere-Querini, P.; Clementi, S.; Clementi, B. Cell Death: Tipping the Balance of Autoimmunity and Tissue Repair. *Curr. Pharm. Des.* **2008**, *14*, 269–277. [CrossRef]
42. Kaltschmidt, B.; Kaltschmidt, C.; Hofmann, T.; Hehner, S.; Dröge, W.; Schmitz, M. The pro- or anti-apoptotic function of NF-κB is determined by the nature of the apoptotic stimulus. *Eur. J. Biochem.* **2000**, *267*, 3828–3835. [CrossRef]
43. Moret, I.; Cerrillo, E.; Navarro-Puche, A.; Iborra, M.; Rausell, F.; Tortosa, L.; Beltrán, B. Estrés oxidativo en la enfermedad de Crohn. *Gastroenterol. Hepatol.* **2014**, *37*, 28–34. [CrossRef]
44. Thornton, C.; Leaw, B.; Mallard, C.; Nair, S.; Jinnai, M.; Hagberg, H. Cell Death in the Developing Brain after Hypoxia-Ischemia. *Front. Cell. Neurosci.* **2017**, *11*, 248. [CrossRef]
45. Carella, F.; Feist, S.; Bignell, J.; De Vico, G. Comparative pathology in bivalves: Aetiological agents and disease processes. *J. Invertebr. Pathol.* **2015**, *131*, 107–120. [CrossRef]
46. Connon, R.; D'Abronzo, L.; Hostetter, N.; Javidmehr, A.; Roby, D.D.; Evans, A.; Loge, F.; Werner, I. Transcription Profiling in Environmental Diagnostics: Health Assessments in Columbia River Basin Steelhead (*Oncorhynchus mykiss*). *Environ. Sci. Technol.* **2012**, *46*, 6081–6087. [CrossRef]
47. Stark, R.; Grzelak, M.; Hadfield, J. RNA sequencing: The teenage years. *Nat. Rev. Genet.* **2019**, *20*, 631–656. [CrossRef]
48. Sun, Y.; Zhang, X.; Wang, Y.; Day, R.; Yang, H.; Zhang, Z. Immunity-related genes and signaling pathways under hypoxic stresses in *Haliotis diversicolor*: A transcriptome analysis. *Sci. Rep.* **2019**, *9*, 19741. [CrossRef]
49. Gallardo-Escarate, C.; Valenzuela-Munoz, V.; Gustavo, N.; Valenzuela-Miranda, D.; Tapia, F.; Yevenes, M.; Gajardo, G.; Toro, J.; Oyarzun, P.; Arriagada, G.; et al. Chromosome-Level Genome Assembly of the Blue Mussel *Mytilus chilensis* Reveals Molecular Signatures Facing the Marine Environment. *Genes* **2023**, *14*, 876. [CrossRef]
50. Yévenes, M.; Núñez-Acuña, G.; Gallardo-Escárate, C.; Gajardo, G. Adaptive mitochondrial genome functioning in ecologically different farm-impacted natural seedbeds of the endemic blue mussel *Mytilus chilensis*. *Comp. Biochem. Physiol. Part D Genom. Proteom.* **2022**, *42*, 100955. [CrossRef]
51. Núñez-Acuña, G.; Gallardo-Escárate, C. Identification of immune-related SNPs in the transcriptome of *Mytilus chilensis* through high-throughput sequencing. *Fish Shellfish Immunol.* **2013**, *35*, 1899–1905. [CrossRef]
52. Detree, C.; Nunez-Acuna, G.; Roberts, S.; Gallardo-Escarate, C. Uncovering the Complex Transcriptome Response of Mytilus chilensis against Saxitoxin: Implications of Harmful Algal Blooms on Mussel Populations. *PLoS ONE* **2016**, *11*, e0165231. [CrossRef] [PubMed]
53. Malachowicz, M.; Wenne, R. Mantle transcriptome sequencing of *Mytilus spp.* and identification of putative biomineralization genes. *PeerJ* **2019**, *6*, e6245. [CrossRef]
54. Lohrmann, K.; Bustos, E.; Rojas, R.; Navarrete, F.; Robotham, H.; Bignell, J. Histopathological assessment of the health status of *Mytilus chilensis* (Hupé 1854) in southern Chile. *Aquaculture* **2019**, *503*, 40–50. [CrossRef]
55. Osores, S.; Lagos, N.; San Martín, V.; Manríquez, P.; Vargas, C.; Torres, R.; Navarro, J.; Poupin, J.; Saldías, G.; Lardies, M. Plasticity and inter-population variability in physiological and life-history traits of the mussel *Mytilus chilensis*: A reciprocal transplant experiment. *J. Exp. Mar. Biol. Ecol.* **2017**, *490*, 1–12. [CrossRef]

56. Ríos, V.; Ocampo, N.; Astorga, M. Proximal chemical composition and morphometry of the ribbed (*Aulacomya ater*, Molina 1782) and the blue (*Mytilus chilensis*, Hupé, 1854) mussels commercialized in the Region of Magallanes. *An. Inst. Patagon.* **2018**, *46*, 49–58. [CrossRef]
57. Navarro, J.; Duarte, C.; Manríquez, P.; Lardies, M.; Torres, R.; Acuña, K.; Vargas, C.; Lagos, N. Ocean warming and elevated carbon dioxide: Multiple stressor impacts on juvenile mussels from southern Chile. *ICES J. Mar. Sci.* **2016**, *73*, 764–771. [CrossRef]
58. Subpesca. Mejillón. Available online: https://www.subpesca.cl/portal/616/w3-article-843.html#presentacion (accessed on 1 May 2023).
59. Oyarzún, P.; Toro, E.; Jaramillo, R.; Guiñez, R.; Briones, C.; Astorga, M. Gonadal cycle of the mussel *Mytilus chilensis* (Bivalvia: Mytilidae) at two localities in southern of Chile. *Lat. Am. J. Aquat. Res.* **2011**, *39*, 512–525. [CrossRef]
60. Salas-Yanquin, L.; Navarro, J.; Pechenik, J.; Montory, J.; Chaparro, O. Volcanic ash in the water column: Physiological impact on the suspension-feeding bivalve *Mytilus chilensis*. *Mar. Pollut. Bull.* **2018**, *127*, 342–351. [CrossRef] [PubMed]
61. Molinet, C.; Diaz, M.; Marin, S.; Astorga, M.; Ojeda, M.; Cares, L.; Asencio, E. Relation of mussel spatfall on natural and artificial substrates: Analysis of ecological implications ensuring long-term success and sustainability for mussel farming. *Aquaculture* **2017**, *467*, 211–218. [CrossRef]
62. IFOP. Innovaciones en la Tecnología de Cultivo de Chorito (Mytilus chilensis), Tendientes a Mejorar la Calidad y Rentabilidad de la Actividad Mitícola en la X Región. Available online: https://www.ifop.cl/wp-content/contenidos/uploads/biblioteca/libros_digitales/Curso_Cultivo_de_choritos.pdf (accessed on 9 January 2023).
63. Subpesca. Informe Sectorial de Pesca y Acuicultura Consolidado (2020–2021). Available online: https://www.subpesca.cl/portal/618/articles-114306_documento.pdf (accessed on 1 October 2023).
64. ProChile. Chile se Convierte en el Mayor Proveedor Mundial de 28 Productos Liderados por Cobre, Cerezas y Salmón. Available online: https://www.prochile.gob.cl/noticias/detalle-noticia/2021/08/12/chile-se-convierte-en-el-mayor-proveedor-mundial-de-28-productos-liderados-por-cobre-cerezas-y-salm%C3%B3n (accessed on 3 October 2023).
65. Blanc, J.; Molinet, C.; Subiabre, R.; Díaz, P. Cadmium determination in Chilean blue mussels *Mytilus chilensis*: Implications for environmental and agronomic interest. *Mar. Pollut. Bull.* **2018**, *129*, 913–917. [CrossRef]
66. Yevenes, M.; Lagos, N.; Farías, L.; Vargas, C. Greenhouse gases, nutrients and the carbonate system in the Reloncaví Fjord (Northern Chilean Patagonia): Implications on aquaculture of the mussel, *Mytilus chilensis*, during an episodic volcanic eruption. *Sci. Total Environ.* **2019**, *669*, 49–61. [CrossRef]
67. Walker, C.; Beneden, R.; Muttray, A.; Böttger, A.; Kelley, M.; Tucker, A.; Kelley, T. *Chapter One—p53 Superfamily Proteins in Marine Bivalve Cancer and Stress Biology*; Michael, L., Ed.; Academic Press: Cambridge, MA, USA, 2011; Volume 59, pp. 1–36.
68. Venier, P.; De Pittà, C.; Pallavicini, A.; Marsano, F.; Varotto, L.; Romualdi, C.; Dondero, F.; Viarengo, A.; Lanfranchi, G. Development of mussel mRNA profiling: Can gene expression trends reveal coastal water pollution? *Mutat. Res./Fundam. Mol. Mech. Mutagen.* **2006**, *602*, 121–134. [CrossRef] [PubMed]
69. Baqueiro–Cárdenas, E.; Borabe, L.; Goldaracena–Islas, C.; Rodríguez–Navarro, J. Mollusks and pollution. A review. *Rev. Mex. Biodivers.* **2007**, *78*, 1–7.
70. Hernández-Miranda, E.; Quiñones, R.; Aedo, G.; Valenzuela, A.; Mermoud, N.; Román, C.; Yañez, F. A major fish stranding caused by a natural hypoxic event in a shallow bay of the eastern South Pacific Ocean. *J. Fish Biol.* **2010**, *76*, 1543–1564. [CrossRef]
71. Hernández-Miranda, E.; Veas, R.; Labra, F.; Salamanca, M.; Quiñones, R. Response of the epibenthic macrofaunal community to a strong upwelling-driven hypoxic event in a shallow bay of the southern Humboldt Current System. *Mar. Environ. Res.* **2012**, *79*, 16–28. [CrossRef]
72. Labra, F.; Hernández-Miranda, E.; Quiñones, R. Dynamic relationships between body size, species richness, abundance, and energy use in a shallow marine epibenthic faunal community. *Ecol. Evol.* **2015**, *5*, 391–408. [CrossRef] [PubMed]
73. Clark, M.; Husmann, G.; Thorne, M.; Burns, G.; Truebano, M.; Peck, L.; Abele, D.; Philipp, E. Hypoxia impacts large adults first: Consequences in a warming world. *Glob. Change Biol.* **2013**, *19*, 2251–2263. [CrossRef]
74. Gu, H.; Shang, Y.; Clements, J.; Dupont, S.; Wang, T.; Wei, S.; Wang, X.; Chen, J.; Huang, W.; Hu, M.; et al. Hypoxia aggravates the effects of ocean acidification on the physiological energetics of the blue mussel *Mytilus edulis*. *Mar. Pollut. Bull.* **2019**, *149*, 110538. [CrossRef] [PubMed]
75. Piontkivska, H.; Chung, S.; Ivanina, A.; Sokolov, E.; Techa, S.; Sokolova, I. Molecular characterization and mRNA expression of two key enzymes of hypoxia-sensing pathways in eastern oysters *Crassostrea virginica* (Gmelin): Hypoxia-inducible factor α (HIF-α) and HIF-prolyl hydroxylase (PHD). *Comp. Biochem. Physiol. Part D Genom. Proteom.* **2011**, *6*, 103–114. [CrossRef]
76. Coxe, N.; Casas, S.; Marshall, D.; La Peyre, M.; Kelly, M.; La Peyre, J. Differential hypoxia tolerance of eastern oysters from the northern Gulf of Mexico at elevated temperature. *J. Exp. Mar. Biol. Ecol.* **2023**, *559*, 151840. [CrossRef]
77. Wang, X.; Zhang, T.; Zhang, Q.; Xue, R.; Qu, Y.; Wang, Q.; Dong, Z.; Zhao, J. Different patterns of hypoxia aggravate the toxicity of polystyrene nanoplastics in the mussels *Mytilus galloprovincialis*: Environmental risk assessment of plastics under global climate change. *Sci. Total Environ.* **2022**, *818*, 151818. [CrossRef] [PubMed]
78. Li, Q.; Zhang, F.; Sun, S. The survival and responses of blue mussel *Mytilus edulis* to 16-day sustained hypoxia stress. *Mar. Environ. Res.* **2022**, *176*, 105601. [CrossRef] [PubMed]
79. Gostyukhina, O.; Yu, A.; Chelebieva, E.; Vodiasova, E.; Lantushenko, A.; Kladchenko, E. Adaptive potential of the Mediterranean mussel *Mytilus galloprovincialis* to short-term environmental hypoxia. *Fish Shellfish Immunol.* **2022**, *131*, 654–661. [CrossRef] [PubMed]

80. Kotsyuba, E.; Dyachuk, V. Effect of Air Exposure-Induced Hypoxia on Neurotransmitters and Neurotransmission Enzymes in Ganglia of the Scallop *Azumapecten farreri*. *Int. J. Mol. Sci.* **2022**, *23*, 2027. [CrossRef] [PubMed]
81. Salmond, N.; Wing, S. Sub-lethal and lethal effects of chronic ammonia exposure and hypoxia on a New Zealand bivalve. *J. Exp. Mar. Biol. Ecol.* **2022**, *549*, 151696. [CrossRef]
82. Andreyeva, A.; Gostyukhina, O.; Kladchenko, E.; Afonnikov, D.; Rasskazov, D.; Lantushenko, A.; Vodiasova, E. Hypoxia exerts oxidative stress and changes in expression of antioxidant enzyme genes in gills of *Mytilus galloprovincialis* (Lamarck, 1819). *Mar. Biol. Res.* **2021**, *17*, 369–379. [CrossRef]
83. Khan, F.; Chen, H.; Gu, H.; Wang, T.; Dupont, S.; Kong, H.; Shang, Y.; Wang, X.; Lu, W.; Hu, M.; et al. Antioxidant responses of the mussel *Mytilus coruscus* co-exposed to ocean acidification, hypoxia and warming. *Mar. Pollut. Bull.* **2021**, *162*, 111869. [CrossRef] [PubMed]
84. Xu, G.; Kong, H.; Chang, X.; Dupont, S.; Chen, H.; Deng, Y.; Hu, M.; Wang, Y. Gonadal antioxidant responses to seawater acidification and hypoxia in the marine mussel *Mytilus coruscus*. *Environ. Sci. Pollut. Res.* **2021**, *28*, 53847–53856. [CrossRef]
85. Sokolov, E.; Adzigbli, L.; Markert, S.; Bundgaard, A.; Fago, A.; Becher, D.; Hirschfeld, C.; Sokolova, I. Intrinsic Mechanisms Underlying Hypoxia-Tolerant Mitochondrial Phenotype During Hypoxia-Reoxygenation Stress in a Marine Facultative Anaerobe, the Blue Mussel *Mytilus edulis*. *Front. Mar. Sci.* **2021**, *8*, 773734. [CrossRef]
86. Altschul, S.; Madden, T.; Schaffer, A.; Zhang, J.; Zhang, Z.; Miller, W.; Lipman, D. Gapped BLAST and PSI-BLAST: A new generation of protein database search programs. *Nucleic Acids Res.* **1998**, *12*, 3389–3402. [CrossRef]
87. Bateman, A.; Martin, M.; Orchard, S.; Magrane, M.; Ahmad, S.; Alpi, E.; Bowler-Barnett, E.; Britto, R.; Cukura, A.; Denny, P.; et al. UniProt: The Universal Protein Knowledgebase in 2023. *Nucleic Acids Res.* **2022**, *51*, D523–D531. [CrossRef]
88. Aleksander, S.; Balhoff, J.; Carbon, S.; Cherry, J.; Drabkin, H.; Ebert, D.; Feuermann, M.; Gaudet, P.; Harris, N.; Hill, D.; et al. The Gene Ontology knowledgebase in 2023. *Genetics* **2023**, *224*, iyad031. [CrossRef]
89. Tatusov, R.; Natale, D.; Garkavtsev, I.; Tatusova, T.; Shankavaram, U.; Rao, B.; Kiryutin, B.; Galperin, M.; Fedorova, N.; Koonin, E. The COG database: New developments in phylogenetic classification of proteins from complete genomes. *Nucleic Acids Res.* **2001**, *29*, 22–28. [CrossRef]
90. Kanehisa, M.; Sato, Y.; Kawashima, M. KEGG mapping tools for uncovering hidden features in biological data. *Protein Sci.* **2022**, *31*, 47–53. [CrossRef]
91. Chen, C.; Chen, H.; Zhang, Y.; Thomas, H.; Frank, M.; He, Y.; Xia, R. TBtools: An Integrative Toolkit Developed for Interactive Analyses of Big Biological Data. *Mol. Plant* **2020**, *13*, 1194–1202. [CrossRef]
92. Ge, S.; Jung, D.; Yao, R. ShinyGO: A graphical gene-set enrichment tool for animals and plants. *Bioinformatics* **2020**, *36*, 2628–2629. [CrossRef]
93. Valenzuela-Muñoz, V.; Gallardo-Escárate, C.; Benavente, B.; Valenzuela-Miranda, D.; Núñez-Acuña, G.; Escobar-Sepulveda, H.; Váldes, J. Whole-Genome Transcript Expression Profiling Reveals Novel Insights into Transposon Genes and Non-Coding RNAs during Atlantic Salmon Seawater Adaptation. *Biology* **2022**, *11*, 1. [CrossRef]
94. Cui, Z.; Cui, Y.; Zang, T.; Wang, Y. Genome analysis interacCircos: An R package based on JavaScript libraries for the generation of interactive circos plots. *Bioinformatics* **2021**, *37*, 3642–3644. [CrossRef]
95. Lee, S.; Choi, E.; Kim, T.; Hwang, J.; Lee, J. AtHAD1, A haloacid dehalogenase-like phosphatase, is involved in repressing the ABA response. *Biochem. Biophys. Res. Commun.* **2022**, *587*, 119–125. [CrossRef]
96. Du, Z.; Deng, S.; Wu, Z.; Wang, C. Genome-wide analysis of haloacid dehalogenase genes reveals their function in phosphate starvation responses in rice. *PLoS ONE* **2021**, *16*, e0245600. [CrossRef]
97. Pandey, B.; Mehra, P.; Verma, L.; Bhadouria, J.; Giri, J. OsHAD1, a Haloacid Dehalogenase-Like APase, Enhances Phosphate Accumulation. *Plant Physiol.* **2017**, *174*, 2316–2332. [CrossRef]
98. Levin, L. Oxygen Minimum Zone Benthos: Adaptation and Community Response to Hypoxia. In *Oceanography and Marine Biology, An Annual Review*, 1st ed.; Gibson, R., Atkinson, A., Eds.; Taylor & Francis: London, UK, 2003; Volume 41, pp. 1–45.
99. Rabalais, N.; Cai, W.; Carstensen, J.; Conley, D.; Fry, B.; Hu, X.; Quiñones-Rivera, Z.; Rosenberg, R.; Slomp, C.; Turner, R.; et al. Eutrophication-driven deoxygenation in the coastal ocean. *Oceanography* **2014**, *27*, 172–183. [CrossRef]
100. Nie, H.; Wang, H.; Jiang, K.; Yan, X. Transcriptome analysis reveals differential immune related genes expression in *Ruditapes philippinarum* under hypoxia stress: Potential HIF and NF-κB crosstalk in immune responses in clam. *BMC Genom.* **2020**, *21*, 318. [CrossRef]
101. Yan, X.; Nie, H.; Huo, Z.; Ding, J.; Li, Z.; Yan, L.; Jiang, L.; Mu, Z.; Wang, H.; Meng, X.; et al. Clam Genome Sequence Clarifies the Molecular Basis of Its Benthic Adaptation and Extraordinary Shell Color Diversity. *iScience* **2019**, *19*, 1225–1237. [CrossRef]
102. Philipp, E.; Wessels, W.; Gruber, H.; Strahl, J.; Wagner, A.; Ernst, I.; Rimbach, G.; Kraemer, L.; Schreiber, S.; Abele, D.; et al. Gene Expression and Physiological Changes of Different Populations of the Long-Lived Bivalve *Arctica islandica* under Low Oxygen Conditions. *PLoS ONE* **2012**, *7*, e44621. [CrossRef]
103. Wang, Y.; Zhou, S.; Liu, T.; Chen, M.; Li, W.; Zhang, X. The transcriptomic responses of the ark shell, *Anadara broughtonii*, to sulfide and hypoxia exposure. *Mol. Biol. Rep.* **2019**, *46*, 4245–4257. [CrossRef]
104. Lee, J.; Bae, S.; Jeong, J.; Kim, S.; Kim, K. Hypoxia-inducible factor (HIF-1)α: Its protein stability and biological functions. *Exp. Mol. Med.* **2004**, *36*, 1–12. [CrossRef]

105. Bravo, R.; Parra, V.; Gatica, D.; Rodriguez, A.; Torrealba, N.; Paredes, F.; Wang, Z.; Zorzano, A.; Hill, J.; Jaimovich, E.; et al. Endoplasmic Reticulum and the Unfolded Protein Response: Dynamics and Metabolic Integration. In *International Review of Cell and Molecular Biology*; Jeon, K., Ed.; Elsevier Academic Press Inc.: San Diego, CA, USA, 2013; Volume 301, pp. 215–290.
106. Steffen, J.; Falfushynska, H.; Piontkivska, H.; Sokolova, I. Molecular Biomarkers of the Mitochondrial Quality Control Are Differently Affected by Hypoxia-Reoxygenation Stress in Marine Bivalves *Crassostrea gigas* and *Mytilus edulis*. *Front. Mar. Sci.* **2020**, *7*, 604411. [CrossRef]
107. Sun, S.; Zhao, G.; Jia, M.; Jiang, Q.; Li, S.; Wang, H.; Li, W.; Wang, Y.; Bian, X.; Zhao, Y.; et al. Stay in touch with the endoplasmic reticulum. *Sci. China Life Sci.* **2024**, *67*, 230–257. [CrossRef]
108. Di Conza, G.; Ho, P.; Cubillos-Ruiz, J.; Huang, S. Control of immune cell function by the unfolded protein response. *Nat. Rev. Immunol.* **2023**, *23*, 546–562. [CrossRef]
109. Adams, C.; Kopp, M.; Larburu, N.; Nowak, P.; Ali, M. Structure and Molecular Mechanism of ER Stress Signaling by the Unfolded Protein Response Signal Activator IRE1. *Front. Mol. Biosci.* **2019**, *6*, 11. [CrossRef]
110. Noulsri, E.; Lerdwana, S. Reducing erythroblast apoptosis in β-thalassemia via unfolded protein response (UPR) signaling. *Med. Hypotheses* **2023**, *177*, 111117. [CrossRef]
111. Wang, L.; Alzayady, K.; Yule, D. Proteolytic fragmentation of inositol 1,4,5-trisphosphate receptors: A novel mechanism regulating channel activity? *J. Physiol.* **2016**, *594*, 2867–2876. [CrossRef]
112. Kokott-Vuong, A.; Jung, J.; Fehr, A.; Kirschfink, N.; Noristani, R.; Voigt, A.; Reich, A.; Schulz, J.; Huber, M.; Habib, P. Increased Post-Hypoxic Oxidative Stress and Activation of the PERK Branch of the UPR in *Trap1*-Deficient *Drosophila melanogaster* Is Abrogated by Metformin. *Int. J. Mol. Sci.* **2021**, *22*, 11586. [CrossRef]
113. Colgan, S.; Hashimi, A.; Austin, R. Endoplasmic reticulum stress and lipid dysregulation. *Expert Rev. Mol. Med.* **2011**, *13*, e4. [CrossRef]
114. Stevenson, J.; Huang, E.; Olzmann, J. Endoplasmic Reticulum-Associated Degradation and Lipid Homeostasis. In *Annual Review of Nutrition*; Stover, P., Ed.; Annual Reviews: Palo Alto, CA, USA, 2016; Volume 36, pp. 511–542.
115. Gerhardtova, I.; Jankech, T.; Majerova, P.; Piestansky, J.; Olesova, D.; Kovac, A.; Jampilek, J. Recent Analytical Methodologies in Lipid Analysis. *Int. J. Mol. Sci.* **2024**, *25*, 2249. [CrossRef]
116. Storrie, B. Maintenance of Golgi apparatus structure in the face of continuous protein recycling to the endoplasmic reticulum: Making ends meet. In *International Review of Cytology—A Survey of Cell Biology*; Jeon, K., Ed.; Elsevier Academic Press Inc.: San Diego, CA, USA, 2005; Volume 244, pp. 69–94.
117. Hetz, C.; Zhang, K.; Kaufman, R. Mechanisms, regulation and functions of the unfolded protein response. *Nat. Rev. Mol. Cell Biol.* **2020**, *21*, 421–438. [CrossRef] [PubMed]
118. He, J.; Zhou, Y.; Sun, L. Emerging mechanisms of the unfolded protein response in therapeutic resistance: From chemotherapy to Immunotherapy. *Cell Commun. Signal.* **2024**, *22*, 89. [CrossRef] [PubMed]
119. Hall, S.; Méthe, D.; Stewart-Clark, S.; Clark, F. Size and site specific transcriptomic responses of blue mussel (*Mytilus edulis*) to acute hypoxia. *Mar. Genom.* **2023**, *71*, 101060. [CrossRef] [PubMed]
120. Soldatov, A.A.; Andreenko, T.I.; Sysoeva, I.V.; Sysoev, A.A. Tissue specificity of metabolism in bivalve mollusc Anadara inaequivalvis Br. under conditions of experimental anoxia. *Comp. Ontog. Biochem.* **2009**, *45*, 284–289. [CrossRef]
121. Dezwaan, A.; Cortesi, P.; Vandenthillart, G.; Roos, J.; Storey, K. Differential sensitivities to hypoxia by two anoxia-tolerant marine molluscs: A biochemical analysis. *Mar. Biol.* **1991**, *111*, 343–351. [CrossRef]
122. Cook, K.; Shen, H.; McKelvey, K.; Gee, H.; Hau, E. Targeting Glucose Metabolism of Cancer Cells with Dichloroacetate to Radiosensitize High-Grade Gliomas. *Int. J. Mol. Sci.* **2021**, *22*, 7265. [CrossRef] [PubMed]
123. Gillen, S.; Waldron, J.; Bushell, M. Codon optimality in cancer. *Oncogene* **2021**, *40*, 6309–6320. [CrossRef] [PubMed]
124. Chen, X.; Cubillos-Ruiz, J. Endoplasmic reticulum stress signals in the tumour and its microenvironment. *Nat. Rev. Cancer* **2021**, *21*, 71–88. [CrossRef] [PubMed]
125. Gebert, M.; Slawski, J.; Kalinowski, L.; Collawn, J.; Bartoszewski, R. The Unfolded Protein Response: A Double-Edged Sword for Brain Health. *Antioxidants* **2023**, *12*, 1648. [CrossRef] [PubMed]
126. Appenzeller-Herzog, C.; Hall, M. Bidirectional crosstalk between endoplasmic reticulum stress and mTOR signaling. *Trends Cell Biol.* **2012**, *22*, 274–282. [CrossRef] [PubMed]
127. Marcondes-de-Castro, I.; Reis-Barbosa, P.; Marinho, T.; Aguila, M.; Mandarim-de-Lacerda, C. AMPK/mTOR pathway significance in healthy liver and non-alcoholic fatty liver disease and its progression. *J. Gastroenterol. Hepatol.* **2023**, *38*, 1868–1876. [CrossRef]
128. Giannetto, A.; Maisano, M.; Cappello, T.; Oliva, S.; Parrino, V.; Natalotto, A.; De Marco, G.; Barberi, C.; Romeo, O.; Mauceri, A.; et al. Hypoxia-Inducible Factor α and Hif-prolyl Hydroxylase Characterization and Gene Expression in Short-Time Air-Exposed *Mytilus galloprovincialis*. *Mar. Biotechnol.* **2015**, *17*, 768–781. [CrossRef] [PubMed]
129. Thomas, Y.; Flye-Sainte-Marie, J.; Chabot, D.; Aguirre-Velarde, A.; Marques, G.; Pecquerie, L. Effects of of hypoxia on metabolic functions in marine organisms: Observed patterns and modelling assumptions within the context of Dynamic Energy Budget (DEB) theory. *J. Sea Res.* **2019**, *143*, 231–242. [CrossRef]
130. Wu, R. Hypoxia: From molecular responses to ecosystem responses. *Mar. Pollut. Bull.* **2002**, *45*, 35–45. [CrossRef]
131. Woo, S.; Denis, V.; Won, H.; Shin, K.; Lee, G.; Lee, T.; Yum, S. Expressions of oxidative stress-related genes and antioxidant enzyme activities in *Mytilus galloprovincialis* (Bivalvia, Mollusca) exposed to hypoxia. *Zool. Stud.* **2013**, *52*, 15. [CrossRef]

132. Aguirre-Velarde, A.; Thouzeau, G.; Jean, F.; Mendo, J.; Cueto-Vega, R.; Kawazo-Delgado, M.; Vásquez-Spencer, J.; Herrera-Sanchez, D.; Vega-Espinoza, A.; Flye-Sainte-Marie, J. Chronic and severe hypoxic conditions in Paracas Bay, Pisco, Peru: Consequences on scallop growth, reproduction, and survival. *Aquaculture* **2019**, *512*, 734259. [CrossRef]
133. Sui, Y.; Hu, M.; Shang, Y.; Wu, F.; Huang, X.; Dupont, S.; Storch, D.; Pörtner, H.; Li, J.; Lu, W.; et al. Antioxidant response of the hard shelled mussel *Mytilus coruscus* exposed to reduced pH and oxygen concentration. *Ecotoxicol. Environ. Saf.* **2017**, *137*, 94–102. [CrossRef] [PubMed]
134. Parisi, M.; Mauro, M.; Sarà, G.; Cammarata, M. Temperature increases, hypoxia, and changes in food availability affect immunological biomarkers in the marine mussel *Mytilus galloprovincialis*. *J. Comp. Physiol. B Biochem. Syst. Environ. Physiol.* **2017**, *187*, 1117–1126. [CrossRef] [PubMed]

Capítulo 2: La disbiosis de la microbiota en *Mytilus chilensis* es inducida por la hipoxia, lo que tiene consecuencias moleculares y funcionales.

Cita entera del artículo publicado: Montúfar-Romero, M.; Valenzuela-Miranda, D.; Valenzuela-Muñoz, V.; Morales-Rivera, M.F.; Gallardo-Escárate, C. Microbiota Dysbiosis in *Mytilus chilensis* Is Induced by Hypoxia, Leading to Molecular and Functional Consequences. Microorganisms 2025, 13, 825.

Resumen

La microbiota de los bivalvos desempeña un papel fundamental en la salud del huésped, ya que contribuye al procesamiento de nutrientes, la inmunidad y la resistencia a las enfermedades. Sin embargo, el aumento de la hipoxia en las aguas costeras chilenas, causado por el cambio climático y la eutrofización, amenaza con alterar este equilibrio microbiano, lo que podría favorecer la proliferación de patógenos y afectar a funciones esenciales. *Mytilus chilensis* es vulnerable a los ciclos de hipoxia-reoxigenación, pero los efectos sobre su microbiota siguen sin conocerse bien. Este estudio investiga el impacto de la hipoxia en la estructura y el potencial funcional de las comunidades microbianas que residen en las branquias y las glándulas digestivas de *M. chilensis*. Mediante la secuenciación completa del gen 16S rRNA, exploramos los efectos de la hipoxia en la diversidad microbiana y la capacidad

funcional. Nuestros resultados revelaron alteraciones significativas en la composición microbiana, con un cambio hacia anaerobios facultativos que prosperan en entornos con bajo nivel de oxígeno. Cabe destacar que se produjo una disminución de los taxa bacterianos dominantes, como Rhodobacterales, mientras que los patógenos oportunistas, como *Vibrio* y *Aeromonas*, mostraron una mayor abundancia. El análisis funcional indicó una disminución de las funciones microbianas críticas asociadas al metabolismo de los nutrientes y al apoyo inmunológico, lo que podría poner en peligro la salud y la supervivencia del huésped. Este estudio arroja luz sobre las complejas interacciones entre la microbiota asociada al huésped y los factores de estrés ambientales, subrayando la importancia de gestionar la microbiota ante el cambio climático y las prácticas acuícolas.

microorganisms

MDPI

Article

Microbiota Dysbiosis in *Mytilus chilensis* Is Induced by Hypoxia, Leading to Molecular and Functional Consequences

Milton Montúfar-Romero [1,2], Diego Valenzuela-Miranda [1,3,*], Valentina Valenzuela-Muñoz [1,4], María F. Morales-Rivera [1] and Cristian Gallardo-Escárate [1,4,*]

[1] Interdisciplinary Center for Aquaculture Research (INCAR), Universidad de Concepción, P.O. Box 160-C, Concepción 4030000, Chile; mba.ing.ac.milton.montufar@gmail.com (M.M.-R.); valevalenzuela@udec.cl (V.V.-M.); marimoralesr@udec.cl (M.F.M.-R.)
[2] Instituto Público de Investigación de Acuicultura y Pesca (IPIAP), Guayaquil 090314, Ecuador
[3] Centro de Biotecnología, Universidad de Concepción, P.O. Box 160-C, Concepción 4030000, Chile
[4] Center for Oceanographic Research COPAS COASTAL, Universidad de Concepción, Concepción 4070409, Chile
* Correspondence: divalenzuela@udec.cl (D.V.-M.); crisgallardo@udec.cl (C.G.-E.); Tel.: +56-956677962 (D.V.-M.); +56-412204402 (C.G.-E.)

Abstract: Bivalve microbiota play a vital role in host health, supporting nutrient processing, immunity, and disease resistance. However, the increasing hypoxia in Chilean coastal waters, caused by climate change and eutrophication, threatens to disrupt this microbial balance, potentially promoting pathogens and impairing essential functions. *Mytilus chilensis* is vulnerable to hypoxia-reoxygenation cycles, yet the effects on its microbiota remain poorly understood. This study investigates the impact of hypoxia on the structure and functional potential of the microbial communities residing in the gills and digestive glands of *M. chilensis*. Employing full-length 16S rRNA gene sequencing, we explored hypoxia's effects on microbial diversity and functional capacity. Our results revealed significant alterations in the microbial composition, with a shift towards facultative anaerobes thriving in low oxygen environments. Notably, there was a decrease in dominant bacterial taxa such as Rhodobacterales, while opportunistic pathogens such as *Vibrio* and *Aeromonas* exhibited increased abundance. Functional analysis indicated a decline in critical microbial functions associated with nutrient metabolism and immune support, potentially jeopardizing the health and survival of the host. This study sheds light on the intricate interactions between host-associated microbiota and environmental stressors, underlining the importance of managing the microbiota in the face of climate change and aquaculture practices.

Keywords: gills; digestive gland; 16s rRNA sequencing; facultative anaerobes; metabolic efficiency; aquaculture; microbial dysbiosis

Academic Editors: Aglaia Pappa and Alex Galanis

Received: 24 February 2025
Revised: 22 March 2025
Accepted: 29 March 2025
Published: 5 April 2025

Citation: Montúfar-Romero, M.; Valenzuela-Miranda, D.; Valenzuela-Muñoz, V.; Morales-Rivera, M.F.; Gallardo-Escárate, C. Microbiota Dysbiosis in *Mytilus chilensis* Is Induced by Hypoxia, Leading to Molecular and Functional Consequences. *Microorganisms* **2025**, *13*, 825. https://doi.org/10.3390/microorganisms13040825

1. Introduction

Dissolved oxygen (DO) levels are critical for the survival and health of marine organisms [1]. In coastal marine ecosystems, reference thresholds have been established to consider the biological and ecological effects of dissolved oxygen levels in the ocean [2–8]. Normoxia is defined as the condition in which DO levels range between 9.0 and 3.0 mg L^{-1}, while hypoxia occurs when DO levels fall between 2.0 and 0.1 mg L^{-1} [2–8]. Hypoxia on the south-central coast of Chile is a pressing issue severely affecting the region's bivalve mollusks, with potentially severe consequences for the marine ecosystem [9–13]. Long-term research reveals that hypoxic zones occupy substantial portions of the water column during upwelling seasons, with an intensifying trend linked to climate change and altered

oceanographic processes [14]. These trends portend a grim outlook for marine organisms reliant on stable oxygen availability [14].

Hypoxia-induced stress can severely impact bivalves, ranging from physiological to molecular levels [15,16]. Physiologically, this stress can increase clearance and respiration rates and reduce food intake, potentially resulting in stunted growth in these organisms [15,17]. Additionally, hypoxic stress can negatively affect the immune system of bivalves, increasing their susceptibility to pathogen infections [18,19]. At the cellular level, hypoxia can trigger autophagy, increase oxidative stress, and reduce cell viability [20]. Molecularly, prolonged hypoxia can affect protein metabolism, inflammation-related genes, and programmed cell death [20,21]. In extreme cases, hypoxic stress can lead to mass mortality and stranding of bivalves [10].

Within bivalve mollusks, the microbiota is characterized as a dynamic and interactive consortium of microorganisms, encompassing bacteria, archaea, viruses, fungi, and protozoa, which establish residence within diverse biological niches, including the mantle, gills, digestive gland, hemolymph, gonad, byssus gland, adductor muscle, and mucus. This engagement results in intricate symbiotic relationships with the host, modulating and executing critical physiological processes [22–30]. The microbiota associated with the host plays a crucial role in animal health by providing vital functions such as disease protection and nutrient processing [15,22]. Moreover, microbiota composition influences the host's physiology, stress tolerance, and fitness [31]. The microbiota is considered an organ that regulates host metabolism and is essential for maintaining a healthy balance in the host immune system due to its relationship with specific diseases [32–35]. Recent studies have shown that a diverse and balanced microbiota can indicate better metabolic health [36]. Greater microbiota diversity is associated with improved lipid profiles, lower levels of pro-inflammatory cytokines, and higher levels of anti-inflammatory cytokines [36]. Furthermore, bivalve mollusks have also shown correlations between microbiota diversity, enzyme activity, and genetic pathways related to metabolism and health [36–38].

Intestinal microbiota significantly influence the host's physiology, reproduction, development, energy balance, behavior, and life history [39]. The intestinal microbiota of bivalve mollusks play an essential role in their health and nutrition [40]. The diversity and abundance of microorganisms in their digestive tract assist in food digestion, strengthen the immune system, and may influence their growth and development [40–42]. However, stress-induced alterations in microbial communities, such as those caused by hypoxia, may increase disease risk and compromise bivalve health [43,44]. For example, the proliferation of opportunistic pathogens, including those from the *Vibrio* and *Arcobacter* genera, could significantly increase the host's susceptibility to diseases, contributing to increased mortality [45]. Furthermore, fluctuations in the external environment, such as abiotic factors, can alter the structure, species richness, and diversity of intestinal microbiota [15].

Mytilus chilensis is a bivalve species of ecological and economic importance in the coastal waters of the Los Lagos Region in Chile [46,47]. Climate change, manifested in declining oxygen levels in the water, induces systematic changes in bivalve mollusks and their bacterial symbionts [15,48,49]. Economically valuable bivalve species, including *M. chilensis*, are increasingly exposed to hypoxic conditions, threatening their viability and sustainability [50,51]. The aquaculture industry in southern Chile, heavily relies on seed collection from the Reloncaví Fjord and grow out operations around Chiloé Island, faces recurrent hypoxia episodes exacerbated by seasonal upwelling and anthropogenic eutrophication [52,53].

The Reloncaví system, comprising the Reloncaví Fjord and Reloncaví Sound, is particularly vulnerable to hypoxia due to the influx of suspended allochthonous organic matter from rivers, especially during late winter and early spring [53–55]. This period is marked

by glacial meltwater contributions, dominating precipitation-driven runoff [53–55]. Major riverine inputs, including the Puelo, Petrohué, and Cochamó Rivers, deliver substantial organic material, fueling microbial decomposition and oxygen consumption [56,57]. Recent risk assessments identify the Reloncaví estuarine system as a hotspot for high inorganic nutrient concentrations, intense phytoplankton blooms, and elevated chlorophyll levels, particularly in late winter (August–September) [58–60]. These conditions, driven by eutrophication from intensive salmon aquaculture, promote the formation of low dissolved oxygen water (LDOW) zones, where stratification and particulate organic matter deposition exacerbate oxygen depletion [60]. The prolonged water residence times in the Reloncaví system, coupled with high biological oxygen demand—including phytoplankton respiration and bacterial remineralization of organic material—underscore the urgent need to investigate hypoxia's impact on *M. chilensis*, particularly at the microbiota level [53,60–63].

Therefore, our objective is to understand the influence of hypoxia on the intestinal and gill microbiota of the native mussel *M. chilensis*. Specifically, a comparative evaluation of the bacterial communities in the intestine and gills of *M. chilensis* exposed to hypoxia was conducted using 16S rRNA sequencing with nanopore technology. Our study is the first to investigate the effects of hypoxia on *M. chilensis* from a hologenome concept. This knowledge could enhance our understanding of host-specific microbiotas and their roles in supporting host ecology. Additionally, it can help elucidate the physiological responses of *M. chilensis* to hypoxia and infer potential health and disease changes that may arise from future stress factors.

2. Materials and Methods

2.1. Experimental Design (Mussel Acclimatization, Hypoxia Challenge, and Sampling for Microbiological Analysis)

Understanding marine bivalves' physiological and microbiological responses to hypoxic stress is crucial for assessing the impacts of climate change and coastal eutrophication on aquaculture species. While numerous studies have examined short-term hypoxia (15 min to 36 h) and subsequent reoxygenation cycles (10 min to 24 h) [20,21,64–71], research on prolonged hypoxic exposure remains limited despite reports of hypoxia lasting up to six days [21,60] in some coastal environments and 25 days [72–74] in others. This study was designed to simulate long-term progressive hypoxia rather than replicate singular hypoxic events, which naturally persist for at least two days in Chilean coastal ecosystems [14]. To approximate future oxygen variability, the experimental design was based on tidal coefficients obtained from publicly available tidal data (https://tablademareas.com accessed on 7 March 2022), reflecting fluctuations in tidal amplitude within the study area over approximately 10 days. The southern Chilean fjords, characterized by their complex coastal morphology and low water exchange rates (e.g., a residence time of approximately 98 days in the Reloncaví fjord), provide an ideal setting to investigate the impacts of prolonged hypoxia [53,75,76].

This study employed a controlled experimental approach to assess the systemic effects of long-term hypoxia and reoxygenation on *M. chilensis*, with a particular emphasis on microbiological shifts in gill and digestive gland tissues. The experimental design simulated environmental conditions projected under climate change and eutrophication scenarios.

Blue mussels (*M. chilensis*) utilized in this study were sourced in April 2022 from the experimental laboratory at the Marine Biological Station of the Universidad de Concepción, Chile. The experiment spanned 50 days and consisted of alternating hypoxic (dissolved oxygen concentrations of 2.0 mg/L) and normoxic (dissolved oxygen concentrations of 7.2 $\pm$ 0.2 mg/L) phases.

From an initial pool of 480 individuals, 36 mussels were selected and distributed into three experimental replicates (n = 12 mussels per replicate). The duration of each hypoxic exposure was determined based on methodologies established in prior studies [77]. The experimental design incorporated a structured sampling regime: Gill and digestive gland samples of three mussels were collected under hypoxic conditions at day 10 (n = 9 total mussels across replicates); gill and digestive gland samples of three mussels were taken following reoxygenation (normoxic conditions) at day 20 (n = 9); gill and digestive gland samples of three mussels were collected following reoxygenation at day 40 (n = 9); and gill and digestive gland samples of three mussels were sampled under hypoxic conditions at day 50 (n = 9). In total, 18 gill and digestive gland mussel samples were under hypoxia, and 18 were under reoxygenation. In the present experimental design, a control group was not included due to the primary focus on direct comparisons between hypoxic and reoxygenation conditions. Furthermore, a singular sampling event on days 10 and 20 would have critically compromised the study's temporal resolution, precluding the detection of progressive effects or prolonged microbial shifts. The serial sampling at days 40 and 50 provided a detailed perspective on the long-term, cumulative effects of hypoxia and reoxygenation, essential for evaluating the impacts of oxygen variability on bivalves under climate change and eutrophication scenarios. This approach is fundamental for developing effective management and conservation strategies for *M. chilensis* in the face of evolving environmental conditions.

Before the hypoxia challenge, mussels were acclimatized for 38 days in filtered seawater (12.5 $\pm$ 0.94 °C) under continuous flow, aeration, and feeding. Following acclimatization, dissolved oxygen concentrations within the recirculation system were monitored daily and adjusted using nitrogen gas injection to maintain the target hypoxic level of 2.0 mg/L.

Gill and digestive gland tissues were selected due to their critical roles in bivalve physiology. Gills, as the primary interface between the organism and its environment, are central to respiration and filter feeding [78,79]. Given their constant exposure to ambient conditions, gills are particularly susceptible to hypoxia-induced physiological stress. Consequently, microbial changes within gill tissues were investigated as potential biomarkers of hypoxia-induced stress [80].

In addition to gills, the digestive gland was analyzed due to its multifunctional role in nutrient assimilation, metabolic regulation, and immune response [81–84]. Under hypoxic conditions, bivalves often exhibit valve closure, significantly reducing filtration and respiration rates [85,86]. Since hypoxia impacts filtration-dependent nutrient processing and metabolic activity, the digestive gland microbiota shifts were examined to elucidate the broader physiological consequences of hypoxia-induced dysbiosis. This study aimed to identify shared perturbation patterns and assess the physiological implications of hypoxia exposure in *M. chilensis* by examining microbial dynamics in both gill and digestive gland tissues.

To reduce inter-individual variability in the microbiota associated with gill and digestive gland tissues, samples from three mussels were pooled to create a single biological replicate, with each sequencing sample representing nine pooled individuals [87]. This pooling strategy, utilizing nine individuals per sequencing sample, was implemented to enhance the detection of consistent microbial patterns while optimizing sequencing resources. Figure 1A,B, 3, 4, and 7 present microbiota composition from pooled samples at control time points (days 20 and 40, n = 9 mussels each) and hypoxic phases (days 10 and 50, n = 9 mussels each). Conversely, Figure 1C, 2, 5, and 6 display microbiota composition from combined normoxic samples at days 20 and 40 (n = 18 total mussels) and combined hypoxic samples at days 10 and 50 (n = 18 total mussels).

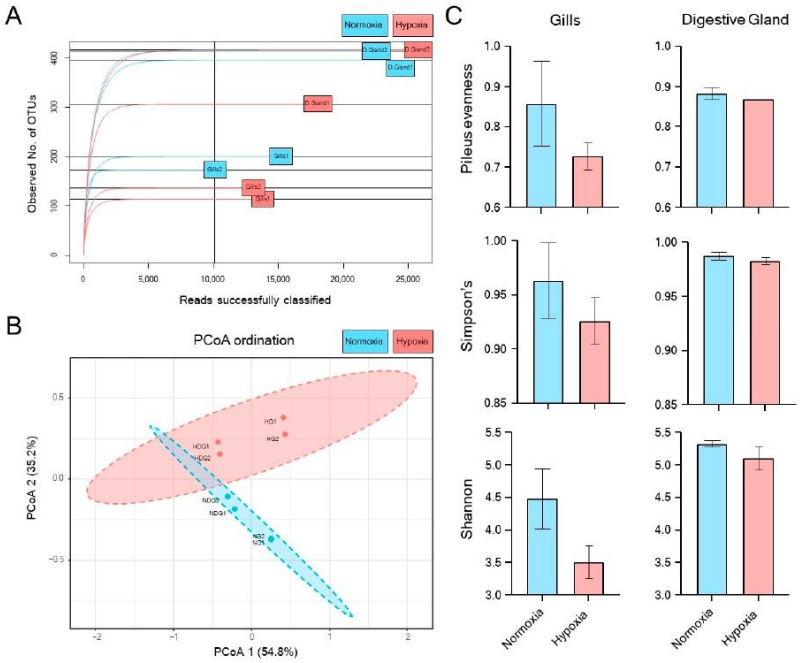

Figure 1. Alpha and beta-diversity analysis for *M. chilensis* microbiota exposed to normoxia (blue) and hypoxia (red). The figure shows the rarefaction curves for all the samples. The digestive gland is represented as D. Gland (**A**). In the principal coordinate analysis (PCoA), the digestive gland is represented as NDG (normoxia) and HDG (hypoxia), while the gills are denoted as NG (normoxia) and HG (hypoxia) (**B**). Different alpha diversity indexes were estimated for gills and digestive glands under the experimental conditions (**C**).

The samples were preserved in molecular-grade ethanol, transported at 4 °C, and stored at −80 °C until further processing for microbiological analysis.

2.2. *DNA Isolation and 16S Amplification*

Total bacterial DNA was isolated from homogenized gill and digestive gland tissues of mussels using the phenol-chloroform extraction method.

Gill and digestive gland tissues (20–30 mg) were collected from three mussels per group (nine per treatment), thawed, washed, minced, and vortexed to facilitate homogenization using ceramic beads. Each sample was then mixed with 1 mL of lysis buffer (10 mM Tris-HCl, 400 mM NaCl, 100 mM EDTA, 0.4% SDS, and 100 µg/mL Proteinase K, pH 8.0) and incubated at 37 °C for 2 h under constant agitation to ensure complete lysis [88].

After incubation, 1 volume of phenol-chloroform was added to each sample, followed by centrifugation at 12,000 rpm for 5 min at room temperature. The aqueous phase was carefully collected, and an equal volume of chloroform was added, followed by an additional centrifugation at 12,000 rpm for 5 min. The resulting aqueous phase was mixed with molecular grade absolute ethanol and transferred to a DNeasy Blood and Tissue column (Qiagen, Germantown, MD, USA) to continue purification following the manufacturer's protocol.

The quality and purity of the extracted DNA were assessed using a Nanodrop One spectrophotometer (Thermo Scientific, Waltham, MA, USA), and its integrity was verified through electrophoresis in a 1% agarose gel prepared in TAE buffer (Tris-Acetic Acid-EDTA). DNA concentration was further quantified by fluorescence using a Qubit 4 fluorometer (Thermo Scientific, Waltham, MA, USA) with the dsDNA BR Assay Kit (Thermo Scientific, Waltham, MA, USA).

For 16S rRNA gene amplification, the isolated DNA was diluted to a concentration of 50 ng/μL and used as a template in a 25 μL PCR reaction containing LongAmp Taq DNA polymerase (New England Biolabs, MA, USA) and universal 16S primers: 27F (5′-AGAGTTTGATCCTGGCTCAG-3′) and 1492R (5′-GGTTACCTTGTTACGACTT-3′) [88]. The thermal cycling conditions included an initial denaturation step at 95 °C for 1 min, followed by 25 cycles of 95 °C for 20 s, 56 °C for 30 s, and 65 °C for 2 min, with a final extension at 65 °C for 5 min. The resulting 16S rRNA PCR amplicons were confirmed by electrophoresis in a 1.2% agarose gel prepared in TAE buffer.

2.3. Library Preparation and Nanopore Sequencing

Nanopore sequencing is an advanced technique for characterizing microbial communities by sequencing the 16S rRNA gene amplicon [89]. Following the PCR amplification of the 16S rRNA gene, the resulting amplicons were pooled according to the experimental groups and purified using Agencourt AMPure XP beads (Beckman Coulter, Brea, CA, USA) to remove primer dimers and nonspecific amplification products. The purified amplicons were then quantified using a Qubit 4 fluorometer (Thermo Scientific, Waltham, MA, USA) to ensure the appropriate library concentration for sequencing.

Library preparation was conducted using the 16S Barcoding Kit (SQK-16S024, Oxford Nanopore Technologies, Oxford, UK) following the manufacturer's protocol. The amplicons were barcoded through a PCR reaction using LongAmp Taq polymerase (New England Biolabs, Ipswich, MA, USA) and purified according to the supplier's instructions.

The quality and size distribution of the prepared libraries were evaluated using the 2200 TapeStation system (Agilent, Santa Clara, CA, USA) with DNA ScreenTape (Agilent, CA, USA). This ensured that the amplicons were within the expected size range and minimized the presence of adapter dimers or residual primers. The final library concentration was determined using the Qubit 4 fluorometer with the High Sensitivity D5000 ScreenTape (Agilent, Santa Clara, CA, USA). A mock microbial community (ZymoBiomics Microbial Community Standard, Zymo Research, Irvine, CA, USA) was included in the analysis as a quality control standard to ensure accuracy and mitigate potential batch effects.

According to the manufacturer's guidelines, libraries were pooled at equimolar concentrations for multiplexing and loaded onto a Spot-ON Flow Cell for sequencing using the MinION platform (Oxford Nanopore Technologies, Oxford, UK). The sequencing efficiency and run quality were monitored in real-time using the MinKNOW software (Oxford Nanopore Technologies) version: 5.8.12, enabling comprehensive and high-resolution microbial community profiling.

2.4. Data Processing and Taxonomic Assignment

A rigorous data processing pipeline was applied to the nanopore sequencing reads to ensure robust and reliable results. First, base-calling was performed using the Guppy software (version 6.3.2), which ensured high-quality nucleotide base identification. Subsequently, a strict quality filter (Q-score ≥ 7) was applied to remove low-quality reads, thereby maintaining the resulting dataset's integrity.

The resulting FASTQ files were processed using Porechop to remove adapter sequences and to demultiplex the reads, assigning them to their respective samples [90].

The demultiplexed reads were then used as input for taxonomic classification through the Emu algorithm, specifically designed to annotate full-length 16S rRNA sequences generated from nanopore sequencing [91]. Emu utilizes an expectation-maximization approach, which enables precise and reliable taxonomic assignments, minimizing false positives and negatives [91].

To further refine taxonomic assignment, a customized 16S rRNA database was constructed by combining reference databases with sequences derived from previous studies. A minimum abundance threshold of 0.01 was established to exclude low-representative taxa or potential artifacts. Classified reads were grouped into operational taxonomic units (OTUs) at a 97% similarity threshold, which enabled the operational definition of the different bacterial species present in the samples.

2.5. Community Profiling and Statistical Testing

The resulting OTU table was analyzed using the Microbiome Analyst software version 2.0 to obtain a comprehensive overview of the microbial community structure and diversity. Initially, singleton OTUs—those present in only one sample—were removed to reduce noise and enhance the robustness of the analyses. Subsequently, a logarithmic transformation was applied to the abundance data to normalize the distribution and improve the interpretability of the results.

Principal Coordinates Analysis (PCoA) was performed based on a Bray-Curtis distance matrix to assess differences in the microbial community composition across sample groups. This analysis facilitated the visualization of sample relationships and the identification of clusters with similar microbial compositions. In addition, an Analysis of Similarities (ANOSIM) was conducted to determine whether statistically significant differences existed in community structure between the compared groups.

Furthermore, a rarefaction curve was constructed using the Vegan package in R to evaluate sampling coverage and microbial community richness [92]. This curve assessed whether the number of sequences obtained was sufficient to capture the total community diversity and if there were differences in richness between the sample groups.

2.6. Data Processing and Heat Tree Visualization of Microbial Communities

The heat tree analysis was performed using the R programming language (version 4.3.3) and the integrated development environment RStudio. Several R libraries were utilized, including Metacoder for hierarchical taxonomic data analysis and visualization, Dplyr for efficient data manipulation, and Vegan for ecological diversity analysis [92,93]. These tools were selected for their robustness and widespread use in microbiota data analysis.

The microbiota dataset used in this study was derived from 16S rRNA sequencing data processed through the MicrobiomeAnalyst pipeline [94]. The dataset comprised two primary files: one containing taxonomic read abundance per sample and another with metadata detailing sample attributes, such as experimental treatments and tissue sources. Both files were imported into R, and an initial exploratory analysis was conducted to assess data integrity and structure.

A rigorous filtering process was implemented to ensure data reliability and mitigate the influence of sequencing artifacts. Taxa with low read counts, specifically those with fewer than five reads, were removed to minimize the impact of sequencing errors. Furthermore, taxa exhibiting zero abundance across all samples were excluded. A prevalence threshold of 20% was applied, ensuring that only taxa present in at least 20% of the samples were retained. This filtering process was conducted separately for tissue types, including gills and digestive glands, for potential tissue-specific variations in microbial communities.

The heat tree visualization was generated using the Metacoder package, which enables the hierarchical representation of microbial communities [95]. In this visualization, node size corresponds to taxon abundance, while node color indicates statistical differences across experimental conditions. Prior to visualization, the dataset was transformed into a format compatible with the Metacoder package. Taxonomic hierarchies were structured according to lineage, and a taxmap object was created to organize and analyze taxonomic relationships.

2.7. Linear Discriminant Analysis Effect Size (LEfSe) and Correlation Network Analysis

The linear discriminant analysis effect size (LEfSe) method was employed to identify significant differences in bacterial species abundance between gill samples from challenged and controlled individuals. A significance threshold of FDR-adjusted p-value < 0.05 and a logarithmic, linear discriminant analysis (LDA) score $\geq$ 4.0 were set as cut-off values to identify differentially abundant taxa. The top 15 discriminative features were visualized using a dot plot highlighting the primary bacterial taxa driving the differences between groups.

To further explore microbial interactions, a network correlation analysis was performed to evaluate the co-occurrence patterns of microbial taxa in the samples. Networks were constructed using the Sparse Correlations for Compositional Data (SparCC) algorithm, which is particularly suited for microbiota data due to its ability to handle compositional structures. The correlation network was estimated using 100 bootstrap permutations, with a significance threshold of $p < 0.05$ and a minimum correlation coefficient of 0.3. These parameters were chosen to ensure the identified associations' robustness and minimize the inclusion of spurious correlations. This approach helps identify potential interactions and dependencies among bacterial species within the microbiota.

2.8. Prediction of Metagenomic Functional Potential

PICRUSt2 (Phylogenetic Investigation of Communities by Reconstruction of Unobserved States) was employed to infer the functional potential of the microbiota in the gill and digestive gland tissues of *M. chilensis* under hypoxic conditions based on marker gene sequences [96]. The R package ggpicrust2 was used to facilitate the functional analysis and visualization [97]. Given that PICRUSt2 is optimized for short-read sequencing data, a preprocessing step was necessary to adapt our long-read amplicon sequences generated through nanopore technology. The software HyperEx v0.1.0 extracted the V3–V4 regions from the full-length 16S rRNA sequences, generating a FASTA file suitable for downstream processing.

The resulting FASTA and BIOM files generated from the operational taxonomic unit (OTU) table were used as input for PICRUSt2 analysis. The functional pathways were constructed using the MetaCyc database to provide a comprehensive functional profile of the microbial communities [98]. The relative abundances of pathways were visualized using the R software version 4.3.3. Statistical Analysis of Metagenomic Profiles (STAMP) was employed [99] to test for significant differences in pathway contributions between groups. A chi-square test corrected with the Benjamini–Hochberg false discovery rate (FDR) was applied to control for multiple comparisons, with a significance threshold set at an FDR-adjusted p-value of <0.05.

For visualization purposes, the final plots included only data with a minimum relative abundance of 0.5% to focus on the most relevant functional changes. This approach enabled a detailed evaluation of pathway-level functional shifts associated with the microbiota's response to hypoxic stress, providing insights into the potential functional adaptations within the microbial community.

2.9. Data Availability

The nanopore data for DNA analysis were deposited in the National Center for Biotechnology Information Short Reads Archive (NCBI-SRA) under the BioProject accession number PRJNA1240298.

3. Results

3.1. Alpha and Beta Diversity Analysis of *M. chilensis* Microbiota Under Normoxia and Hypoxia

Alpha and beta diversity analyses of the *M. chilensis* microbiota under normoxic and hypoxic conditions revealed significant differences in microbial composition and structure across both studied tissues (gills and digestive gland) (Figure 1). Rarefaction curves (Figure 1A) showed an apparent decrease in microbial diversity under hypoxia compared to normoxia, particularly pronounced in the gills. The digestive gland showed lower diversity only during the first hypoxic sampling. Principal Coordinate Analysis (PCoA) (Figure 1B) revealed a distinct clustering of normoxic and hypoxic samples for both tissues, indicating substantial shifts in microbial community composition. Alpha diversity indices (Figure 1C) confirmed a significant decrease in microbial diversity in both tissues under hypoxia. This decline was more pronounced in the gills, suggesting a greater sensitivity of the microbial community present to low oxygen compared to the digestive gland.

3.2. Taxonomic Shifts in the Microbiota of *M. chilensis* Under Normoxia and Hypoxia

Figure 2 presents a heat tree analysis, where branch color reflects the log2 of the mean ratio between bacterial taxa's relative abundance under normoxia (blue) and hypoxia (red). This approach visualizes taxonomic changes across hierarchical levels, highlighting variations induced by oxygen conditions.

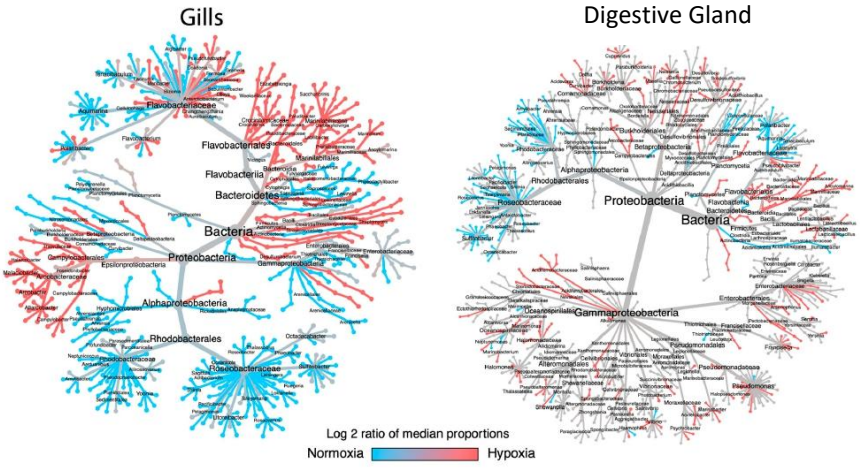

Figure 2. Heat tree analysis evidencing the taxonomical changes in the microbiota of gills and digestive gland of *M. chilensis* exposed to different levels of oxygenation. The color of the branches represents the log2 ratio of median proportions between normoxia (blue) and hypoxia (red).

In gills, an apparent decrease in the relative abundance of specific taxa under hypoxia was observed, while others exhibited an increase. This difference is represented by branch color: taxa with decreased abundance under hypoxia are blue, and those with increased abundance are red. Dominant taxa under normoxia included Roseobacteraceae, *Oceanicola*, *Roseobacter*, *Thalassobius*, *Phaeobacter*, Octadecabacter, *Sulfitobacter*, *Leisingera*, *Ruegeria*, *Loktanella*, *Tateyamaria*, *Roseovarius*, *Litoreibacter*, *Pelagimonas*, *Pacifibacter*, *Shimia*, *Actibacterium*, *Saggitula*, Rhodobacteraceae, *Aliiroseovarius*, *Yoonia*, *Pseudophaeobacter*, *Planktotalea*, *Sedimentitalea*, *Amylibacter*, *Aestuariibius*, and *Neptunicoccus*. Conversely, taxa representative of hypoxia included Campylobacterales, *Poseidonibacter*, Arcobacteraceae, Campylobacteraceae, Campylobacter, *Aliarcobacter*, *Arcobacter*, *Malaciobacter*, *Halarcobacter*, Thiovulaceae, *Elizabethkingia*, *Weeksellaceae*, *Saccharicrinis*, *Paludibacter*, *Crocinitomix*, Crocinitomicaceae, *Labilibacter*, Prolixibacteraceae, *Marinifilum*, *Olleya*, *Antarticcibacterium*, Firmicutes, and Bacillales.

The digestive gland displayed a similar response, with differential patterns in taxonomic abundance under hypoxia. Hypoxia significantly altered the microbiota composition, with several taxa exhibiting notable changes in relative abundance. Dominant taxa under normoxia included *Octadecabacter*, *Sulfitobacter*, *Thalassobius*, *Phaeobacter*, *Roseobacter*, *Leisingera*, *Antarctobacter*, *Roseovarius*, *Tateyamaria*, *Shimia*, *Pacificibacter*, *Litoreibacter*, *Pelagimonas*, *Aliiroseovarius*, *Amylibacter*, *Sedimentitalea*, *Planktotalea*, Rhodobacteraceae, Lacipirellulaceae, *Polaribacter*, and *Aquimarina*. In contrast, taxa enriched under hypoxia were *Acidovorax*, *Delftia*, *Curvibacter*, *Burkholderia*, *Cupriavidus*, *Paraburkholderia*, *Neisseria*, *Massilia*, *Desulfovibrio*, *Solidesulfovibrio*, *Pseudodesulfovibrio*, *Acidithiobacillus*, Acidiferrobacteraceae, Nevskiales, Steroidobacteraceae, Ectothiorhodospiraceae, *Marinobacterium*, *Pseudoalteromonas*, *Shewanella*, *Vibrio*, *Francisella*, *Yersinia*, *Serratia*, Pectobacteriaceae, Enterobacteriaceae, *Ancylomarina*, Marinifilaceae, Marinilabiliales, Bacteroidales, and Flavobacteriales.

3.3. Analysis of Bacterial Genus Relative Abundance in the Microbiota of M. chilensis Under Normoxia and Hypoxia

Heatmap analysis revealed distinct shifts in the relative abundance of bacterial genera in the gill and digestive gland microbiotas of *M. chilensis* under normoxic and hypoxic conditions (Figures 3 and 4). The microbial communities clustered into two distinct groups in both tissues, reflecting differential responses to oxygen availability. Figures 3A and 4A illustrate these patterns, with normoxic (blue) and hypoxic (red) conditions highlighting specific genera that were differentially distributed, suggesting a tissue-specific microbial adaptation to hypoxia.

Cluster 1 consisted of bacterial genera that showed a marked decrease in abundance under hypoxic conditions. In the gills (Figure 3B), these genera exhibited a significant reduction in relative abundance during hypoxia exposure, with a similar trend observed in the digestive gland (Figure 4B). Representative genera in the gill cluster included *Salmonella*, *Thalassobius*, *Roseobacter*, *Cocleimonas*, *Nitratireductor*, *Planktomarina*, *Marinicella*, *Yoonia*, *Neptunicoccus*, *Tenacibaculum*, *Cellulophaga*, *Leucothrix*, *Tritonibacter*, *Jannaschia*, *Lacinutrix*, *Boseongicola*, *Sedimentitalea*, *Pseudahrensia*, *Pseudoruegeria*, and *Phaeobacter*. In the digestive gland, prominent genera included *Thiomicrorhabdus*, *Mobilisporobacter*, *Klebsiella*, *Helicobacter*, *Spongiibacter*, *Paraglaciecola*, *Citrobacter*, *Shewanella*, *Cellvibrio*, *Vibrio*, *Solidesulfovibrio*, *Rheinheimera*, *Serratia*, *Aquella*, *Glaciecola*, *Franconibacter*, *Latilactobacillus*, *Oceaniserpentilla*, *Lacticaseibacillus*, and *Labilibaculum*.

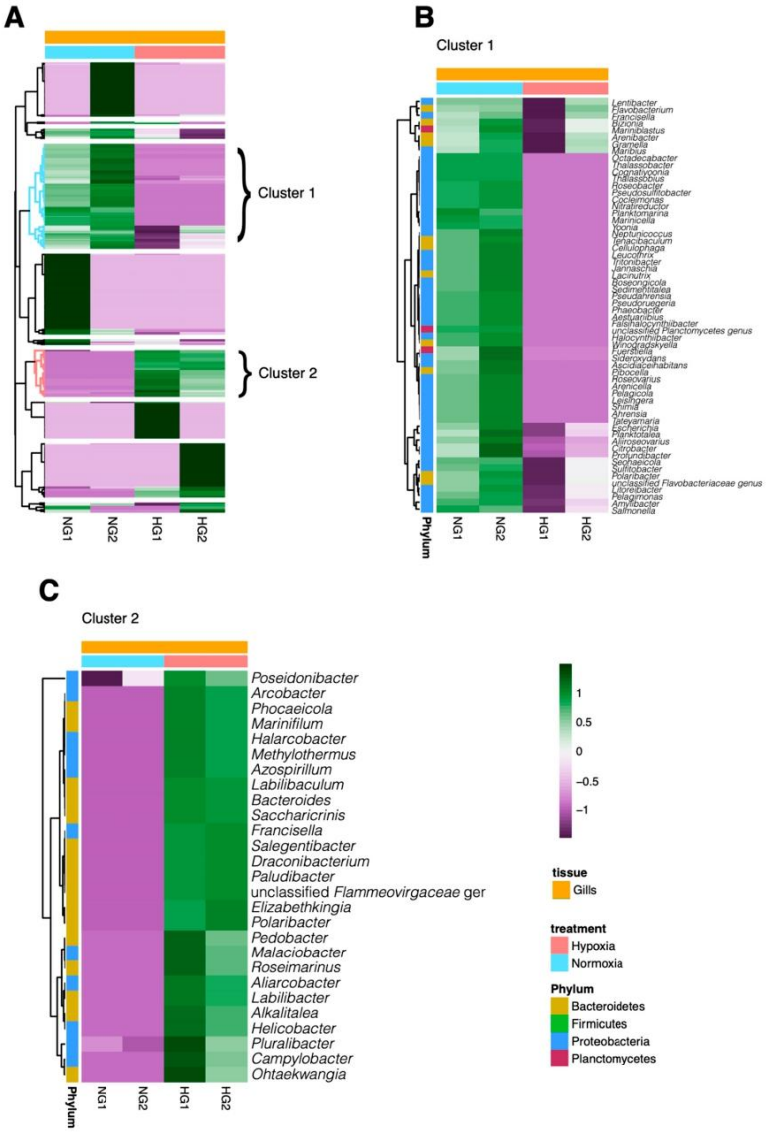

Figure 3. Heatmaps showing the relative abundance of various bacterial genera in the microbiota of gills (**A**) of *M. chilensis* exposed to normoxia (blue) and hypoxia (red). For each condition, two clusters were identified. "Cluster 1" includes genera that exhibited decreased abundance in the gills of mussels exposed to hypoxia (**B**). In contrast, "Cluster 2" comprises genera that increased their abundance in hypoxic conditions in the gills (**C**).

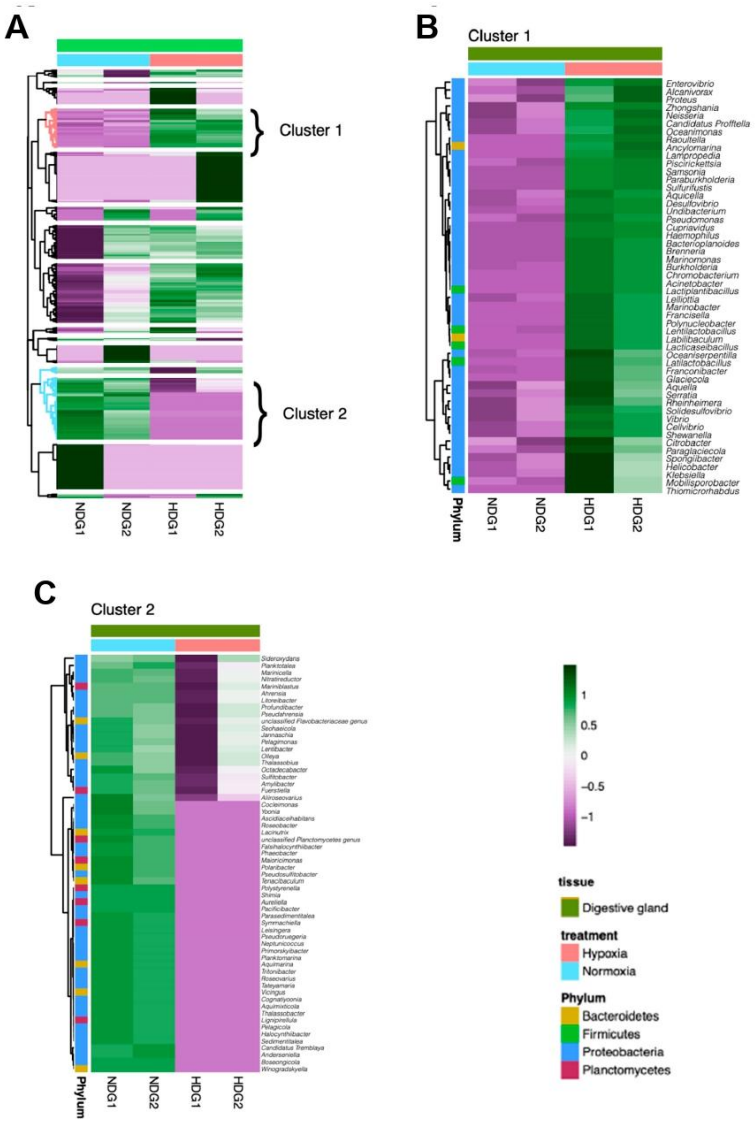

Figure 4. Heatmaps illustrating the relative abundance of different bacterial genera in the microbiota of the digestive gland (**A**) of *M. chilensis* exposed to normoxia (blue) and hypoxia (red). Two distinct clusters were identified for each condition. "Cluster 1" consists of genera that decreased in abundance in the digestive glands of mussels exposed to hypoxia (**B**), while "Cluster 2" includes genera that increased in abundance under hypoxic conditions (**C**).

In contrast, Cluster 2 comprised bacterial genera that increased in abundance under hypoxia. In the gills (Figure 3C), these genera showed a significant rise in relative abundance in response to hypoxic exposure, and a similar pattern was evident in the digestive gland (Figure 4C). The predominant gill genera under hypoxia included *Poseidonibacter*, *Arcobacter*, *Phocaeicola*, *Marinifilum*, *Halarcobacter*, *Methylothermus*, *Azospirillum*, *Labilibaculum*, *Bacteroides*, *Saccharicrinis*, *Francisella*, *Salegentibacter*, *Draconibacterium*, *Paludibacter*, *Elizabethkingia*, *Polaribacter*, *Pedobacter*, *Malaciobacter*, *Roseimarinus*, and *Aliarcobacter*. The digestive gland featured hypoxia-associated genera such as *Sideroxydans*, *Planktotalea*, *Marinicella*, *Nitratireductor*, *Mariniblastus*, *Ahrensia*, *Litoreibacter*, *Profundibacter*, *Pseudahrensia*, *Seohaeicola*, *Jannaschia*, *Pelagimonas*, *Lentibacter*, *Olleya*, *Thalassobius*, *Octadecabacter*, *Sulfitobacter*, *Amylibacter*, *Fuerstiella*, and *Aliiroseovarius*.

3.4. Linear Discriminant Analysis

Linear Discriminant Analysis (LDA) demonstrated distinct bacterial community compositions in the gills and digestive gland of *M. chilensis* under normoxic and hypoxic conditions (Figure 5).

In the gills (Figure 5A), 31 bacterial species were significantly more abundant under normoxia, including *Aquimarina macrocephali*, *Aquimarina muelleri*, and *Flavobacteriaceae bacterium*. Conversely, 19 species exhibited increased abundance under hypoxia, such as *Poseidonibacter parvus*, *Poseidonibacter lekithochrous*, and *Arcobacter nitrofigilis*.

Similarly, the digestive gland (Figure 5B) displayed 14 bacterial species enriched under normoxia, including *Polaribacter* sp. *ALD11*, *Polaribacter* sp. *BM10*, and *Plaribacter atrinae*. In contrast, six species showed increased abundance under hypoxia, including *Francisella tularensis*, *Citrobacter freundii*, and *Shigella sonnei*.

3.5. Functional Potential Prediction of the M. chilensis Microbiota Under Normoxia and Hypoxia

Picrust2 analysis revealed alterations in the functional potential of the *M. chilensis* microbiota between normoxia and hypoxia conditions (Figure 6). Among the metabolic pathways analyzed, only the degradation/utilization/assimilation category showed a significant difference between conditions (Figure 6A,B). Notably, both tissues exhibited a higher proportion of sequences assigned to degradation/utilization/assimilation pathways under normoxia compared to hypoxia (Figure 6C,D).

The metabolic pathways enriched under normoxia and hypoxia differed between the gills and digestive gland (Figure 6E,F). All degradation/utilization/assimilation pathways were different for both tissues, except for the TCA cycle which was more enriched than other pathways in the digestive gland. In the gills, normoxia favored pathways related to cofactor, prosthetic group, and electron carrier biosynthesis, as well as fatty acid, lipid, and carbohydrate biosynthesis, whereas the digestive gland exhibited a predominance of the TCA cycle, amine and polyamine degradation, and aspartate metabolism. Under hypoxia (Figure 6E), the gills showed an increase in cofactor, prosthetic group, electron carrier biosynthesis, carbohydrate biosynthesis, and the TCA cycle, accompanied by a decline in fatty acid and lipid biosynthesis, nucleoside and nucleotide degradation, and secondary metabolite degradation. In the digestive gland (Figure 6F), hypoxia induced an upregulation of the TCA cycle and hexuronide and hexuronate degradation, while pathways related to amine and polyamine degradation, aspartate metabolism, S-adenosyl-L-methionine biosynthesis, and the methylaspartate cycle were downregulated.

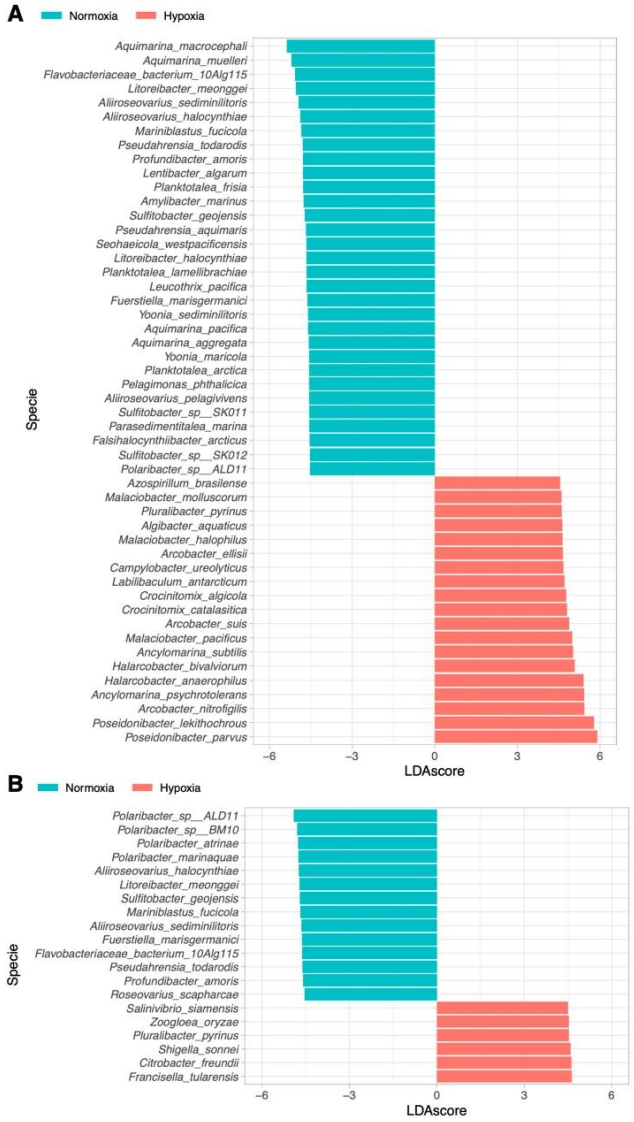

Figure 5. Linear Discriminant Analysis (LDA) scores of differentially abundant species in mussels exposed to normoxia and hypoxia conditions for gills (**A**) and digestive gland (**B**). Species with blue bars were significantly abundant in normoxia conditions, while the red ones were more abundant in hypoxic conditions.

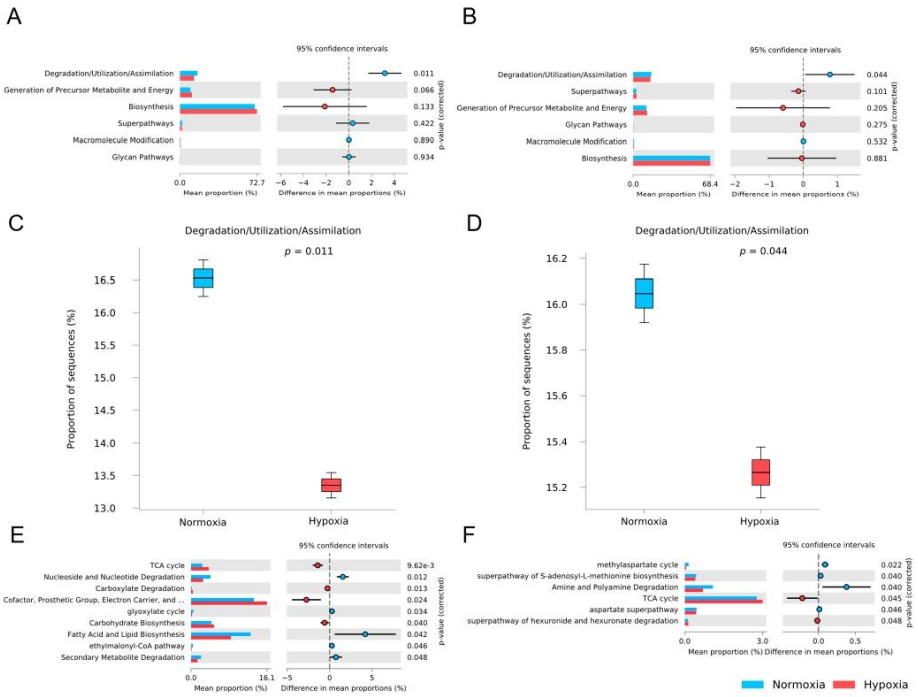

Figure 6. Prediction of the functional potential of the microbiota from gills and digestive gland of *M. chilensis* based on Picrust2. Bars represent the mean proportions of microbiota pathways in normoxia (blue) and hypoxia (red) individuals. The differences between the conditions for the Metacyc top level are presented for gills (**A**) and digestive gland (**B**) with their respective corrected *p*-values. (**C**,**D**) show the specific values for the degradation/utilization/assimilation pathways for gills and digestive gland, respectively. Finally, the Metacyc secondary levels for degradation/utilization/assimilation with significant differences (corrected *p*-value < 0.05) within experimental conditions are also presented for gills (**E**) and digestive gland (**F**).

3.6. Dynamics of Bacterial Pathogens

We evaluated the presence and abundance of specific groups to explore whether changes in the microbiota due to hypoxia lead to an increase in the community of pathogenic bacteria. The objective was to assess whether hypoxia promotes bivalves as reservoirs for aquatic pathogens. Figure 7 presents a scatter plot illustrating the dynamics in the relative abundance of various fish bacterial pathogens in *M. chilensis* under normoxic and hypoxic conditions. Each point on the graph represents the relative abundance of a specific pathogen at different levels of oxygen.

In the gills of *M. chilensis*, an increase in the relative abundance of some bacterial pathogens was observed under hypoxic conditions compared to normoxia. Pathogens that showed a significant increase included *Arcobacter cryaerophilus*, with smaller increases seen in *Citrobacter freundii* and *Klebsiella pneumoniae*. Conversely, some bacterial pathogens in the gills of *M. chilensis* disappeared under hypoxic conditions compared to normoxia.

These pathogens included *Flavobacterium columnare*, *Salmonella enterica*, and *Tenacibaculum ovolyticum*.

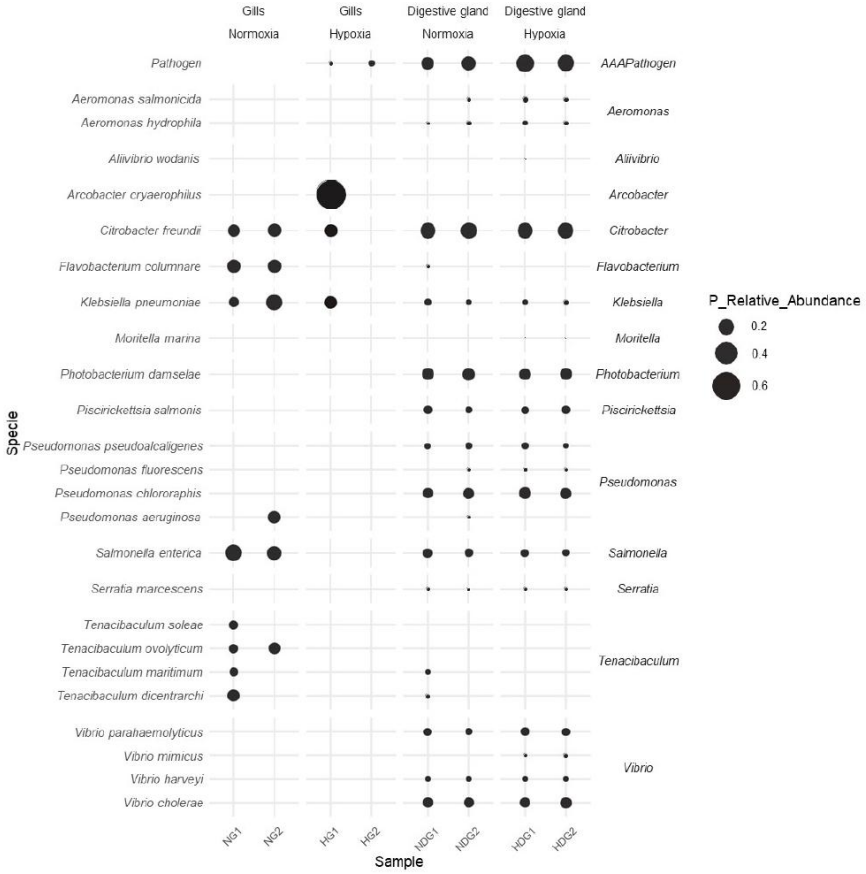

Figure 7. Dot plot showing the dynamics in the relative abundance of fish bacterial pathogens associated with gills and digestive glands of *M. chilensis* exposed to different oxygenation levels.

Similarly, the digestive gland of *M. chilensis* also experienced an increase in the relative abundance of several bacterial pathogens under hypoxia. Pathogens that showed a notable increase included *Aliivibrio wodanis*, *Pseudomonas fluorescens*, *Moritella marina*, and *Vibrio mimicus*. Additionally, in the digestive gland of *M. chilensis*, several bacterial pathogens disappeared under hypoxic conditions compared to normoxia. Pathogens that disappeared included *Flavobacterium columnare*, *Tenacibaculum maritimum*, and *Tenacibaculum dicentrarchi*. Moreover, a reduction in the relative abundance of *Vibrio cholerae*, *Pseudomonas chlororaphis*, and *Citrobacter freundii* was also observed.

4. Discussion

This study highlights the importance of conducting controlled hypoxia exposure experiments to understand and predict changes in the microbiota of bivalve mollusks, such as *M. chilensis*, under environmental stress associated with climate change [15]. Hypoxia, regarded as a significant environmental stressor, interacts in complex ways with other environmental factors, significantly affecting the health and performance of marine organisms [100,101]. Advancing our understanding of the microbiota's role in the physiological response of organisms to these stressors has become essential, as it can reveal critical mechanisms of adaptation and resilience [30,102–104]. Expanding on previous studies, this work focused on evaluating the impact of hypoxia on the gill and digestive gland microbiota of *M. chilensis* [15,105,106].

In this context, our study is pioneering in demonstrating the effects of oceanic hypoxia on the gill and digestive gland microbiota of mussels at the species level. The gills, in addition to their respiratory function, play a key role in nutrition and immune defense, hosting symbiotic microbial communities that contribute to carbon and nitrogen fixation [107–110]. Our results indicate that hypoxia induces profound changes in both the composition and function of the microbiota in these tissues, primarily by eliminating bacterial groups unable to tolerate low oxygen conditions. The observed restructuring of the microbiota under hypoxia suggests adaptive and selective effects, reinforcing the microbiota's ability to respond to environmental stress. These changes likely result from selective pressure favoring bacterial communities with greater tolerance to hypoxic conditions, possibly mediated by adaptive mechanisms such as quorum sensing, which regulate colonization, virulence, and stress resistance in oxygen-depleted environments [27,28,108,111–115]. However, this adaptive capacity also presents potential risks. The selective pressure exerted by hypoxia may facilitate the proliferation of opportunistic pathogens, potentially compromising the host's immune system and its ability to resist infections and other environmental stressors. Our results provide evidence of this selective pressure, manifested in a reduction of bacterial species richness and diversity, particularly in the gills, aligning with responses observed in other aquatic ecosystems [1,116,117]. Functional changes in the microbiota of *M. chilensis*, especially in lipid and fatty acid biosynthesis pathways, suggest metabolic adaptations to hypoxia. These findings corroborate previous studies in other bivalves [15]. These changes are likely strategies to optimize energy efficiency and minimize biomass production in resource-limited environments [16,118].

Alterations in the functionality of the microbiota have direct implications for host physiology [119]. Reducing the production of essential metabolites, such as vitamins and amino acids, may affect the nutrition and overall health of *M. chilensis* [120]. Additionally, the decrease in microbial diversity and functionality could limit the microbiota's ability to contribute to critical metabolic processes, such as nutrient digestion and the production of immunomodulatory compounds [121]. The results reveal a decrease in the activity of degradation, utilization, and nutrient assimilation pathways in the digestive gland under hypoxic conditions. This phenomenon could affect essential cellular processes, such as proliferation and differentiation, limiting the mussel's growth and adaptive capacity in response to additional stress factors [122,123]. The complex interaction between biosynthesis, metabolite generation, and degradation pathways under hypoxia indicates a co-evolutionary adaptation process between *M. chilensis* and its microbiota. This symbiotic relationship is crucial for maintaining host homeostasis; any disruption in this balance may lead to dysbiosis, increasing susceptibility to opportunistic or polymicrobial infections. In aquaculture and marine environments, dysbiosis has been associated with mass mortality events and disease outbreaks, underscoring the importance of the microbiota in host health [124].

The variation in the intestinal microbiota composition of *Mytilus* across individuals and populations reflects the influence of diet, host genetics, and environmental conditions [125–130]. Aquaculture practices also shape this microbial structure, as seen in the differences between the microbiota of farmed and wild mussels [131]. In the gills of *M. chilensis*, the increased presence of bacterial groups associated with hypoxic environments is a clear consequence of the selective pressure of low oxygen availability. These adaptations may involve the production of antioxidants and the utilization of alternative metabolic pathways, indicating a complex metabolic interaction between the bacteria and the host [132,133].

The dominant microbiota in the digestive gland of *M. chilensis* includes bacteria from the phyla Actinobacteria, Proteobacteria, Bacteroidetes, and Firmicutes, consistent with other mussel species and aquatic organisms [15,44,134–148]. In contrast, the gill microbiota is dominated by Proteobacteria and Firmicutes, suggesting specialized and complementary roles in mussel physiology. Our findings are consistent with previous studies in other aquatic environments [136]. The prevalence of Bacteroidetes and Firmicutes in the digestive tract indicates a specialized symbiotic relationship with an enzymatic arsenal for degrading complex polysaccharides, such as cellulose and chitin, found in plankton and marine detritus [135,149–151]. These bacteria produce various bioactive compounds, such as antibiotics and pigments, which can benefit both the host and the microbiota [152]. Antibiotics may protect the host from pathogens, while pigments may function as antioxidants, reducing oxidative stress [153,154]. Firmicutes, with their ability to form spores, contribute to the stability of the intestinal microbiota under stressful conditions [155–157]. Additionally, some Firmicutes produce short-chain fatty acids as fermentation byproducts, which have anti-inflammatory properties and modulate the host's immune response [158].

Hypoxia significantly altered the microbial community structure of *M. chilensis*, favoring facultative anaerobes and opportunistic pathogens while reducing beneficial microbial functions. Proteobacteria in the gills of *M. chilensis* participate in the degradation of organic matter in marine environments [159–162]. Their metabolic versatility allows them to utilize a wide range of organic compounds, significantly contributing to nutrient cycling [163–168]. However, a shift toward *Vibrio*, *Aeromonas*, and *Desulfovibrio* was observed under hypoxic conditions, indicating an increased risk of pathogenicity and altered sulfur metabolism [169–171]. The selective pressure exerted by low oxygen availability may enhance the survival of bacteria capable of utilizing alternative electron acceptors, potentially increasing oxidative stress in the host and disrupting metabolic homeostasis [172–176].

The study of the microbiota associated with *M. chilensis* reveals the dominance of bacteria belonging to the classes Alphaproteobacteria, Bacteroidia, Epsilonproteobacteria, and Gammaproteobacteria in the gills and digestive gland. These classes exhibit diverse and ecologically relevant metabolic functions in aquatic ecosystems, participating in biogeochemical and ecological cycles [167,177–181]. The presence of Epsilonproteobacteria in the gills suggests an adaptation to sulfuric niches and a potential symbiotic role in the oxidation of reduced compounds [182,183]. Alphaproteobacteria and Gammaproteobacteria are key components of the *M. chilensis* microbiota, particularly under normoxic conditions. Their abundance may correlate with water quality, serving as potential bioindicators of dissolved organic matter from anthropogenic sources [184,185]. Gammaproteobacteria play a crucial role in the degradation of complex organic compounds, contributing to nutrient biogeochemical cycles [186–188]. The order Rhodobacterales, within the class Alphaproteobacteria, dominates the gill and digestive microbiota of *M. chilensis*. These bacteria break down organic matter, facilitating the host's nutrient absorption [181]. Furthermore, they may modulate the immune response, enhancing the mussel's survival in challenging

environments [189,190]. A significant aspect is the Roseobacteraceae family's sensitivity to hypoxia. The reduction of these bacteria under low oxygen conditions suggests a disruption in microbial trophic networks, potentially affecting host health [191–193].

The taxonomic analysis of the digestive gland reveals the dominant presence of bacterial genera *Shewanella*, *Aeromonas*, and *Vibrio* as key components of the core bacterial community in the digestive gland. These bacteria are known for their pathogenic potential and ability to act as reservoirs of plasmids encoding antibiotic resistance genes [194–196]. The horizontal transfer of these genes, facilitated by conjugation, transformation, and transduction mechanisms, increases the risk of antimicrobial resistance dissemination, posing a significant public health concern [197–202]. This phenomenon is not limited to clinical settings but has also been documented in natural aquatic ecosystems, suggesting that these environments can serve as global reservoirs of resistance genes [203–205].

The increasing antimicrobial resistance, exacerbated by climate change and the indiscriminate use of antibiotics in aquaculture, highlights the urgent need to develop more effective control strategies [206–211]. Under hypoxic conditions, a reduction in the populations of *Shewanella* and *Vibrio* was observed, while *Aeromonas* demonstrated a remarkable ability to adapt and maintain its presence. This adaptability may be related to its diverse genetic repertoire, which includes virulence factors and the ability to form biofilms [212–217].

Pathogenic species such as *Aeromonas hydrophila* and *Aeromonas salmonicida* cause significant losses in aquaculture and pose a global health threat due to their ability to acquire antibiotic resistance genes [201,206,218–227]. The coevolution between Aeromonas and hosts such as *M. chilensis* suggests a symbiotic relationship in which the bacteria may facilitate digestion and offer protection against other pathogens [228–246]. However, this symbiosis can be disrupted under environmental stress, such as hypoxia, promoting Aeromonas as an opportunistic pathogen.

The decrease in *Shewanella* under hypoxic conditions is noteworthy, considering its ability to utilize nitrate as an electron acceptor in anaerobic environments [247–249]. This reduction in abundance could be due to competition for nutrients or the production of antimicrobial compounds by other microbial species'. The presence of *Vibrio* in the core microbiota of *M. chilensis* suggests a potential mutualistic relationship, which is consistent with other studies [240,250,251]. However, some *Vibrio* species are pathogenic to both bivalves and humans [250,252–257]. Although *Vibrio* demonstrates ecological adaptability, its dependence on oxygen reduces its prevalence under hypoxic conditions. This decrease may benefit the health of *M. chilensis* by reducing *Vibrio*-induced diseases, but it could also increase vulnerability to other pathogenic species such as *Vibrio mimicus*. This pathogen has been associated with disease outbreaks in various bivalve species, causing high mortality rates and significant economic losses in aquaculture [258]. *V. mimicus* thrives in hypoxic conditions and poses a threat due to biofilm formation, antibiotic resistance, and zoonotic potential [259,260]. An increase in the genus *Acinetobacter* was observed in the digestive gland under hypoxic conditions. This genus is notable for its ability to persist in diverse environments and facilitate horizontal gene transfer, including those conferring resistance to multiple clinically relevant antibiotic classes. Pathogenic strains of *Acinetobacter*, characterized by their multidrug resistance, represent a critical public health threat in both clinical settings and natural ecosystems [222].

Our findings confirm the absence of *Psychrilyobacter* in farmed *M. chilensis* compared to wild populations, indicating that habitat characteristics significantly influence microbial composition [131]. Anaerobic conditions in natural ecosystems support *Psychrilyobacter* colonization, whereas suspended aquaculture systems limit such environments [163,261–264]. Reduced microbial diversity in aquaculture could impair mussel adaptation to environmental changes and increase susceptibility to pathogens over time [265]. The presence of

Aquimarina macrocephali in the gills of *M. chilensis* under normoxic conditions suggests an adaptation to this oxygen-rich environment. This is supported by its enzymatic profile for reducing oxidative stress and its potential role in the degradation of organic matter [266]. This bacterium may contribute to the cleaning of gill surfaces, facilitating nutrient acquisition and enhancing host health. Additionally, its ability to degrade chitin suggests a possible symbiotic interaction with the mussel, as chitin is a common structural component in plankton and microorganisms that form part of the bivalve diet [151,266]. However, *A. macrocephali*'s resistance to multiple antibiotics raises concerns about its role as a reservoir of resistance genes, potentially facilitating the spread of these genetic elements within the marine ecosystem and the food chain [266–270]. Antibiotic resistance in *A. macrocephali* could be linked to acquiring plasmids and exposure to subtherapeutic antibiotic doses in the aquatic environment, stemming from aquaculture and wastewater [271,272].

The comprehensive integration of transcriptomic and microbiota profiling in *M. chilensis* exposed to hypoxic stress has revealed a tightly interconnected network of metabolic reprogramming, immune modulation, and microbial community restructuring, underscoring the profound physiological consequences of oxygen deprivation. Hypoxia-induced metabolic shifts, characterized by the suppression of aerobic respiration and the upregulation of anaerobic pathways, were accompanied by significant alterations in the microbiota, favoring facultative anaerobes and opportunistic pathogens, thereby indicating microbial dysbiosis that could compromise host metabolic efficiency and overall homeostasis. Concurrently, immunosuppression was evident through the downregulation of immune-related genes, increased oxidative stress marked by elevated reactive oxygen species (ROS) levels, and a greater abundance of pathogenic taxa, collectively suggesting heightened host vulnerability to infections. The response exhibited tissue specificity, with gill tissues displaying more pronounced transcriptomic and microbial shifts than the digestive gland, potentially engaging compensatory metabolic pathways to mitigate hypoxia-induced stress [77].

A more personalized approach will be required to effectively manipulate immune functions through microbiota-based therapies, one that identifies specific microorganism-host relationships [104]. In the context of bivalves, high-throughput sequencing has been instrumental in managing diseases in aquaculture [273,274]. Prebiotics and probiotics in mussel farming offer a promising approach to enhancing larval resistance to adverse effects such as climate change [273,275]. These adaptations could support the survival of populations in an evolving marine environment. Early colonization by a complex microbiota or specific symbionts can induce lasting epigenetic modifications, promoting protective immunity and greater resilience to environmental stressors associated with climate change [276–278]. These early epigenetic alterations can have long-term protective effects, reducing the risk of diseases in later life stages and enhancing the organism's adaptive capacity [276–278]. Additionally, molecular research on the interactions between hypoxia and other environmental factors, such as temperature, pH, and salinity, is crucial for managing the impacts of hypoxia on aquatic ecosystems [274,279]. Monitoring oxygenation conditions in marine habitats will be essential to maintaining the health and robustness of key species. Identifying bacterial genera sensitive or resistant to hypoxia will provide critical insights for developing sustainable management strategies.

An integrated approach based on the hologenome concept is recommended. This approach includes developing predictive models that incorporate environmental, microbial, and host factors to better understand and manage the effects of hypoxia in these ecosystems. Moreover, expanding studies on the *M. chilensis* hologenome, which includes viruses and microeukaryotes whose identities and functions are still in the early stages of research, is necessary [280]. Implementing sustainable management practices, such as reducing

eutrophication and restoring coastal habitats, could improve water quality and protect marine biodiversity.

5. Conclusions

This study represents the first comprehensive report on the effects of hypoxia, a global environmental concern, on the gills and digestive glands of the mussel *M. chilensis*. Our findings show that hypoxia significantly affects the structure, relative abundance, community composition, species richness, and diversity of microbial communities associated with these tissues. The changes in the microbiota induced by hypoxia have substantial implications for mussel physiology, influencing essential processes such as digestion, nutrient absorption, and immune response. Additionally, our results suggest that hypoxia encourages the growth of opportunistic and pathogenic bacteria, underscoring the need for further investigation into the underlying mechanisms of these changes and their functional implications for the organism. Thus, maintaining optimal dissolved oxygen levels in aquaculture systems is crucial for preserving the health of *M. chilensis* and ensuring the sustainability of aquaculture practices. Future research is necessary to develop mitigation strategies that can reduce the negative impacts of this stressor on aquatic ecosystems.

Author Contributions: Conceptualization, M.M.-R., V.V.-M., D.V.-M. and C.G.-E.; methodology, M.M.-R., V.V.-M., D.V.-M. and C.G.-E.; software, V.V.-M., D.V.-M., M.F.M.-R. and C.G.-E.; validation, M.M.-R., V.V.-M., M.F.M.-R., D.V.-M. and C.G.-E.; formal analysis, M.M.-R., V.V.-M., D.V.-M., M.F.M.-R. and C.G.-E.; investigation, M.M.-R., V.V.-M. and C.G.-E.; resources, M.M.-R., V.V.-M. and C.G.-E.; data curation, M.F.M.-R., V.V.-M., D.V.-M. and C.G.-E.; writing—original draft preparation, M.M.-R., V.V.-M., D.V.-M. and C.G.-E.; writing—review and editing, M.M.-R., V.V.-M., D.V.-M. and C.G.-E.; visualization, M.M.-R., V.V.-M., D.V.-M. and C.G.-E.; supervision, M.M.-R., V.V.-M., D.V.-M. and C.G.-E.; project administration, M.M.-R., V.V.-M., D.V.-M. and C.G.-E.; funding acquisition, M.M.-R., V.V.-M. and C.G.-E. All authors have read and agreed to the published version of the manuscript.

Funding: This work was funded by ANID-Chile, FONDAP N°1522A0004, and COPAS Coastal ANID FB210021. Additionally, the author (M.M.-R.) acknowledges financial support from the Secretaría de Educación Superior, Ciencia, Tecnología e Innovación (SENESCYT)-Ecuador/Contrato Nro. CZ05-000735-2018, as well as from the Agencia Nacional de Investigación y Desarrollo (ANID)–Chile, Subdirección de Capital Humano/Beca de Doctorado Nacional 2019-Folio 21190791.

Institutional Review Board Statement: The study was approved by the Ethics Committee of the Universidad de Concepción (protocol code CEBB 1356-2023, approved in 1 March 2023).

Informed Consent Statement: Not applicable.

Data Availability Statement: The original contributions presented in the study are included in the article; further inquiries can be directed to the corresponding authors.

Acknowledgments: We would like to thank Constanza Sáez-Vera for her invaluable contributions and technical support throughout this research. We also wish to acknowledge Claudia Fuentealba for her essential administrative assistance, which greatly facilitated the progress of this project.

Conflicts of Interest: The authors declare no conflicts of interest.

Abbreviations

The following abbreviations are used in this manuscript:

°C	grados Celsius
ANID	Agencia Nacional de Investigación y Desarrollo
ANOSIM	Analysis of Similarities
CA	California
CEBB	Ethics Committee of the Universidad de Concepción

C.G.-E.	Cristian Gallardo Escárate
D.V.-M	Diego Valenzuela Miranda
DO	Dissolved oxygen
FDR	false discovery rate
FONDAP	Fondo de Financiamiento de Centros de Investigación en Áreas Prioritarias
INCAR	Interdisciplinary Center for Aquaculture Research
IPIAP	Instituto Público de Investigación de Acuicultura
LDA	linear discriminant analysis
LDOW	low dissolved oxygen water
LEfSe	Linear Discriminant Analysis Effect Size
$\log_2$	logarithm base 2
M. chilensis	Mytilus chilensis
MA	Massachusetts
MDPI	Multidisciplinary Digital Publishing Institute
mg/L	milligrams per liter
M.M.-R	Milton Montúfar Romero
M.F.M.-R	María Fernanda Morales-Rivera
n	sample size
NCBI	National Center for Biotechnology Information
OTUs	operational taxonomic units
PCoA	Principal Coordinates Analysis
PCR	Polymerase Chain Reaction
pH	potential of hydrogen
PICRUSt2	Phylogenetic Investigation of Communities by Reconstruction of Unobserved States
Q-score	Quality score
rRNA	ribosomal ribonucleic acid
SENESCYT	Secretaría de Educación Superior, Ciencia, Tecnología e Innovación
SparCC	Sparse Correlations for Compositional Data
SRA	Sequence Read Archive
STAMP	Statistical Analysis of Metagenomic Profiles
TCA	Tricarboxylic Acid Cycle
UK	United Kingdom
USA	United States of America
V.V.-M	Valentina Valenzuela-Muñoz

References

1. Fan, S.; Li, H.; Zhao, R. Effects of normoxic and hypoxic conditions on the immune response and gut microbiota of *Bostrichthys sinensis*. *Aquaculture* **2020**, *525*, 735336. [CrossRef]
2. Choumiline, K.; Pérez-Cruz, L.; Gray, A.; Bates, S.; Lyons, T. Scenarios of Deoxygenation of the Eastern Tropical North Pacific During the Past Millennium as a Window Into the Future of Oxygen Minimum Zones. *Front. Earth Sci.* **2019**, *7*, 237. [CrossRef]
3. Conley, D.; Carstensen, J.; Vaquer-Sunyer, R.; Duarte, C. Ecosystem thresholds with hypoxia. *Hydrobiologia* **2009**, *629*, 21–29. [CrossRef]
4. Diaz, R.; Rosenberg, R. Spreading Dead Zones and Consequences for Marine Ecosystems. *Science* **2008**, *321*, 926–929. [CrossRef]
5. Hofmann, A.; Peltzer, E.; Walz, P.; Brewer, P. Hypoxia by degrees: Establishing definitions for a changing ocean. *Deep. Sea Res. Part I Oceanogr. Res. Pap.* **2011**, *58*, 1212–1226. [CrossRef]
6. McArley, T.; Hickey, A.; Herbert, N. Hyperoxia increases maximum oxygen consumption and aerobic scope of intertidal fish facing acutely high temperatures. *J. Exp. Biol.* **2018**, *221*, jeb189993. [CrossRef]
7. Moffitt, S.; Moffitt, R.; Sauthoff, W.; Davis, C.; Hewett, K.; Hill, T. Paleoceanographic insights on recent oxygen minimum zone expansion: Lessons for modern oceanography. *PLoS ONE* **2015**, *10*, e0115246. [CrossRef]
8. Sattari, M.; Bagherzadeh, F.; Sharifpour, I.; Kazemi, R. Effect of hypoxia, normoxia and hyperoxia conditions on gill histopathology in two weight groups of beluga (*Huso huso*). *Casp. J. Environ. Sci.* **2013**, *11*, 77–84.
9. Hernández-Miranda, E.; Quiñones, R.; Aedo, G.; Valenzuela, A.; Mermoud, N.; Román, C.; Yañez, F. A major fish stranding caused by a natural hypoxic event in a shallow bay of the eastern South Pacific Ocean. *J. Fish Biol.* **2010**, *76*, 1543–1564. [CrossRef]

10. Hernández-Miranda, E.; Veas, R.; Anabalón, V.; Quiñones, R. Short-term alteration of biotic and abiotic components of the pelagic system in a shallow bay produced by a strong natural hypoxia event. *PLoS ONE* **2017**, *12*, e0179023. [CrossRef]
11. Hernández-Miranda, E.; Veas, R.; Labra, F.; Salamanca, M.; Quiñones, R. Response of the epibenthic macrofaunal community to a strong upwelling-driven hypoxic event in a shallow bay of the southern Humboldt Current System. *Mar. Environ. Res.* **2012**, *79*, 16–28. [CrossRef]
12. Labra, F.; Hernández-Miranda, E.; Quiñones, R. Dynamic relationships between body size, species richness, abundance, and energy use in a shallow marine epibenthic faunal community. *Ecol. Evol.* **2015**, *5*, 391–408. [CrossRef] [PubMed]
13. Ali, J.; Yang, Y.; Pan, G. Oxygen micro-nanobubbles for mitigating eutrophication induced sediment pollution in freshwater bodies. *J. Environ. Manag.* **2023**, *331*, 117281. [CrossRef] [PubMed]
14. De la Maza, L.; Farias, L. The intensification of coastal hypoxia off central Chile: Long term and high frequency variability. *Front. Earth Sci.* **2023**, *10*, 929271. [CrossRef]
15. Khan, F.; Shang, Y.; Chang, X.; Kong, H.; Zuberi, A.; Fang, J.; Liu, W.; Peng, J.; Zhang, X.; Hu, M.; et al. Effects of Ocean Acidification, Hypoxia, and Warming on the Gut Microbiota of the Thick Shell Mussel *Mytilus coruscus* Through 16S rRNA Gene Sequencing. *Front. Mar. Sci.* **2021**, *8*, 736338. [CrossRef]
16. Andreyeva, A.; Gostyukhina, O.; Kladchenko, E.; Afonnikov, D.; Rasskazov, D.; Lantushenko, A.; Vodiasova, E. Hypoxia exerts oxidative stress and changes in expression of antioxidant enzyme genes in gills of *Mytilus galloprovincialis* (Lamarck, 1819). *Mar. Biol. Res.* **2021**, *17*, 369–379. [CrossRef]
17. Gu, H.; Shang, Y.; Clements, J.; Dupont, S.; Wang, T.; Wei, S.; Wang, X.; Chen, J.; Huang, W.; Hu, M.; et al. Hypoxia aggravates the effects of ocean acidification on the physiological energetics of the blue mussel *Mytilus edulis*. *Mar. Pollut. Bull.* **2019**, *149*, 110538. [CrossRef]
18. Wang, Y.; Hu, M.; Li, Q.; Li, J.; Lin, D.; Lu, W. Immune toxicity of TiO_2 under hypoxia in the green-lipped mussel *Perna viridis* based on flow cytometric analysis of hemocyte parameters. *Sci. Total Environ.* **2014**, *470*, 791–799. [CrossRef]
19. Wang, Y.; Hu, M.; Cheung, S.; Shin, P.; Lu, W.; Li, J. Immune parameter changes of hemocytes in green-lipped mussel *Perna viridis* exposure to hypoxia and hyposalinity. *Aquaculture* **2012**, *356*, 22–29. [CrossRef]
20. Falfushynska, H.; Piontkivska, H.; Sokolova, I. Effects of intermittent hypoxia on cell survival and inflammatory responses in the intertidal marine bivalves *Mytilus edulis* and *Crassostrea gigas*. *J. Exp. Biol.* **2020**, *223*, jeb217026. [CrossRef]
21. Haider, F.; Falfushynska, H.; Timm, S.; Sokolova, I. Effects of hypoxia and reoxygenation on intermediary metabolite homeostasis of marine bivalves *Mytilus edulis* and *Crassostrea gigas*. *Comp. Biochem. Physiol. Part A Mol. Integr. Physiol.* **2020**, *242*, 110657. [CrossRef]
22. Sweet, M.; Bulling, M. On the Importance of the Microbiome and Pathobiome in Coral Health and Disease. *Front. Mar. Sci.* **2017**, *4*, 9. [CrossRef]
23. Berg, G.; Rybakova, D.; Fischer, D.; Cernava, T.; Vergès, M.; Charles, T.; Chen, X.; Cocolin, L.; Eversole, K.; Corral, G.; et al. Microbiome definition re-visited: Old concepts and new challenges. *Microbiome* **2020**, *8*, 103. [CrossRef]
24. Cheng, F.; Wang, L.; Lai, Y.; Chiang, C. The utility of microbiome (microbiota) and exosomes in dentistry. *J. Dent. Sci.* **2024**, *19*, 1313–1319. [CrossRef] [PubMed]
25. Quigley, E.; Stanton, C.; Murphy, E. The gut microbiota and the liver. Pathophysiological and clinical implications. *J. Hepatol.* **2013**, *58*, 1020–1027. [CrossRef] [PubMed]
26. Baudoin, L.; Sapinho, D.; Maddi, A.; Miotti, L. Scientometric analysis of the term 'microbiota' in research publications (1999-2017): A second youth of a century-old concept. *FEMS Microbiol. Lett.* **2019**, *366*, fnz138. [CrossRef]
27. Lokmer, A.; Wegner, K. Hemolymph microbiome of Pacific oysters in response to temperature, temperature stress and infection. *Int. Soc. Microb. Ecol. J.* **2015**, *9*, 670–682. [CrossRef]
28. Green, T.; Barnes, A. Bacterial diversity of the digestive gland of Sydney rock oysters, *Saccostrea glomerata* infected with the paramyxean parasite, *Marteilia sydneyi*. *J. Appl. Microbiol.* **2010**, *109*, 613–622. [CrossRef]
29. Zurel, D.; Benayahu, Y.; Or, A.; Kovacs, A.; Gophna, U. Composition and dynamics of the gill microbiota of an invasive Indo-Pacific oyster in the eastern Mediterranean Sea. *Environ. Microbiol.* **2011**, *13*, 1467–1476. [CrossRef]
30. Dubé, C.; Ky, C.; Planes, S. Microbiome of the Black-Lipped Pearl Oyster *Pinctada margaritifera*, a Multi-Tissue Description With Functional Profiling. *Front. Microbiol.* **2019**, *10*, 1548. [CrossRef]
31. Voolstra, C.; Ziegler, M. Adapting with Microbial Help: Microbiome Flexibility Facilitates Rapid Responses to Environmental Change. *Bioessays* **2020**, *42*, 2000004. [CrossRef] [PubMed]
32. Rastelli, M.; Cani, P.; Knauf, C. The Gut Microbiome Influences Host Endocrine Functions. *Endocr. Rev.* **2019**, *40*, 1271–1284. [CrossRef] [PubMed]
33. Soen, Y. Environmental disruption of host-microbe co-adaptation as a potential driving force in evolution. *Front. Genet.* **2014**, *5*, 168. [CrossRef]
34. Suzuki, T.; Ley, R. The role of the microbiota in human genetic adaptation. *Science* **2020**, *370*, eaaz6827. [CrossRef]

35. McLaren, M.; Callahan, B. Pathogen resistance may be the principal evolutionary advantage provided by the microbiome. *Philos. Trans. R. Soc. B Biol. Sci.* **2020**, *375*, 20190592. [CrossRef]
36. Zeb, F.; Osaili, T.; Obaid, R.; Naja, F.; Radwan, H.; Ismail, L.; Hasan, H.; Hashim, M.; Alam, I.; Sehar, B.; et al. Gut Microbiota and Time-Restricted Feeding/Eating: A Targeted Biomarker and Approach in Precision Nutrition. *Nutrients* **2023**, *15*, 259. [CrossRef]
37. Masanja, F.; Yang, K.; Xu, Y.; He, G.; Liu, X.; Xu, X.; Jiang, X.; Luo, X.; Mkuye, R.; Deng, Y.; et al. Bivalves and microbes: A mini-review of their relationship and potential implications for human health in a rapidly warming ocean. *Front. Mar. Sci.* **2023**, *10*, 1182438. [CrossRef]
38. Xie, C.; Han, Y.; Dong, M.; Zhang, Y.; Song, H.; Huang, H.; Zhang, H.; Liu, Y.; Wei, L.; Wang, X. Analysis of microbial communities on the coloured mantle surface of three common bivalves. *Aquac. Rep.* **2024**, *37*, 102220. [CrossRef]
39. Semova, I.; Carten, J.; Stombaugh, J.; Mackey, L.; Knight, R.; Farber, S.; Rawls, J. Microbiota Regulate Intestinal Absorption and Metabolism of Fatty Acids in the Zebrafish. *Cell Host Microbe* **2012**, *12*, 277–288. [CrossRef] [PubMed]
40. Akter, S.; Wos-Oxley, M.; Catalano, S.; Hassan, M.; Li, X.; Qin, J.; Oxley, A. Host Species and Environment Shape the Gut Microbiota of Cohabiting Marine Bivalves. *Microb. Ecol.* **2023**, *86*, 1755–1772. [CrossRef]
41. Valenzuela, T.; Rilling, J.; Larama, G.; Acuna, J.; Campos, M.; Inostroza, N.; Araya, M.; Altamirano, K.; Fujiyoshi, S.; Yarimizu, K.; et al. 16S rRNA-Based Analysis Reveals Differences in the Bacterial Community Present in Tissues of *Choromytilus chorus* (Mytilidae, Bivalvia) Grown in an Estuary and a Bay in Southern Chile. *Diversity* **2021**, *13*, 209. [CrossRef]
42. Auguste, M.; Lasa, A.; Pallavicini, A.; Gualdi, S.; Vezzulli, L.; Canesi, L. Exposure to TiO_2 nanoparticles induces shifts in the microbiota composition of *Mytilus galloprovincialis* hemolymph. *Sci. Total Environ.* **2019**, *670*, 129–137. [CrossRef] [PubMed]
43. Khan, B.; Clinton, S.; Hamp, T.; Oliver, J.; Ringwood, A. Potential impacts of hypoxia and a warming ocean on oyster microbiomes. *Mar. Environ. Res.* **2018**, *139*, 27–34. [CrossRef]
44. Li, Y.; Yang, N.; Liang, X.; Yoshida, A.; Osatomi, K.; Power, D.; Batista, F.; Yang, J. Elevated Seawater Temperatures Decrease Microbial Diversity in the Gut of *Mytilus coruscus*. *Front. Physiol.* **2018**, *9*, 839. [CrossRef]
45. Li, Y.; Xu, J.; Chen, Y.; Ding, W.; Shao, A.; Liang, X.; Zhu, Y.; Yang, J. Characterization of Gut Microbiome in the Mussel *Mytilus galloprovincialis* in Response to Thermal Stress. *Front. Physiol.* **2019**, *10*, 1086. [CrossRef]
46. Diaz-Puente, B.; Pita, A.; Uribe, J.; Cuellar-Pinzon, J.; Guinez, R.; Presa, P. A biogeography-based management for *Mytilus chilensis*: The genetic hodgepodge of Los Lagos versus the pristine hybrid zone of the Magellanic ecotone. *Aquat. Conserv.-Mar. Freshw. Ecosyst.* **2020**, *30*, 412–425. [CrossRef]
47. Santibañez, P.; Romalde, J.; Fuentes, D.; Figueras, A.; Figueroa, J. Health Status of *Mytilus chilensis* from Intensive Culture Areas in Chile Assessed by Molecular, Microbiological, and Histological Analyses. *Pathogens* **2022**, *11*, 494. [CrossRef]
48. Liu, M.; Li, Q.; Tan, L.; Wang, L.; Wu, F.; Li, L.; Zhang, G. Host-microbiota interactions play a crucial role in oyster adaptation to rising seawater temperature in summer. *Environ. Res.* **2023**, *216*, 114585. [CrossRef]
49. Hughes, D.; Alderdice, R.; Cooney, C.; Kuhl, M.; Pernice, M.; Voolstra, C.; Suggett, D. Coral reef survival under accelerating ocean deoxygenation. *Nat. Clim. Change* **2020**, *10*, 296–307. [CrossRef]
50. Salmond, N.; Wing, S. Sub-lethal and lethal effects of chronic and extreme multiple stressors on a critical New Zealand bivalve under hypoxia. *Mar. Ecol. Prog. Ser.* **2023**, *703*, 81–93. [CrossRef]
51. Iriarte, J.; Pantoja, S.; Daneri, G. Oceanographic Processes in Chilean Fjords of Patagonia: From small to large-scale studies. *Prog. Oceanogr.* **2014**, *129*, 1–7. [CrossRef]
52. Yevenes, M.; Lagos, N.; Farías, L.; Vargas, C. Greenhouse gases, nutrients and the carbonate system in the Reloncaví Fjord (Northern Chilean Patagonia): Implications on aquaculture of the mussel, *Mytilus chilensis*, during an episodic volcanic eruption. *Sci. Total Environ.* **2019**, *669*, 49–61. [CrossRef] [PubMed]
53. Silva, N.; Vargas, C. Hypoxia in Chilean Patagonian Fjords. *Prog. Oceanogr.* **2014**, *129*, 62–74. [CrossRef]
54. Linford, P.; Pérez-Santos, I.; Montes, I.; Dewitte, B.; Buchan, S.; Narváez, D.; Saldías, G.; Pinilla, E.; Garreaud, R.; Díaz, P.; et al. Recent Deoxygenation of Patagonian Fjord Subsurface Waters Connected to the Peru-Chile Undercurrent and Equatorial Subsurface Water Variability. *Glob. Biogeochem. Cycles* **2023**, *37*, e2022GB007688. [CrossRef]
55. Díaz, P.; Pérez-Santos, I.; Basti, L.; Garreaud, R.; Pinilla, E.; Barrera, F.; Tello, A.; Schwerter, C.; Arenas-Uribe, S.; Soto-Riquelme, C.; et al. The impact of local and climate change drivers on the formation, dynamics, and potential recurrence of a massive fish-killing microalgal bloom in Patagonian fjord. *Sci. Total Environ.* **2023**, *865*, 161288. [CrossRef] [PubMed]
56. Castillo, M.; Cifuentes, U.; Pizarro, O.; Djurfeldt, L.; Caceres, M. Seasonal hydrography and surface outflow in a fjord with a deep sill: The Reloncaví fjord, Chile. *Ocean Sci.* **2016**, *12*, 533–544. [CrossRef]
57. Schneider, W.; Pérez-Santos, I.; Ross, L.; Bravo, L.; Seguel, R.; Hernández, F. On the hydrography of Puyuhuapi Channel, Chilean Patagonia. *Prog. Oceanogr.* **2014**, *129*, 8–18. [CrossRef]
58. Pérez-Santos, I.; Díaz, P.; Silva, N.; Garreaud, R.; Montero, P.; Henríquez-Castillo, C.; Barrera, F.; Linford, P.; Amaya, C.; Contreras, S.; et al. Oceanography time series reveals annual asynchrony input between oceanic and estuarine waters in Patagonian fjords. *Sci. Total Environ.* **2021**, *798*, 149241. [CrossRef]

59. Soto, D.; León-Muñoz, J.; Garreaud, R.; Quinoñes, R.; Morey, F. Scientific warnings could help to reduce farmed salmon mortality due to harmful algal blooms. *Mar. Policy* **2021**, *132*, 104705. [CrossRef]
60. Linford, P.; Pérez-Santos, I.; Montero, P.; Díaz, P.; Aracena, C.; Pinilla, E.; Barrera, F.; Castillo, M.; Alvera-Azcárate, A.; Alvarado, M.; et al. Oceanographic processes driving low-oxygen conditions inside Patagonian fjords. *Biogeosciences* **2024**, *21*, 1433–1459. [CrossRef]
61. Mardones, J.; Paredes, J.; Godoy, M.; Suarez, R.; Norambuena, L.; Vargas, V.; Fuenzalida, G.; Pinilla, E.; Artal, O.; Rojas, X.; et al. Disentangling the environmental processes responsible for the world's largest farmed fish-killing harmful algal bloom: Chile, 2016. *Sci. Total Environ.* **2021**, *766*, 144383. [CrossRef] [PubMed]
62. Montero, P.; Daneri, G.; González, H.; Iriarte, J.; Tapia, F.; Lizárraga, L.; Sanchez, N.; Pizarro, O. Seasonal variability of primary production in a fjord ecosystem of the Chilean Patagonia: Implications for the transfer of carbon within pelagic food webs. *Cont. Shelf Res.* **2011**, *31*, 202–215. [CrossRef]
63. Daneri, G.; Montero, P.; Lizárraga, L.; Torres, R.; Iriarte, J.L.; Jacob, B.; González, H.E.; Tapia, F.J. Primary Productivity and heterotrophic activity in an enclosed marine area of central Patagonia (Puyuhuapi channel; 44° S, 73° W). *Biogeosciences Discuss.* **2012**, *2012*, 5929–5968. [CrossRef]
64. Adzigbli, L.; Sokolov, E.; Ponsuksili, S.; Sokolova, I. Tissue- and substrate-dependent mitochondrial responses to acute hypoxia-reoxygenation stress in a marine bivalve (*Crassostrea gigas*). *J. Exp. Biol.* **2022**, *225*, jeb243304. [CrossRef]
65. Sokolov, E.; Markert, S.; Hinzke, T.; Hirschfeld, C.; Becher, D.; Ponsuksili, S.; Sokolova, I. Effects of hypoxia-reoxygenation stress on mitochondrial proteome and bioenergetics of the hypoxia-tolerant marine bivalve *Crassostrea gigas*. *J. Proteom.* **2019**, *194*, 99–111. [CrossRef]
66. Steffen, J.; Falfushynska, H.; Piontkivska, H.; Sokolova, I. Molecular Biomarkers of the Mitochondrial Quality Control Are Differently Affected by Hypoxia-Reoxygenation Stress in Marine Bivalves *Crassostrea gigas* and *Mytilus edulis*. *Front. Mar. Sci.* **2020**, *7*, 19. [CrossRef]
67. Amorim, K.; Piontkivska, H.; Zettler, M.; Sokolov, E.; Hinzke, T.; Nair, A.; Sokolova, I. Transcriptional response of key metabolic and stress response genes of a nuculanid bivalve, *Lembulus bicuspidatus* from an oxygen minimum zone exposed to hypoxia-reoxygenation. *Comp. Biochem. Physiol. B-Biochem. Mol. Biol.* **2021**, *256*, 110617. [CrossRef]
68. Falfushynska, H.; Sokolov, E.; Piontkivska, H.; Sokolova, I. The Role of Reversible Protein Phosphorylation in Regulation of the Mitochondrial Electron Transport System During Hypoxia and Reoxygenation Stress in Marine Bivalves. *Front. Mar. Sci.* **2020**, *7*, 467. [CrossRef]
69. Liu, T.; Lu, Y.; Sun, M.; Shen, H.; Niu, D. Effects of acute hypoxia and reoxygenation on histological structure, antioxidant response, and apoptosis in razor clam *Sinonovacula constricta*. *Fish Shellfish. Immunol.* **2024**, *145*, 109310. [CrossRef]
70. Adzigbli, L.; Ponsuksili, S.; Sokolova, I. Mitochondrial responses to constant and cyclic hypoxia depend on the oxidized fuel in a hypoxia-tolerant marine bivalve *Crassostrea gigas*. *Sci. Rep.* **2024**, *14*, 9658. [CrossRef]
71. Ivanina, A.; Sokolova, I. Effects of intermittent hypoxia on oxidative stress and protein degradation in molluscan mitochondria. *J. Exp. Biol.* **2016**, *219*, 3794–3802. [CrossRef] [PubMed]
72. Yang, C.; Wu, H.; Chen, J.; Liao, Y.; Mkuye, R.; Deng, Y.; Du, X. Integrated transcriptomic and metabolomic analysis reveals the response of pearl oyster (*Pinctada fucata martensii*) to long-term hypoxia. *Mar. Environ. Res.* **2023**, *191*, 106133. [CrossRef]
73. Yang, C.; Yang, J.; Hao, R.; Du, X.; Deng, Y. Molecular characterization of *OSR1* in *Pinctada fucata martensii* and association of allelic variants with growth traits. *Aquaculture* **2020**, *516*, 734617. [CrossRef]
74. Li, X.; Shi, H.; Xia, H.; Zhou, Y.; Qiu, Y. Seasonal hypoxia and its potential forming mechanisms in the Mirs Bay, the northern South China Sea. *Cont. Shelf Res.* **2014**, *80*, 1–7. [CrossRef]
75. Calvete, C.; Sobarzo, M. Quantification of the surface brackish water layer and frontal zones in southern Chilean fjords between Boca del Guafo (43°30′S) and Estero Elefantes (46°30′S). *Cont. Shelf Res.* **2011**, *31*, 162–171. [CrossRef]
76. Cáceres, M.; Valle-Levinson, A.; Sepúlveda, H.; Holderied, K. Transverse variability of flow and density in a Chilean fjord. *Cont. Shelf Res.* **2002**, *22*, 1683–1698. [CrossRef]
77. Montúfar-Romero, M.; Valenzuela-Muñoz, V.; Valenzuela-Miranda, D.; Gallardo-Escárate, C. Hypoxia in the Blue Mussel *Mytilus chilensis* Induces a Transcriptome Shift Associated with Endoplasmic Reticulum Stress, Metabolism, and Immune Response. *Genes* **2024**, *15*, 658. [CrossRef]
78. Sun, B.; Hu, M.; Lan, X.; Waiho, K.; Lv, X.; Xu, C.; Wang, Y. Nano-titanium dioxide exacerbates the harmful effects of perfluorooctanoic acid on the health of mussels. *Environ. Int.* **2024**, *187*, 108681. [CrossRef]
79. Mardones, M.; Mardones-Toledo, D.; Büchner-Miranda, J.; Salas-Yanquin, L.; Gray, M.; Cubillos, V.; Montory, J.; Chaparro, O. Food acquisition by the intertidal filter feeder bivalve *Perumytilus purpuratus*: Can the gill explain a differential performance between smaller individuals and the larger ones? *J. Exp. Mar. Biol. Ecol.* **2024**, *571*, 151982. [CrossRef]
80. Haque, M.; Eom, H.; Nam, S.; Shin, Y.; Rhee, J. Chlorothalonil induces oxidative stress and reduces enzymatic activities of Na^+/K^+-ATPase and acetylcholinesterase in gill tissues of marine bivalves. *PLoS ONE* **2019**, *14*, e0214236. [CrossRef]

81. Sforzini, S.; Moore, M.; Oliveri, C.; Volta, A.; Jha, A.; Banni, M.; Viarengo, A. Role of mTOR in autophagic and lysosomal reactions to environmental stressors in molluscs. *Aquat. Toxicol.* **2018**, *195*, 114–128. [CrossRef] [PubMed]
82. Otegui, M.; Fiori, S.; Menechella, A.; Dos Santos, E.; Gimenez, J. Histological characterization and morphological alterations in gill and digestive gland in non-native bivalve from the Province of Buenos Aires: Spatial and seasonal evaluation. *Zool. Anz.* **2024**, *312*, 11–19. [CrossRef]
83. Kim, Y.; Kim, W.; Shin, Y.; Lee, D.; Kim, Y.; Kim, J.; Rhee, J. Microcystin-LR bioconcentration induces antioxidant responses in the digestive gland of two marine bivalves *Crassostrea gigas* and *Mytilus edulis*. *Aquat. Toxicol.* **2017**, *188*, 119–129. [CrossRef]
84. Borkovic-Mitic, S.; Pavlovic, S.; Perendija, B.; Despotovic, S.; Gavric, J.; Gacic, Z.; Saicic, Z. Influence of some metal concentrations on the activity of antioxidant enzymes and concentrations of vitamin E and SH-groups in the digestive gland and gills of the freshwater bivalve *Unio tumidus* from the Serbian part of Sava River. *Ecol. Indic.* **2013**, *32*, 212–221. [CrossRef]
85. Tang, B.; Riisgård, H. Relationship between oxygen concentration, respiration and filtration rate in blue mussel *Mytilus edulis*. *J. Oceanol. Limnol.* **2018**, *36*, 395–404. [CrossRef]
86. Porter, E.; Porter, F. A Strain Gauge Monitor (SGM) for Continuous Valve Gape Measurements in Bivalve Molluscs in Response to Laboratory Induced Diel-cycling Hypoxia and pH. *JoVE-J. Vis. Exp.* **2018**, *138*, 57404. [CrossRef]
87. Sun, S.; Yang, M.; Fu, H.; Ge, X.; Zou, J. Altered intestinal microbiota induced by chronic hypoxia drives the effects on lipid metabolism and the immune response of oriental river prawn *Macrobrachium nipponense*. *Aquaculture* **2020**, *526*, 735431. [CrossRef]
88. Valenzuela-Miranda, D.; Valenzuela-Muñoz, V.; Benavente, B.; Muñoz-Trorcoso, M.; Nuñez-Acuña, G.; Gallardo-Escárate, C. The Atlantic salmon microbiome infected with the sea louse *Caligus rogercresseyi* reveals tissue-specific functional dysbiosis. *Aquaculture* **2024**, *580*, 740328. [CrossRef]
89. Ciuffreda, L.; Rodríguez-Pérez, H.; Flores, C. Nanopore sequencing and its application to the study of microbial communities. *Comput. Struct. Biotechnol. J.* **2021**, *19*, 1497–1511. [CrossRef]
90. Bonenfant, Q.; Noé, L.; Touzet, H. Porechop_ABI: Discovering unknown adapters in Oxford Nanopore Technology sequencing reads for downstream trimming. *Bioinform. Adv.* **2023**, *3*, vbac085. [CrossRef]
91. Curry, K.; Wang, Q.; Nute, M.; Tyshaieva, A.; Reeves, E.; Soriano, S.; Wu, Q.; Graeber, E.; Finzer, P.; Mendling, W.; et al. Emu: Species-level microbial community profiling of full-length 16S rRNA Oxford Nanopore sequencing data. *Nat. Methods* **2022**, *19*, 845–853. [CrossRef]
92. Dixon, P. VEGAN, a package of R functions for community ecology. *J. Veg. Sci.* **2003**, *14*, 927–930. [CrossRef]
93. Beckerman, A.; Childs, D.; Petchey, O. *Data Management, Manipulation, and Exploration with Dplyr*; Oxford University Press: New York, NY, USA, 2017; pp. 57–77.
94. Lu, Y.; Zhou, G.; Ewald, J.; Pang, Z.; Shiri, T.; Xia, J. MicrobiomeAnalyst 2.0: Comprehensive statistical, functional and integrative analysis of microbiome data. *Nucleic Acids Res.* **2023**, *51*, W310–W318. [CrossRef]
95. Foster, Z.; Sharpton, T.; Grünwald, N. Metacoder: An R package for visualization and manipulation of community taxonomic diversity data. *PLOS Comput. Biol.* **2017**, *13*, e1005404. [CrossRef] [PubMed]
96. Douglas, G.; Maffei, V.; Zaneveld, J.; Yurgel, S.; Brown, J.; Taylor, C.; Huttenhower, C.; Langille, M. PICRUSt2 for prediction of metagenome functions. *Nat. Biotechnol.* **2020**, *38*, 685–688. [CrossRef]
97. Yang, C.; Mai, J.; Cao, X.; Burberry, A.; Cominelli, F.; Zhang, L. ggpicrust2: An R package for PICRUSt2 predicted functional profile analysis and visualization. *Bioinformatics* **2023**, *39*, btad470. [CrossRef]
98. Caspi, R.; Billington, R.; Ferrer, L.; Foerster, H.; Fulcher, C.; Keseler, I.; Kothari, A.; Krummenacker, M.; Latendresse, M.; Mueller, L.; et al. The MetaCyc database of metabolic pathways and enzymes and the BioCyc collection of pathway/genome databases. *Nucleic Acids Res.* **2016**, *44*, D471–D480. [CrossRef]
99. Parks, D.; Tyson, G.; Hugenholtz, P.; Beiko, R. STAMP: Statistical analysis of taxonomic and functional profiles. *Bioinformatics* **2014**, *30*, 3123–3124. [CrossRef]
100. Todgham, A.; Stillman, J. Physiological Responses to Shifts in Multiple Environmental Stressors: Relevance in a Changing World. *Integr. Comp. Biol.* **2013**, *53*, 539–544. [CrossRef]
101. Earhart, M.; Blanchard, T.; Harman, A.; Schulte, P. Hypoxia and High Temperature as Interacting Stressors: Will Plasticity Promote Resilience of Fishes in a Changing World? *Biol. Bull.* **2022**, *243*, 149–170. [CrossRef]
102. Howard, R.; Schul, M.; Bravo, L.; Altieri, A.; Meyer, J. Shifts in the coral microbiome in response to *in situ* experimental deoxygenation. *Appl. Environ. Microbiol.* **2023**, *89*, e00577-23. [CrossRef] [PubMed]
103. Lozupone, C. Unraveling Interactions between the Microbiome and the Host Immune System To Decipher Mechanisms of Disease. *mSystems* **2018**, *3*, 00183-17. [CrossRef]
104. Clavel, T.; Gomes-Neto, J.; Lagkouvardos, I.; Ramer-Tait, A. Deciphering interactions between the gut microbiota and the immune system via microbial cultivation and minimal microbiomes. *Immunol. Rev.* **2017**, *279*, 8–22. [CrossRef] [PubMed]
105. Xie, Z.; Li, Y.; Xiong, K.; Tu, Z.; Waiho, K.; Yang, C.; Deng, Y.; Li, S.; Fang, J.; Hu, M.; et al. Combined effect of salinity and hypoxia on digestive enzymes and intestinal microbiota in the oyster *Crassostrea hongkongensis*. *Environ. Pollut.* **2023**, *331*, 121921. [CrossRef]

106. Hemraj, D.; Falkenberg, L.; Cheung, K.; Man, L.; Carini, A.; Russell, B. Acidification and hypoxia drive physiological trade-offs in oysters and partial loss of nutrient cycling capacity in oyster holobiont. *Front. Ecol. Evol.* **2023**, *11*, 1083315. [CrossRef]
107. Allam, B.; Espinosa, E. Bivalve immunity and response to infections: Are we looking at the right place? *Fish Shellfish. Immunol.* **2016**, *53*, 4–12. [CrossRef]
108. González, R.; Henríquez-Castillo, C.; Lohrmann, K.; Romero, M.; Ramajo, L.; Schmitt, P.; Brokordt, K. The Gill Microbiota of *Argopecten purpuratus* Scallop Is Dominated by Symbiotic Campylobacterota and Upwelling Intensification Differentially Affects Their Abundance. *Microorganisms* **2022**, *10*, 2330. [CrossRef]
109. Dor-Roterman, Y.; Benayahu, Y.; Reshef, L.; Gophna, U. Host-Microbiome Interactions in a Changing Sea: The Gill Microbiome of an Invasive Oyster under Drastic Temperature Changes. *Microorganisms* **2024**, *12*, 197. [CrossRef]
110. Assié, A.; Borowski, C.; van der Heijden, K.; Raggi, L.; Geier, B.; Leisch, N.; Schimak, M.; Dubilier, N.; Petersen, J. A specific and widespread association between deep-sea *Bathymodiolus* mussels and a novel family of Epsilonproteobacteria. *Environ. Microbiol. Rep.* **2016**, *8*, 805–813. [CrossRef]
111. Brown, E.; Sadarangani, M.; Finlay, B. The role of the immune system in governing host-microbe interactions in the intestine. *Nat. Immunol.* **2013**, *14*, 660–667. [CrossRef]
112. Shade, A.; Handelsman, J. Beyond the Venn diagram: The hunt for a core microbiome. *Environ. Microbiol.* **2012**, *14*, 4–12. [CrossRef] [PubMed]
113. Contreras-Ramos, M.; Mansell, T. Leveraging quorum sensing to manipulate microbial dynamics. *Curr. Opin. Biomed. Eng.* **2021**, *19*, 100306. [CrossRef]
114. Soto-Aceves, M.; Diggle, S.; Greenberg, E. Microbial Primer: LuxR- LuxI Quorum Sensing. *Microbiology* **2023**, *169*, 001343. [CrossRef] [PubMed]
115. Kamath, A.; Shukla, A.; Patel, D. Quorum Sensing and Quorum Quenching: Two sides of the same coin. *Physiol. Mol. Plant Pathol.* **2023**, *123*, 101927. [CrossRef]
116. Chan, Y.; Li, A.; Gopalakrishnan, S.; Shin, P.; Wu, R.; Pointing, S.; Chiu, J. Interactive effects of hypoxia and polybrominated diphenyl ethers (PBDEs) on microbial community assembly in surface marine sediments. *Mar. Pollut. Bull.* **2014**, *85*, 400–409. [CrossRef] [PubMed]
117. Mori, F.; Umezawa, Y.; Kondo, R.; Wada, M. Effects of bottom-water hypoxia on sediment bacterial community composition in a seasonally hypoxic enclosed bay (Omura Bay, West Kyushu, Japan). *FEMS Microbiol. Ecol.* **2018**, *94*, fiy053. [CrossRef]
118. Seibel, B.; Häfker, N.; Trübenbach, K.; Zhang, J.; Tessier, S.; Pörtner, H.; Rosa, R.; Storey, K. Metabolic suppression during protracted exposure to hypoxia in the jumbo squid, *Dosidicus gigas*, living in an oxygen minimum zone. *J. Exp. Biol.* **2014**, *217*, 2555–2568. [CrossRef]
119. Sommer, F.; Bäckhed, F. The gut microbiota—Masters of host development and physiology. *Nat. Rev. Microbiol.* **2013**, *11*, 227–238. [CrossRef]
120. Pohlenz, C.; Gatlin, D. Interrelationships between fish nutrition and health. *Aquaculture* **2014**, *431*, 111–117. [CrossRef]
121. Jin, Y.; Dong, H.; Xia, L.; Yang, Y.; Zhu, Y.; Shen, Y.; Zheng, H.; Yao, C.; Wang, Y.; Lu, S. The Diversity of Gut Microbiome is Associated With Favorable Responses to Anti-Programmed Death 1 Immunotherapy in Chinese Patients With NSCLC. *J. Thorac. Oncol.* **2019**, *14*, 1378–1389. [CrossRef]
122. Lenis, Y.; Elmetwally, M.; Maldonado-Estrada, J.; Bazer, F. Physiological importance of polyamines. *Zygote* **2017**, *25*, 244–255. [CrossRef] [PubMed]
123. Zahedi, K.; Barone, S.; Soleimani, M. Polyamines and Their Metabolism: From the Maintenance of Physiological Homeostasis to the Mediation of Disease. *Med. Sci.* **2022**, *10*, 38. [CrossRef]
124. Egan, S.; Gardiner, M. Microbial Dysbiosis: Rethinking Disease in Marine Ecosystems. *Front. Microbiol.* **2016**, *7*, 991. [CrossRef]
125. Pierce, M.; Ward, J. Gut Microbiomes of the Eastern Oyster (*Crassostrea virginica*) and the Blue Mussel (*Mytilus edulis*): Temporal Variation and the Influence of Marine Aggregate-Associated Microbial Communities. *mSphere* **2019**, *4*, 00730-19. [CrossRef]
126. Trabal, N.; Mazón-Suástegui, J.; Vázquez-Juárez, R.; Asencio-Valle, F.; Morales-Bojórquez, E.; Romero, J. Molecular Analysis of Bacterial Microbiota Associated with Oysters (*Crassostrea gigas* and *Crassostrea corteziensis*) in Different Growth Phases at Two Cultivation Sites. *Microb. Ecol.* **2012**, *64*, 555–569. [CrossRef] [PubMed]
127. Fernández, N.; Mazón-Suástegui, J.; Vázquez-Juárez, R.; Ascencio-Valle, F.; Romero, J. Changes in the composition and diversity of the bacterial microbiota associated with oysters (*Crassostrea corteziensis*, *Crassostrea gigas* and *Crassostrea sikamea*) during commercial production. *FEMS Microbiol. Ecol.* **2014**, *88*, 69–83. [CrossRef]
128. Utermann, C.; Parrot, D.; Breusing, C.; Stuckas, H.; Staufenberger, T.; Blümel, M.; Labes, A.; Tasdemir, D. Combined genotyping, microbial diversity and metabolite profiling studies on farmed *Mytilus* spp. from Kiel Fjord. *Sci. Rep.* **2018**, *8*, 7983. [CrossRef]
129. Li, J.; Ni, J.; Li, J.; Wang, C.; Li, X.; Wu, S.; Zhang, T.; Yu, Y.; Yan, Q. Comparative study on gastrointestinal microbiota of eight fish species with different feeding habits. *J. Appl. Microbiol.* **2014**, *117*, 1750–1760. [CrossRef]
130. Auguste, M.; Lasa, A.; Balbi, T.; Pallavicini, A.; Vezzulli, L.; Canesi, L. Impact of nanoplastics on hemolymph immune parameters and microbiota composition in *Mytilus galloprovincialis*. *Mar. Environ. Res.* **2020**, *159*, 105017. [CrossRef]

131. Santibáñez, P.; Romalde, J.; Maldonado, J.; Fuentes, D.; Figueroa, J. First characterization of the gut microbiome associated with *Mytilus chilensis* collected at a mussel farm and from a natural environment in Chile. *Aquaculture* **2022**, *548*, 737644. [CrossRef]
132. van der Meer, D.; van den Thillart, G.; Witte, F.; de Bakker, M.; Besser, J.; Richardson, M.; Spaink, H.; Leito, J.; Bagowski, C. Gene expression profiling of the long-term adaptive response to hypoxia in the gills of adult zebrafish. *Am. J. Physiol.-Regul. Integr. Comp. Physiol.* **2005**, *289*, R1512–R1519. [CrossRef] [PubMed]
133. Huang, C.; Lin, H.; Lin, C. Effects of hypoxia on ionic regulation, glycogen utilization and antioxidative ability in the gills and liver of the aquatic air-breathing fish *Trichogaster microlepis*. *Comp. Biochem. Physiol. Part A Mol. Integr. Physiol.* **2015**, *179*, 25–34. [CrossRef]
134. Yang, L.; Lv, L.; Liu, H.; Wang, M.; Sui, Y.; Wang, Y. Effects of Ocean Acidification and Microplastics on Microflora Community Composition in the Digestive Tract of the Thick Shell Mussel *Mytilus coruscus* Through 16S RNA Gene Sequencing. *Bull. Environ. Contam. Toxicol.* **2021**, *107*, 616–625. [CrossRef] [PubMed]
135. Song, H.; Yu, Z.; Yang, M.; Zhang, T.; Wang, H. Analysis of microbial abundance and community composition in esophagus and intestinal tract of wild veined rapa whelk (*Rapana venosa*) by 16S rRNA gene sequencing. *J. Gen. Appl. Microbiol.* **2018**, *64*, 158–166. [CrossRef]
136. Lu, G.; Wang, F.; Yu, Z.; Lu, M.; Wang, Y.; Liu, C.; Xue, Z.; Wu, Y.; Wang, L.; Song, L. Bacterial communities in gills and intestines of yesso scallop (*Patinopecten yessoensis*) and its habitat waters in Changhai (Dalian, China). *ISJ-Invertebr. Surviv. J.* **2017**, *14*, 340–351.
137. Li, Z.; Li, L.; Sokolova, I.; Shang, Y.; Huang, W.; Khor, W.; Fang, J.; Wang, Y.; Hu, M. Effects of elevated temperature and different crystal structures of TiO_2 nanoparticles on the gut microbiota of mussel *Mytilus coruscus*. *Mar. Pollut. Bull.* **2024**, *199*, 115979. [CrossRef] [PubMed]
138. Gao, Y.; He, J.; He, Z.; Li, Z.; Zhao, B.; Mu, Y.; Lee, J.; Chu, Z. Effects of fulvic acid on growth performance and intestinal health of juvenile loath *Paramisgurnus dabryanus* (Sauvage). *Fish Shellfish. Immunol.* **2017**, *62*, 47–56. [CrossRef]
139. Zheng, Y.; Wu, W.; Hu, G.; Qiu, L.; Meng, S.; Song, C.; Fan, L.; Zhao, Z.; Bing, X.; Chen, J. Gut microbiota analysis of juvenile genetically improved farmed tilapia (*Oreochromis niloticus*) by dietary supplementation of different resveratrol concentrations. *Fish Shellfish. Immunol.* **2018**, *77*, 200–207. [CrossRef]
140. Zhou, M.; Liang, R.; Mo, J.; Yang, S.; Gu, N.; Wu, Z.; Babu, V.; Li, J.; Huang, Y.; Lin, L. Effects of brewer's yeast hydrolysate on the growth performance and the intestinal bacterial diversity of largemouth bass (*Micropterus salmoides*). *Aquaculture* **2018**, *484*, 139–144. [CrossRef]
141. Dishaw, L.; Flores-Torres, J.; Lax, S.; Gemayel, K.; Leigh, B.; Melillo, D.; Mueller, M.; Natale, L.; Zucchetti, I.; De Santis, R.; et al. The Gut of Geographically Disparate *Ciona intestinalis* Harbors a Core Microbiota. *PLoS ONE* **2014**, *9*, e93386. [CrossRef]
142. Zhao, J.; Shi, B.; Jiang, Q.; Ke, C. Changes in gut-associated flora and bacterial digestive enzymes during the development stages of abalone (*Haliotis diversicolor*). *Aquaculture* **2012**, *338*, 147–153. [CrossRef]
143. King, G.; Judd, C.; Kuske, C.; Smith, C. Analysis of Stomach and Gut Microbiomes of the Eastern Oyster (*Crassostrea virginica*) from Coastal Louisiana, USA. *PLoS ONE* **2012**, *7*, e51475. [CrossRef] [PubMed]
144. Rungrassamee, W.; Klanchui, A.; Maibunkaew, S.; Chaiyapechara, S.; Jiravanichpaisal, P.; Karoonuthaisiri, N. Characterization of Intestinal Bacteria in Wild and Domesticated Adult Black Tiger Shrimp (*Penaeus monodon*). *PLoS ONE* **2014**, *9*, e91853. [CrossRef]
145. Givens, C.; Burnett, K.; Burnett, L.; Hollibaugh, J. Microbial communities of the carapace, gut, and hemolymph of the Atlantic blue crab, *Callinectes sapidus*. *Mar. Biol.* **2013**, *160*, 2841–2851. [CrossRef]
146. Hakim, J.; Koo, H.; Dennis, L.; Kumar, R.; Ptacek, T.; Morrow, C.; Lefkowitz, E.; Powell, M.; Bej, A.; Watts, S. An abundance of Epsilonproteobacteria revealed in the gut microbiome of the laboratory cultured sea urchin, *Lytechinus variegatus*. *Front. Microbiol.* **2015**, *6*, 1047. [CrossRef]
147. Musella, M.; Wathsala, R.; Tavella, T.; Rampelli, S.; Barone, M.; Palladino, G.; Biagi, E.; Brigidi, P.; Turroni, S.; Franzellitti, S.; et al. Tissue-scale microbiota of the Mediterranean mussel (*Mytilus galloprovincialis*) and its relationship with the environment. *Sci. Total Environ.* **2020**, *717*, 137209. [CrossRef]
148. Griffin, T.; Baer, J.; Ward, J. Direct Comparison of Fecal and Gut Microbiota in the Blue Mussel (*Mytilus edulis*) Discourages Fecal Sampling as a Proxy for Resident Gut Community. *Microb. Ecol.* **2021**, *81*, 180–192. [CrossRef]
149. Deegan, L.; Peterson, B.; Portier, R. Stable isotopes and cellulase activity as evidence for detritus as a food source for juvenile Gulf menhaden. *Estuaries* **1990**, *13*, 14–19. [CrossRef]
150. McKee, L.; La Rosa, S.; Westereng, B.; Eijsink, V.; Pope, P.; Larsbrink, J. Polysaccharide degradation by the Bacteroidetes: Mechanisms and nomenclature. *Environ. Microbiol. Rep.* **2021**, *13*, 559–581. [CrossRef]
151. Shahbaz, U. Chitin, Characteristic, Sources, and Biomedical Application. *Curr. Pharm. Biotechnol.* **2020**, *21*, 1433–1443. [CrossRef]
152. Brinkmann, S.; Spohn, M.; Schäberle, T. Bioactive natural products from Bacteroidetes. *Nat. Prod. Rep.* **2022**, *39*, 1045–1065. [CrossRef] [PubMed]
153. Wolf, A.; Asoh, S.; Hiranuma, H.; Ohsawa, I.; Iio, K.; Satou, A.; Ishikura, M.; Ohta, S. Astaxanthin protects mitochondrial redox state and functional integrity against oxidative stress. *J. Nutr. Biochem.* **2010**, *21*, 381–389. [CrossRef]

154. Fischbach, M.; Walsh, C. Antibiotics for Emerging Pathogens. *Science* **2009**, *325*, 1089–1093. [CrossRef]
155. Sathe, P.; Laxman, K.; Myint, M.; Dobretsov, S.; Richter, J.; Dutta, J. Bioinspired nanocoatings for biofouling prevention by photocatalytic redox reactions. *Sci. Rep.* **2017**, *7*, 3624. [CrossRef]
156. Fimlaid, K.; Shen, A. Diverse mechanisms regulate sporulation sigma factor activity in the Firmicutes. *Curr. Opin. Microbiol.* **2015**, *24*, 88–95. [CrossRef] [PubMed]
157. Vesth, T.; Ozen, A.; Andersen, S.; Kaas, R.; Lukjancenko, O.; Bohlin, J.; Nookaew, I.; Wassenaar, T.; Ussery, D. *Veillonella*, *Firmicutes*: Microbes disguised as Gram negatives. *Stand. Genomis Sci.* **2013**, *9*, 431–448. [CrossRef]
158. Xiao, S.; Jiang, S.; Qian, D.; Duan, J. Modulation of microbially derived short-chain fatty acids on intestinal homeostasis, metabolism, and neuropsychiatric disorder. *Appl. Microbiol. Biotechnol.* **2020**, *104*, 589–601. [CrossRef] [PubMed]
159. Lin, G.; Sun, F.; Wang, C.; Zhang, L.; Zhang, X. Assessment of the effect of *Enteromorpha prolifera* on bacterial community structures in aquaculture environment. *PLoS ONE* **2017**, *12*, e0179792. [CrossRef]
160. Zhao, G.; He, H.; Wang, H.; Liang, Y.; Guo, C.; Shao, H.; Jiang, Y.; Wang, M. Variations in Marine Bacterial and Archaeal Communities during an *Ulva prolifera* Green Tide in Coastal Qingdao Areas. *Microorganisms* **2022**, *10*, 1204. [CrossRef]
161. Fernández-Gómez, B.; Richter, M.; Schüler, M.; Pinhassi, J.; Acinas, S.; González, J.; Pedrós-Alió, C. Ecology of marine Bacteroidetes: A comparative genomics approach. *ISME J.* **2013**, *7*, 1026–1037. [CrossRef]
162. Bergauer, K.; Fernandez-Guerra, A.; Garcia, J.; Sprenger, R.; Stepanauskas, R.; Pachiadaki, M.; Jensen, O.; Herndl, G. Organic matter processing by microbial communities throughout the Atlantic water column as revealed by metaproteomics. *Proc. Natl. Acad. Sci. USA* **2018**, *115*, E400–E408. [CrossRef] [PubMed]
163. Newell, R. Ecosystem influences of natural and cultivated populations of suspension-feeding bivalve molluscs: A review. *J. Shellfish. Res.* **2004**, *23*, 51–61.
164. Zehr, J.; Jenkins, B.; Short, S.; Steward, G. Nitrogenase gene diversity and microbial community structure: A cross-system comparison. *Environ. Microbiol.* **2003**, *5*, 539–554. [CrossRef] [PubMed]
165. Liao, Y.; Cai, C.; Yang, C.; Zheng, Z.; Wang, Q.; Du, X.; Deng, Y. Effect of protein sources in formulated diets on the growth, immune response, and intestinal microflora of pearl oyster *Pinctada fucata martensii*. *Aquac. Rep.* **2020**, *16*, 100253. [CrossRef]
166. Amin, S.; Parker, M.; Armbrust, E. Interactions between Diatoms and Bacteria. *Microbiol. Mol. Biol. Rev.* **2012**, *76*, 667–684. [CrossRef]
167. Buchan, A.; LeCleir, G.; Gulvik, C.; González, J. Master recyclers: Features and functions of bacteria associated with phytoplankton blooms. *Nat. Rev. Microbiol.* **2014**, *12*, 686–698. [CrossRef]
168. Goecke, F.; Thiel, V.; Wiese, J.; Labes, A.; Imhoff, J. Algae as an important environment for bacteria—Phylogenetic relationships among new bacterial species isolated from algae. *Phycologia* **2013**, *52*, 14–24. [CrossRef]
169. Shin, N.; Whon, T.; Bae, J. Proteobacteria: Microbial signature of dysbiosis in gut microbiota. *Trends Biotechnol.* **2015**, *33*, 496–503. [CrossRef]
170. Bryukhanov, A.; Korneeva, V.; Dinarieva, T.; Karnachuk, O.; Netrusov, A.; Pimenov, N. Components of antioxidant systems in the cells of aerotolerant sulfate-reducing bacteria of the genus *Desulfovibrio* (strains A2 and TomC) isolated from metal mining waste. *Microbiology* **2016**, *85*, 649–657. [CrossRef]
171. Schoenborn, L.; Abdollahi, H.; Tee, W.; Dyall-Smith, M.; Janssen, P. A member of the delta subgroup of proteobacteria from a pyogenic liver abscess is a typical sulfate reducer of the genus *Desulfovibrio*. *J. Clin. Microbiol.* **2001**, *39*, 787–790. [CrossRef]
172. Finster, K.; Kjeldsen, K. *Desulfovibrio oceani* subsp *oceani* sp nov., subsp nov and *Desulfovibrio oceani* subsp *galateae* subsp nov., novel sulfate-reducing bacteria isolated from the oxygen minimum zone off the coast of Peru. *Antonie Van Leeuwenhoek Int. J. Gen. Mol. Microbiol.* **2010**, *97*, 221–229. [CrossRef]
173. Pereira, P.; He, Q.; Xavier, A.; Zhou, J.; Pereira, I.; Louro, R. Transcriptional response of *Desulfovibrio vulgaris* Hildenborough to oxidative stress mimicking environmental conditions. *Arch. Microbiol.* **2008**, *189*, 451–461. [CrossRef] [PubMed]
174. Ramel, F.; Amrani, A.; Pieulle, L.; Lamrabet, O.; Voordouw, G.; Seddiki, N.; Brèthes, D.; Company, M.; Dolla, A.; Brasseur, G. Membrane-bound oxygen reductases of the anaerobic sulfate-reducing *Desulfovibrio vulgaris* Hildenborough: Roles in oxygen defence and electron link with periplasmic hydrogen oxidation. *Microbiology* **2013**, *159*, 2663–2673. [CrossRef] [PubMed]
175. Cypionka, H. Oxygen respiration by *Desulfovibrio* species. *Annu. Rev. Microbiol.* **2000**, *54*, 827–848. [CrossRef]
176. Abdollahi, H.; Wimpenny, J. Effects of Oxygen on the Growth of *Desulfovibrio desulfuricans*. *J. Gen. Microbiol.* **1990**, *136*, 1025–1030. [CrossRef]
177. Lopez-Sánchez, R.; Rebollar, E.; Gutierrez-Rios, R.; Garciarrubio, A.; Juarez, K.; Segovia, L. Metagenomic analysis of carbohydrate-active enzymes and their contribution to marine sediment biodiversity. *World J. Microbiol. Biotechnol.* **2024**, *40*, 95. [CrossRef]
178. Eppinger, M.; Baar, C.; Raddatz, G.; Huson, D.; Schuster, S. Comparative analysis of four Campylobacterales. *Nat. Rev. Microbiol.* **2004**, *2*, 872–885. [CrossRef]
179. Gupta, R. Molecular signatures (unique proteins and conserved indels) that are specific for the epsilon proteobacteria (*Campylobacterales*). *BMC Genom.* **2006**, *7*, 167. [CrossRef]

180. Van Goethem, M.; Makhalanyane, T.; Cowan, D.; Valverde, A. Cyanobacteria and Alphaproteobacteria May Facilitate Cooperative Interactions in Niche Communities. *Front. Microbiol.* **2017**, *8*, 2099. [CrossRef]
181. Lu, Y.; Cheung, S.; Koh, X.; Xia, X.; Jing, H.; Lee, P.; Kao, S.; Gan, J.; Dai, M.; Liu, H. Active degradation-nitrification microbial assemblages in the hypoxic zone in a subtropical estuary. *Sci. Total Environ.* **2023**, *904*, 166694. [CrossRef]
182. Waite, D.; Vanwonterghem, I.; Rinke, C.; Parks, D.; Zhang, Y.; Takai, K.; Sievert, S.; Simon, J.; Campbell, B.; Hanson, T.; et al. Comparative Genomic Analysis of the Class *Epsilonproteobacteria* and Proposed Reclassification to Epsilonbacteraeota (phyl. nov.). *Front. Microbiol.* **2017**, *8*, 682. [CrossRef] [PubMed]
183. On, S. Taxonomy of *Campylobacter*, *Arcobacter*, *Helicobacter* and related bacteria:: Current status, future prospects and immediate concerns. *J. Appl. Microbiol.* **2001**, *90*, 1S–15S. [CrossRef] [PubMed]
184. Gazdag, O.; Takács, T.; Ködöböcz, L.; Krett, G.; Szili-Kovács, T. Alphaproteobacteria communities depend more on soil types than land managements. *Acta Agric. Scand. Sect. B-Soil Plant Sci.* **2019**, *69*, 147–154. [CrossRef]
185. Bagagnan, S.; Guerin-Rechdaoui, S.; Marconi, A.; Rocher, V.; Giusti-Miller, S.; Moilleron, R.; Jusselme, M. Overview of microbial communities in the surface water of the Seine River to understand their response to climate change and human activities. *Aquat. Ecol.* **2024**, *58*, 1067–1089. [CrossRef]
186. Gao, F.; Li, F.; Tan, J.; Yan, J.; Sun, H. Bacterial Community Composition in the Gut Content and Ambient Sediment of Sea Cucumber *Apostichopus japonicus* Revealed by 16S rRNA Gene Pyrosequencing. *PLoS ONE* **2014**, *9*, e100092. [CrossRef]
187. Phoma, S.; Vikram, S.; Jansson, J.; Ansorge, I.; Cowan, D.; Van de Peer, Y.; Makhalanyane, T. Agulhas Current properties shape microbial community diversity and potential functionality. *Sci. Rep.* **2018**, *8*, 10542. [CrossRef]
188. Papale, M.; Rizzo, C.; Caruso, G.; Amalfitano, S.; Maimone, G.; Miserocchi, S.; La Ferla, R.; Aspholm, P.; Decembrini, F.; Azzaro, F.; et al. Ice Melt-Induced Variations of Structural and Functional Traits of the Aquatic Microbial Community along an Arctic River (Pasvik River, Norway). *Water* **2021**, *13*, 2297. [CrossRef]
189. Voloshina, E.; Kosiakova, N.; Prokhorenko, I. Lipopolysaccharide from *Rhodobacter capsulatus* Counteracts the Effects of Toxic Lipopolysaccharides and Inhibits the Release of TNF-α, IL-6, and IL-1β in Human Whole Blood. *Biol. Membr.* **2013**, *30*, 357–363. [CrossRef]
190. Song, Z.; Li, K.; Li, K. Acute effects of the environmental probiotics *Rhodobacter sphaeroides* on intestinal bacteria and transcriptome in shrimp *Penaeus vannamei*. *Fish Shellfish. Immunol.* **2024**, *145*, 109316. [CrossRef]
191. Yoon, J. *Thetidibacter halocola* gen. nov., sp. nov., a novel member within the family *Roseobacteraceae* isolated from seawater. *Antonie Van Leeuwenhoek Int. J. Gen. Mol. Microbiol.* **2023**, *116*, 631–641. [CrossRef]
192. Nedashkovskaya, O.; Otstavnykh, N.; Balabanova, L.; Bystritskaya, E.; Kim, S.; Zhukova, N.; Tekutyeva, L.; Isaeva, M. *Rhodoalgimonas zhirmunskyi* gen. nov., sp. nov., a Marine Alphaproteobacterium Isolated from the Pacific Red Alga *Ahnfeltia tobuchiensis*: Phenotypic Characterization and Pan-Genome Analysis. *Microorganisms* **2023**, *11*, 2463. [CrossRef] [PubMed]
193. Wu, Y.; Ren, W.; Zhong, Y.; Guo, L.; Zhou, P.; Xu, X. *Thiosulfatihalobacter marinus* gen. nov. sp. nov., a novel member of the family *Roseobacteraceae*, isolated from the West Pacific Ocean. *Int. J. Syst. Evol. Microbiol.* **2022**, *72*, 005286. [CrossRef]
194. Dutta, D.; Kaushik, A.; Kumar, D.; Bag, S. Foodborne Pathogenic Vibrios: Antimicrobial Resistance. *Front. Microbiol.* **2021**, *12*, 638331. [CrossRef]
195. Zago, V.; Veschetti, L.; Patuzzo, C.; Malerba, G.; Lleo, M. Resistome, Mobilome and Virulome Analysis of *Shewanella algae* and *Vibrio* spp. Strains Isolated in Italian Aquaculture Centers. *Microorganisms* **2020**, *8*, 572. [CrossRef] [PubMed]
196. Dubey, S.; Ager-Wick, E.; Kumar, J.; Karunasagar, I.; Karunasagar, I.; Peng, B.; Evensen, O.; Sorum, H.; Munang'andu, H. *Aeromonas* species isolated from aquatic organisms, insects, chicken, and humans in India show similar antimicrobial resistance profiles. *Front. Microbiol.* **2022**, *13*, 1008870. [CrossRef]
197. Ng, W.; Shum, H.; To, K.; Sridhar, S. Emerging Infections Due to *Shewanella* spp.: A Case Series of 128 Cases Over 10 Years. *Front. Med.* **2022**, *9*, 850938. [CrossRef]
198. Zong, Z. Nosocomial peripancreatic infection associated with *Shewanella xiamenensis*. *J. Med. Microbiol.* **2011**, *60*, 1387–1390. [CrossRef]
199. Antonelli, A.; Di Palo, D.; Galano, A.; Becciani, S.; Montagnani, C.; Pecile, P.; Galli, L.; Rossolini, G. Intestinal carriage of *Shewanella xiamenensis* simulating carriage of OXA-48-producing Enterobacteriaceae. *Diagn. Microbiol. Infect. Dis.* **2015**, *82*, 1–3. [CrossRef]
200. Janda, J.; Abbott, S. The genus *Shewanella*: From the briny depths below to human pathogen. *Crit. Rev. Microbiol.* **2014**, *40*, 293–312. [CrossRef]
201. Bello-López, J.; Cabrero-Martínez, O.; Ibáñez-Cervantes, G.; Hernández-Cortez, C.; Pelcastre-Rodríguez, L.; Gonzalez-Avila, L.; Castro-Escarpulli, G. Horizontal Gene Transfer and Its Association with Antibiotic Resistance in the Genus *Aeromonas* spp. *Microorganisms* **2019**, *7*, 363. [CrossRef]
202. Lerminiaux, N.; Cameron, A. Horizontal transfer of antibiotic resistance genes in clinical environments. *Can. J. Microbiol.* **2019**, *65*, 34–44. [CrossRef] [PubMed]
203. Yu, K.; Huang, Z.; Xiao, Y.; Wang, D. *Shewanella* infection in humans: Epidemiology, clinical features and pathogenicity. *Virulence* **2022**, *13*, 1515–1532. [CrossRef]

204. Samreen; Ahmad, I.; Malak, H.; Abulreesh, H. Environmental antimicrobial resistance and its drivers: A potential threat to public health. *J. Glob. Antimicrob. Resist.* **2021**, *27*, 101–111. [CrossRef]
205. Pavón, A.; Riquelme, D.; Jaña, V.; Iribarren, C.; Manzano, C.; Lopez-Joven, C.; Reyes-Cerpa, S.; Navarrete, P.; Pavez, L.; García, K. The High Risk of Bivalve Farming in Coastal Areas With Heavy Metal Pollution and Antibiotic-Resistant Bacteria: A Chilean Perspective. *Front. Cell. Infect. Microbiol.* **2022**, *12*, 867446. [CrossRef] [PubMed]
206. Lamy, B.; Baron, S.; Barraud, O. *Aeromonas*: The multifaceted middleman in the *One Health* world. *Curr. Opin. Microbiol.* **2022**, *65*, 24–32. [CrossRef] [PubMed]
207. Jones, D.; LaMartina, E.; Lewis, J.; Dahl, A.; Nadig, N.; Szabo, A.; Newton, R.; Skwor, T. One Health and Global Health View of Antimicrobial Susceptibility through the "Eye" of *Aeromonas*: Systematic Review and Meta-Analysis. *Int. J. Antimicrob. Agents* **2023**, *62*, 106848. [CrossRef]
208. Yang, C.; Guo, M.; Yang, H.; Wen, Y.; Zhu, Z.; Wang, T.; Zhu, J.; Chen, L.; Du, H. bla_{KPC-24}-Harboring *Aeromonas veronii* from the Hospital Sewage Samples in China. *Microbiol. Spectr.* **2022**, *10*, e00555-22. [CrossRef]
209. Grilo, M.; Pereira, A.; Sousa-Santos, C.; Robalo, J.; Oliveira, M. Climatic Alterations Influence Bacterial Growth, Biofilm Production and Antimicrobial Resistance Profiles in *Aeromonas* spp. *Antibiotics* **2021**, *10*, 1008. [CrossRef]
210. Gufe, C.; Hodobo, T.; Mbonjani, B.; Majonga, O.; Marumure, J.; Musari, S.; Jongi, G.; Makaya, P.; Machakwa, J. Antimicrobial Profiling of Bacteria Isolated from Fish Sold at Informal Market in Mufakose, Zimbabwe. *Int. J. Microbiol.* **2019**, *2019*, 8759636. [CrossRef]
211. Montezzi, L.; Campana, E.; Corrêa, L.; Justo, L.; Paschoal, R.; da Silva, I.; Souza, M.; Drolshagen, M.; Picao, R. Occurrence of carbapenemase-producing bacteria in coastal recreational waters. *Int. J. Antimicrob. Agents* **2015**, *45*, 174–177. [CrossRef]
212. Rahman, M.; Akter, S.; Ashrafudoulla, M.; Chowdhury, M.; Mahamud, A.; Park, S.; Ha, S. Insights into the mechanisms and key factors influencing biofilm formation by *Aeromonas hydrophila* in the food industry: A comprehensive review and bibliometric analysis. *Food Res. Int.* **2024**, *175*, 113671. [CrossRef]
213. Sherik, M.; Eves, R.; Guo, S.; Lloyd, C.; Klose, K.; Davies, P. Sugar-binding and split domain combinations in repeats-in-toxin adhesins from *Vibrio cholerae* and *Aeromonas veronii* mediate cell-surface recognition and hemolytic activities. *mBio* **2024**, *15*, e02291-23. [CrossRef] [PubMed]
214. Semwal, A.; Kumar, A.; Kumar, N. A review on pathogenicity of *Aeromonas hydrophila* and their mitigation through medicinal herbs in aquaculture. *Heliyon* **2023**, *9*, e14088. [CrossRef] [PubMed]
215. Li, J.; Ni, X.; Liu, Y.; Lu, C. Detection of three virulence genes *alt*, *ahp* and *aerA* in *Aeromonas hydrophila* and their relationship with actual virulence to zebrafish. *J. Appl. Microbiol.* **2011**, *110*, 823–830. [CrossRef] [PubMed]
216. Chen, J.; Hsu, G.; Hsu, B.; Yang, P.; Kuo, Y.; Wang, J.; Hussain, B.; Huang, S. Prevalence, virulence-gene profiles, antimicrobial resistance, and genetic diversity of human pathogenic *Aeromonas* spp. from shellfish and aquatic environments. *Environ. Pollut.* **2021**, *287*, 117361. [CrossRef]
217. Roger, F.; Marchandin, H.; Jumas-Bilak, E.; Kodjo, A.; Lamy, B.; ColBVH, S.G. Multilocus genetics to reconstruct aeromonad evolution. *BMC Microbiol.* **2012**, *12*, 62. [CrossRef]
218. Majeed, S.; De Silva, L.; Kumarage, P.; Heo, G. Occurrence of potential virulence determinants in *Aeromonas* spp. isolated from different aquatic environments. *J. Appl. Microbiol.* **2023**, *134*, lxad031. [CrossRef]
219. Dien, L.; Ngo, T.; Nguyen, T.; Kayansamruaj, P.; Salin, K.; Mohan, C.; Rodkhum, C.; Dong, H. Non-antibiotic approaches to combat motile *Aeromonas* infections in aquaculture: Current state of knowledge and future perspectives. *Rev. Aquac.* **2022**, *15*, 333–366. [CrossRef]
220. Kikuchi, Y.; Graf, J. Spatial and temporal population dynamics of a naturally occurring two-species microbial community inside the digestive tract of the medicinal leech. *Appl. Environ. Microbiol.* **2007**, *73*, 1984–1991. [CrossRef]
221. Kari, Z.; Wee, W.; Sukri, S.; Harun, H.; Reduan, M.; Khoo, M.; Doan, H.; Goh, K.; Wei, L. Role of phytobiotics in relieving the impacts of *Aeromonas hydrophila* infection on aquatic animals: A mini-review. *Front. Vet. Sci.* **2022**, *9*, 1023784. [CrossRef]
222. Milligan, E.; Calarco, J.; Davis, B.; Keenum, I.; Liguori, K.; Pruden, A.; Harwood, V. A Systematic Review of Culture-Based Methods for Monitoring Antibiotic-Resistant *Acinetobacter*, *Aeromonas*, and *Pseudomonas* as Environmentally Relevant Pathogens in Wastewater and Surface Water. *Curr. Environ. Health Rep.* **2023**, *10*, 154–171. [CrossRef] [PubMed]
223. Pessoa, R.; de Oliveira, W.; Correia, M.; Fontes, A.; Coelho, L. Aeromonas and Human Health Disorders: Clinical Approaches. *Front. Microbiol.* **2022**, *13*, 868890. [CrossRef]
224. Piotrowska, M.; Popowska, M. Insight into the mobilome of *Aeromonas* strains. *Front. Microbiol.* **2015**, *6*, 494. [CrossRef]
225. Chen, F.; Yu, T.; Yin, Z.; Wang, P.; Lu, X.; He, J.; Zheng, Y.; Zhou, D.; Gao, B.; Mu, K. Uncovering the hidden threat: The widespread presence of chromosome-borne accessory genetic elements and novel antibiotic resistance genetic environments in *Aeromonas*. *Virulence* **2023**, *14*, 2271688. [CrossRef]
226. Tekedar, H.; Kumru, S.; Blom, J.; Perkins, A.; Griffin, M.; Abdelhamed, H.; Karsi, A.; Lawrence, M. Comparative genomics of *Aeromonas veronii*: Identification of a pathotype impacting aquaculture globally. *PLoS ONE* **2019**, *14*, e0221018. [CrossRef]

227. Subirats, J.; Sànchez-Melsió, A.; Borrego, C.; Balcázar, J.; Simonet, P. Metagenomic analysis reveals that bacteriophages are reservoirs of antibiotic resistance genes. *Int. J. Antimicrob. Agents* **2016**, *48*, 163–167. [CrossRef]
228. Ott, B.; Cruciger, M.; Dacks, A.; Rio, R. Hitchhiking of host biology by beneficial symbionts enhances transmission. *Sci. Rep.* **2014**, *4*, 5825. [CrossRef]
229. Bomar, L.; Graf, J. Investigation into the Physiologies of *Aeromonas veronii in vitro* and Inside the Digestive Tract of the Medicinal Leech Using RNA-seq. *Biol. Bull.* **2012**, *223*, 155–166.
230. McFall-Ngai, M. Negotiations between animals and bacteria: The 'diplomacy' of the squid-vibrio symbiosis. *Comp. Biochem. Physiol. Part A Mol. Integr. Physiol.* **2000**, *126*, 471–480.
231. Braschler, T.; Merino, S.; Tomás, J.; Graf, J. Complement resistance is essential for colonization of the digestive tract of *Hirudo medicinalis* by *Aeromonas* strains. *Appl. Environ. Microbiol.* **2003**, *69*, 4268–4271. [CrossRef]
232. Maltz, M.; LeVarge, B.; Graf, J. Identification of iron and heme utilization genes in *Aeromonas* and their role in the colonization of the leech digestive tract. *Front. Microbiol.* **2015**, *6*, 763. [CrossRef] [PubMed]
233. Bücker, R.; Krug, S.; Rosenthal, R.; Günzel, D.; Fromm, A.; Zeitz, M.; Chakraborty, T.; Fromm, M.; Epple, H.; Schulzke, J. Aerolysin From *Aeromonas hydrophila* Perturbs Tight Junction Integrity and Cell Lesion Repair in Intestinal Epithelial HT-29/B6 Cells. *J. Infect. Dis.* **2011**, *204*, 1283–1292. [CrossRef]
234. von Graevenitz, A. The role of *Aeromonas* in diarrhea: A review. *Infection* **2007**, *35*, 59–64. [CrossRef] [PubMed]
235. Janda, J. Recent Advances in the Study of the Taxonomy, Pathogenicity, and Infectious Syndromes Associated with the Genus Aeromonas. *Clin. Microbiol. Rev.* **1991**, *4*, 397–410. [CrossRef]
236. Nelson, M.; Graf, J. Bacterial symbioses of the medicinal leech *Hirudo verbana*. *Gut Microbes* **2012**, *3*, 322–331. [CrossRef] [PubMed]
237. Knobloch, K.; Gohritz, A.; Busch, K.; Spies, M.; Vogt, P. Hirudo medicinalis-leech applications in plastic and reconstructive microsurgery—A literature review. *Handchir. Mikkrochirurgie Plast. Chir.* **2007**, *39*, 103–107. [CrossRef] [PubMed]
238. Vaelli, P.; Theis, K.; Williams, J.; O'Connell, L.; Foster, J.; Eisthen, H. The skin microbiome facilitates adaptive tetrodotoxin production in poisonous newts. *eLife* **2020**, *9*, e53898. [CrossRef]
239. Zhang, F.; Dashti, N.; Hynes, R.; Smith, D. Plant growth-promoting rhizobacteria and soybean [*Glycine max* (L) Merr] growth and physiology at suboptimal root zone temperatures. *Ann. Bot.* **1997**, *79*, 243–249. [CrossRef]
240. Lichty, K.; Loughran, R.; Ushijima, B.; Richards, G.; Boyd, E. Osmotic stress response of the coral and oyster pathogen *Vibrio coralliilyticus*: Acquisition of catabolism gene clusters for the compatible solute and signaling molecule *myo*-inositol. *Appl. Environ. Microbiol.* **2024**, *90*, e00920-24. [CrossRef]
241. Dempsey, A.; Kitting, C.; Rosson, R. Bacterial variability among individual penaeid shrimp digestive tracts. *Crustaceana* **1989**, *56*, 267–278. [CrossRef]
242. Indergand, S.; Graf, J. Ingested blood contributes to the specificity of the symbiosis of *Aeromonas veronii* biovar sobria and *Hirudo medicinalis*, the medicinal leech. *Appl. Environ. Microbiol.* **2000**, *66*, 4735–4741.
243. Graf, J. Lessons from Digestive-Tract Symbioses Between Bacteria and Invertebrates. *Annu. Rev. Microbiol.* **2016**, *70*, 375–393. [CrossRef]
244. Silver, A.; Graf, J. Innate and procured immunity inside the digestive tract of the medicinal leech. *ISJ-Invertebr. Surviv. J.* **2011**, *8*, 173–178.
245. Nyholm, S.; Graf, J. Knowing your friends: Invertebrate innate immunity fosters beneficial bacterial symbioses. *Nat. Rev. Microbiol.* **2012**, *10*, 815–827. [CrossRef] [PubMed]
246. Mardeni, J.; McClure, E.; Beka, L.; Graf, J. Host Matters: Medicinal Leech Digestive-Tract Symbionts and Their Pathogenic Potential. *Front. Microbiol.* **2016**, *7*, 1569. [CrossRef]
247. Mukherjee, M.; Zaiden, N.; Teng, A.; Hu, Y.; Cao, B. *Shewanella* biofilm development and engineering for environmental and bioenergy applications. *Curr. Opin. Chem. Biol.* **2020**, *59*, 84–92. [CrossRef]
248. Lemaire, O.; Méjean, V.; Iobbi-Nivol, C. The *Shewanella* genus: Ubiquitous organisms sustaining and preserving aquatic ecosystems. *FEMS Microbiol. Rev.* **2020**, *44*, 155–170. [CrossRef]
249. Chen, Y.; Wang, F. Insights on nitrate respiration by Shewanella. *Front. Mar. Sci.* **2015**, *1*, 80. [CrossRef]
250. Sampaio, A.; Silva, V.; Poeta, P.; Aonofriesei, F. *Vibrio* spp.: Life Strategies, Ecology, and Risks in a Changing Environment. *Diversity* **2022**, *14*, 97. [CrossRef]
251. Visick, K.; Stabb, E.; Ruby, E. A lasting symbiosis: How *Vibrio fischeri* finds a squid partner and persists within its natural host. *Nat. Rev. Microbiol.* **2021**, *19*, 654–665. [CrossRef]
252. Brauge, T.; Mougin, J.; Ells, T.; Midelet, G. Sources and contamination routes of seafood with human pathogenic *Vibrio* spp.: A *Farm-to-Fork* approach. *Compr. Rev. Food Sci. Food Saf.* **2024**, *23*, e13283. [CrossRef]
253. Mancini, M.; Alessiani, A.; Donatiello, A.; Didonna, A.; D'Attoli, L.; Faleo, S.; Occhiochiuso, G.; Carella, F.; Di Taranto, P.; Pace, L.; et al. Systematic Survey of *Vibrio* spp. and *Salmonella* spp. in Bivalve Shellfish in Apulia Region (Italy): Prevalence and Antimicrobial Resistance. *Microorganisms* **2023**, *11*, 450. [CrossRef] [PubMed]

254. Walton, M.; Cubillejo, I.; Nag, D.; Withey, J. Advances in cholera research: From molecular biology to public health initiatives. *Front. Microbiol.* **2023**, *14*, 1178538. [CrossRef]
255. Dubert, J.; Barja, J.; Romalde, J. New Insights into Pathogenic Vibrios Affecting Bivalves in Hatcheries: Present and Future Prospects. *Front. Microbiol.* **2017**, *8*, 762. [CrossRef]
256. Beaz-Hidalgo, R.; Balboa, S.; Romalde, J.; Figueras, M. Diversity and pathogenecity of *Vibrio* species in cultured bivalve molluscs. *Environ. Microbiol. Rep.* **2010**, *2*, 34–43. [CrossRef]
257. Tercero-Alburo, J.; González-Márquez, H.; Bonilla-González, E.; Quiñones-Ramírez, E.; Vázquez-Salinas, C. Identification of capsule, biofilm, lateral flagellum, and type IV pili in *Vibrio mimicus* strains. *Microb. Pathog.* **2014**, *76*, 77–83. [CrossRef]
258. Muñoz, D.; de Marín, C.; Marval, H.; Martínez, C. Identification of Bacteria of the Genus *Vibrio* Associated to Zones of Bivalve Mollusks Extraction, Sucre State, Venezuela. *Rev. Científica-Fac. Cienc. Vet.* **2012**, *22*, 459–467.
259. Pruzzo, C.; Gallo, G.; Canesi, L. Persistence of vibrios in marine bivalves: The role of interactions with haemolymph components. *Environ. Microbiol.* **2005**, *7*, 761–772. [CrossRef] [PubMed]
260. Zhao, R.; Qin, Z.; Feng, Y.; Geng, Y.; Huang, X.; Ouyang, P.; Chen, D.; Guo, H.; Deng, H.; Fang, J.; et al. Sialic acid catabolism contributes to *Vibrio mimicus* virulence. *Aquaculture* **2023**, *574*, 739660. [CrossRef]
261. Zhao, J.; Manno, D.; Hawari, J. *Psychrilyobacter atlanticus* gen. nov., sp nov., a marine member of the phylum *Fusobacteria* that produces H_2 and degrades nitramine explosives under low temperature conditions. *Int. J. Syst. Evol. Microbiol.* **2009**, *59*, 491–497. [CrossRef]
262. Diaz, R.; Rosenberg, R. Marine benthic hypoxia: A review of its ecological effects and the behavioral responses of benthic macrofauna. *Oceanogr. Mar.Biol. Annu. Rev.* **1995**, *33*, 245–303.
263. Olivier, A.; Jones, L.; Le Vay, L.; Christie, M.; Wilson, J.; Malham, S. A global review of the ecosystem services provided by bivalve aquaculture. *Rev. Aquac.* **2020**, *12*, 3–25. [CrossRef]
264. Yadav, S.; Koenen, M.; Bale, N.; Damsté, J.; Villanueva, L. The physiology and metabolic properties of a novel, low-abundance *Psychrilyobacter* species isolated from the anoxic Black Sea shed light on its ecological role. *Environ. Microbiol. Rep.* **2021**, *13*, 899–910. [CrossRef]
265. Boutin, S.; Bernatchez, L.; Audet, C.; Derôme, N. Network Analysis Highlights Complex Interactions between Pathogen, Host and Commensal Microbiota. *PLoS ONE* **2013**, *8*, e84772. [CrossRef] [PubMed]
266. Miyazaki, M.; Nagano, Y.; Fujiwara, Y.; Hatada, Y.; Nogi, Y. *Aquimarina macrocephali* sp. nov., isolated from sediment adjacent to sperm whale carcasses. *Int. J. Syst. Evol. Microbiol.* **2010**, *60*, 2298–2302. [CrossRef]
267. Santos, L.; Ramos, F. Antimicrobial resistance in aquaculture: Current knowledge and alternatives to tackle the problem. *Int. J. Antimicrob. Agents* **2018**, *52*, 135–143. [CrossRef]
268. El-Saadony, M.; Alagawany, M.; Patra, A.; Kar, I.; Tiwari, R.; Dawood, M.; Dhama, K.; Abdel-Latif, H. The functionality of probiotics in aquaculture: An overview. *Fish Shellfish. Immunol.* **2021**, *117*, 36–52. [CrossRef]
269. Quinn, R.; Hazra, S.; Smolowitz, R.; Chistoserdov, A. Real-time PCR assay for *Aquimarina macrocephali* subsp homaria and its distribution in shell disease lesions of *Homarus americanus*, Milne-Edwards, 1837, and environmental samples. *J. Microbiol. Methods* **2017**, *139*, 61–67. [CrossRef]
270. Park, S.; Choe, H.; Baik, K.; Seong, C. *Aquimarina mytili* sp nov., isolated from the gut microflora of a mussel, *Mytilus coruscus*, and emended description of *Aquimarina macrocephali*. *Int. J. Syst. Evol. Microbiol.* **2012**, *62*, 1974–1979. [CrossRef]
271. Jadeja, N.; Worrich, A. From gut to mud: Dissemination of antimicrobial resistance between animal and agricultural niches. *Environ. Microbiol.* **2022**, *24*, 3290–3306. [CrossRef]
272. Subirats, J.; Triadó-Margarit, X.; Mandaric, L.; Acuña, V.; Balcázar, J.; Sabater, S.; Borrego, C. Wastewater pollution differently affects the antibiotic resistance gene pool and biofilm bacterial communities across streambed compartments. *Mol. Ecol.* **2017**, *26*, 5567–5581. [CrossRef] [PubMed]
273. Bentzon-Tilia, M.; Sonnenschein, E.; Gram, L. Monitoring and managing microbes in aquaculture—Towards a sustainable industry. *Microb. Biotechnol.* **2016**, *9*, 576–584. [CrossRef] [PubMed]
274. Gómez-Chiarri, M.; Guo, X.; Tanguy, A.; He, Y.; Proestou, D. The use of -omic tools in the study of disease processes in marine bivalve mollusks. *J. Invertebr. Pathol.* **2015**, *131*, 137–154. [CrossRef]
275. Habteweld, H.; Asfaw, T. Novel Dietary Approach with Probiotics, Prebiotics, and Synbiotics to Mitigate Antimicrobial Resistance and Subsequent Out Marketplace of Antimicrobial Agents: A Review. *Infect. Drug Resist.* **2023**, *16*, 3191–3211. [CrossRef] [PubMed]
276. Arrieta, M.; Stiemsma, L.; Amenyogbe, N.; Brown, E.; Finlay, B. The intestinal microbiome in early life: Health and disease. *Front. Immunol.* **2014**, *5*, 427. [CrossRef]
277. Destoumieux-Garzón, D.; Montagnani, C.; Dantan, L.; Nicolas, N.; Travers, M.; Duperret, L.; Charrière, G.; Toulza, E.; Mitta, G.; Cosseau, C.; et al. Cross-talk and mutual shaping between the immune system and the microbiota during an oyster's life. *Philos. Trans. R. Soc. B-Biol. Sci.* **2024**, *379*, 20230065. [CrossRef]

278. Majnik, A.; Lane, R. The relationship between early-life environment, the epigenome and the microbiota. *Epigenomics* **2015**, *7*, 1173–1184. [CrossRef]
279. Camara, M.; Griffith, S.; Evans, S. Can selective breeding reduce the heavy metals content of pacific oysters (*Crassostrea gigas*), and are there trade-offs with growth or survival? *J. Shellfish. Res.* **2005**, *24*, 979–986.
280. Dupont, S.; Lokmer, A.; Corre, E.; Auguet, J.; Petton, B.; Toulza, E.; Montagnani, C.; Tanguy, G.; Pecqueur, D.; Salmeron, C.; et al. Oyster hemolymph is a complex and dynamic ecosystem hosting bacteria, protists and viruses. *Anim. Microbiome* **2020**, *2*, 12. [CrossRef]

Capítulo 3: Secuenciación Directa de ARN Mediante Nanoporo Revela Reconfiguración Epitranscriptómica y Dinámica Postranscripcional en *Mytilus chilensis* Bajo Estrés Hipóxico

Resumen

Las modificaciones epitranscriptómicas como la N6-metiladenosina (m^6A), 5-metilcitosina (m^5C) y la pseudouridina (Ψ) han emergido como capas fundamentales de regulación post-transcripcional en eucariotas. En organismos marinos como *Mytilus chilensis*, la comprensión de estos mecanismos es aún limitada, particularmente bajo condiciones de estrés ambiental como la hipoxia, fenómeno cada vez más frecuente en sistemas costeros debido al cambio climático. En este estudio, se utilizó secuenciación directa de ARN mediante la plataforma Nanopore para caracterizar de manera integral las modificaciones epitranscriptómicas inducidas por hipoxia en tejidos de branquia y glándula digestiva. El análisis reveló un perfil diferencial en la distribución y frecuencia de metilaciones m^6A y m^5C entre condiciones de normoxia e hipoxia, con un incremento significativo en la cantidad de genes metilados en regiones 3' UTR y CDS bajo hipoxia. Se detectó además un enriquecimiento de motivos específicos como GGACA y AGACT en sitios de m^6A, así como una redistribución cromosómica de genes

modificados. La hipoxia también produjo una reducción generalizada en la longitud de las colas poli(A), lo que sugiere una regulación activa de la estabilidad y degradación del ARN. Por otro lado, el análisis de pseudouridina evidenció patrones de modificación dependientes de la condición ambiental, sin correlación significativa con la profundidad de lectura, lo cual valida la robustez del enfoque. Estos hallazgos evidencian una reprogramación epitranscriptómica inducida por hipoxia en *M. chilensis*, y subrayan el papel funcional de estas marcas químicas como posibles mediadores adaptativos ante cambios ambientales. La presente investigación establece las bases para el desarrollo de biomarcadores epitranscriptómicos en moluscos y aporta nuevas herramientas para el monitoreo de salud ambiental en ecosistemas costeros.

Palabras clave: m^6A, m^5C, Pseudouridina, Modificaciones químicas del ARN, Biomarcadores ambientales, Adaptación al estrés

Introducción

Las modificaciones epitranscriptómicas del ARN, particularmente N6-metiladenosina (m^6A), 5-metilcitosina (m^5C) y pseudouridina (Ψ), han emergido como capas críticas de regulación post-transcripcional en eucariotas, modulando procesos clave como la estabilidad del ARN, la eficiencia de traducción y la respuesta a señales ambientales (Li et al., 2017; Zaccara et al., 2019). A diferencia de las modificaciones epigenéticas del ADN, las marcas epitranscriptómicas son dinámicas y reversibles, lo que permite a las células responder rápidamente a condiciones cambiantes del entorno, incluyendo el estrés hipóxico.

La hipoxia representa un estrés ambiental significativo que desencadena reprogramaciones transcripcionales y post-transcripcionales, especialmente en organismos acuáticos expuestos a zonas de oxígeno reducido por causas naturales o antrópicas (Shen et al., 2023; Vaquer-Sunyer & Duarte, 2008). En moluscos bivalvos, como *M. chilensis*, especie endémica de importancia ecológica y comercial en el cono sur de Sudamérica, la adaptación a fluctuaciones en la disponibilidad de oxígeno es fundamental para su supervivencia,

distribución y rendimiento acuícola. Sin embargo, a pesar de su relevancia, el paisaje epitranscriptómico de esta especie en respuesta a hipoxia permanece inexplorado.

Estudios previos en modelos vertebrados y vegetales han demostrado que la hipoxia puede modular la deposición y eliminación de marcas como m^6A, impactando la estabilidad y destino de los transcritos asociados a metabolismo energético, respuesta oxidativa y muerte celular (Frye M. et al., 2018; Zhou et al., 2016). En paralelo, se ha documentado que m^5C participa en la regulación del transporte nuclear del ARN y la traducción en condiciones de estrés (Yang et al., 2017), mientras que la pseudouridilación contribuye a la arquitectura secundaria del ARN y a su interacción con ribonucleoproteínas (Carlile et al., 2014). La aplicación de tecnologías de secuenciación directa de ARN, como Oxford Nanopore, ha permitido detectar estas modificaciones de forma simultánea, sin requerir retrotranscripción ni amplificación, preservando así las señales nativas del ARN (Workman et al., 2019).

En este contexto, el presente estudio se propuso caracterizar por primera vez el epitranscriptoma de *M. chilensis* bajo condiciones experimentales de hipoxia y normoxia, utilizando secuenciación directa de ARN por Nanopore. Se analizó de forma integrada la expresión diferencial, la distribución de metilaciones m^6A y m^5C, los motivos nucleotídicos asociados, la pseudouridina y la dinámica de la cola poli(A). Esta aproximación busca no solo expandir el conocimiento básico sobre regulación post-transcripcional en bivalvos, sino también sentar las bases para el desarrollo de biomarcadores moleculares aplicables en estudios de ecotoxicología, fisiología comparada y adaptación marina al cambio climático.

Metodología

Diseño experimental y condiciones de exposición

Se utilizaron ejemplares de *M. chilensis* provenientes de cultivos ubicados en el sistema estuarino de Reloncaví, Región de Los Lagos, Chile. Los organismos fueron aclimatados durante 38 días en condiciones controladas de laboratorio ($12{,}5 \pm 0{,}94$ °C, agua de mar

filtrada, flujo continuo y alimentación regular), previo al inicio del tratamiento experimental. El experimento tuvo una duración de 50 días y consistió en la exposición alternante de los organismos a condiciones de hipoxia (2,0 mg/L de oxígeno disuelto) y normoxia ($7{,}2 \pm 0{,}2$ mg/L). La hipoxia fue inducida mediante inyección controlada de nitrógeno gaseoso y los niveles de oxígeno se monitorearon diariamente utilizando sondas multiparamétricas calibradas.

Muestreo y extracción de ARN

Las muestras biológicas fueron recolectadas en cuatro puntos temporales: días 10 y 50 bajo hipoxia, y días 20 y 40 bajo normoxia. En cada punto de muestreo se extrajeron tejidos de branquias y glándulas digestivas de tres individuos por réplica biológica, totalizando nueve individuos por condición. Los tejidos fueron preservados en etanol molecular, transportados a 4 °C y almacenados a −80 °C hasta su procesamiento. Se generó un pool de tejidos por réplica experimental para minimizar la variabilidad interindividual. La extracción de ARN total se realizó mediante homogeneización tisular en buffer lítico y posterior separación orgánica con fenol-cloroformo. La calidad e

integridad del ARN se verificaron mediante electroforesis en gel y espectrofotometría, y las fracciones de ARNm fueron purificadas y seleccionadas para análisis epitranscriptómico.

Preparación de bibliotecas y secuenciación directa de ARN

Se empleó secuenciación directa de ARN de molécula única usando la plataforma de tercera generación Nanopore (Oxford Nanopore Technologies®). Esta metodología evitó la necesidad de retrotranscripción y amplificación enzimática, permitiendo preservar la orientación nativa del ARN y sus modificaciones epitranscriptómicas. Las bibliotecas se prepararon mediante ligación de adaptadores poli(dT) y adaptadores motores conforme a las especificaciones del fabricante, con carga posterior en flowcells activas.

Durante la secuenciación, las moléculas de ARN generaron señales de corriente iónica al atravesar los poros de proteína, las cuales fueron decodificadas mediante el algoritmo de red neuronal GUPPY. Los archivos fast5 fueron convertidos a formato fastq, y posteriormente

sometidos a un control de calidad que excluyó lecturas con puntuación inferior a Q7 y longitud menor a 50 pb.

Mapeo al genoma de referencia y anotación de transcritos

Las lecturas depuradas fueron alineadas al genoma de referencia *de M. chilensis* utilizando alineadores especializados en lecturas largas. Solo se conservaron lecturas con alineamientos únicos. Para construir y cuantificar los transcritos consenso se empleó FLAIR (v1.5.0), y su refinamiento estructural se realizó con StringTie (v2.1.4). Para comparar los transcritos obtenidos con las anotaciones genómicas existentes, se utilizó gffcompare (v0.12.1), identificando 5.237 nuevos transcritos, de los cuales 4.796 no mostraron homología con regiones previamente descritas.

Predicción de regiones codificantes y optimización estructural

TransDecoder (v5.5.0) fue utilizado para predecir regiones codificantes (CDS) en los transcritos no anotados. Las regiones 5′ y 3′ de los transcritos fueron extendidas cuando se detectaron límites no

coincidentes con las anotaciones previas, lo que permitió una mejora sustancial en la definición de los UTRs y de los límites génicos.

Análisis de expresión diferencial

Los conteos de lectura por transcripto fueron procesados mediante el paquete edgeR (v3.32.1). Se consideraron como diferencialmente expresados aquellos transcritos con FDR < 0,05 y |logFC| > 1, lo que permitió detectar alteraciones significativas en la expresión entre las condiciones de hipoxia y normoxia.

Identificación de modificaciones epitranscriptómicas (m^6A, m^5C y Ψ)

La detección de sitios m^5C se realizó mediante el modelo alternativo de Tombo, mientras que los sitios m^6A fueron identificados usando el modelo de novo del mismo software, complementado con el pipeline MINES. Para la pseudouridina (Ψ), se empleó el software Nanopsu con un umbral de probabilidad posterior superior a 0,9, permitiendo una detección robusta de esta modificación estructural.

Análisis de motivos y distribución epigenómica

Los motivos de metilación fueron evaluados mediante análisis de secuencias flanqueantes a los sitios modificados. Asimismo, se analizó la distribución cromosómica y estructural de los genes modificados, discriminando entre regiones CDS, UTRs y secuencias no anotadas.

Análisis estadístico y validación

Las diferencias en la fracción de expresión de regiones modificadas fueron evaluadas mediante pruebas ANOVA de Welch, con ajustes por Bonferroni para comparaciones múltiples. La asociación entre profundidad de lectura y probabilidad de motivo fue examinada mediante correlaciones de Pearson y Spearman, sin hallarse significancia estadística, lo que respalda la consistencia técnica de la detección de motivos independientemente del nivel de cobertura.

Visualización y procesamiento de datos

Los análisis estadísticos y gráficos fueron realizados en R (versión 4.2.2), utilizando paquetes como ggplot2, dplyr, data.table y ggpubr. Los análisis epitranscriptómicos fueron complementados con herramientas especializadas como Tombo y Nanocompore. Los criterios de inclusión de eventos modificados consideraron un umbral de probabilidad ≥ 0.95 para asegurar la confiabilidad en la identificación de las modificaciones epitranscriptómicas.

Resultados

El análisis de la distribución de genes con metilación m^6A en función de sus regiones estructurales reveló patrones diferenciales entre condiciones de normoxia e hipoxia en *M. chilensis* (Figura 1). Se observaron incrementos consistentes en el número de genes modificados bajo hipoxia en todas las regiones estructurales evaluadas, lo que sugiere una intensificación global de la regulación epitranscriptómica ante la disminución del oxígeno ambiental.

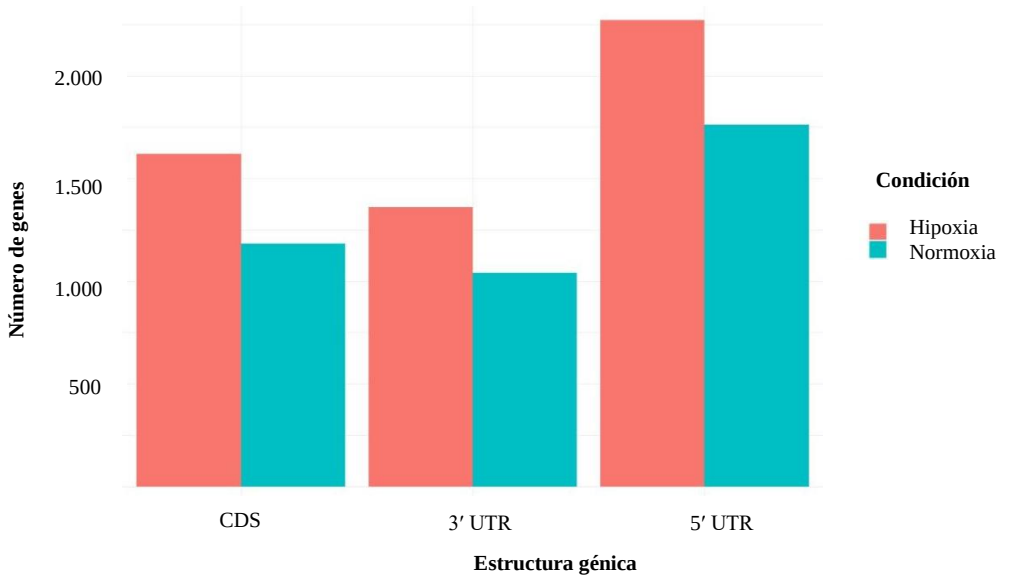

FIGURA 1. Distribución de genes modificados con m^6A según regiones estructurales del transcrito en *M. chilensis* bajo condiciones de hipoxia y normoxia. El gráfico de barras representa el número de genes asociados a metilación m^6A en distintas regiones del ARN mensajero: secuencia codificante (CDS), región no traducida 5′ (5′ UTR) y región no traducida 3′ (3′ UTR), en condiciones de hipoxia (rojo) y normoxia (azul)

La región 3′ UTR fue la más frecuentemente modificada, destacando un total de 2.273 genes bajo hipoxia frente a 1.762 en normoxia. Esta observación sugiere que la metilación m^6A en dicha región podría desempeñar un papel clave en la modulación de la estabilidad del ARNm, el silenciamiento post-transcripcional y el reclutamiento de proteínas de unión bajo condiciones de estrés hipóxico.

Asimismo, la secuencia codificante (CDS) mostró un aumento considerable en hipoxia (1.619 genes) en comparación con normoxia (1.183 genes), indicando una posible participación directa de la

metilación en la regulación de genes funcionales esenciales durante la adaptación fisiológica. Del mismo modo, la región 5′ UTR presentó una mayor frecuencia de modificación bajo hipoxia (1.361 vs. 1.042 genes), lo cual podría relacionarse con mecanismos que afectan la eficiencia de la traducción o la selección de sitios de inicio alternativos.

El análisis comparativo de motivos epitranscriptómicos asociados a sitios de metilación m^6A en *M. chilensis* reveló un enriquecimiento diferencial dependiente de la condición ambiental (Figura 2). Se identificaron cinco motivos principales (AGACT, GGACA, GGACC, GGACT y NA), cuya frecuencia varió significativamente entre normoxia e hipoxia.

El motivo GGACA fue el más representado en ambos grupos, con una frecuencia notablemente mayor bajo hipoxia (~2.000 vs. ~1.550 en normoxia), lo que sugiere un posible rol regulador central en condiciones de bajo oxígeno. El motivo AGACT también mostró una mayor prevalencia en hipoxia (~1.600 frente a ~1.250), lo que podría reflejar su implicación en rutas transcripcionales específicas inducidas por estrés hipóxico. Del mismo modo, los motivos GGACT y GGACC exhibieron

frecuencias elevadas bajo hipoxia (~1.000 vs. ~750 y ~650 vs. ~450, respectivamente), reforzando el patrón de enriquecimiento selectivo de secuencias reconocidas por las metiltransferasas m m^6A A en ambientes de oxígeno reducido.

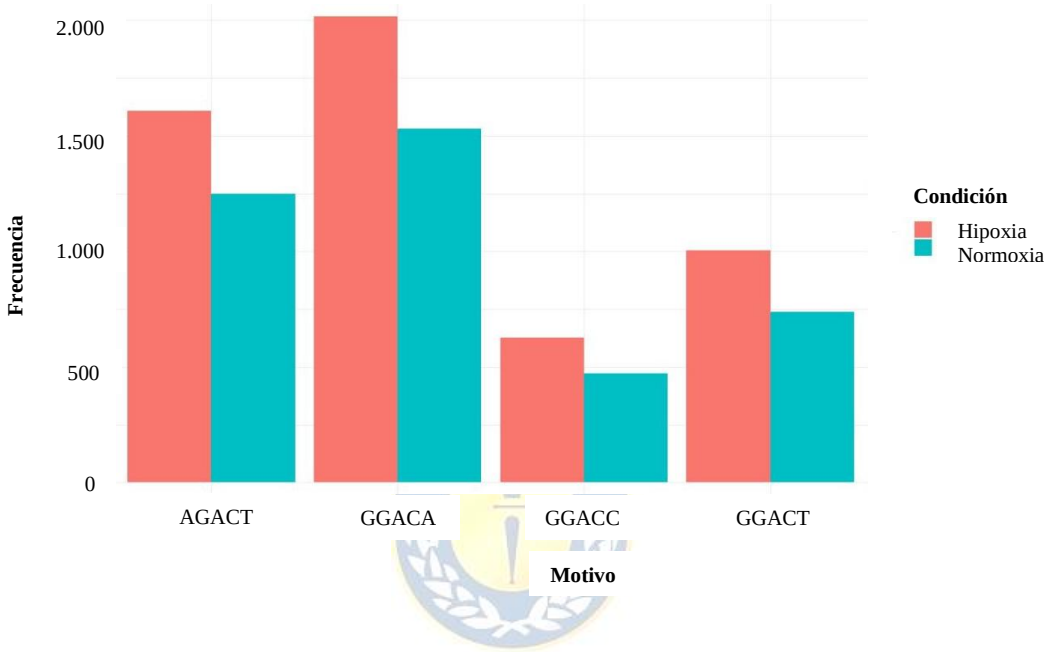

FIGURA 2. Frecuencia comparativa de motivos de metilación m^6A en *M. chilensis* bajo condiciones de hipoxia y normoxia. El gráfico de barras muestra la distribución de cinco motivos nucleotídicos asociados a sitios de metilación m^6A en condiciones de hipoxia (rojo) y normoxia (azul).

El perfil de poliadenilación reveló una variación dependiente de las condiciones en las distribuciones de la longitud de la cola poli(A) en *M. chilensis* sometida a estrés hipóxico (Figura 3). Se analizaron un total de 93.870 transcritos en el grupo normóxico (control), que mostraron una longitud media de la cola poli(A) de 77,19 nucleótidos, con valores del

primer cuartil (Q25), mediana (Q50) y tercer cuartil (Q75) de 39.37, 64.52 y 104.03 nucleótidos, respectivamente. Por el contrario, el grupo tratado con hipoxia incluyó 138.950 transcripciones con una longitud media de la cola poli(A) ligeramente reducida de 74,07 nucleótidos, y valores cuartiles de 39,21 (Q25), 62,04 (Q50) y 97,81 (Q75). El análisis del gráfico de violín confirmó visualmente un cambio global hacia colas de poli(A) más cortas en condiciones de hipoxia.

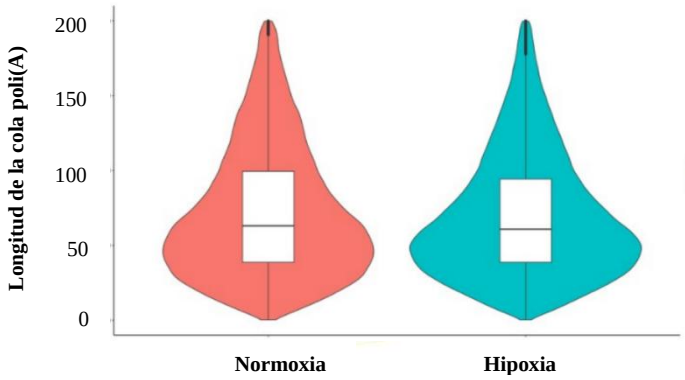

FIGURA 3. Distribución de la longitud de la cola poli(A) en *M. chilensis*. Gráficos de violín que ilustran la distribución comparativa de las longitudes de la cola poli(A) en muestras normóxicas (control, rojo) frente a hipóxicas (tratamiento, azul).

El análisis genómico completo de los sitios de metilación del ARN en condiciones normóxicas reveló una distribución cromosómica distintiva de las modificaciones de 5-metilcitosina (m^5C) y N6-metiladenosina (m^6A) en *M. chilensis* (Figura 4). La distribución de los sitios de modificación m^5C (panel izquierdo) mostró una amplia cobertura en múltiples cromosomas, con sitios dispersos por todo el

genoma, aunque con regiones de mayor densidad de metilación en cromosomas específicos, lo que sugiere una regulación epitranscriptómica localizada. Por el contrario, los sitios m^6A (panel derecho) mostraron una distribución más desigual, caracterizada por una agrupación prominente dentro de regiones cromosómicas distintas. Este patrón indica posibles puntos críticos para la regulación del ARN mediada por m^6A.

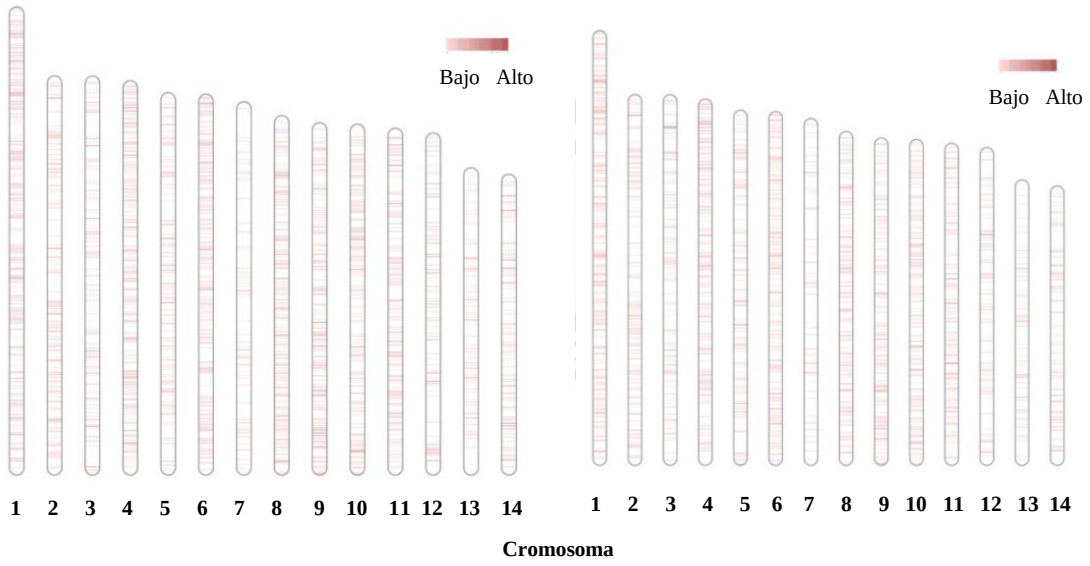

FIGURA 4. Distribución cromosómica de los sitios de modificación por metilación del ARN en *M. chilensis* en condiciones normóxicas. Distribución cromosómica de los sitios de modificación por metilación del ARN en *M. chilensis* en condiciones normóxicas. Panel izquierdo: Distribución y densidad de los sitios identificados de 5-metilcitosina (m^5C) en los cromosomas. Panel derecho: Distribución y densidad de los sitios de modificación de N6-metiladenosina (m^6A) identificados. Los gráficos ilustran la localización espacial y la abundancia relativa de cada tipo de metilación del ARN en todo el genoma, reflejando los patrones epitranscriptómicos de referencia en condiciones de normoxia.

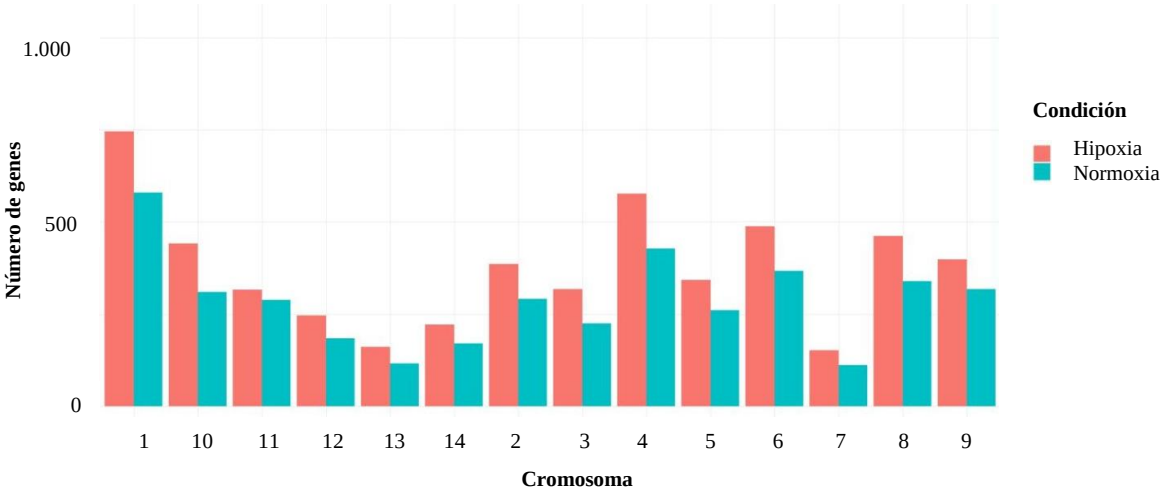

FIGURA 5. Distribución cromosómica de genes asociados a metilación m^6A en *M. chilensis* bajo condiciones de normoxia e hipoxia. El gráfico de barras muestra el número de genes con modificaciones m^6A distribuidos por cromosoma en condiciones de normoxia (azul) e hipoxia (rojo). Se observa una tendencia general hacia un mayor número de genes modificados bajo hipoxia en prácticamente todos los cromosomas, lo que sugiere una respuesta transcripcional dependiente de la condición ambiental.

El análisis de la distribución cromosómica de genes con modificaciones m^6A en *M. chilensis* reveló una reconfiguración significativa en respuesta a la hipoxia (Figura 5). En casi todos los cromosomas, se observó un aumento en el número de genes modificados en condiciones hipóxicas en comparación con normoxia, lo cual sugiere una activación diferencial del epitranscriptoma bajo estrés por baja disponibilidad de oxígeno.

Tabla 1. Distribución cromosómica de genes asociados a metilación m^6A en *M. chilensis* bajo condiciones de normoxia e hipoxia

Cromosoma (Hipoxia)	Conteo de Genes (Hipoxia)	Cromosoma (Normoxia)	Conteo de Genes (Normoxia)
Cromosoma 1	746	Cromosoma 1	579
Cromosoma 4	576	Cromosoma 4	427
Cromosoma 6	488	Cromosoma 6	368
Cromosoma 8	462	Cromosoma 8	339
Cromosoma 10	442	Cromosoma 9	317
Cromosoma 9	398	Cromosoma 10	310
Cromosoma 2	386	Cromosoma 2	292
Cromosoma 5	342	Cromosoma 11	288
Cromosoma 3	317	Cromosoma 5	260
Cromosoma 11	316	Cromosoma 3	224
Cromosoma 12	246	Cromosoma 12	184
Cromosoma 14	221	Cromosoma 14	171
Cromosoma 13	161	Cromosoma 13	116
Cromosoma 7	152	Cromosoma 7	11
Total	5253		3886

Los cromosomas 1, 4, 6 y 8 concentraron el mayor número absoluto de genes con metilación m^6A en hipoxia, con diferencias notables respecto a normoxia (Tabla 1). Estos resultados destacan estas regiones cromosómicas como posibles núcleos funcionales de regulación epitranscriptómica en respuesta a condiciones hipóxicas.

En contraste, los cromosomas 13, 14 y 7 presentaron la menor representación en ambos estados, aunque mantuvieron la tendencia de mayor frecuencia bajo hipoxia (Tabla 1), lo que sugiere que incluso en regiones de baja expresión global, la hipoxia genera una reprogramación selectiva del patrón de metilación.

FIGURA 6. Motivos secuenciales que rodean los sitios de modificación por metilación del ARN en *M. chilensis*. Panel izquierdo: Distribución de secuencias de nucleótidos (9 pb) que flanquean los sitios de modificación por 5-metilcitosina (m^5C) identificados. Panel derecho: Distribución de secuencias de nucleótidos (5 pb) que flanquean los sitios de modificación de N6-metiladenosina (m^6A). Los logotipos de secuencia ilustran la frecuencia de nucleótidos en cada posición, donde la altura de las letras representa la frecuencia relativa y la conservación, destacando las preferencias de motivos dependientes del contexto para la metilación del ARN en respuesta a condiciones hipóxicas.

Los análisis de motivos secuenciales revelaron preferencias contextuales distintas en torno a los sitios de metilación del ARN en *M. chilensis* (Figura 6). Concretamente, la distribución de los nucleótidos que flanquean los sitios de modificación de 5-metilcitosina (m^5C) identificados indicó un motivo consenso conservado de cinco bases en el que destacan los residuos de citosina (C) en la posición central, con

residuos de adenina (A) enriquecidos situados predominantemente upstream (posiciones -2 y -1) y residuos de uracilo (U) downstream (posiciones +1 y +2). Por el contrario, los sitios de modificación de N6-metiladenosina (m^6A) mostraban un motivo consenso de cinco bases diferente, caracterizado por un fuerte enriquecimiento de residuos de guanina (G) en las posiciones -2 y -1, adenina (A) en el sitio de modificación central y una presencia constante de citosina (C) y uracilo (U) en las posiciones aguas abajo (+1 y +2).

El perfil epitranscriptómico de *M. chilensis* bajo condiciones de normoxia e hipoxia reveló patrones diferenciados en la abundancia relativa de eventos de metilación del ARN en sitios m^5C y m^6A (Figura 7). El análisis de diagramas de caja mostró que la metilación m^6A presentó una reducción pronunciada bajo hipoxia, evidenciada por una mediana más baja y un rango intercuartílico reducido en comparación con las condiciones normóxicas. En contraste, la metilación m^5C mantuvo una distribución más estable entre ambas condiciones experimentales, con medianas y dispersión similares.

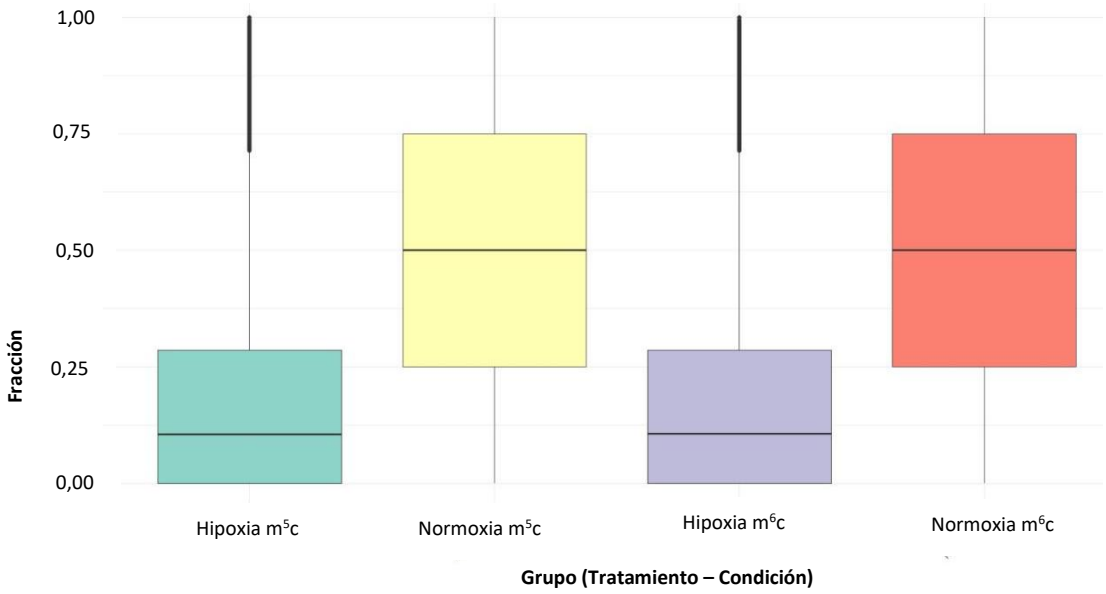

FIGURA 7. Distribución comparativa de sitios de metilación de ARN en nucleótidos m^5C y m^6A en *M. chilensis* bajo condiciones de hipoxia y normoxia. Las proporciones fueron estimadas a partir de secuenciación directa de ARN mediante tecnología de nanoporo, utilizando los modelos de detección de Tombo para m^5C y la combinación Tombo + MINES para m^6A. Los diagramas de caja representan el rango intercuartílico (IQR), con la línea horizontal indicando la mediana y los puntos individuales representando valores atípicos. Se evidenció una reducción significativa en la frecuencia relativa de modificaciones m^6A bajo hipoxia, mientras que las modificaciones m^5C mostraron una distribución más estable. Estos resultados reflejan una reconfiguración epitranscriptómica sensible al estado redox, con posibles implicancias en la regulación post-transcripcional de genes relacionados al metabolismo energético y respuesta al estrés ambiental.

Bajo normoxia, la señal de m^6A exhibió mayor variabilidad y una fracción de modificación significativamente más alta, lo que indica un paisaje de metilación más activo y extendido en presencia de niveles óptimos de oxígeno. Por el contrario, la supresión de m^6A bajo hipoxia sugiere una posible regulación negativa, a nivel transcripcional o enzimático, del sistema de metilación m^6A en respuesta a condiciones de

bajo oxígeno. Estos hallazgos evidencian una reprogramación epitranscriptómica dependiente del estado redox, donde la marca m^6A se muestra especialmente sensible. La estabilidad relativa de la metilación m^5C entre condiciones sugiere funciones regulatorias distintas, posiblemente orientadas al mantenimiento de la estabilidad transcripcional básica frente al estrés ambiental.

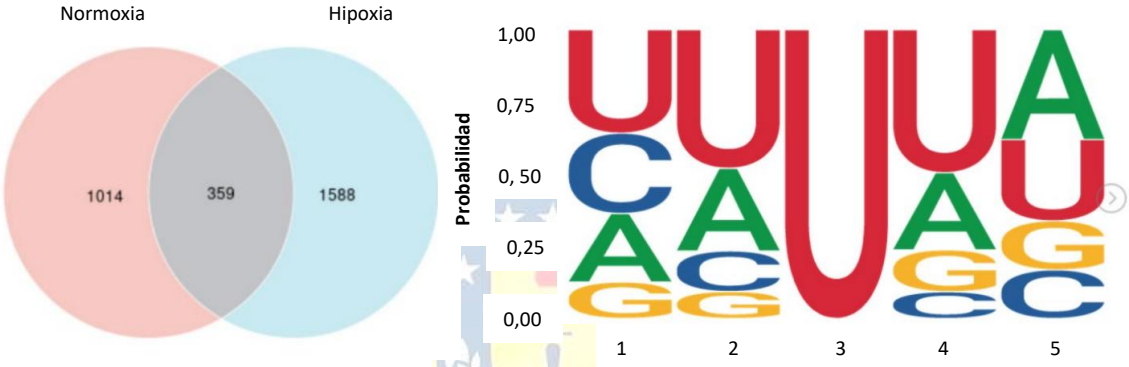

FIGURA 8. Diagrama de Venn y logotipo del motivo secuencial que representan los sitios de modificación de pseudouridina (Ψ) en *M. chilensis*. Panel izquierdo: diagrama de Venn que ilustra la superposición y la singularidad de los sitios de pseudouridina identificados en muestras de control frente a muestras tratadas con hipoxia. Panel derecho: logotipo del motivo secuencial consensuado que representa la preferencia de nucleótidos y la probabilidad posicional relativa que rodea a los sitios de modificación de pseudouridina. La altura de cada nucleótido corresponde a su frecuencia en la posición respectiva, lo que destaca un contexto conservado rico en U.

El perfil de los sitios de modificación de pseudouridina (Ψ) reveló patrones de distribución distintos entre las muestras de *M. chilensis* del grupo de control y las tratadas con hipoxia (Figura 8). El análisis del diagrama de Venn mostró un total de 1.373 sitios únicos de modificación de pseudouridina en el grupo de control, 1.947 sitios únicos en el grupo

tratado con hipoxia y 359 sitios compartidos entre ambas condiciones. Además, el análisis de motivos secuenciales adyacentes a los sitios de pseudouridina reveló un motivo consenso conservado y enriquecido en uridina, caracterizado predominantemente por residuos consecutivos de uridina con alta frecuencia en las posiciones -2, -1, +1 y +2 con respecto al sitio de modificación, lo que sugiere un contexto estructural y funcional conservado para la pseudouridilación en las transcripciones de *M. chilensis* bajo estrés ambiental.

El análisis de la relación entre la profundidad de secuenciación y la probabilidad de detección de motivos para sitios de pseudouridina (Ψ) en *M. chilensis* (Figura 9) mostró patrones consistentes bajo condiciones de normoxia e hipoxia. En normoxia, la mayor concentración de puntos se observó en profundidades de lectura entre 0 y 200, con probabilidades de detección de motivos predominantemente comprendidas entre 0,925 y 1,0, destacando una fuerte densidad en torno a 0,95. Esta distribución indica que la detección de motivos de pseudouridina se mantiene estable y con alta confianza a través de un amplio rango de profundidades de secuenciación, lo que evidencia una uniformidad en la predicción de modificaciones incluso en condiciones de baja cobertura.

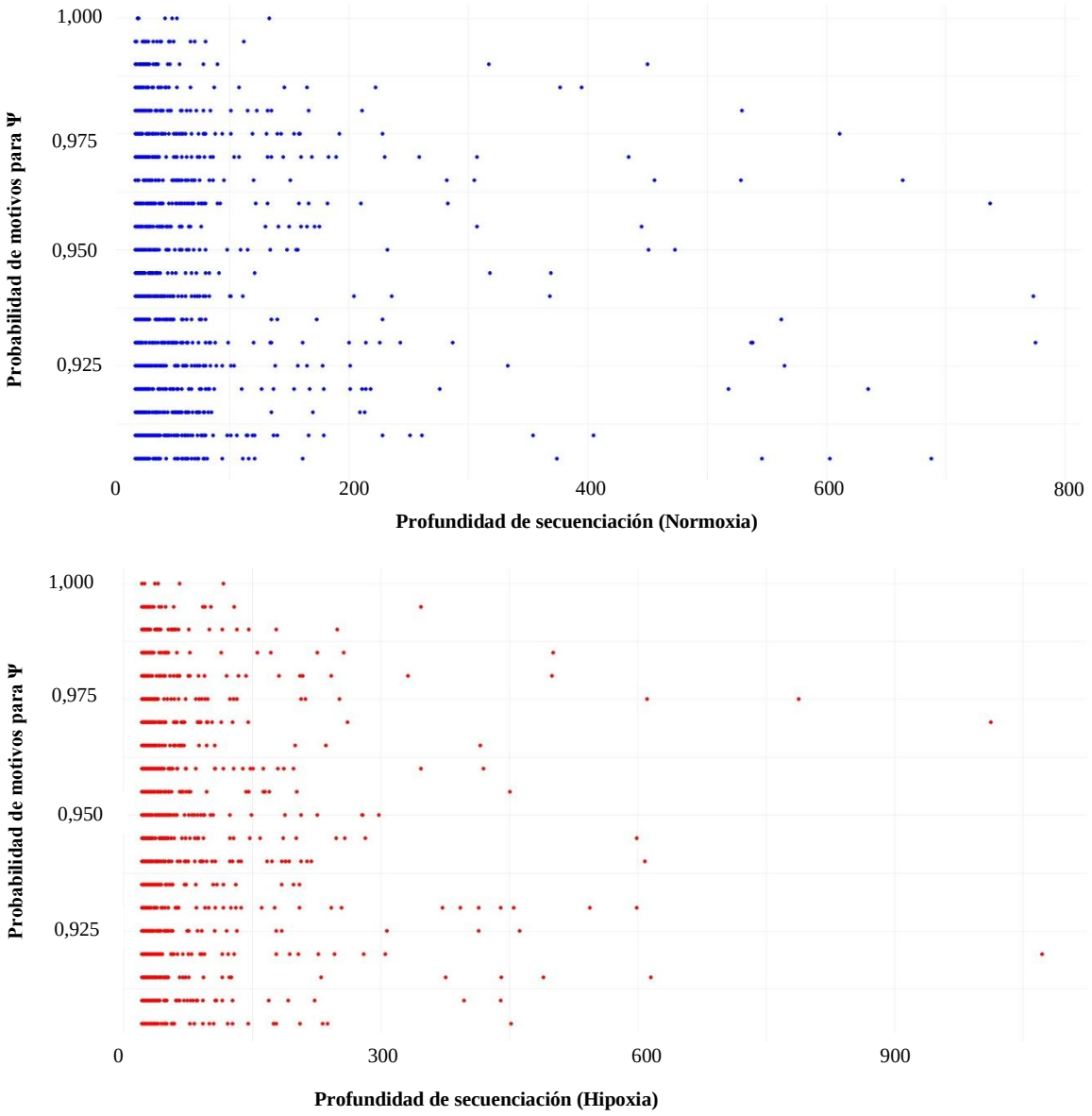

FIGURA 9. Relación entre la profundidad de secuenciación y la probabilidad de detección de motivos para sitios de pseudouridina (Ψ) en condiciones de normoxia e hipoxia en *M. chilensis*. Los gráficos de dispersión ilustran la asociación entre la profundidad de lectura (eje X) y la probabilidad de detección de motivos (eje Y) en transcritos modificados con pseudouridina, identificados mediante secuenciación directa de ARN. (A) Las muestras normóxicas (azul) presentan una alta densidad de motivos con probabilidades de modificación consistentemente elevadas a lo largo de un amplio rango de profundidades de secuenciación. (B) Las muestras hipóxicas (rojo) muestran una distribución global comparable, aunque con una mayor dispersión en profundidades bajas, lo que sugiere una variabilidad dependiente de la condición en la detección de motivos de pseudouridina.

Bajo condiciones de hipoxia, la distribución general fue comparable, aunque se registró una mayor dispersión en los niveles de baja profundidad de secuenciación. A pesar de esta variabilidad, las probabilidades de detección de motivos permanecieron consistentemente elevadas, cercanas a 1,0 en la mayoría de los casos, lo que confirma la solidez del procedimiento analítico aplicado. En conjunto, los resultados señalan que la probabilidad de detección de motivos de pseudouridina es altamente robusta frente a variaciones en la profundidad de lectura, aportando respaldo a la fiabilidad de la identificación de modificaciones epitranscriptómicas en transcritos con representación diferencial bajo condiciones ambientales contrastantes.

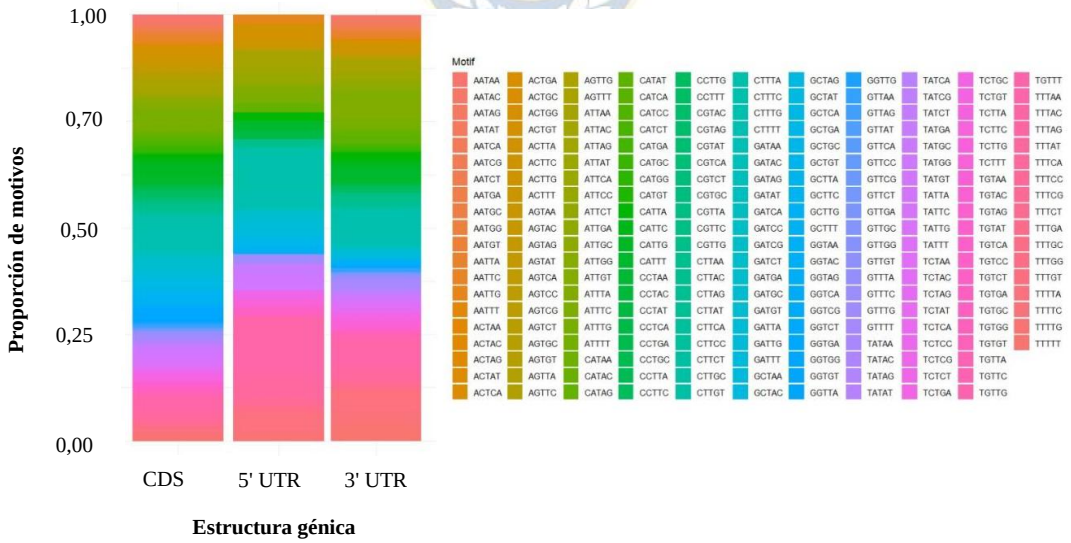

FIGURA 10. Relación entre la estructura génica y la distribución de motivos en *M. chilensis* bajo condiciones normóxicas. El gráfico de barras apiladas normalizadas representa la proporción relativa de motivos de pseudouridina (Ψ) detectados en diferentes regiones estructurales del ARN mensajero: CDS, 5' UTR y 3' UTR. Cada segmento de color dentro de las barras indica un motivo específico, y la altura relativa

de cada segmento refleja su frecuencia proporcional dentro de la estructura correspondiente.

El análisis de distribución proporcional de motivos de pseudouridina en diferentes estructuras génicas reveló una alta homogeneidad composicional entre regiones codificantes (CDS) y regiones no traducidas (5'UTR y 3'UTR). La representación gráfica mediante barras apiladas normalizadas permitió visualizar las proporciones relativas de motivos identificados en cada categoría estructural, indicando una distribución amplia y compartida de secuencias modificadas en todas las regiones analizadas.

Las regiones CDS y 3'UTR presentaron la mayor diversidad de motivos, con patrones de color altamente coincidentes, lo que sugiere una distribución funcionalmente redundante de modificaciones Ψ en segmentos tanto codificantes como post-traduccionales. La categoría 5'UTR, en contraste, mostró una menor diversidad de motivos, posiblemente reflejando restricciones estructurales o selectividad funcional en regiones implicadas en la iniciación de la traducción.

El análisis estadístico mediante prueba de independencia Chi-cuadrado no arrojó diferencias significativas en la composición de motivos entre las estructuras génicas ($p = 0,4853$), lo que respalda la hipótesis de una distribución no estructuralmente preferencial de los motivos de pseudouridina. Este patrón sugiere que la deposición de Ψ podría estar regulada de forma contexto-independiente, o bien que múltiples estructuras funcionales comparten mecanismos comunes de modificación epitranscriptómica.

Discusión

Los resultados de este estudio proporcionan la primera evidencia sistemática de una reprogramación epitranscriptómica inducida por hipoxia en *M. chilensis*, abarcando las principales modificaciones químicas del ARN: N6-metiladenosina (m^6A), 5-metilcitosina (m^5C) y pseudouridina (Ψ). Esta caracterización revela una plasticidad molecular altamente sensible al estado redox del entorno, con implicancias funcionales relevantes para la regulación postranscripcional en bivalvos marinos no modelo.

Uno de los hallazgos más notables es la redistribución diferencial de sitios m^6A bajo hipoxia, con un enriquecimiento significativo de motivos como GGACA, AGACT y GGACC. Este resultado se asemeja a otras investigaciones en donde entre las metilaciones de ARN detectadas, la abundancia de m^6A del motivo GGACA fue la más alta, seguida de GGACC y AGACT (Xu et al., 2023). En bivalvos, si bien las enzimas writer-reader-eraser no han sido plenamente caracterizadas, nuestros datos sugieren que *M. chilensis* podría contar con ortólogos funcionales capaces de inducir una remodelación epitranscriptómica dependiente del ambiente.

La observación de una mayor frecuencia de modificaciones m^6A en regiones estructurales funcionalmente relevantes —como CDS y 3′ UTR— bajo hipoxia, refuerza la noción de un control fino sobre la eficiencia de traducción, estabilidad del ARNm y localización subcelular. Estudios recientes han descrito una nueva vía de degradación del ARNm que depende del m^6A en la secuencia codificante del ARNm (CDS) (Zlotorynski, 2025). En este contexto, el patrón observado en *M. chilensis* sugiere una posible estrategia de priorización funcional mediada por metilación.

En paralelo, la modificación m^5C se mantuvo relativamente estable entre condiciones, lo que sugiere un rol más constitutivo que adaptativo, posiblemente asociado al mantenimiento de la integridad transcripcional y la homeostasis génica básica. Este hallazgo difiere de estudios en peces donde m^5C es upregulated en condiciones de hipoxia (Li et al., 2022). Asimismo, la plasticidad de m^6A refuerza su rol como marcador dinámico de la respuesta al estrés ambiental.

Respecto a la pseudouridina, los resultados muestran un patrón de deposición homogénea entre estructuras génicas, con ausencia de preferencias estructurales significativas. Esto podría indicar una función global en la estabilización del ARN mensajero o en el mantenimiento de la conformación secundaria, independientemente de la región genómica. Estudios recientes en células humanas han reportado que Ψ puede actuar como modulador estructural bajo condiciones de estrés oxidativo y privación de oxígeno (Luo et al., 2023), lo que sugiere funciones evolutivamente conservadas.

La modulación de la cola poli(A) también constituye un aspecto destacado. Bajo hipoxia se observó un acortamiento significativo de la

longitud media, lo cual se ha asociado en plantas en donde la hipoxia provoca un aumento del número de isoformas de ARNm con extremos 3′ poliadenilados que se mapean en regiones 5′ no traducidas (UTR), intrones y regiones codificadoras de proteínas (de Lorenzo et al., 2017). Esta dinámica sugiere que la hipoxia no solo reconfigura las modificaciones químicas del ARN, sino también los procesos de maduración y degradación postranscripcional, lo que representa un nivel de regulación adicional aún inexplorado en moluscos.

Desde una perspectiva genómica, la redistribución de genes metilados a lo largo de los cromosomas bajo hipoxia sugiere la existencia de zonas reguladoras epitranscriptómicas activadas diferencialmente por el ambiente. Este hallazgo coincide con la noción emergente de "hotspots epitranscriptómicos" observada en animales y plantas (Dominissini et al., 2012; Shen, 2025) donde determinadas regiones cromosómicas concentran modificaciones asociadas a funciones específicas.

En cuanto a la robustez metodológica, la ausencia de correlación significativa entre la profundidad de lectura y la probabilidad de detección de motivos valida la estabilidad del pipeline analítico y

refuerza la reproducibilidad de los resultados. El empleo de secuenciación directa de ARN mediante nanoporo, en combinación con algoritmos como Tombo, Nanocompore y Nanopsu, permitió una detección precisa y contexto-específica de las modificaciones, superando las limitaciones clásicas de métodos indirectos como MeRIP-Seq o m^5C bisulfito.

Sin embargo, el estudio también presenta limitaciones que deben ser abordadas en trabajos futuros. La falta de validación funcional mediante ensayos de ganancia/pérdida de función impide establecer relaciones causales entre modificaciones y expresión génica. Asimismo, la carencia de anotaciones específicas para las enzimas writer/reader/eraser en *M. chilensis* limita la interpretación mecanística, subrayando la necesidad de profundizar en la genómica funcional de especies no modelo. También es importante considerar que, aunque se emplearon umbrales conservadores de detección, la resolución intrínseca de la secuenciación por nanoporo aún puede introducir sesgos en la identificación de sitios con estructuras secundarias complejas.

En conjunto, este estudio amplía el horizonte de la epitranscriptómica ambiental en moluscos marinos, revelando una reprogramación adaptativa del ARN mensajero frente a la hipoxia. La integración de estos hallazgos con datos transcriptómicos, proteómicos y fisiológicos permitirá avanzar hacia una comprensión holística de la plasticidad fenotípica en ambientes costeros vulnerables.

Conclusión

Este estudio constituye la primera caracterización epitranscriptómica integral en *M. chilensis* bajo condiciones controladas de hipoxia, utilizando tecnología de secuenciación directa de ARN por Nanopore. Los resultados obtenidos revelan una reconfiguración epitranscriptómica sustancial asociada al estrés hipóxico, evidenciada por alteraciones en los patrones de metilación m^6A y m^5C, redistribución cromosómica de genes modificados, enriquecimiento específico de motivos nucleotídicos, y una reducción generalizada en la longitud de las colas poli(A), lo cual sugiere una modulación post-transcripcional dependiente del oxígeno ambiental.

La identificación de motivos como GGACA y AGACT como elementos prevalentes bajo hipoxia sugiere que estas secuencias podrían representar sitios funcionalmente relevantes en la regulación adaptativa. Asimismo, la estabilidad de los patrones m^5C frente a la plasticidad observada en m^6A resalta la existencia de mecanismos diferenciales de sensibilidad epitranscriptómica frente a condiciones ambientales adversas. La incorporación del análisis de pseudouridina complementó este panorama, sugiriendo una remodelación estructural adicional del ARN como parte de la respuesta al estrés.

Estos hallazgos no solo expanden el conocimiento actual sobre la regulación post-transcripcional en moluscos bivalvos, sino que también abren nuevas perspectivas para el desarrollo de biomarcadores epitranscriptómicos aplicables en estudios de ecotoxicología, acuicultura sostenible y resiliencia marina frente al cambio climático. En conjunto, esta investigación posiciona a la epitranscriptómica como un componente clave en la comprensión de la biología adaptativa en organismos no modelo sometidos a presiones ambientales emergentes.

DISCUSIÓN

Los resultados obtenidos en esta tesis doctoral consolidan un marco integrador para comprender la respuesta fisiológica, molecular y microbiana de *M. chilensis* frente a condiciones de hipoxia y reoxigenación. Se evidencia una dinámica coordinada entre el hospedador y su microbioma, lo que refuerza la noción del holobionte como unidad funcional de adaptación ecológica, en línea con planteamientos recientes sobre la integración funcional entre genoma y microbioma en organismos acuáticos (Khan et al., 2021)

El presente estudio demuestra, mediante una aproximación multiómica sin precedentes en *M. chilensis*, que la hipoxia no actúa como un estresor aislado, sino como un disruptor sistémico que reconfigura la fisiología del hospedador a través de una interacción dinámica entre su transcriptoma, epitranscriptoma y microbioma. Esta interacción define un fenotipo integrado de tolerancia que trasciende la respuesta individual de cada capa molecular (Wang et al., 2024).

En este sentido, la integración crítica de los resultados revela que la disbiosis inducida por hipoxia (aumento de *Vibrio* y *Aeromonas*) no

puede entenderse de forma aislada, sino en interacción con la reprogramación epitranscriptómica. La pérdida de bacterias mutualistas, como Rhodobacterales, podría intensificar el estrés del retículo endoplasmático (Catta-Preta et al., 2022; Kumar et al., 2020; Li et al., 2021), mientras que la metilación diferencial de m^6A en genes de la vía Toll-like modula la traducción de receptores inmunitarios que responden a señales bacterianas (Karikó et al., 2005; Zong et al., 2021). Esta interdependencia muestra que la hipoxia reestructura simultáneamente rutas metabólicas internas y el diálogo hospedador-microbioma, generando un círculo de retroalimentación negativa que compromete la resiliencia.

La reconfiguración transcriptómica observada en tejidos metabólicamente activos como branquias y glándula digestiva, con una modulación significativa de las vías mTOR y del ciclo del ácido cítrico, es consistente con mecanismos adaptativos descritos en otros bivalvos. En *Mytilus edulis*, por ejemplo, se ha documentado que la hipoxia induce fosforilación reversible de proteínas mitocondriales, facilitando la reorientación del flujo respiratorio y mitigando el estrés oxidativo durante la reoxigenación (Sokolov et al., 2021). Asimismo, se destaca la

capacidad de los mitílidos para modular la expresión génica y activar rutas de depresión metabólica y metabolismo anaerobio, lo que respalda los hallazgos de esta tesis (Tomanek, 2015).

Desde una perspectiva eco-evolutiva, los resultados sugieren que esta plasticidad molecular y microbiana no representa un simple ajuste fisiológico, sino una estrategia adaptativa conservada en la familia Mytilidae. La plasticidad fenotípica observada en *M. chilensis* puede considerarse un mecanismo de resiliencia evolutiva, donde el holobionte (hospedador + microbioma) actúa como unidad de selección bajo escenarios de hipoxia recurrente, contribuyendo a explicar su éxito en ecosistemas costeros variables. Estudios comparativos en especies vegetales como *Solanum habrochaites* también han demostrado que la adaptación a la hipoxia implica una reprogramación transcripcional y proteómica orientada a la flexibilidad metabólica y la homeostasis energética, lo que sugiere que estos mecanismos podrían estar conservados evolutivamente en distintos reinos biológicos (Zhang et al., 2025).

En cuanto a la regulación epitranscriptómica, los resultados adquieren especial relevancia al revelar modificaciones como m^6A, m^5C y pseudouridinas, junto con una correlación entre la longitud de la cola poli(A) y los niveles de expresión génica. Estos hallazgos sugieren que la regulación post-transcripcional constituye un eje crítico para la respuesta rápida al estrés (Hernández-Elvira & Sunnerhagen, 2022).

La metilación diferencial de m^6A, particularmente el enriquecimiento de motivos GGACA, GGACC y AGACT en condiciones de hipoxia, sugiere la existencia de un código de metilación hipoxia-dependiente. Este código probablemente regula la estabilidad y traducción de transcritos claves involucrados en la apoptosis (e.g., caspasas), la autofagia y el estrés del retículo endoplasmático, amortiguando así los efectos deletéreos de la hipoxia a nivel postranscripcional (Cai et al., 2025). Además, la significativa reducción en la longitud de la cola poli(A) bajo hipoxia refuerza este hallazgo, indicando una activación global de mecanismos de decaimiento del ARNm para reconfigurar rápidamente el proteoma celular sin un coste energético transcripcional elevado (Wang et al., 2021).

Esta plasticidad reguladora ha sido reportada en *Apostichopus japonicus*, donde la hipoxia combinada con temperatura elevada induce una reprogramación epitranscriptómica en genes antioxidantes e inmunológicos (Wang et al., 2025). Además, estudios recientes han demostrado que la epitranscriptómica modula la respuesta al estrés térmico en peces (Jiang et al., 2025), y que tecnologías como Nanopore permiten detectar una amplia gama de modificaciones post-transcripcionales con alta resolución (Vujaklija et al., 2024). Estos datos refuerzan la idea de que la epitranscriptómica es una estrategia conservada en organismos acuáticos para enfrentar fluctuaciones ambientales.

Desde el punto de vista microbiológico, la alteración de la microbiota inducida por hipoxia en *M. chilensis* se alinea con investigaciones en *Mytilus coruscus*, donde estresores combinados como acidificación, temperatura elevada e hipoxia provocan una alteración profunda del microbioma intestinal (Khan et al., 2021).

En este estudio, se observó una disbiosis caracterizada por el declive de comensales mutualistas como Rhodobacterales—cruciales en

el ciclado de nutrientes y la síntesis de vitaminas—y la proliferación de patógenos oportunistas como *Vibrio* y *Aeromonas*. Esta disbiosis no es meramente una consecuencia pasiva, sino un factor activo que exacerba el estado de estrés. La pérdida de funciones microbianas inferidas, especialmente aquellas relacionadas con el metabolismo de aminoácidos y la biosíntesis de cofactores, probablemente priva al hospedador de metabolitos esenciales precisamente cuando más los necesita, creando un círculo vicioso de disfunción metabólica e inmunosupresión (Ingala et al., 2021; Liu et al., 2023; Murga-Garrido et al., 2023).

La relación entre disbiosis e inmunidad es crítica, como lo demuestran investigaciones que reportan que la hipoxia en vertebrados genera un desorden metabólico y compromete la función inmune, aumentando la susceptibilidad a enfermedades (Villareal & Xue, 2024; Zhang et al., 2022)

A nivel ecológico y evolutivo, estudios sobre diferenciación genética en genes inmunológicos y metabólicos entre poblaciones silvestres y de cultivo de *M. chilensis* aportan una perspectiva complementaria (Yévenes et al., 2022). Esta variabilidad

interpoblacional sugiere que los resultados transcriptómicos y microbiológicos podrían estar modulados por el origen genético de las poblaciones, lo que debe ser considerado en futuras investigaciones. Además, una revisión sistemática reciente sobre la sensibilidad de la familia Mytilidae a estresores ambientales combinados (Rynkowski et al., 2025) contextualiza la relevancia de los mecanismos adaptativos identificados en esta tesis. La plasticidad del transcriptoma y del microbioma de *M. chilensis* podría explicar su resiliencia relativa frente a perturbaciones ambientales, sugiriendo la existencia de mecanismos compensatorios que favorecen su supervivencia en escenarios de cambio climático (Ross et al., 2023).

La integración de los resultados obtenidos permite proponer un modelo conceptual unificado en el que la exposición cíclica y prolongada a episodios de hipoxia seguidos de reoxigenación desencadena una repriorización epitranscriptómica en el hospedador, orientada a optimizar la supervivencia celular. Esta reprogramación molecular conlleva una respuesta inmunometabólica compensatoria, caracterizada por la supresión de vías inmunológicas de alta demanda energética y por una modificación estructural en la composición del microbioma (Burnett

& Burnett, 2022; Sui et al., 2017; Zhan et al., 2022). En este contexto, se favorece la selección de comunidades microbianas más anaerobias y con menor grado de mutualismo (Golub et al., 2024). La disfunción microbiana resultante intensifica el estrés fisiológico del organismo, comprometiendo su homeostasis y afectando negativamente su salud a largo plazo (Miro-Blanch & Yanes, 2019). Esta interacción dinámica y bidireccional entre el hospedador y su microbiota, bajo condiciones sostenidas de estrés oxidativo y restricción energética, emerge como un eje central en los mecanismos de resiliencia ambiental observados en bivalvos (Balbi et al., 2021).

Si bien este estudio sienta las bases transcriptómicas, epitranscriptómicas y microbiológicas de la respuesta al estrés, un marco verdaderamente integrador del holobionte requiere la incorporación de capas ómicas adicionales. Estudios futuros deberían dirigirse hacia una aproximación multiómica que incluya la epigenómica, para descifrar los mecanismos de memoria transcripcional a largo plazo inducidos por la hipoxia (Brown & Rupert, 2014; Leung et al., 2013); la proteómica, para validar funcionalmente los cambios observados a nivel de ARN y cuantificar las respuestas enzimáticas clave (Kim et al., 2025); y la

metabolómica, para caracterizar el perfil de metabolitos resultante y cerrar la brecha entre la expresión génica y el fenotipo fisiológico final (Yang et al., 2023). La integración de estos datos mediante enfoques de biología de sistemas permitiría modelar las redes de regulación del holobionte en su totalidad, identificando nodos críticos de resiliencia.

Además, futuros estudios deberían incorporar tecnologías de célula única (single-cell y single-nucleus RNA-seq), capaces de resolver la heterogeneidad celular en tejidos clave como branquias y glándula digestiva (Denisenko et al., 2020; Jin et al., 2025). Este enfoque permitiría identificar subpoblaciones celulares con distinta sensibilidad a la hipoxia, mapear circuitos inmunometabólicos específicos y descubrir células centinela responsables de coordinar la respuesta del holobionte. Integrar estos datos con otras capas ómicas abriría la posibilidad de construir atlas celulares de resiliencia en bivalvos, recurso estratégico para la investigación básica y la acuicultura adaptativa.

Más allá de su valor en la investigación básica, los resultados de esta tesis presentan implicancias directas para la acuicultura sostenible. Las firmas epitranscriptómicas identificadas, como los motivos GGACA

y GGACC, podrían ser utilizadas como biomarcadores tempranos de estrés hipóxico en sistemas de monitoreo ambiental. A largo plazo, la caracterización funcional de las enzimas writers y erasers de m^{6}A en *M. chilensis* abre la posibilidad de desarrollar estrategias nutracéuticas o programas de selección genética orientados a promover individuos con respuestas epitranscriptómicas más resilientes (Pilala et al., 2025). De forma complementaria, la manipulación específica del microbioma mediante consorcios probióticos diseñados —por ejemplo, formulaciones orientadas a la reposición de bacterias del orden Rhodobacterales— (Zhao et al., 2025) se perfila como una estrategia prometedora de manejo microbiológico para mitigar la disbiosis inducida por hipoxia y optimizar la productividad en condiciones de oxigenación fluctuante.

De igual modo, la aplicación de técnicas de enriquecimiento para modificaciones epitranscriptómicas, la validación funcional de genes clave mediante herramientas como CRISPR-Cas9, y el uso de metagenómica shotgun para una caracterización funcional más profunda del microbioma, representan pasos lógicos para avanzar en la comprensión del holobionte (Sandoval-Quintana et al., 2023; Sarkar et

al., 2021; Yang et al., 2025). Asimismo, la evaluación de estresores múltiples y la comparación entre poblaciones genéticamente diferenciadas permitirán extrapolar los resultados a contextos ecológicos más amplios y robustos.

En conjunto, esta investigación demuestra que la resiliencia de *M. chilensis* frente a la hipoxia es una propiedad emergente del holobionte, resultado de interacciones dinámicas entre la expresión génica del hospedador, la regulación epitranscriptómica y la composición de su microbioma. Estos hallazgos no solo profundizan la comprensión de los mecanismos moleculares y ecológicos que sustentan la adaptación de los bivalvos, sino que también proporcionan un marco conceptual robusto y herramientas técnicas aplicables al desarrollo de estrategias de manejo sostenible en acuicultura, especialmente en el contexto de creciente presión ambiental derivada del cambio climático.

CONCLUSIÓN

La presente tesis doctoral abordó de manera integral la respuesta fisiológica y molecular del molusco bivalvo *M. chilensis* frente al estrés por hipoxia y posterior reoxigenación, mediante un enfoque multiescala que integró análisis transcriptómicos, epitranscriptómicos y microbiológicos. Los resultados obtenidos permiten delinear un modelo de afectación sistémica que compromete tanto al hospedador como a sus comunidades microbianas asociadas, consolidando el concepto de holobionte como unidad funcional de estudio en contextos de estrés ambiental.

En el primer capítulo, se evidenció una notable plasticidad transcriptómica en tejidos clave —branquias, glándula digestiva y músculo aductor— bajo condiciones de hipoxia prolongada. La modulación de rutas metabólicas centrales, como el ciclo de Krebs, junto con la regulación de vías de señalización asociadas a mTOR y apoptosis, sugiere una estrategia adaptativa orientada a la conservación energética y a la inmunosupresión sistémica. Estos hallazgos revelan una priorización funcional por parte del hospedador destinada a optimizar su supervivencia en entornos adversos.

El segundo capítulo demostró que estas alteraciones fisiológicas se correlacionan con una disbiosis microbiana significativa. El análisis del microbioma, mediante secuenciación del gen 16S rRNA, evidenció una transición hacia comunidades dominadas por anaerobios facultativos, acompañada de una disminución de taxa comensales beneficiosos como *Rhodobacterales*, y un aumento en la abundancia de géneros patógenos oportunistas como *Vibrio* y *Aeromonas*. Este desequilibrio compromete la funcionalidad del holobionte, afectando negativamente procesos metabólicos e inmunológicos esenciales.

En el tercer capítulo, la aplicación de secuenciación directa de ARN mediante tecnología Nanopore permitió una caracterización sin precedentes de la regulación génica post-transcripcional. La identificación de modificaciones epitranscriptómicas como m^5C, m^6A y pseudouridinas, junto con la correlación entre la longitud de la cola poli(A) y los niveles de expresión génica, resalta el rol central de la epitranscriptómica en la respuesta rápida de *M. chilensis* frente a condiciones hipóxicas. Además, se generó un catálogo funcionalmente

anotado de transcritos, constituyendo un recurso bioinformático de alto valor para investigaciones futuras en genómica funcional de bivalvos.

En conjunto, esta investigación demuestra que la resiliencia de *M. chilensis* frente a la hipoxia constituye una propiedad emergente del holobionte, resultado de interacciones dinámicas entre la expresión génica del hospedador y la estructura de su microbioma. Los hallazgos aquí presentados no solo profundizan en la comprensión de los mecanismos moleculares y ecológicos que subyacen a la adaptación de los bivalvos, sino que también proporcionan un marco conceptual robusto y herramientas técnicas aplicables al desarrollo de estrategias de manejo sostenible en acuicultura, particularmente en un escenario de creciente presión ambiental asociada al cambio climático.

REFERENCIAS

.

Adli, M., Merkhofer, E., Cogswell, P., & Baldwin, A. (2010). IKKalpha and IKKbeta each function to regulate NF-kappaB activation in the TNF-induced/canonical pathway. *PloS one*, *5*(2), 1-7. https://doi.org/10.1371/journal.pone.0009428

Adzigbli, L., Ponsuksili, S., & Sokolova, I. (2024). Mitochondrial responses to constant and cyclic hypoxia depend on the oxidized fuel in a hypoxia-tolerant marine bivalve *Crassostrea gigas*. *Scientific Reports*, *14*(1), 1-15. https://doi.org/10.1038/s41598-024-60261-w

Adzigbli, L., Sokolov, E., Ponsuksili, S., & Sokolova, I. (2022). Tissue- and substrate-dependent mitochondrial responses to acute hypoxia-reoxygenation stress in a marine bivalve (*Crassostrea gigas*). *Journal of Experimental Biology*, *225*(1), 1-13. https://doi.org/10.1242/jeb.243304

Akalin, A., Kormaksson, M., Li, S., Garrett-Bakelman, F., Figueroa, M., Melnick, A., & Mason, C. (2012). methylKit: a comprehensive R package for the analysis of genome-wide DNA methylation profiles. *Genome Biology*, *13*(10), 1-9. https://doi.org/10.1186/gb-2012-13-10-R87

Aleksander, S., Balhoff, J., Carbon, S., Cherry, J., Drabkin, H., Ebert, D.,…Westerfield, M. (2023). The Gene Ontology knowledgebase in 2023. *Genetics*, *224*(1), 1-14. https://doi.org/10.1093/genetics/iyad031

Alkhammash, A. (2025). Pharmacology of epitranscriptomic modifications: Decoding the therapeutic potential of RNA modifications in drug resistance. *European Journal of Pharmacology*, *994*, 1-19. https://doi.org/10.1016/j.ejphar.2025.177397

Alonso, A., Pérez, M., Vidal, Z., & Vidal, A. (2016). Papel de la reprogramación metabólica en la carcinogénesis. *Correo Científico Médico*, *20*, 292-304.

Altschul, S., Madden, T., Schaffer, A., Zhang, J., Zhang, Z., Miller, W., & Lipman, D. (1998). Gapped BLAST and PSI-BLAST: A new generation of protein database search programs. *Nucleic Acids Research*, *12*(8), 3389-3402. https://doi.org/10.1093/nar/25.17.3389

Amorim, K., Piontkivska, H., Zettler, M., Sokolov, E., Hinzke, T., Nair, A., & Sokolova, I. (2021). Transcriptional response of key metabolic and stress response genes of a nuculanid bivalve, *Lembulus bicuspidatus* from an oxygen minimum zone exposed to hypoxia-reoxygenation [Article]. *Comparative Biochemistry and Physiology B-Biochemistry & Molecular Biology*, *256*, 1-9, Article 110617. https://doi.org/10.1016/j.cbpb.2021.110617

Angelo, A., Rovere-Querini, P., Clementi, S., & Clementi, B. (2008). Cell Death: Tipping the Balance of Autoimmunity and Tissue Repair. *Current Pharmaceutical Design*, *14*(3), 269-277. https://doi.org/10.2174/138161208783413275

Antunes, F., Erustes, A., Costa, A., Nascimento, A., Bincoletto, C., Ureshino, R.,…Smaili, S. (2018). Autophagy and intermittent fasting: the connection for cancer therapy? *Clinics (Sao Paulo, Brazil)*, *73*(1), 1-7. https://doi.org/10.6061/clinics/2018/e814s

Babarro, J., & De Zwaan, A. (2008). Anaerobic survival potential of four bivalves from different habitats. A comparative survey. *Comparative Biochemistry and Physiology Part A: Molecular & Integrative Physiology*, *151*(1), 108-113. https://doi.org/https://doi.org/10.1016/j.cbpa.2008.06.006

Bakun, A., Black, B., Bograd, S., García-Reyes, M., Miller, A., Rykaczewski, R., & Sydeman, W. (2015). Anticipated Effects of Climate Change on Coastal Upwelling Ecosystems. *Current Climate Change Reports*, *1*(2), 85-93. https://doi.org/10.1007/s40641-015-0008-4

Balbi, T., Auguste, M., Ciacci, C., & Canesi, L. (2021). Immunological Responses of Marine Bivalves to Contaminant Exposure: Contribution of the -Omics Approach. *Frontiers in Immunology*, *12*, 1-11. https://doi.org/10.3389/fimmu.2021.618726

Bateman, A., Martin, M., Orchard, S., Magrane, M., Ahmad, S., Alpi, E.,…UniProt, C. (2022). UniProt: the Universal Protein Knowledgebase in 2023. *Nucleic Acids Research*, *51*, D523–D531. https://doi.org/10.1093/nar/gkac1052

Beckerman, A., Childs, D., & Petchey, O. (2017). *Data Management, Manipulation, and Exploration with dplyr* [Article; Book Chapter]. Oxford University Press. https://doi.org/10.1093/acprof:oso/9780198787839.003.0003

Beleneva, I., Zhukova, N., & Maslennikova, E. (2003). Comparative study of microbial communities from cultured and natural populations of the mussel *Mytilus trossulus* in Peter the Great Bay. *Microbiology*, *72*(4), 472-477. https://doi.org/10.1023/A:1025005025620

Bell, G., & Eggleston, D. (2005). Species-specific avoidance responses by blue crabs and fish to chronic and episodic hypoxia. *Marine Biology*, *146*(4), 761-770. https://doi.org/10.1007/s00227-004-1483-7

Bianchi, T., Arndt, S., Austin, W., Benn, D., Bertrand, S., Cui, X.,…Syvitski, J. (2020). Fjords as Aquatic Critical Zones (ACZs). *Earth-Science Reviews*, *203*, 1-25. https://doi.org/https://doi.org/10.1016/j.earscirev.2020.103145

Blanc, J., Molinet, C., Subiabre, R., & Díaz, P. (2018). Cadmium determination in Chilean blue mussels *Mytilus chilensis*: Implications for environmental and agronomic interest. *Marine Pollution Bulletin*, *129*(2), 913-917. https://doi.org/10.1016/j.marpolbul.2017.10.048

Boccaletto, P., Machnicka, M., Purta, E., Piatkowski, P., Baginski, B., Wirecki, T.,…Bujnicki, J. (2018). MODOMICS: a database of RNA modification pathways. 2017 update. *Nucleic Acids Research*, *46*(D1), D303-D307. https://doi.org/10.1093/nar/gkx1030

Bonenfant, Q., Noé, L., & Touzet, H. (2023). Porechop_ABI: discovering unknown adapters in Oxford Nanopore Technology sequencing reads for downstream trimming. *Bioinformatics Advances*, *3*(1), 1-4. https://doi.org/10.1093/bioadv/vbac085

Boo, S., & Kim, Y. (2020). The emerging role of RNA modifications in the regulation of mRNA stability. *Experimental and Molecular Medicine*, *52*(3), 400-408. https://doi.org/10.1038/s12276-020-0407-z

Borenfreund, E., & Puerner, J. (1985). Toxicity determined in vitro by morphological alterations and neutral red absorption. *Toxicology Letters*, *24*(2), 119-124. https://doi.org/10.1016/0378-4274(85)90046-3

Borkovic-Mitic, S., Pavlovic, S., Perendija, B., Despotovic, S., Gavric, J., Gacic, Z., & Saicic, Z. (2013). Influence of some metal concentrations on the activity of antioxidant enzymes and concentrations of vitamin E and SH-groups in the digestive gland and gills of the freshwater bivalve *Unio tumidus* from the Serbian part of Sava River. *Ecological Indicators, 32*, 212-221. https://doi.org/10.1016/j.ecolind.2013.03.024

Bouallegui, Y. (2019). Immunity in mussels: An overview of molecular components and mechanisms with a focus on the functional defenses. *Fish & Shellfish Immunology*, *89*, 158-169. https://doi.org/https://doi.org/10.1016/j.fsi.2019.03.057

Breitburg, D., Hondorp, D., Audemard, C., Carnegie, R., Burrell, R., Trice, M., & Clark, V. (2015). Landscape-Level Variation in Disease Susceptibility Related to Shallow-Water Hypoxia. *Plos One*, *10*(2), 1-27. https://doi.org/10.1371/journal.pone.0116223

Breitburg, D., Levin, L. A., Oschlies, A., Grégoire, M., Chavez, F. P., Conley, D. J.,…Zhang, J. (2018). Declining oxygen in the global ocean and coastal waters. *Science*, *359*(6371), 1-11. https://doi.org/10.1126/science.aam7240

Brown, C., & Rupert, J. (2014). Hypoxia and Environmental Epigenetics. *High Altitude Medicine & Biology*, *15*(3), 323-330. https://doi.org/10.1089/ham.2014.1016

Burnett, K., & Burnett, L. (2022). Immune Defense in Hypoxic Waters: Impacts of CO_2 Acidification. *Biological Bulletin*, *243*(2), 120-133. https://doi.org/10.1086/721322

Cai, J., Wang, X., Wang, Z., Sheng, S., Tang, F., & Zhang, Z. (2025). ZC3H13-Mediated m^6A Modification Ameliorates Acute Myocardial Infarction through Preventing Inflammation, Oxidative Stress and Ferroptosis by Targeting lncRNA93358. *Inflammation*, *48*(3), 1270-1284. https://doi.org/10.1007/s10753-024-02116-0

Calle, X., Jiménez-Gallegos, D., Muñoz-Córdova, F., Sánchez, P., & Lavandero, S. (2019). Mecanismo sensor y de adaptación a los niveles de oxígeno y su implicancia en las enfermedades cardiovasculares: a propósito del Premio Nobel de Fisiología-Medicina 2019. *Revista chilena de cardiología*, *38*, 225-235.

Calvete, C., & Sobarzo, M. (2011). Quantification of the surface brackish water layer and frontal zones in southern Chilean fjords between Boca del Guafo (43°30′S) and Estero Elefantes (46°30′S). *Continental Shelf Research*, *31*(3-4), 162-171. https://doi.org/10.1016/j.csr.2010.09.013

Capet, A., Beckers, J., & Grégoire, M. (2013). Drivers, mechanisms and long-term variability of seasonal hypoxia on the Black Sea northwestern shelf – is there any recovery after eutrophication? *Biogeosciences*, *10*(6), 3943-3962. https://doi.org/10.5194/bg-10-3943-2013

Carella, F., Feist, S., Bignell, J., & De Vico, G. (2015). Comparative pathology in bivalves: Aetiological agents and disease processes. *Journal of Invertebrate Pathology*, *131*, 107-120. https://doi.org/10.1016/j.jip.2015.07.012

Carlile, T., Rojas-Duran, M., Zinshteyn, B., Shin, H., Bartoli, K., & Gilbert, W. (2014). Pseudouridine profiling reveals regulated mRNA pseudouridylation in yeast

and human cells. *Nature*, *515*(7525), 143-159. https://doi.org/10.1038/nature13802

Carvajal, C. (2019). Especies reactivas del oxígeno: formación, funcion y estrés oxidativo. *Medicina Legal de Costa Rica*, *36*, 91-100.

Caspi, R., Billington, R., Ferrer, L., Foerster, H., Fulcher, C., Keseler, I.,…Karp, P. (2016). The MetaCyc database of metabolic pathways and enzymes and the BioCyc collection of pathway/genome databases. *Nucleic Acids Research*, *44*, D471-D480. https://doi.org/10.1093/nar/gkv1164

Catta-Preta, C., de Azevedo-Martins, A., de Souza, W., & Motta, M. (2022). Effect of the endoplasmic reticulum stressor tunicamycin in *Angomonas deanei* heat-shock protein expression and on the association with the endosymbiotic bacterium. *Experimental Cell Research*, *417*(1), 1-10. https://doi.org/10.1016/j.yexcr.2022.113162

Cavallo, R., Acquaviva, M., & Stabili, L. (2009). Culturable heterotrophic bacteria in seawater and *Mytilus galloprovincialis* from a Mediterranean area (Northern Ionian Sea-Italy). *Environmental Monitoring and Assessment*, *149*(1-4), 465-475. https://doi.org/10.1007/s10661-008-0223-8

Cerda, M., Knoppers, B., Valdés, J., Fettah, A., Ortlieb, L., & Sabadini-Santos, E. (2010). Variación espacial y temporal de las masas de agua, nutrientes y sedimentación de la materia orgánica e inorgánica en la bahía Mejillones del sur (23° S), Chile. *Revista chilena de historia natural*, *83*, 409-420.

Cerneckis, J., Ming, G., Song, H., He, C., & Shi, Y. (2024). The rise of epitranscriptomics: recent developments and future directions. *Trends in Pharmacological Sciences*, *45*(1), 24-38. https://doi.org/10.1016/j.tips.2023.11.002

Cheng, H., Peng, Z., Zhao, C., Jin, H., Bao, Y., & Liu, M. (2024). The transcriptomic and biochemical responses of blood clams (*Tegillarca granosa*) to prolonged intermittent hypoxia [Article]. *Comparative Biochemistry and Physiology B-Biochemistry & Molecular Biology*, *270*, Article 110923. https://doi.org/10.1016/j.cbpb.2023.110923

Chokkalla, A., Mehta, S., & Vemuganti, R. (2020). Epitranscriptomic regulation by m^6A RNA methylation in brain development and diseases. *Journal of Cerebral Blood Flow and Metabolism*, *40*(12), 2331-2349. https://doi.org/10.1177/0271678X20960033

Choumiline, K., Pérez-Cruz, L., Gray, A., Bates, S., & Lyons, T. (2019). Scenarios of Deoxygenation of the Eastern Tropical North Pacific During the Past Millennium as a Window Into the Future of Oxygen Minimum Zones. *Frontiers in Earth Science*, *7*, 1-23. https://doi.org/10.3389/feart.2019.00237

Chu, J., Curkan, C., & Tunnicliffe, V. (2018). Drivers of temporal beta diversity of a benthic community in a seasonally hypoxic fjord. *Royal Society Open Science*, *5*(4), 1-18. https://doi.org/10.1098/rsos.172284

Clark, M., Husmann, G., Thorne, M., Burns, G., Truebano, M., Peck, L.,…Philipp, E. (2013). Hypoxia impacts large adults first: consequences in a warming world. *Global Change Biology*, *19*(7), 2251-2263. https://doi.org/10.1111/gcb.12197

Conley, D., Carstensen, J., Vaquer-Sunyer, R., & Duarte, C. (2009). Ecosystem thresholds with hypoxia. *Hydrobiologia*, *629*(1), 21-29. https://doi.org/10.1007/s10750-009-9764-2

Cossío-Bayúgar, R., Miranda-Miranda, E., Aguilar-Díaz, H., Narváez-Padilla, V., & Reynaud, E. (2024). Transcriptomic dataset of the development and maturation of the *Rhipicephalus microplus* ovary. *Data in Brief*, *55*, 1-11. https://doi.org/10.1016/j.dib.2024.110661

Cui, Z., Cui, Y., Zang, T., & Wang, Y. (2021). Genome analysis interacCircos: an R package based on JavaScript libraries for the generation of interactive circos plots. *Bioinformatics*, *37*(20), 3642-3644. https://doi.org/10.1093/bioinformatics/btab232

Curry, K., Wang, Q., Nute, M., Tyshaieva, A., Reeves, E., Soriano, S.,…Treangen, T. (2022). Emu: species-level microbial community profiling of full-length 16S rRNA Oxford Nanopore sequencing data. *Nature Methods*, *19*(7), 845-853. https://doi.org/10.1038/s41592-022-01520-4

Cáceres, M., Valle-Levinson, A., Sepúlveda, H., & Holderied, K. (2002). Transverse variability of flow and density in a Chilean fjord. *Continental Shelf Research*, *22*(11-13), 1683-1698.

Daneri, G., Montero, P., Lizárraga, L., Torres, R., Iriarte, J. L., Jacob, B.,…Tapia, F. J. (2012). Primary Productivity and heterotrophic activity in an enclosed marine area of central Patagonia (Puyuhuapi channel; 44° S, 73° W). *Biogeosciences Discuss.*, *2012*, 5929-5968. https://doi.org/10.5194/bgd-9-5929-2012

de Lorenzo, L., Sorenson, R., Bailey-Serres, J., & Hunt, A. (2017). Noncanonical Alternative Polyadenylation Contributes to Gene Regulation in Response to Hypoxia. *Plant Cell*, *29*(6), 1262-1277. https://doi.org/10.1105/tpc.16.00746

Denisenko, E., Guo, B., Jones, M., Hou, R., de Kock, L., Lassmann, T.,…Forrest, A. (2020). Systematic assessment of tissue dissociation and storage biases in single-cell and single-nucleus RNA-seq workflows. *Genome Biology*, *21*(1), 1-25. https://doi.org/10.1186/s13059-020-02048-6

Destoumieux-Garzón, D., Montagnani, C., Dantan, L., Nicolas, N., Travers, M., Duperret, L.,…Escoubas, J. (2024). Cross-talk and mutual shaping between the immune system and the microbiota during an oyster's life [Review]. *Philosophical Transactions of The Royal Society B-Biological Sciences*, *379*, 1-12, Article 20230065. https://doi.org/10.1098/rstb.2023.0065

Deutsch, C., Ferrel, A., Seibel, B., Pörtner, H., & Huey, R. (2015). Climate change tightens a metabolic constraint on marine habitats. *Science*, *348*(6239), 1132-1135. https://doi.org/10.1126/science.aaa1605

Diaz, R. (2001). Overview of Hypoxia around the World. *Journal of Environmental Quality*, *30*(2), 275-281. https://doi.org/https://doi.org/10.2134/jeq2001.302275x

Diaz, R., & Rosenberg, R. (1995). Marine benthic hypoxia: A review of its ecological effects and the behavioral responses of benthic macrofauna. *Oceanography and Morine Biology: an Annual Review*, *33*, 245-303.

Diaz, R., & Rosenberg, R. (2008). Spreading Dead Zones and Consequences for Marine Ecosystems. *Science*, *321*(5891), 926-929. https://doi.org/10.1126/science.1156401

Dittami, S., Arboleda, E., Auguet, J., Bigalke, A., Briand, E., Cárdenas, P.,…Not, F. (2021). A community perspective on the concept of marine holobionts: current

status, challenges, and future directions. *Peerj*, *9*, 1-34. https://doi.org/10.7717/peerj.10911

Dixon, P. (2003). VEGAN, a package of R functions for community ecology. *Journal of vegetation science*, *14*(6), 927-930. https://doi.org/10.1111/j.1654-1103.2003.tb02228.x

Dominissini, D., Moshitch-Moshkovitz, S., Schwartz, S., Salmon-Divon, M., Ungar, L., Osenberg, S.,…Rechavi, G. (2012). Topology of the human and mouse m6A RNA methylomes revealed by m^6A-seq. *Nature*, *485*(7397), 201-U284. https://doi.org/10.1038/nature11112

Douglas, G., Maffei, V., Zaneveld, J., Yurgel, S., Brown, J., Taylor, C.,…Langille, M. (2020). PICRUSt2 for prediction of metagenome functions. *Nature Biotechnology*, *38*, 685-688. https://doi.org/10.1038/s41587-020-0548-6

Du, L., Gao, R., & Chen, Z. (2025). 5-Methylcytosine Methylation-Linked Hippo Pathway Molecular Interactions Regulate Lipid Metabolism. *International Journal of Molecular Sciences*, *26*(6), 1-17. https://doi.org/10.3390/ijms26062560

Duarte, C., Conley, D., Carstensen, J., & Sánchez-Camacho, M. (2009). Return to Neverland: Shifting Baselines Affect Eutrophication Restoration Targets. *Estuaries and Coasts*, *32*(1), 29-36. https://doi.org/10.1007/s12237-008-9111-2

Dunkai, T., Bogatyrenko, E., & Kim, A. (2023). Biodiversity and Metabolic Properties of Bacterial Communities from the Digestive System of the Bivalve *Crenomytilus grayanus*. *Microbiology*, *92*(4), 552-563. https://doi.org/10.1134/S0026261723600982

Echeverri, R., & Mockus, S. (2008). Factor nuclear κB (NF-κB): signalosoma y su importancia en enfermedades inflamatorias y cáncer. *Revista de la Facultad de Medicina*, *56*, 133-146.

Escribano, R., Marin, V., & Irribarren, C. (2000). Distribution of *Euphausia mucronata* at the upwelling area of Peninsula Mejillones, northern Chile: The influence of the oxygen minimum layer. *Scientia Marina*, *64*(1), 69-77. https://doi.org/10.3989/scimar.2000.64n169

Essington, T., & Paulsen, C. (2010). Quantifying Hypoxia Impacts on an Estuarine Demersal Community Using a Hierarchical Ensemble Approach. *Ecosystems*, *13*(7), 1035-1048. https://doi.org/10.1007/s10021-010-9372-z

Falfushynska, H., Piontkivska, H., & Sokolova, I. (2020). Effects of intermittent hypoxia on cell survival and inflammatory responses in the intertidal marine bivalves *Mytilus edulis* and *Crassostrea gigas*. *Journal of Experimental Biology*, *223*(4), 1-13. https://doi.org/10.1242/jeb.217026

Fang, I., & Trewyn, B. (2012). Application of mesoporous silica nanoparticles in intracellular delivery of molecules and proteins. *Methods in Enzymology*, *508*, 41-59. https://doi.org/10.1016/b978-0-12-391860-4.00003-3

FAO. (2018). *El estado mundial de la pesca y la acuicultura 2018. Cumplir los objetivos de desarrollo sostenible*. Organización de las Naciones Unidas para la Alimentación y la Agricultura.

Fava, L., Bock, F., Geley, S., & Villunger, A. (2012). Caspase-2 at a glance. *Journal of Cell Science*, *125*(24), 5911-5915. https://doi.org/10.1242/jcs.115105

Follo, C., Vidoni, C., Morani, F., Ferraresi, A., Seca, C., & Isidoro, C. (2019). Amino acid response by Halofuginone in Cancer cells triggers autophagy through proteasome degradation of mTOR. *Cell Communication and Signaling*, *17*(1), 1-18. https://doi.org/10.1186/s12964-019-0354-2

Frye, M., Jaffrey, S., Pan, T., Rechavi, G., & Suzuki, T. (2016). RNA modifications: what have we learned and where are we headed? *Nature Reviews Genetics*(17), 365–372. https://doi.org/10.1038/nrg.2016.47

Frye M., Harada B., Behm, M., & He, C. (2018). RNA modifications modulate gene expression during development. *Science*, *361*(6409), 1346-1349. https://doi.org/10.1126/science.aau1646

Gallardo-Escarate, C., Valenzuela-Munoz, V., Gustavo, N., Valenzuela-Miranda, D., Tapia, F., Yevenes, M.,…Gerdol, M. (2023). Chromosome-Level Genome Assembly of the Blue Mussel *Mytilus chilensis* Reveals Molecular Signatures Facing the Marine Environment. *Genes*, *14*(4), 1-27. https://doi.org/10.3390/genes14040876

García, N., Puentes, O., & Montalvo, J. (2008). Contaminación orgánica en el sector de la Bahía de Buena Vista cercano a la desembocadura de Río Guanó, Villa Clara, Cuba. *Revista Cubana de Química*, *20*(3), 39-46.

Gatsiou, A., & Stellos, K. (2018). Dawn of Epitranscriptomic Medicine. *Circulation-Genomic and Precision Medicine*, *11*(9), 1-15. https://doi.org/10.1161/CIRCGEN.118.001927

Gattuso, J., Magnan, A., Billé, R., Cheung, W., Howes, E., Joos, F.,…Turley, C. (2015). Contrasting futures for ocean and society from different anthropogenic CO_2 emissions scenarios. *Royal Society open science*, *5*(4), 1-18. https://doi.org/10.1126/science.aac4722

Giannetto, A., Maisano, M., Cappello, T., Oliva, S., Parrino, V., Natalotto, A.,…Fasulo, S. (2015). Hypoxia-Inducible Factor α and Hif-prolyl Hydroxylase Characterization and Gene Expression in Short-Time Air-Exposed *Mytilus galloprovincialis* [Article]. *Marine Biotechnology*, *17*(6), 768-781. https://doi.org/10.1007/s10126-015-9655-7

Gilbert, W., Bell, T., & Schaening, C. (2016). Messenger RNA modifications: Form, distribution, and function. *Science*, *352*(6292), 1408-1412. https://doi.org/10.1126/science.aad8711

Golub, N., Soldatov, A., Ryabushko, V., Kuznetsov, A., Kurchenko, V., & Budkevich, E. (2024). Effect of Hypoxia on Amino Acid Content in Hemolymph and Protein Hydrolysate of the Bivalve Mollusk *Anadara kagoshimensis*. *Journal of Evolutionary Biochemistry and Physiology*, *60*(1), 136-150. https://doi.org/10.1134/S0022093024010101

Goodman, L., & Campbell, J. (2007). Lethal levels of hypoxia for gulf coast estuarine animals. *Marine Biology*, *152*(1), 37-42. https://doi.org/10.1007/s00227-007-0685-1

Grantham, B., Chan, F., Nielsen, K., Fox, D., Barth, J., Huyer, A.,…Menge, B. (2004). Upwelling-driven nearshore hypoxia signals ecosystem and oceanographic changes in the northeast Pacific. *Nature*, *429*(6993), 749-754. https://doi.org/10.1038/nature02605

Green, T., Siboni, N., King, W., Labbate, M., Seymour, J., & Raftos, D. (2019). Simulated Marine Heat Wave Alters Abundance and Structure of Vibrio

Populations Associated with the Pacific Oyster Resulting in a Mass Mortality Event. *Microbial Ecology*, *77*(3), 736-747. https://doi.org/10.1007/s00248-018-1242-9

Greenwood, N., Parker, E., Fernand, L., Sivyer, D., Weston, K., Painting, S.,…Laane, R. (2010). Detection of low bottom water oxygen concentrations in the North Sea; implications for monitoring and assessment of ecosystem health. *Biogeosciences*, *7*(4), 1357 – 1373. https://doi.org/10.5194/bg-7-1357-2010

Grieshaber, M., Hardewig, I., Kreutzer, U., & Pörtner, H. (1994). Physiological and metabolic responses to hypoxia in invertebrates. *Reviews of Physiology, Biochemistry and Pharmacology.*, *125*, 43-147. https://doi.org/10.1007/BFb0030909

Grijalba-Uche, M., & Echarte, L. (2015). Homeostasis y representaciones intelectuales: una aproximación a la conducta moral desde la teoría de la teoría de la emoción de Antonio Damasio. *Persona y Bioética*, *19*, 80-98. https://doi.org/10.5294/PEBI.2015.19.1.7

Gu, H., Shang, Y., Clements, J., Dupont, S., Wang, T., Wei, S.,…Wang, Y. (2019). Hypoxia aggravates the effects of ocean acidification on the physiological energetics of the blue mussel *Mytilus edulis*. *Marine Pollution Bulletin*, *149*, 1-7. https://doi.org/https://doi.org/10.1016/j.marpolbul.2019.110538

Gutiérrez, D., Sifeddine, A., Field, D., Ortlieb, L., Vargas, G., Chávez, F.,…Baumgartner, T. (2009). Rapid reorganization in ocean biogeochemistry off Perú towards the end of the Little Ice Age. *Biogeosciences*, *6*(5), 835-848. https://doi.org/10.5194/bg-6-835-2009

Haider, F., Falfushynska, H., Timm, S., & Sokolova, I. (2020). Effects of hypoxia and reoxygenation on intermediary metabolite homeostasis of marine bivalves *Mytilus edulis* and *Crassostrea gigas*. *Comparative Biochemistry and Physiology Part A: Molecular & Integrative Physiology*, *242*, 1-16. https://doi.org/https://doi.org/10.1016/j.cbpa.2020.110657

Hall, S., Méthe, D., Stewart-Clark, S., & Clark, F. (2023). Size and site specific transcriptomic responses of blue mussel (*Mytilus edulis*) to acute hypoxia. *Marine Genomics*, *71*, 1-9. https://doi.org/10.1016/j.margen.2023.101060

Hashem, Z. (2025). Bacterial Metabolites in Defense: A Crucial Aspect of Microbial Interaction and Host Protection. In S. S. M. Soliman & M. I. Husseiny (Eds.), *Metabolic Dynamics in Host-Microbe Interaction* (pp. 101-120). Springer Nature Singapore. https://doi.org/10.1007/978-981-96-1305-2_5

Hatano, K., Orita, R., Kimura, K., Nagano, Y., & Suzuki, N. (2025). Gene expression dataset of the blood clam *Anadara kagoshimensis* in relation to anoxic stress. *Data in Brief*, *59*, 1-7. https://doi.org/10.1016/j.dib.2025.111341

Hernroth, B., & Baden, S. (2018). Alteration of host-pathogen interactions in the wake of climate change – Increasing risk for shellfish associated infections? *Environmental Research*, *161*, 425-438. https://doi.org/https://doi.org/10.1016/j.envres.2017.11.032

Hernández-Elvira, M., & Sunnerhagen, P. (2022). Post-transcriptional regulation during stress. *FEMS Yeast Research*, *22*(1), 1-11. https://doi.org/10.1093/femsyr/foac025

Hernández-Miranda, E., Quiñones, R., Aedo, G., Valenzuela, A., Mermoud, N., Román, C., & Yañez, F. (2010). A major fish stranding caused by a natural

hypoxic event in a shallow bay of the eastern South Pacific Ocean. *Journal of Fish Biology*, *76*(7), 1543-1564. https://doi.org/10.1111/j.1095-8649.2010.02580.x

Hernández-Miranda, E., Veas, R., Anabalón, V., & Quiñones, R. (2017). Short-term alteration of biotic and abiotic components of the pelagic system in a shallow bay produced by a strong natural hypoxia event. *PLoS One*, *12*(7), 1-25. https://doi.org/10.1371/journal.pone.0179023

Hernández-Miranda, E., Veas, R., Labra, F., Salamanca, M., & Quiñones, R. (2012). Response of the epibenthic macrofaunal community to a strong upwelling-driven hypoxic event in a shallow bay of the southern Humboldt Current System. *Marine Environmental Research*, *79*, 16-28. https://doi.org/10.1016/j.marenvres.2012.04.004

Hickey, M., & Lee, J. (2018). A comprehensive review of *Vibrio* (*Listonella*) *anguillarum*: ecology, pathology and prevention. *Reviews in Aquaculture*, *10*(3), 585-610. https://doi.org/https://doi.org/10.1111/raq.12188

Hill, R., Wyse, G., & Anderson, M. (2012). *Animal Physiology* (Tercera edición ed.). Editorial Médica Panamericana S.A.

Hofmann, A., Peltzer, E., Walz, P., & Brewer, P. (2011). Hypoxia by degrees: Establishing definitions for a changing ocean. *Deep Sea Research Part I: Oceanographic Research Papers*, *58*(12), 1212-1226. https://doi.org/https://doi.org/10.1016/j.dsr.2011.09.004

Hopkins, S. (2003). The pathophysiological role of cytokines. *Legal Medicine*, *5*, 45-57. https://doi.org/https://doi.org/10.1016/S1344-6223(02)00088-3

Hu, J., Cai, J., Xu, T., & Kang, H. (2022). Epitranscriptomic mRNA modifications governing plant stress responses: underlying mechanism and potential application. *Plant Biotechnology Journal*, *20*(12), 2245-2257. https://doi.org/10.1111/pbi.13913

Huang, R., & Zhou, P. (2020). HIF-1 signaling: A key orchestrator of cancer radioresistance. *Radiation Medicine and Protection*, *1*(1), 7-14. https://doi.org/https://doi.org/10.1016/j.radmp.2020.01.006

IFOP. (2000). *Innovaciones en la tecnología de cultivo de chorito (Mytilus chilensis), tendientes a mejorar la calidad y rentabilidad de la actividad mitícola en la X Región*. Retrieved from https://www.ifop.cl/wp-content/contenidos/uploads/biblioteca/libros_digitales/Curso_Cultivo_de_choritos.pdf

Ingala, M., Simmons, N., Dunbar, M., Wultsch, C., Krampis, K., & Perkins, S. (2021). You are more than what you eat: potentially adaptive enrichment of microbiome functions across bat dietary niches. *Animal Microbiome*, *3*(1), 1-17. https://doi.org/10.1186/s42523-021-00139-8

Iriarte, J., Pantoja, S., & Daneri, G. (2014). Oceanographic Processes in Chilean Fjords of Patagonia: From small to large-scale studies *Progress in Oceanography*, *129*, 1-7. https://doi.org/10.1016/j.pocean.2014.10.004

Ivanina, A., & Sokolova, I. (2016). Effects of intermittent hypoxia on oxidative stress and protein degradation in molluscan mitochondria. *Journal of Experimental Biology*, *219*(23), 3794-3802. https://doi.org/10.1242/jeb.134700

Jain, M., Abu-Shumays, R., Olsen, H., & Akeson, M. (2022). Advances in nanopore direct RNA sequencing. *Nature Methods*, *19*(10), 1160-1164. https://doi.org/10.1038/s41592-022-01633-w

Jiang, J., Zhang, Y., Wang, J., Qin, Y., Zhao, C., He, K.,…Kalueff, A. (2025). Using Zebrafish Models to Study Epitranscriptomic Regulation of CNS Functions. *Journal of Neurochemistry*, *169*(1), 1-11. https://doi.org/10.1111/jnc.16311

Jin, S., Plikus, M., & Nie, Q. (2025). CellChat for systematic analysis of cell-cell communication from single-cell transcriptomics. *Nature Protocols*, *20*(1), 180-219. https://doi.org/10.1038/s41596-024-01045-4

Jung, Y., & Goldman, D. (2018). Role of RNA modifications in brain and behavior. *Genes Brain and Behavior*, *17*(3), 1-9. https://doi.org/10.1111/gbb.12444

Jung-whan, K., Tchernyshyov, I., Semenza, L., & Dang, V. (2006). *HIF-1*-mediated expression of pyruvate dehydrogenase kinase: A metabolic switch required for cellular adaptation to hypoxia. *Cell Metabolism*, *3*(3), 177-185. https://doi.org/https://doi.org/10.1016/j.cmet.2006.02.002

Kaltschmidt, B., Kaltschmidt, C., Hofmann, T., Hehner, S., Dröge, W., & Schmitz, M. (2000). The pro- or anti-apoptotic function of NF-κB is determined by the nature of the apoptotic stimulus. *European Journal of Biochemistry*, *267*(12), 3828-3835. https://doi.org/10.1046/j.1432-1327.2000.01421.x

Kanehisa, M., Sato, Y., & Kawashima, M. (2022). KEGG mapping tools for uncovering hidden features in biological data. *Protein Science*, *31*(1), 47-53. https://doi.org/10.1002/pro.4172

Karikó, K., Buckstein, M., Ni, H., & Weissman, D. (2005). Suppression of RNA recognition by Toll-like receptors: The impact of nucleoside modification and the evolutionary origin of RNA. *Immunity*, *23*(2), 165-175. https://doi.org/10.1016/j.immuni.2005.06.008

Karikó, K., Muramatsu, H., Welsh, F., Ludwig, J., Kato, H., Akira, S., & Weissman, D. (2008). Incorporation of Pseudouridine Into mRNA Yields Superior Nonimmunogenic Vector With Increased Translational Capacity and Biological Stability. *Molecular Therapy*, *16*(11), 1833-1840. https://doi.org/10.1038/mt.2008.200

Keppel, A., Breitburg, D., Wikfors, G., Burrell, R., & Clark, V. (2015). Effects of co-varying diel-cycling hypoxia and pH on disease susceptibility in the eastern oyster Crassostrea virginica. *Marine Ecology Progress Series*, *538*, 169-183. https://doi.org/10.3354/meps11479

Khan, B., Clinton, S., Hamp, T., Oliver, J., & Ringwood, A. (2018). Potential impacts of hypoxia and a warming ocean on oyster microbiomes. *Marine Environmental Research*, *139*, 27-34. https://doi.org/10.1016/j.marenvres.2018.04.018

Khan, F., Shang, Y., Chang, X., Kong, H., Zuberi, A., Fang, J.,…Wang, Y. (2021). Effects of Ocean Acidification, Hypoxia, and Warming on the Gut Microbiota of the Thick Shell Mussel *Mytilus coruscus* Through 16S rRNA Gene Sequencing. *Frontiers in Marine Science*, *8*, 1-12, Article 736338. https://doi.org/10.3389/fmars.2021.736338

Kim, C. (2018). Immune regulation by microbiome metabolites. *Immunology*, *154*(2), 220-229. https://doi.org/10.1111/imm.12930

Kim, C., Park, C., Kim, E., & Nam, Y. (2021). Transcriptional modulation patterns of abalone *Haliotis discus hannai* hypoxia inducible factor-1α (HIF-1α) in interdependent crosstalk between hypoxia, infection, and environmental stresses. *Aquaculture Reports*, *19*, 1-10. https://doi.org/https://doi.org/10.1016/j.aqrep.2020.100566

Kim, J., Kajino, N., Shin, J., Yang, H., Lee, H., Choi, K., & Hong, H. (2025). Combined effects of hypoxia and thermal stress on hemocyte response in Pacific oysters (*Crassostrea gigas*): Insights from transcriptomic and proteomic analyses. *Comparative Biochemistry and Physiology D-Genomics & Proteomics*, *56*, 1-17. https://doi.org/10.1016/j.cbd.2025.101626

King, M. (2000). Detection of dead cells and measurement of cell killing by flow cytometry. *Journal of Immunological Methods*, *243*(1), 155-166. https://doi.org/10.1016/S0022-1759(00)00232-5

Kogut, M., Lee, A., & Santin, E. (2020). Microbiome and pathogen interaction with the immune system. *Poultry Science*, *99*(4), 1906-1913. https://doi.org/10.1016/j.psj.2019.12.011

Korthauer, K., Kimes, P., Duvallet, C., Reyes, A., Subramanian, A., Teng, M.,…Hicks, S. (2019). A practical guide to methods controlling false discoveries in computational biology. *Genome Biology*, *20*, 1-21. https://doi.org/10.1186/s13059-019-1716-1

Kroemer, G., Galluzzi, L., Vandenabeele, P., Abrams, J., Alnemri, E., Baehrecke, E.,…Melino, G. (2009). Classification of cell death: recommendations of the Nomenclature Committee on Cell Death 2009. *Cell Death & Differentiation*, *16*(1), 3-11. https://doi.org/10.1038/cdd.2008.150

Kueh, C., & Chan, K. (1985). Bacteria in Bivalve Shellfish with Special Reference to the Oyster. *Journal of Applied Bacteriology*, *59*(1), 41-47. https://doi.org/10.1111/j.1365-2672.1985.tb01773.x

Kumar, A., Singh, P., Zhang, K., & Kumar, A. (2020). Toll-like receptor 2 (TLR2) engages endoplasmic reticulum stress sensor IRE1α to regulate retinal innate responses in *Staphylococcus aureus* endophthalmitis. *FASEB Journal*, *34*(10), 13826-13838. https://doi.org/10.1096/fj.202001393R

Kumar, S., & Mohapatra, T. (2021). Deciphering Epitranscriptome: Modification of mRNA Bases Provides a New Perspective for Post-transcriptional Regulation of Gene Expression. *Frontiers in Cell and Developmental Biology*, *9*, 1-22. https://doi.org/10.3389/fcell.2021.628415

Labra, F., Hernández-Miranda, E., & Quiñones, R. (2015). Dynamic relationships between body size, species richness, abundance, and energy use in a shallow marine epibenthic faunal community. *Ecology and Evolution*, *5*(2), 391-408. https://doi.org/10.1002/ece3.1343

Lacedonia, D., Carpagnano, G., Crisetti, E., Cotugno, G., Palladino, G., Patricelli, G.,…Foschino, M. (2015). Mitochondrial DNA alteration in obstructive sleep apnea. *Respiratory Research*, *16*(1), 1-7. https://doi.org/10.1186/s12931-015-0205-7

Lagos, N., Benítez, S., Duarte, C., Lardies, M., Broitman, B., Tapia, C.,…Vargas, C. (2015). Effects of temperature and ocean acidification on shell characteristics of *Argopecten purpuratus*: implications for scallop aquaculture in an

upwelling-influenced area. *Aquaculture Environment Interactions*, *8*, 357-370. https://doi.org/10.3354/aei00183

Lasa, A., & Romalde, J. (2021). Coevolution of Molluscs and Their Microbes. In *Microbes: The Foundation Stone of the Biosphere* (pp. 513-526). Springer International Publishing. https://doi.org/10.1007/978-3-030-63512-1_24

Ledesma, C., Bonansea, M., Rodriguez, C., & Sánchez, A. (2013). Determinación de indicadores de eutrofización en el embalse Río Tercero, Córdoba (Argentina). *Revista Ciência Agronômica*, *44*, 419-425.

Leung, J., Cheung, S., Qiu, J., Ang, P., Chiu, J., Thiyagarajan, V., & Shin, P. (2013). Effect of parental hypoxic exposure on embryonic development of the offspring of two serpulid polychaetes: Implication for transgenerational epigenetic effect. *Marine Pollution Bulletin*, *74*(1), 149-155. https://doi.org/10.1016/j.marpolbul.2013.07.014

Levin, L. (2003). Oxygen Minimum Zone Benthos: Adaptation and Community Response to Hypoxia. *Oceanography and Marine Biology, An Annual Review*, *41*, 1-45.

Levin, L., Ekau, W., Gooday, A., Jorissen, F., Middelburg, J., Naqvi, S.,…Zhang, J. (2009). Effects of natural and human-induced hypoxia on coastal benthos. *Biogeosciences*, *6*(10), 2063-2098. https://doi.org/10.5194/bg-6-2063-2009

León-Muñoz, J., Aguayo, R., Marcé, R., Catalán, N., Woelfl, S., Nimptsch, J.,…Miranda, A. (2021). Climate and Land Cover Trends Affecting Freshwater Inputs to a Fjord in Northwestern Patagonia. *Frontiers in Marine Science*, *8*, 1-21. https://doi.org/10.3389/fmars.2021.628454

Li, H., Yang, Q., Gao, X., Su, H., Wang, J., & He, C. (2012). Identification and expression of a putative LPS-induced TNF-α factor from Asiatic hard clam *Meretrix meretrix*. *Molecular biology reports*, *39*(2), 865-871. https://doi.org/10.1007/s11033-011-0810-6

Li, M., Xie, Y., Zhao, K., Chen, K., Cao, Y., Zhang, J.,…Li, H. (2021). Endoplasmic reticulum stress exacerbates inflammation in chronic rhinosinusitis with nasal polyps via the transcription factor XBP1. *Clinical Immunology*, *223*, 1-11. https://doi.org/10.1016/j.clim.2020.108659

Li, W., Li, X., Ma, X., Xiao, W., & Zhang, J. (2022). Mapping the m^1A, m^5C, m^6A and m^7G methylation atlas in zebrafish brain under hypoxic conditions by MeRIP-seq. *BMC Genomics*, *23*(1), 1-19. https://doi.org/10.1186/s12864-022-08350-w

Li, X., Shi, H., Xia, H., Zhou, Y., & Qiu, Y. (2014). Seasonal hypoxia and its potential forming mechanisms in the Mirs Bay, the northern South China Sea. *Continental Shelf Research*, *80*, 1-7. https://doi.org/10.1016/j.csr.2014.03.003

Li, X., Xiong, X., & Yi, C. (2017). Epitranscriptome sequencing technologies: decoding RNA modifications. *Nature Methods*, *14*(1), 23-31. https://doi.org/10.1038/NMETH.4110

Li, Y., Chen, Y., Xu, J., Ding, W., Shao, A., Zhu, Y.,…Yang, J. (2019). Temperature elevation and *Vibrio cyclitrophicus* infection reduce the diversity of haemolymph microbiome of the mussel *Mytilus coruscus*. *Scientific Reports*, *9*(1), 1-10. https://doi.org/10.1038/s41598-019-52752-y

Li, Y., Yang, N., Liang, X., Yoshida, A., Osatomi, K., Power, D.,…Yang, J. (2018). Elevated Seawater Temperatures Decrease Microbial Diversity in the Gut of

Mytilus coruscus. *Frontiers in Physiology*, *9*, 1-9. https://doi.org/10.3389/fphys.2018.00839

Liao, M., Zhu, Y., Zhu, X., Somero, G., & Dong, Y. (2025). RNA editing generates mRNA isoforms with distinct stabilities that may expand the thermal tolerance of mRNA and proteins in *Mytilus* species. *Zoological Research*, *46*(3), 527-537. https://doi.org/10.24272/j.issn.2095-8137.2024.383

Linford, P., Pérez-Santos, I., Montero, P., Díaz, P., Aracena, C., Pinilla, E.,…Soto-Riquelme, C. (2024). Oceanographic processes driving low-oxygen conditions inside Patagonian fjords. *Biogeosciences*, *21*(6), 1433-1459. https://doi.org/10.5194/bg-21-1433-2024

Liu, C., Liang, H., Wan, A., Xiao, M., Sun, L., Yu, Y.,…Wan, G. (2025). Decoding the m^6A epitranscriptomic landscape for biotechnological applications using a direct RNA sequencing approach. *Nature Communications*, *16*(1), 1-15. https://doi.org/10.1038/s41467-025-56173-6

Liu, T., Lu, Y., Sun, M., Shen, H., & Niu, D. (2024). Effects of acute hypoxia and reoxygenation on histological structure, antioxidant response, and apoptosis in razor clam *Sinonovacula constricta*. *Fish & Shellfish Immunology*, *145*, 1-12. https://doi.org/10.1016/j.fsi.2023.109310

Liu, Y., Wilson, A., Han, J., Hui, A., O'Sullivan, L., Huan, T., & Haney, C. (2023). Amino Acid Availability Determines Plant Immune Homeostasis in the *Rhizosphere Microbiome*. *MBIO*, *14*(2), 1-16. https://doi.org/10.1128/mbio.03424-22

Lohrmann, K., Bustos, E., Rojas, R., Navarrete, F., Robotham, H., & Bignell, J. (2019). Histopathological assessment of the health status of *Mytilus chilensis* (Hupé 1854) in southern Chile. *Aquaculture*, *503*, 40-50. https://doi.org/https://doi.org/10.1016/j.aquaculture.2018.12.080

Lokmer, A., & Mathias, K. (2015). Hemolymph microbiome of Pacific oysters in response to temperature, temperature stress and infection. *The International Society for Microbial Ecology Journal*, *9*(3), 670-682. https://doi.org/10.1038/ismej.2014.160

Lorenz, D., Sathe, S., Einstein, J., & Yeo, G. (2020). Direct RNA sequencing enables m6A detection in endogenous transcript isoforms at base-specific resolution. *RNA*, *26*(1), 19-28. https://doi.org/10.1261/rna.072785.119

Luo, W., Xu, Z., Wang, H., Lu, Z., Ding, L., Wang, R.,…Xia, L. (2023). HIF1A-repressed PUS10 regulates NUDC/Cofilin1 dependent renal cell carcinoma migration by promoting the maturation of miR-194-5p. *Cell & Bioscience*, *13*(1-20), 153. https://doi.org/10.1186/s13578-023-01094-4

Luo, Y., Lu, G., Chen, Y., Liu, F., Xu, G., Yin, J., & Gao, Y. (2013). Long-term cycles of hypoxia and normoxia increase the contents of liver mitochondrial DNA in rats. *European Journal of Applied Physiology*, *113*(1), 223-232. https://doi.org/10.1007/s00421-012-2414-9

Mardones, J., Paredes, J., Godoy, M., Suarez, R., Norambuena, L., Vargas, V.,…Hallegraeff, G. (2021). Disentangling the environmental processes responsible for the world's largest farmed fish-killing harmful algal bloom: Chile, 2016. *Science of The Total Environment*, *766*, 1-19. https://doi.org/https://doi.org/10.1016/j.scitotenv.2020.144383

Mardones, M., Mardones-Toledo, D., Büchner-Miranda, J., Salas-Yanquin, L., Gray, M., Cubillos, V.,…Chaparro, O. (2024). Food acquisition by the intertidal filter feeder bivalve *Perumytilus purpuratus*: Can the gill explain a differential performance between smaller individuals and the larger ones? *Journal of Experimental Marine Biology and Ecology*, *571*, 1-9. https://doi.org/10.1016/j.jembe.2023.151982

Martínez, M., González-Aravena, M., Held, C., & Abele, D. (2023). A molecular perspective on the invasibility of the southern ocean benthos: The impact of hypoxia and temperature on gene expression in South American and Antarctic *Aequiyoldia bivalves*. *Frontiers in Physiology*, *14*, 1-12. https://doi.org/10.3389/fphys.2023.1083240

McArley, T., Hickey, A., & Herbert, N. (2018). Hyperoxia increases maximum oxygen consumption and aerobic scope of intertidal fish facing acutely high temperatures. *Journal of Experimental Biology*, *221*(22), 1-31. https://doi.org/10.1242/jeb.189993

Melzner, F., Thomsen, J., Koeve, W., Oschlies, A., Gutowska, M. A., Bange, H. W.,…Körtzinger, A. (2013). Future ocean acidification will be amplified by hypoxia in coastal habitats. *Marine Biology*, *160*(8), 1875-1888. https://doi.org/10.1007/s00227-012-1954-1

Miro-Blanch, J., & Yanes, O. (2019). Epigenetic Regulation at the Interplay Between Gut Microbiota and Host Metabolism. *Frontiers in Genetics*, *10*, 1-9. https://doi.org/10.3389/fgene.2019.00638

Mizutani, Y., Orita, R., Kimura, K., & Funabara, D. (2025). Hypoxia-induced changes in the gill and hepatopancreatic bacterial communities of the ark shell *Anadara kagoshimensis*. *Marine Biotechnology*, *27*(2), 1-11. https://doi.org/10.1007/s10126-025-10430-3

Moffitt, S., Moffitt, R., Sauthoff, W., Davis, C., Hewett, K., & Hill, T. (2015). Paleoceanographic insights on recent oxygen minimum zone expansion: lessons for modern oceanography. *PloS one*, *10*(1), 1-39. https://doi.org/10.1371/journal.pone.0115246

Montero, P., Daneri, G., González, H., Iriarte, J., Tapia, F., Lizárraga, L.,…Pizarro, O. (2011). Seasonal variability of primary production in a fjord ecosystem of the Chilean Patagonia: Implications for the transfer of carbon within pelagic food webs. *Continental Shelf Research*, *31*(3), 202-215. https://doi.org/https://doi.org/10.1016/j.csr.2010.09.003

Moret, I., Cerrillo, E., Navarro-Puche, A., Iborra, M., Rausell, F., Tortosa, L., & Beltrán, B. (2014). Estrés oxidativo en la enfermedad de Crohn. *Gastroenterología y Hepatología*, *37*, 28-34. https://doi.org/10.1016/j.gastrohep.2013.01.008

Movassagh, M., & Foo, R. (2008). Simplified apoptotic cascades. *Heart Failure Reviews*, *13*(2), 111-119. https://doi.org/10.1007/s10741-007-9070-x

Munari, M., Matozzo, V., Riedl, V., Pastore, P., Badocco, D., & Marin, M. (2020). Eat Breathe Excrete Repeat: Physiological Responses of the Mussel *Mytilus galloprovincialis* to Diclofenac and Ocean Acidification. *Journal of Marine Science and Engineering*, *8*(11), 1-12. https://doi.org/10.3390/jmse8110907

Murga-Garrido, S., Ulloa-Pérez, E., Díaz-Benítez, C., Orbe-Orihuela, Y., Cornejo-Granados, F., Ochoa-Leyva, A.,…Lagunas-Martínez, A. (2023). Virulence

Factors of the Gut Microbiome Are Associated with BMI and Metabolic Blood Parameters in Children with Obesity. *Microbiology Spectrum*, *11*(2), 1-18. https://doi.org/10.1128/spectrum.03382-22

Nance, K., & Meier, J. (2021). Modifications in an Emergency: The Role of N1-Methylpseudouridine in COVID-19 Vaccines. *ACS Central Science*, *7*(5), 748-756. https://doi.org/10.1021/acscentsci.1c00197

Narváez, D., Vargas, C., Cuevas, L., García-Loyola, S., Lara, C., Segura, C.,…Broitman, B. (2019). Dominant scales of subtidal variability in coastal hydrography of the Northern Chilean Patagonia. *Journal of Marine Systems*, *193*, 59-73. https://doi.org/https://doi.org/10.1016/j.jmarsys.2018.12.008

Navarro, J., Duarte, C., Manríquez, P., Lardies, M., Torres, R., Acuña, K.,…Lagos, N. (2016). Ocean warming and elevated carbon dioxide: multiple stressor impacts on juvenile mussels from southern Chile. *ICES Journal of Marine Science.*, *73*(3), 764–771. https://doi.org/https://doi.org/10.1093/icesjms/fsv249

Nishikura, K. (2016). A-to-I editing of coding and non-coding RNAs by ADARs. *Nature Reviews Molecular Cell Biology*, *17*(2), 83-96. https://doi.org/10.1038/nrm.2015.4

Osores, S., Lagos, N., San Martín, V., Manríquez, P., Vargas, C., Torres, R.,…Lardies, M. (2017). Plasticity and inter-population variability in physiological and life-history traits of the mussel *Mytilus chilensis*: A reciprocal transplant experiment. *Journal of Experimental Marine Biology and Ecology*, *490*, 1-12. https://doi.org/https://doi.org/10.1016/j.jembe.2017.02.005

Oyarzún, P., Toro, E., Jaramillo, R., Guiñez, R., Briones, C., & Astorga, M. (2011). Ciclo gonadal del chorito *Mytilus chilensis* (Bivalvia: Mytilidae) en dos localidades del sur de Chile. *Latin american journal of aquatic research*, *39*, 512-525. https://doi.org/10.3856/vol39-issue3-fi1lltext-11

Paillard, C., Gueguen, Y., Wegner, K., Bass, D., Pallavicini, A., Vezzulli, L., & Arzul, I. (2022). Recent advances in bivalve-microbiota interactions for disease prevention in aquaculture. *Current Opinion in Biotechnology*, *73*, 225-232. https://doi.org/10.1016/j.copbio.2021.07.026

Park, C., Lee, S., & Yoon, K. (2020). Epitranscriptomic regulation of transcriptome plasticity in development and diseases of the brain. *BMB Reports*, *53*(11), 551-564. https://doi.org/10.5483/BMBRep.2020.53.11.204

Parks, D., Tyson, G., Hugenholtz, P., & Beiko, R. (2014). STAMP: statistical analysis of taxonomic and functional profiles. *Bioinformatics*, *30*, 3123-3124. https://doi.org/10.1093/bioinformatics/btu494

Pastukh, V., Gorodnya, O., Gillespie, M., & Ruchko, M. (2016). Regulation of mitochondrial genome replication by hypoxia: The role of DNA oxidation in D-loop region. *Free Radical Biology and Medicine*, *96*, 78-88. https://doi.org/10.1016/j.freeradbiomed.2016.04.011

Patil, D., Pickering, B., & Jaffrey, S. (2018). Reading m^6A in the Transcriptome: m^6A-Binding Proteins. *Trends in Cell Biology*, *28*(2), 113-127. https://doi.org/10.1016/j.tcb.2017.10.001

Pawitan, Y., Michiels, S., Koscielny, S., Gusnanto, A., & Ploner, A. (2005). False discovery rate, sensitivity and sample size for microarray studies. *Bioinformatics*, *21*(13), 3017-3024. https://doi.org/10.1093/bioinformatics/bti448

Perillo, B., Ombra, M., Bertoni, A., Cuozzo, C., Sacchetti, S., Sasso, A.,…Avvedimento, E. (2008). DNA oxidation as triggered by H3K9me2 demethylation drives estrogen-induced gene expression. *Science*, *319*(5860), 202-206. https://doi.org/10.1126/science.1147674

Pertea, G., & Pertea, M. (2020). GFF Utilities: GffRead and GffCompare. *F1000Research*, *9*(304), 1-19. https://doi.org/10.12688/f1000research.23297.2

Pertea, M., Pertea, G., Antonescu, C., Chang, T., Mendell, J., & Salzberg, S. (2015). StringTie enables improved reconstruction of a transcriptome from RNA-seq reads. *Nature Biotechnology*, *33*(3), 290-297. https://doi.org/10.1038/nbt.3122

Peña-Sanoja, M., & De Sanctis, J. (2013). Autofagia y respuesta inmunitaria. *Investigación Clínica*, *54*, 325-337.

Pilala, K., Panoutsopoulou, K., Papadimitriou, M., Soureas, K., Scorilas, A., & Avgeris, M. (2025). Exploring the methyl-verse: Dynamic interplay of epigenome and m^6A epitranscriptome. *Molecular Therapy*, *33*(2), 447-464. https://doi.org/10.1016/j.ymthe.2024.12.003

Pohjoismäki, J. L., Boettger, T., Liu, Z., Goffart, S., Szibor, M., & Braun, T. (2012). Oxidative stress during mitochondrial biogenesis compromises mtDNA integrity in growing hearts and induces a global DNA repair response. *Nucleic Acids Research*, *40*(14), 6595-6607. https://doi.org/10.1093/nar/gks301

Pollock, M., Clarke, L., & Dubé, M. (2007). The effects of hypoxia on fishes: from ecological relevance to physiological effects. *Environmental Reviews*, *15*, 1-14. https://doi.org/10.1139/A06-006

Porter, E., & Porter, F. (2018). A Strain Gauge Monitor (SGM) for Continuous Valve Gape Measurements in Bivalve Molluscs in Response to Laboratory Induced Diel-cycling Hypoxia and pH. *Jove-Journal of Visualized Experiments*(138), 1-13. https://doi.org/10.3791/57404

Puerta, H. (1995). *La depuración de los moluscos bivalvos*. Editorial Fundación Caixa Galicia.

Rabalais, N., Cai, W., Carstensen, J., Conley, D., Fry, B., Hu, X.,…Zhang, J. (2014). Eutrophication-driven deoxygenation in the coastal ocean. *Oceanography*, *27*(1), 172–183. https://doi.org/10.5670/oceanog.2014.21

Radbakhsh, S., Najar, M., Merimi, M., Benderdour, M., Fernandes, J., Martel-Pelletier, J.,…Fahmi, H. (2025). RNA Modifications in Osteoarthritis: Epitranscriptomic Insights into Pathogenesis and Therapeutic Targets. *International Journal of Molecular Sciences*, *26*(10), 1-25. https://doi.org/10.3390/ijms26104955

Ramírez-Sagredo, A., Aleman, L., Villa, M., Chávez, N., García, L., & Lavandero, S. (2016). Autofagia en el sistema cardiovascular: pasado, presente y futuro. *Revista chilena de cardiología*, *35*, 228-241.

Reddy, A., Huang, J., Syed, N., Ben-Hur, A., Dong, S., & Gu, L. (2020). Decoding co-/post-transcriptional complexities of plant transcriptomes and epitranscriptome using next-generation sequencing technologies. *Biochemical Society Transactions*, *48*(6), 2399-2414. https://doi.org/10.1042/BST20190492

Reed, D., & Harrison, J. (2016). Linking nutrient loading and oxygen in the coastal ocean: A new global scale model. *Global Biogeochemical Cycles*, *30*(3), 447-459. https://doi.org/10.1002/2015GB005303

Roberts, J., Brandt, S., Fanslow, D., Ludsin, S., Pothoven, S., Scavia, D., & Höök, T. (2011). Effects of Hypoxia on Consumption, Growth, and RNA:DNA Ratios of Young Yellow Perch. *Transactions of the American Fisheries Society*, *140*(6), 1574-1586. https://doi.org/10.1080/00028487.2011.638576

Robinson, M., McCarthy, D., & Smyth, G. (2010). edgeR: a Bioconductor package for differential expression analysis of digital gene expression data. *Bioinformatics*, *26*(1), 139-140. https://doi.org/10.1093/bioinformatics/btp616

Ross, P., Scanes, E., Byrne, M., Ainsworth, T., Donelson, J., Foo, S.,…Parker, L. (2023). Surviving the anthropocene: the resilience of marine animals to climate change. In *Oceanography and marine biology: an annual review, Vol 61* (pp. 35-80). CRC Press-Taylor & Francis Group. https://doi.org/10.1201/9781003363873-3

Roundtree, I., Evans, M., Pan, T., & He, C. (2017). Dynamic RNA Modifications in Gene Expression Regulation. *Cell*, *169*(7), 1187-1200. https://doi.org/10.1016/j.cell.2017.05.045

Rynkowski, L., Ellis, J., Needham, H., & Pilditch, C. (2025). A systematic review and meta-analysis of the cumulative effects of multiple stressors on marine bivalves. *Marine Biology*, *172*(7), 1-21. https://doi.org/10.1007/s00227-025-04671-y

Ríos, V., Ocampo, N., & Astorga, M. (2018). Composición química proximal y morfométría de cholga (*Aulacomya ater*, Molina, 1782) y chorito (*Mytilus chilensis*, Hupé, 1854) comercializados en la Región de Magallanes. *Anales Instituto Patagonia (Chile) 46*(1), 49–58. https://doi.org/http://dx.doi.org/10.4067/S0718-686X2018000100049

Salas-Yanquin, L., Navarro, J., Pechenik, J., Montory, J., & Chaparro, O. (2018). Volcanic ash in the water column: Physiological impact on the suspension-feeding bivalve *Mytilus chilensis*. *Marine Pollution Bulletin*, *127*, 342-351. https://doi.org/https://doi.org/10.1016/j.marpolbul.2017.12.024

Sandoval-Quintana, E., Stangl, C., Huang, L., Renkens, I., Duran, R., van Haaften, G.,…Cagnon, C. (2023). CRISPR-Cas9 enrichment, a new strategy in microbial metagenomics to investigate complex genomic regions: The case of an environmental integron. *Molecular Ecology Resources*, *23*(6), 1288-1298. https://doi.org/10.1111/1755-0998.13798

Sarkar, A., Gasperi, W., Begley, U., Nevins, S., Huber, S., Dedon, P., & Begley, T. (2021). Detecting the epitranscriptome. *Wiley Interdisciplinary Reviews-RNA*, *12*(6), 1-19. https://doi.org/10.1002/wrna.1663

Sattari, M., Bagherzadeh, F., Sharifpour, I., & Kazemi, R. (2013). Effect of hypoxia, normoxia and hyperoxia conditions on gill histopathology in two weight groups of beluga (*Huso huso*). *Caspian Journal of Environmental Sciences*, *11*(1), 77-84.

Scanes, E., Parker, L., Seymour, J., Siboni, N., King, W., Danckert, N.,…Ross, P. (2021). Climate change alters the haemolymph microbiome of oysters. *Marine Pollution Bulletin*, *164*, 1-12. https://doi.org/https://doi.org/10.1016/j.marpolbul.2021.111991

Scanes, E., Scanes, P., & Ross, P. (2020). Climate change rapidly warms and acidifies Australian estuaries. *Nature Communications*, *11*(1), 1-11. https://doi.org/10.1038/s41467-020-15550-z

Schmidtko, S., Stramma, L., & Visbeck, M. (2017). Decline in global oceanic oxygen content during the past five decades. *Nature*, *542*(7641), 335-339. https://doi.org/10.1038/nature21399

Sforzini, S., Moore, M., Oliveri, C., Volta, A., Jha, A., Banni, M., & Viarengo, A. (2018). Role of mTOR in autophagic and lysosomal reactions to environmental stressors in molluscs. *Aquatic Toxicology*, *195*, 114-128. https://doi.org/10.1016/j.aquatox.2017.12.014

Shen, L. (2025). Epitranscriptomic regulation through phase separation in plants. *Trends in Plant Science*, *30*(6), 629-641. https://doi.org/10.1016/tplants.2024.11.012

Shen, Y., Huang, Z., Liu, G., Ke, C., & You, W. (2019). Hemolymph and transcriptome analysis to understand innate immune responses to hypoxia in Pacific abalone. *Comparative Biochemistry and Physiology Part D: Genomics and Proteomics*, *30*, 102-112.

Shen, Y., You, W., Luo, X., Lu, Y., Huang, M., & Ke, C. (2023). An overview of the mechanisms underlying hypoxia tolerance differences in aquatic animals and their inspirations for aquaculture. *Reviews in Fish Biology and Fisheries*, *33*(4), 1223-1236. https://doi.org/10.1007/s11160-023-09793-4

Silva, N., & Vargas, C. (2014). Hypoxia in Chilean Patagonian Fjords. *Progress in Oceanography*, *129*, 62-74. https://doi.org/https://doi.org/10.1016/j.pocean.2014.05.016

Sleight, V., Clark, M., Yap-Chiongco, M., Turner, F., & Kocot, K. (2025). Genomic, transcriptomic and epigenomic signatures of ageing and cold adaptation in the Antarctic clam *Laternula elliptica*. *Open Biology*, *15*(5), 1-14. https://doi.org/10.1098/rsob.250009

Sokolov, E., Adzigbli, L., Markert, S., Bundgaard, A., Fago, A., Becher, D.,…Sokolova, I. (2021). Intrinsic Mechanisms Underlying Hypoxia-Tolerant Mitochondrial Phenotype During Hypoxia-Reoxygenation Stress in a Marine Facultative Anaerobe, the Blue Mussel *Mytilus edulis*. *Frontiers in Marine Science*, *8*, 1-15. https://doi.org/10.3389/fmars.2021.773734

Sokolov, E., Markert, S., Hinzke, T., Hirschfeld, C., Becher, D., Ponsuksili, S., & Sokolova, I. (2019). Effects of hypoxia-reoxygenation stress on mitochondrial proteome and bioenergetics of the hypoxia-tolerant marine bivalve *Crassostrea gigas*. *Journal of Proteomics*, *194*, 99-111. https://doi.org/10.1016/j.jprot.2018.12.009

Sokolov, E., & Sokolova, I. (2019). Compatible osmolytes modulate mitochondrial function in a marine osmoconformer *Crassostrea gigas* (Thunberg, 1793). *Mitochondrion*, *45*, 29-37. https://doi.org/10.1016/j.mito.2018.02.002

Sokolova, I. (2018). Mitochondrial Adaptations to Variable Environments and Their Role in Animals' Stress Tolerance. *Integrative and Comparative Biology*, *58*(3), 519-531. https://doi.org/10.1093/icb/icy017

Sokolova, I., Sokolov, E., & Haider, F. (2019). Mitochondrial Mechanisms Underlying Tolerance to Fluctuating Oxygen Conditions: Lessons from Hypoxia-Tolerant Organisms. *Integrative and Comparative Biology*, *59*(4), 938-952. https://doi.org/10.1093/icb/icz047

Soldatov, A., Andreenko, T., Golovina, I., & Stolbov, A. (2010). Peculiarities of organization of tissue metabolism in molluscs with different tolerance to

external hypoxia. *Journal of Evolutionary Biochemistry and Physiology*, *46*(4), 284-290. https://doi.org/10.1134/S0022093010040022

Soldatov, A., Andreenko, T., Sysoeva, I., & Sysoev, A. (2009). Tissue specificity of metabolism in bivalve mollusc *Anadara inaequivalvis* Br. under conditions of experimental anoxia. *Comparative and Ontogenic Biochemistry*, *45*(3), 284-289. https://doi.org/10.1134/S002209300903003X

Song, Z., Li, K., & Li, K. (2024). Acute effects of the environmental probiotics *Rhodobacter sphaeroides* on intestinal bacteria and transcriptome in shrimp *Penaeus vannamei*. *Fish & Shellfish Immunology*, *145*, 1-11. https://doi.org/10.1016/j.fsi.2023.109316

Steckbauer, A., Ramajo, L., Hendriks, I., Fernandez, M., Lagos, N., Prado, L., & Duarte, C. (2015). Synergistic effects of hypoxia and increasing CO_2 on benthic invertebrates of the central Chilean coast. *Frontiers in Marine Science*, *2*(49), 1-12. https://doi.org/10.3389/fmars.2015.00049

Steffen, J., Falfushynska, H., Piontkivska, H., & Sokolova, I. (2020). Molecular Biomarkers of the Mitochondrial Quality Control Are Differently Affected by Hypoxia-Reoxygenation Stress in Marine Bivalves *Crassostrea gigas* and *Mytilus edulis*. *Frontiers in Marine Science*, *7*, 1- 19. https://doi.org/10.3389/fmars.2020.604411

Stevens, A., & Gobler, C. (2018). Interactive effects of acidification, hypoxia, and thermal stress on growth, respiration, and survival of four North Atlantic bivalves. *Marine Ecology Progress Series*(604), 143–161. https://doi.org/10.3354/meps

Storey, J., & Tibshirani, R. (2003). Statistical significance for genomewide studies. *Proceedings of the National Academy of Sciences of the United States of America*, *100*(16), 9440-9445. https://doi.org/10.1073/pnas.1530509100

Storey, K., & Storey, J. (2004). Metabolic rate depression in animals: transcriptional and translational controls. *Biological Reviews of the Cambridge Philosophical Society*, *79*(1), 207-233. https://doi.org/10.1017/s1464793103006195

Subpesca. (2019). *Informe Sectorial de Pesca y Acuicultura*. Chile: Subsecretaría de Pesca y Acuicultura Retrieved from http://www.subpesca.cl/portal/618/articles-106845_documento.pdf

Subpesca. (2021). *Mejillón*. Chile: Subsecretaría de Pesca y Acuicultura Retrieved from https://www.subpesca.cl/portal/616/w3-article-843.html#presentacion

Sui, Y., Hu, M., Shang, Y., Wu, F., Huang, X., Dupont, S.,…Wang, Y. (2017). Antioxidant response of the hard shelled mussel *Mytilus coruscus* exposed to reduced pH and oxygen concentration. *Ecotoxicology and Environmental Safety*, *137*, 94-102. https://doi.org/10.1016/j.ecoenv.2016.11.023

Sun, B., Hu, M., Lan, X., Waiho, K., Lv, X., Xu, C., & Wang, Y. (2024). Nano-titanium dioxide exacerbates the harmful effects of perfluorooctanoic acid on the health of mussels. *Environmental International*, *187*, 1-15. https://doi.org/10.1016/j.envint.2024.108681

Sun, S., Yang, M., Fu, H., Ge, X., & Zou, J. (2020). Altered intestinal microbiota induced by chronic hypoxia drives the effects on lipid metabolism and the immune response of oriental river prawn *Macrobrachium nipponense*. *Aquaculture*, *526*, 1-10. https://doi.org/10.1016/j.aquaculture.2020.735431

Tanaka, R., Shibata, T., Miyake, H., Mori, T., Tamaru, Y., Ueda, M., & Bossier, P. (2016). Temporal fluctuation in the abundance of alginate-degrading bacteria in the gut of abalone *Haliotis gigantea* over 1 year. *Aquaculture Research*, *47*(9), 2899-2908. https://doi.org/https://doi.org/10.1111/are.12740

Tang, A., Soulette, C., van Baren, M., Hart, K., Hrabeta-Robinson, E., Wu, C., & Brooks, A. (2020). Full-length transcript characterization of SF3B1 mutation in chronic lymphocytic leukemia reveals downregulation of retained introns [Article]. *Nature Communications*, *11*(1), 1-12, Article 1438. https://doi.org/10.1038/s41467-020-15171-6

Tang, B., & Riisgård, H. (2018). Relationship between oxygen concentration, respiration and filtration rate in blue mussel *Mytilus edulis*. *Journal of Oceanology and Limnology*, *36*(2), 395-404. https://doi.org/10.1007/s00343-018-6244-4

Taraska, N., & Anne, B. (2013). Selective initiation and transmission of disseminated neoplasia in the soft shell clam *Mya arenaria* dependent on natural disease prevalence and animal size. *Journal of Invertebrate Pathology*, *112*(1), 94-101. https://doi.org/10.1016/j.jip.2012.10.001

Tatusov, R., Natale, D., Garkavtsev, I., Tatusova, T., Shankavaram, U., Rao, B.,…Koonin, E. (2001). The COG database: new developments in phylogenetic classification of proteins from complete genomes. *Nucleic Acids Research*, *29*(1), 22-28. https://doi.org/10.1093/nar/29.1.22

Thornton, C., Leaw, B., Mallard, C., Nair, S., Jinnai, M., & Hagberg, H. (2017). Cell Death in the Developing Brain after Hypoxia-Ischemia. *Frontiers in Cellular Neuroscience*, *11*, 1-19. https://doi.org/10.3389/fncel.2017.00248

Toche, P. (2012). Visión panorámica del sistema inmune. *Revista Médica Clínica Las Condes*, *23*(4), 446-457. https://doi.org/10.1016/S0716-8640(12)70335-8

Todgham, A., & Stillman, J. (2013). Physiological responses to shifts in multiple environmental stressors: relevance in a changing world. *Integrative and Comparative Biology*, *53*(4), 539-544. https://doi.org/10.1093/icb/ict086

Tomanek, L. (2015). Proteomic responses to environmentally induced oxidative stress. *Journal of Experimental Biology*, *218*(12), 1867-1879. https://doi.org/10.1242/jeb.116475

Tripp-Valdez, M., Harms, L., Pörtner, H., Sicard, T., & Lucassen, M. (2019). De novo transcriptome assembly and gene expression profile of thermally challenged green abalone (*Haliotis fulgens*: Gastropoda) under acute hypoxia and hypercapnia. *Marine Genomics*, *45*, 48-56. https://doi.org/10.1016/j.margen.2019.01.007

Valdés, J., & Ortlieb, L. (2001). Paleoxigenación subsuperficial de la columna de agua en la bahía Mejillones del sur (23°S): Indicadores geoquímicos en testigos de sedimento marino. *Investigaciones marinas*, *29*, 25-35. https://doi.org/10.4067/S0717-71782001000100003

Valenzuela-Miranda, D., Valenzuela-Muñoz, V., Benavente, B., Muñoz-Trorcoso, M., Nuñez-Acuña, G., & Gallardo-Escárate, C. (2024). The Atlantic salmon microbiome infected with the sea louse *Caligus rogercresseyi* reveals tissue-specific functional dysbiosis. *Aquaculture*, *580*, 1-11. https://doi.org/10.1016/j.aquaculture.2023.740328

Valenzuela-Muñoz, V., Gallardo-Escárate, C., Benavente, B., Valenzuela-Miranda, D., Núñez-Acuña, G., Escobar-Sepulveda, H., & Váldes, J. (2022). Whole-Genome Transcript Expression Profiling Reveals Novel Insights into Transposon Genes and Non-Coding RNAs during Atlantic Salmon Seawater Adaptation. *Biology-Basel*, *11*(1), 1-21. https://doi.org/10.3390/biology11010001

Vaquer-Sunyer, R., & Duarte, C. (2008). Thresholds of hypoxia for marine biodiversity. *Proceedings of the National Academy of Sciences*, *105*(40), 15452–15457. https://doi.org/10.1073/pnas.0803833105

Vargas, C., Lagos, N., Lardies, M., Duarte, C., Manríquez, P., Aguilera, V.,…Dupont, S. (2017). Species-specific responses to ocean acidification should account for local adaptation and adaptive plasticity. *Nature Ecology & Evolution*, *1*(4), 1-7. https://doi.org/10.1038/s41559-017-0084

Velasco-Martínez, I., Hernández-Camacho, C., Méndez-Rodríguez, L., & Zenteno-Savín, T. (2016). Purine metabolism in response to hypoxic conditions associated with breath-hold diving and exercise in erythrocytes and plasma from bottlenose dolphins (*Tursiops truncatus*). *Comparative Biochemistry and Physiology, Part A*, *191*, 196-201. https://doi.org/10.1016/j.cbpa.2015.10.021

Villareal, L., & Xue, X. (2024). The emerging role of hypoxia and environmental factors in inflammatory bowel disease. *Toxicological sciences*, *198*(2), 169-184. https://doi.org/10.1093/toxsci/kfae004

Vujaklija, I., Bidin, S., Volaric, M., Bakic, S., Li, Z., Foo, R.,…Sikic, M. (2024). Detecting a wide range of epitranscriptomic modifications using a nanopore-sequencing-based computational approach with 1D score-clustering. *Nucleic Acids Research*, *53*(1), 1-18. https://doi.org/10.1093/nar/gkae1168

Wang, Q., Wu, R., Ji, J., Zhang, J., Niu, S., Tang, B.,…Liang, Z. (2024). Integrated Transcriptomics and Metabolomics Reveal Changes in Cell Homeostasis and Energy Metabolism in *Trachinotus ovatus* in Response to Acute Hypoxic Stress. *International Journal of Molecular Sciences*, *25*(2), 1-30. https://doi.org/10.3390/ijms25021054

Wang, Q., Zhang, S., He, X., Li, S., Xu, X., Feng, Y.,…Sun, G. (2025). Integrated m^6A RNA methylation and transcriptomic analysis of *Apostichopus japonicus* under combined high-temperature and hypoxia stress. *BMC Genomics*, *26*(1), 1-13. https://doi.org/10.1186/s12864-025-11532-x

Wang, Y., Li, L., Hu, M., & Lu, W. (2015). Physiological energetics of the thick shell mussel *Mytilus coruscus* exposed to seawater acidification and thermal stress. *Science of The Total Environment*, *514*, 261-272. https://doi.org/https://doi.org/10.1016/j.scitotenv.2015.01.092

Wang, Y., Yang, B., Lai, Q., Shi, J., Peng, J., Zhang, Y.,…Yin, D. (2021). Reprogramming of m^6A epitranscriptome is crucial for shaping of transcriptome and proteome in response to hypoxia. *RNA Biology*, *18*(1), 131-143. https://doi.org/10.1080/15476286.2020.1804697

Wang, Y., Zhou, S., Liu, T., Chen, M., Li, W., & Zhang, X. (2019). The transcriptomic responses of the ark shell, *Anadara broughtonii*, to sulfide and hypoxia exposure. *Molecular Biology Reports*, *46*(4), 4245-4257. https://doi.org/10.1007/s11033-019-04879-4

Wang, Z., Zhang, G., Ge, G., Wu, L., Wang, Y., Liu, Z.,…Wu, B. (2022). Transcriptome analysis reveals the molecular basis of the response to acute hypoxic stress in blood clam *Scapharca broughtonii*. *Israeli Journal of Aquaculture-Bamidgeh*, *74*, 1-14. https://doi.org/10.46989/001c.66177

White, E. (2012). Deconvoluting the context-dependent role for autophagy in cancer. *Nature Reviews Cancer*, *12*(6), 401-410. https://doi.org/10.1038/nrc3262

Workman, R., Tang, A., Tang, P., Jain, M., Tyson, J., Razaghi, R.,…Timp, W. (2019). Nanopore native RNA sequencing of a human poly(A) transcriptome. *Nature Methods*, *16*(12), 1297-1305. https://doi.org/10.1038/s41592-019-0617-2

Xu, X., Zheng, F., Xu, S., Hu, M., Hang, C., Liu, L.,…Du, L. (2023). Decreased ubiquitin modifying enzyme A20 associated with hyper-responsiveness to ovalbumin challenge following intrauterine growth restriction. *Respiratory Research*, *24*(1-11). https://doi.org/10.1186/s12931-023-02360-2

Yang, B., & Chen, Q. (2021). Cross-Talk between Oxidative Stress and m^6A RNA Methylation in Cancer. *Oxidative Medicine and Cellular Longevity*, *2021*, 1-26. https://doi.org/10.1155/2021/6545728

Yang, C., Wu, H., Chen, J., Liao, Y., Mkuye, R., Deng, Y., & Du, X. (2023). Integrated transcriptomic and metabolomic analysis reveals the response of pearl oyster (*Pinctada fucata martensii*) to long-term hypoxia. *Marine Environmental Research*, *191*, 1-10. https://doi.org/10.1016/j.marenvres.2023.106133

Yang, C., Yang, J., Hao, R., Du, X., & Deng, Y. (2020). Molecular characterization of *OSR1* in *Pinctada fucata martensii* and association of allelic variants with growth traits. *Aquaculture*, *516*, 1-9. https://doi.org/10.1016/j.aquaculture.2019.734617

Yang, J., Qiang, Z., Zhang, D., Hao, H., Wei, J., Maira, H.,…Nie, Z. (2025). Shotgun metagenomics analysis of gut microbiota of three indigenous fish species from the Kizil River, Xinjiang. *Frontiers in Microbiology*, *16*, 1-16. https://doi.org/10.3389/fmicb.2025.1617701

Yang, X., Yang, Y., Sun, B., Chen, Y., Xu, J., Lai, W.,…Yang, Y. (2017). 5-methylcytosine promotes mRNA export-NSUN2 as the methyltransferase and ALYREF as an m^5C reader. *Cell Research*, *27*(5), 606-625. https://doi.org/10.1038/cr.2017.55

Yang, Y., Hsu, P., Chen, Y., & Yang, Y. (2018). Dynamic transcriptomic m^6A decoration: writers, erasers, readers and functions in RNA metabolism. *Cell Research*, *28*(6), 616-624. https://doi.org/10.1038/s41422-018-0040-8

Yevenes, M., Lagos, N., Farías, L., & Vargas, C. (2019). Greenhouse gases, nutrients and the carbonate system in the Reloncaví Fjord (Northern Chilean Patagonia): Implications on aquaculture of the mussel, *Mytilus chilensis*, during an episodic volcanic eruption. *Science of the Total Environment*, *669*, 49-61. https://doi.org/10.1016/j.scitotenv.2019.03.037

Yu, R., & Wu, R. (2006). Hypoxia Affects Sex Differentiation and Development, Leading to a Male-Dominated Population in Zebrafish (*Danio rerio*). *Environmental Science & Technology*, *40*(9), 3118-3122. https://doi.org/10.1021/es0522579

Yévenes, M., Núñez-Acuña, G., Gallardo-Escárate, C., & Gajardo, G. (2022). Adaptive mitochondrial genome functioning in ecologically different farm-impacted natural seedbeds of the endemic blue mussel *Mytilus chilensis*.

Comparative Biochemistry and Physiology Part D: Genomics and Proteomics, *42*, 100955. https://doi.org/10.1016/j.cbd.2021.100955

Zaccara, S., Ries, R., & Jaffrey, S. (2019). Reading, writing and erasing mRNA methylation. *Nature Reviews Molecular Cell Biology*, *20*(10), 608-624. https://doi.org/10.1038/s41580-019-0168-5

Zannella, C., Mosca, F., Mariani, F., Franci, G., Folliero, V., Galdiero, M.,…Galdiero, M. (2017). Microbial Diseases of Bivalve Mollusks: Infections, Immunology and Antimicrobial Defense. *Marine Drugs*, *15*(6), 1-36. https://doi.org/10.3390/md15060182

Zhan, Y., Zha, S., Peng, Z., Lin, Z., & Bao, Y. (2022). Hypoxia-mediated immunotoxicity in the blood clam *Tegillarca granosa*. *Marine Environmental Research*, *177*, 1-8. https://doi.org/10.1016/j.marenvres.2022.105632

Zhang, S., Li, R., Zhang, L., Chen, S., Xie, M., Yang, L.,…Lam, H. (2020). New insights into *Arabidopsis* transcriptome complexity revealed by direct sequencing of native RNAs. *Nucleic Acids Research*, *48*(14), 7700-7711. https://doi.org/10.1093/nar/gkaa588

Zhang, Y., Luo, H., Niu, Y., Yang, X., Li, Z., Wang, K.,…Pang, X. (2022). Chronic intermittent hypoxia induces gut microbial dysbiosis and infers metabolic dysfunction in mice. *Sleep medicine*, *91*, 84-92. https://doi.org/10.1016/j.sleep.2022.02.003

Zhang, Z., Hou, Y., Yin, H., Lu, S., Liu, D., Cheng, L.,…Zhao, Y. (2025). Comparative transcriptomic and proteomic analyses of hypoxia response in wild and cultivated tomato roots. *BMC Genomics*, *26*(1), 1-20. https://doi.org/10.1186/s12864-025-11653-3

Zhang, Z., Park, E., Lin, L., & Xing, Y. (2018). A panoramic view of RNA modifications: exploring new frontiers. *Genome Biology*, *19*, 1-3. https://doi.org/10.1186/s13059-018-1394-4

Zhao, Q., Zhou, K., Zhang, F., Wang, Y., Hao, J., Xie, F., & Yang, Q. (2025). Relations Between Core Taxa and Metabolic Characteristics of Bacterial Communities in *Litopenaeus vannamei* Ponds and Their Probiotic Potential. *Microorganisms*, *13*(2), 1-18. https://doi.org/10.3390/microorganisms13020466

Zhou, Y., Zeng, P., Li, Y., Zhang, Z., & Cui, Q. (2016). SRAMP: prediction of mammalian N6-methyladenosine (m^6A) sites based on sequence-derived features. *Nucleic Acids Research*, *44*(10), 1-12. https://doi.org/10.1093/nar/gkw104

Zlotorynski, E. (2025). m^6A 'encodes' a dedicated mRNA decay pathway. *Nature Reviews Molecular Cell Biology*, *26*(1), 8. https://doi.org/10.1038/s41580-024-00815-y

Zong, X., Xiao, X., Shen, B., Jiang, Q., Wang, H., Lu, Z.,…Wang, Y. (2021). The N^6-methyladenosine RNA-binding protein YTHDF1 modulates the translation of *TRAF6* to mediate the intestinal immune response. *Nucleic Acids Research*, *49*(10), 5537-5552. https://doi.org/10.1093/nar/gkab343

Zou, J., Guo, P., Lv, N., & Huang, D. (2015). Lipopolysaccharide-induced tumor necrosis factor-α factor enhances inflammation and is associated with cancer (Review). *Molecular Medicine Reports*, *12*(5), 6399-6404. https://doi.org/10.3892/mmr.2015.4243